Volume 188, Number 4.2, October 2017 ISSN 0033–7587

Radiation Research

SNOLAB Focus Issue
Guest Editor: Dr. Douglas Boreham

Radiation Research
Official Journal of the Radiation Research Society

VOLUME 188, NUMBER 4.2, OCTOBER 2017

ON THE COVER: Artwork created in Adobe Illustrator

RADIATION RESEARCH

Volume 188, Number 4.2, October 2017

0033-7587/13 $15.00

PRINTED IN THE UNITED STATES OF AMERICA

This journal is printed on acid-free paper.

RADIATION RESEARCH

(ISSN 0033-7587)

Published monthly by the Radiation Research Society, 380 Ice Center Lane, Suite C, Bozeman, MT 59718

2017; volumes 187–188: Price: $780.00 U.S.A. and Canada; $880.00 all other countries

All prices include postage and handling.

All correspondence regarding subscriptions should be addressed to *Radiation Research*, 380 Ice Center Lane, Suite C, Bozeman, MT 59718, USA; phone: (406) 522-1301; e-mail: info@radres.org

Send notices of changes of address at least 6 weeks in advance. Please include both old and new address. POSTMASTER: Send changes of address to Radiation Research, 380 Ice Center Lane, Suite C, Bozeman, MT 59718, USA

Periodical postage paid at Bozeman, Montana, and at additional office.

Editorial office contact information: e-mail: jfye@iupui.edu; (317) 944-1308

Manuscript submission site: radiatres.allentrack.net

The Radiation Research Society gratefully acknowledges the support of the following corporations and institutions:

RRS Corporate Member

Rencel Energy & Metal Limited

RRS Institution Members

Albert Einstein College of Medicine
UAMA, Division of Radiation Health
Colorado State University
Center for Radiological Research, Columbia University
Duke University Medical Center
Institute for Radiological Protection and Nuclear Safety (IRSN)
University of Iowa
MD Anderson Cancer Center
University of Michigan Health System
UT Southwestern Medical Center
Queen's University Belfast
Wake Forest School of Medicine
Yale University of School of Medicine

Annual Meeting

Best Theratronics Ltd.
J. L. Shepherd and Associates Lab Research Inc.
Precision X-Ray Inc.
SNBL
Faxitron
Lovelace Biomedical
Taylor & Francis
CITox Lab
SRI International
Life Sciences in Space Research/Elsevier
Xstrahl Ltd.

Journal Office

Indiana University School of Medicine Department of Radiation Oncology

To learn more about how your company or institution can support the Radiation Research society, please contact:

Radiation Research Society
380 Ice Center Lane, Suite C
Bozeman, MT 59718
Toll free: 877-217-1919

RADIATION RESEARCH

CONTENTS Volume 188, Number 4.2, October 2017

RADIATION RESEARCH **188,** 469 (2017)
0033-7587/17 $15.00

DOI: 10.1667/RR0SNO.1

FOREWORD

It is a pleasure to provide an introductory message for this issue on the biological effects of low-level radiation. We are very happy to have this new research direction at SNOLAB to broaden the set of measurements taking place in our underground laboratory.

SNOLAB originated with the construction of the Sudbury Neutrino Observatory (SNO) experiment starting back in 1990. For this experiment, performed by a large international collaboration, we needed the ultimate in low radioactivity as we were trying to observe one neutrino per hour from the sun without interference from background radioactivity. To do this, we built a detector the size of a ten story building 2-km underground using ultra-clean materials and created an environment that was very free from mine dust containing trace amounts of uranium and thorium, the principal contaminants for our measurements. After excavating the cavity 34 meters high by 22 meters in diameter and lining it with urylon plastic to provide a water-tight and radon-tight volume, everyone working on the construction of the experiment took a shower and dressed in lint-free clothing when they entered the laboratory. We were able to restrict the dust to be less than a total of one gram distributed over the entire detector. Since we were looking for faint bursts of light we had to restrict greatly the cosmic rays that would have made our detector glow like the Northern Lights famous in Northern Canada. The 2-km depth accomplished this very well.

The SNO experiment was very successful and resulted in the award of the 2015 Nobel Prize in Physics for the discovery that neutrinos from the Sun changed from one flavor to another, also implying that they have a finite mass. Both of these properties are outside the predictions of the Standard Model of Elementary Particle Physics and require revisions or extensions to that theory.

The success of this ultra-low radioactivity experiment resulted in an application in 2003 by a consortium led by Professor David Sinclair of Carleton University for the expansion of the underground excavated space by about a factor of three, providing sites in the new SNOLAB for experiments that can benefit from the low radioactivity levels. In addition to the 2-km depth, the same standards of air quality are being maintained in SNOLAB to avoid additional contamination by mine dust in the experiments being performed. There are now a number of new particle astrophysics experiments situated in SNOLAB, ready to provide evidence of neutrinos from a supernova occurring in our galaxy or seeking evidence for interactions of Dark Matter particles. Other future experiments are aimed at the observation of a rare radioactivity known as Neutrino-less Double Beta Decay that could provide further detailed knowledge of neutrino properties.

The REPAIR experiment is a welcome addition to the set of experiments at SNOLAB and brings a new dimension to the type of measurements that can benefit from one of the lowest radioactivity laboratories in the world.

Professor Emeritus Art McDonald,
Queen's University, Kingston Ontario, SNO Collaboration Director,
Co-winner of the 2015 Nobel Prize in Physics

Dr. Nigel Smith,
Director of SNOLAB

RADIATION RESEARCH **188**, 470–474 (2017)
0033-7587/17 $15.00

DOI: 10.1667/RR14654.1

COMMENTARY

The REPAIR Project: Examining the Biological Impacts of Sub-Background Radiation Exposure within SNOLAB, a Deep Underground Laboratory

Christopher Thome,[a,b,1] Sujeenthar Tharmalingam,[a,b,1] Jake Pirkkanen,[b,1] Andrew Zarnke,[b,1] Taylor Laframboise[a] and Douglas R. Boreham[a,b,c,2]

[a] *Division of Medical Sciences, Northern Ontario School of Medicine and* [b] *Department of Biology, Laurentian University, Sudbury, Canada, P3E 2C6; and* [c] *Bruce Power, Tiverton, Canada, N0G 2T0*

Thome, C., Tharmalingam, S., Pirkkanen, J., Zarnke, A., Laframboise, T. and Boreham, D. R. The REPAIR Project: Examining the Biological Impacts of Sub-Background Radiation Exposure within SNOLAB, a Deep Underground Laboratory. *Radiat. Res.* 188, 470–474 (2017).

Considerable attention has been given to understanding the biological effects of low-dose ionizing radiation exposure at levels slightly above background. However, relatively few studies have been performed to examine the inverse, where natural background radiation is removed. The limited available data suggest that organisms exposed to sub-background radiation environments undergo reduced growth and an impaired capacity to repair genetic damage. Shielding from background radiation is inherently difficult due to high-energy cosmic radiation. SNOLAB, located in Sudbury, Ontario, Canada, is a unique facility for examining the effects of sub-background radiation exposure. Originally constructed for astroparticle physics research, the laboratory is located within an active nickel mine at a depth of over 2,000 m. The rock overburden provides shielding equivalent to 6,000 m of water, thereby almost completely eliminating cosmic radiation. Additional features of the facility help to reduce radiological contamination from the surrounding rock. We are currently establishing a biological research program within SNOLAB: Researching the Effects of the Presence and Absence of Ionizing Radiation (REPAIR project). We hypothesize that natural background radiation is essential for life and maintains genomic stability, and that prolonged exposure to sub-background radiation environments will be detrimental to biological systems. Using a combination of whole organism and cell culture model systems, the effects of exposure to a sub-background environment will be examined on growth and development, as well as markers of genomic damage, DNA repair capacity and oxidative stress. The results of this research will provide further insight into the biological effects of low-dose radiation exposure as well as elucidate some of the processes that may drive evolution and selection in living systems. This *Radiation Research* focus issue contains reviews and original articles, which relate to the presence or absence of low-dose ionizing radiation exposure.

INTRODUCTION

Biological systems on earth are continually exposed to natural background ionizing radiation, originating from a combination of cosmic and terrestrial sources. Cosmic radiation includes high-energy charged particles and atomic nuclei, which produce secondary radiation through atmospheric interaction, such as protons, neutrons and cosmogenic nuclides like carbon-14 and tritium. Terrestrial sources consist of long-lived primordial radioisotopes of uranium, thorium and potassium and their associated decay progeny, particularly radon gas. With the increase in man-made medical radiation exposures, considerable attention has been given to understanding the effects of low-dose radiation at levels slightly above natural background. There is growing evidence supporting the sublinear, threshold or hormetic models, where the biological risk at low doses is significantly less (or negative) compared to high-dose estimates (*1–3*). However, relatively few studies have been done to examine the inverse, where natural background radiation is removed.

In early experiments from the 1970s and 1980s, researchers examined the biological effects of sub-background radiation exposure on the protozoa *Paramecium tetraurelia* (*4–6*). Growth rates were significantly reduced when cultures were incubated within a shielded lead box. When a low-dose source was introduced into the shielded container, to artificially reintroduce background radiation, growth rates were restored to baseline levels. This growth inhibition after the removal of background radiation was later verified in other experiments using prokaryotes (*7–9*),

[1] Scholar-in-training, Radiation Research Society.

[2] Address for correspondence: Northern Ontario School of Medicine, Medical Sciences, 935 Ramsey Lake Road, MSE 224, Sudbury, ON P3E 2C6, Canada; email: dboreham@nosm.ca.

single-celled eukaryotes (*10, 11*) and mammalian cell culture models (*10, 12*).

In addition to alterations in growth rate, removal of background radiation promotes genotoxic damage. When grown in a sub-background environment, cultured cells showed an increase in basal levels of DNA damage and mutation rate (*13–15*). Low-background-adapted cells were also found to be more sensitive to induced genetic damage after exposure to a high-dose radiation challenge (*15–18*) or chemical agent (*13, 16, 19*). This increased sensitivity was correlated to a reduction in free radical scavenging ability (*13, 15, 16, 18*). In many cases, changes in repair capacity or growth rate were only observed after prolonged incubation in a sub-background environment on the order of weeks to months (*10, 13, 14, 17, 19–21*).

What makes sub-background experiments so challenging to conduct is the inherent difficulty in shielding from high-energy cosmic radiation. Historically, most experiments have relied on lead or other heavy metals for shielding, achieving only a modest reduction in background dose rates (*4, 6–8, 10, 12, 17, 20, 22*). Designing artificial shielding to obtain a significant reduction in cosmic radiation is impractical. The best way to eliminate cosmic radiation is to conduct experiments within facilities built deep underground. Only a few subterranean laboratories exist in the world. One such facility, SNOLAB, is located in Sudbury, Ontario, Canada.

SNOLAB

The laboratory first opened in 1999 as the Sudbury Neutrino Observatory (SNO) after nearly a decade of construction. The facility was built within Creighton Mine, an active nickel mine, at a depth of 2,070 m. To gain access, laboratory researchers must first travel down the mine shaft to the 6,800 level (6,800 feet underground), followed by a 1.5 km walk along one of the mine drifts (the laboratory was purposefully built to be isolated from the active mining sites). The original SNO experiment consisted of a single detector designed to measure neutrinos. The detector was the largest of its kind at that depth, measuring 12 m in diameter and filled with 1,000 tonnes of heavy water (*23*). Using heavy water enabled SNO to measure all three flavors of neutrino (electron, muon and tau). The 2,070-m overburden of rock effectively shielded out other sources of cosmic radiation, allowing SNO to detect the much lighter and very weakly interacting neutrinos. The SNO experiment provided the first direct evidence for neutrino oscillation, confirming that neutrinos possess mass (*24*). Electron neutrinos produced from solar nuclear fusion can change flavor into muon or tau neutrinos when traveling to earth. The discovery solved the solar neutrino problem: the deficit in early measurements of solar neutrinos compared to what was predicted based on the standard solar model. This breakthrough was recognized with the 2015 Nobel Prize in physics awarded to Dr. Arthur McDonald. The laboratory expanded beginning in 2004 and was renamed SNOLAB. Currently, SNOLAB has 3,060 m^2 of laboratory space (*25*). The original SNO detector is being repurposed to examine lower energy neutrinos and neutrinoless double beta decay using a liquid scintillator. Additional experiments are underway, or are planned, for examining supernovae and dark matter. These experiments all rely on the cosmic ray shielding provided by the 2 km of overhead rock.

In addition to the overburden of rock, which almost completely eliminates cosmic radiation, further measures have been established to help reduce radiation levels within SNOLAB. The experiment area of the laboratory is operated as a class 2000 clean room (fewer than 2,000 particles, 0.5 μm or larger, per cubic foot). All personnel entering the facility must shower and change into clean clothes to reduce contamination from radioactive dust in the mine drift. All equipment and supplies must also be hand washed before entering SNOLAB. Radon levels are reduced through continuous air filtration at a rate of 50 $m^3\ s^{-1}$, resulting in 10 full air changes per hour throughout the laboratory (*25*).

Low levels of radiation are still present in SNOLAB, mainly from radioactive decay in the surrounding norite rock. The largest component is radon gas with levels in the laboratory at approximately 130 Bq m^{-3} (*25*). Additionally, gamma radiation results from the decay of uranium and thorium progeny, and a small amount of neutron radiation is present from alpha particle interactions and spontaneous fission. Experiment specific shielding can be utilized to further control these sources of radiation. Neutrons and gamma rays can be reduced with the addition of water and lead shielding, respectively. Radon gas can be reduced using air-controlled chambers, such as glove boxes, which are filled with air from aged gas cylinders. With a half-life of 3.8 days, radon levels will decay several orders of magnitude within a few weeks.

Several other underground astroparticle physics laboratories exist around the world, however, very few of them have biological research programs. The largest facility for underground biology is the Laboratori Nazionali del Gran Sasso (LNGS) in Italy. Unlike SNOLAB, which was built within a mine, LNGS was tunneled into the side of the Gran Sasso Mountain to achieve cosmic ray shielding. The laboratory at LNGS has a rock overburden of 1,400 m and can achieve background dose rates down to approximately 30 μGy per year, a reduction of over 80-fold (*18*). Due to differences in geological composition, the depth of underground laboratories is generally stated in meters of water equivalent (MWE). LNGS has a MWE of 3,950 m (*26*), significantly less than SNOLAB, which has a MWE of 6,000 m (*27*). Biological experiments have also been conducted within the Waste Isolation Pilot Plant (WIPP), a nuclear waste repository in New Mexico. However, at a depth of 650 m, WIPP has considerably less shielding compared to SNOLAB or LNGS and only reduces background dose rates by a factor of 15 (*9*).

REPAIR PROJECT

We are currently establishing a biological research program within SNOLAB; Researching the Effects of the Presence and Absence of Ionizing Radiation (hereto know as REPAIR project). This program is focused on elucidating the effects of sub-background radiation exposure. The research space within SNOLAB will be the deepest underground biological laboratory in the world. Through utilization of the existing infrastructure, as well as some additional shielding, the REPAIR project will be able to monitor the response of biological systems exposed to one of the lowest background dose rates ever achieved. We hypothesize that because living organisms have evolved in the continual presence of natural background radiation, it is essential for life and helps to maintain genomic stability. Prolonged exposure to sub-background environments will therefore be detrimental to biological systems. This will be tested using a combination of cell culture and whole organism models. We will examine a variety of end points, ranging from simple quantification of growth and development, to more complex metrics for measuring oxidative stress, neoplastic transformation and genomic instability. This focus issue of *Radiation Research* includes three reviews and four original articles relating to the presence or absence of low-dose radiation exposure, which describe relevant findings, methodologies and/or model systems pertaining to the research aims of the REPAIR project.

Cellular transformation assays have been utilized to assess the influence of ionizing radiation and other carcinogenic agents on neoplastic transformation. Evaluating the frequency of events in which normal cells alter phenotypically and become neoplastic, as well as the genetic and epigenetic mechanisms driving this change, provide important information in the evaluation of carcinogenesis. By investigating changes in gene regulation, DNA damage/repair and morphology can be linked to these phenotypic changes to help elucidate what may drive the neoplastic transformation of normal cells. The CGL1 cell line is a pre-neoplastic derivative of a HeLa x normal human fibroblast hybrid (*28*) and is ideal due to its human origin, compared to other similar systems derived from rodent or non-mammalian sources. It is a stable and non-tumorigenic tissue culture system in which cell transformation can be induced by a radiological or chemical stress, and is therefore a good model for quantitatively investigating the effects of ionizing radiation on neoplastic transformation *in vitro* (*40*). Transformed CGL1 cells differentially express intestinal alkaline phosphatase (IAP) as a surface antigen (*29, 30*). This novel characteristic allows for a simplistic and expedited end point. When in the presence of the alkaline phosphatase chromogen Western Blue (WB), transformed cells yield a colored precipitant (*31*), which makes neoplastically transformed colonies easily distinguishable from non-transformed IAP negative foci. This feature makes the CGL1-based transformation assay unique among others, since transformation events can be detected earlier and do not rely on scoring methods such as morphological assessment, which can be imprecise and tedious. Furthermore, the WB substrate is inexpensive compared to antibody immunohistochemical-based detection and scoring methods. In the sub-background radiation environment that SNOLAB provides, the CGL1-based transformation assay is ideal for several reasons: it is sensitive to low-dose and low-dose-rate radiation exposure (*32–34*), has a relatively short assay period of only 21 days and the scoring end point works on viable as well as paraformaldehyde-fixed cells. Therefore, minimal infrastructure and reagent are necessary to complete this assay, making it attractive for utilization underground in SNOLAB.

A topic that is consistently absent from previous experiments is the effect of sub-background radiation exposure on complex multicellular whole organism models. All research to date has utilized either single celled organisms (*4–11, 17, 19, 20*) or *in vitro* cell culture models (*9, 10, 12–16, 18*), and the observed results may not translate to the whole organism level. Animal work in underground facilities such as SNOLAB is hampered by space limitations and restrictions in laboratory access, which makes many species, such as murine models, extremely difficult to work with. Animal models must be low maintenance, have minimal space and resource requirements, and be able to survive for several days without researcher access.

Embryonic development in lake whitefish (*Coregonus clupeaformis*) is an ideal species model for studying sub-background exposure. We have previously examined the effects of low-dose ionizing radiation (above background) on lake whitefish embryogenesis. Embryos responded to small changes in radiation environments, where a chronic exposure as low as 0.06 mGy per day resulted in significant growth stimulation (*41*). Growth stimulation was also observed with four fractionated low doses of 15 mGy radiation, in contrast to growth suppression observed at higher fractions of 2, 6 or 8 Gy (*42*). This sensitivity to low-dose radiation suggests that lake whitefish may be affected by development in a sub-background environment. In addition, embryos can be easily raised in large numbers using only petri dishes, dechlorinated water and standard refrigeration units (*35*). Lake whitefish develop slowly, close to 200 days depending on temperature (*36, 37*). This is important since, in many of the previous sub-background experiments, effects were observed only after prolonged incubation (*10, 13, 14, 17, 19–21*). Lastly, embryos can be easily staged and quantified for growth rate (*38*), which is one of the main end points examined in past studies. We plan to raise lake whitefish embryos within SNOLAB, representing the first sub-background experiment utilizing a complex whole organism model.

One topic of investigation for the REPAIR project will be the response of low-background adapted cells and organisms to induced damage from a high-dose challenge

exposure. Previous sub-background studies have shown reduced repair capacity when background radiation was removed (*13–15, 18, 19, 21*), which challenges the linear no-threshold hypothesis. This coincides with data demonstrating a radiation-induced adaptive response at doses slightly above natural background. At the cellular levels, low-dose exposures below 100 mGy produce an adaptive response towards radiation-induced DNA damage and genomic instability (*39*). At the whole organism level, a low-dose exposure can modify cancer progression. When cancer-prone *Trp*53$^{+/-}$ mice were exposed to multiple CT scans (one weekly scan for 10 weeks, 10 mGy per scan) after the induction of cancer by a previous high-dose exposure, both cancer latency and overall lifespan were increased (*43*). Similarly, cancer latency and lifespan were increased after a single 10 mGy CT scan (*44*). Low-dose radiation can also reduce the incidence of non-cancerous disease such as cardiac impairment and diabetes (*45*). We predict that organisms and cells grown within the sub-background environment in SNOLAB will be more sensitive to induced damage.

Low-linear energy-transfer radiation acts mainly through the production of reactive oxygen intermediates. When cellular antioxidant defense mechanisms are unable to counteract the formation of oxidative stress, the excess free radicals damage biological macromolecules including nucleic acids. Previous results from sub-background experiments have been linked to changes in oxidative stress levels (*13, 15, 16, 18*). Low-dose radiation-induced phenotypic alterations can demonstrate non-Mendelian modes of inheritance. There is emerging evidence that low levels of oxidative stress can cause heritable gene expression modifications by altering the genomic structure, while the underlying DNA nucleotide sequence remains unchanged. These structural genome changes are referred to as epigenetic modifications (*46*). Oxidative stress generated from low doses of ionizing radiation provides a mechanistic link between radiation and epigenetic gene regulation. Cells can adapt to radiation exposure by modifying epigenetic gene regulation. These heritable cellular effects can either provide a positively adaptive phenotype or result in enhanced disease progression. The REPAIR project will aim to elucidate the effects of sub-background radiation exposure on oxidative stress and epigenetic programming.

Overall, the REPAIR project will provide an in-depth evaluation of the biological effects of sub-background radiation exposure, an area of research that still remains poorly understood. SNOLAB is a unique facility and one of few in the world where this type of research can be conducted. We will examine sub-background effects using complex animal systems, such as embryonic development in lake whitefish. Numerous different cellular end points will be used, including transformation frequency, which will provide insight into baseline levels of DNA damage and oxidative stress, as well as cellular repair capacity and genomic instability. The results of this project will extend our knowledge into the biological effects of low-dose ionizing radiation exposure, as we explore what happens in the absence of a physics stressor, given that all living systems have evolved in the presence of low-level ionizing radiation.

ACKNOWLEDGMENTS

We thank SNOLAB and its staff for support through underground space, logistical and technical services. SNOLAB operations are supported by the Canada Foundation for Innovation and the Province of Ontario Ministry of Research and Innovation, with underground access provided by Vale at the Creighton mine site. The REPAIR project is supported through an industrial research grant from Bruce Power, as well as funding from the Natural Sciences and Research Council of Canada and Mitacs.

Received: October 12, 2016; accepted: May 8, 2017; published online: July 19, 2017

REFERENCES

1. Brooks AL, Dauer LT. Advances in radiation biology: effect on nuclear medicine. Semin Nucl Med 2014; 44:179–86.
2. Tang FR, Loke WK. Molecular mechanisms of low dose ionizing radiation-induced hormesis, adaptive responses, radioresistance, bystander effects, and genomic instability. Int J Radiat Biol 2015; 91:13–27.
3. Calabrese EJ, Baldwin LA. U-shaped dose-responses in biology, toxicology, and public health. Annu Rev Public Health 2001; 22:15–33.
4. Planel H, Soleilhavoup JP, Tixador R, Croute F, Richoilley G. Biological and environmental effects of low-level radiation: v. 1 (IAEA Proceedings Series). Vienna: International Atomic Energy Agency; 1976.
5. Croute F, Dupouy D, Charley JP, Soleilhavoup JP, Planel H. Effects of autogamy in Paramecium tetraurelia on catalase activity and on radiosensitivity to natural ionizing radiations. J Protozool 1980; 27:132–5.
6. Planel H, Soleilhavoup JP, Tixador R, Richoilley G, Conter A, Croute F, et al. Influence on cell proliferation of background radiation or exposure to very low, chronic gamma radiation. Health Phys 1987; 52:571–8.
7. Conter A, Dupouy D, Planel H. Demonstration of a biological effect of natural ionizing radiations. Int J Radiat Biol Relat Stud Phys Chem Med 1983; 43:421–32.
8. Conter A. Preirradiation of medium induces a subsequent stimulation or inhibition of growth according to the physiological state in Synechococcus lividus in culture. Radiat Res 1987; 109:342–6.
9. Smith GB, Grof Y, Navarrette A, Guilmette RA. Exploring biological effects of low level radiation from the other side of background. Health Phys 2011; 100:263–5.
10. Kawanishi M, Okuyama K, Shiraishi K, Matsuda Y, Taniguchi R, Shiomi N, et al. Growth retardation of Paramecium and mouse cells by shielding them from background radiation. J Radiat Res 2012; 53:404–10.
11. Luckey TD. Ionizing radiation promotes protozoan reproduction. Radiat Res 1986; 108:215–21.
12. Takizawa Y, Yamashita J, Wakizaka A, Tanooka H. Background radiation can stimulate the proliferation of mouse-L-5178Y cells. In: JAER Institution (now JAEA), editor. International Conference on Radiation Effects and Protection. Naka-Gun, Japan: Japan Atomic Energy Research Institution (now Japan Atomic Energy Agency); 1992.
13. Satta L, Antonelli F, Belli M, Sapora O, Simone G, Sorrentino E, et al. Influence of a low background radiation environment on

biochemical and biological responses in V79 cells. Radiat Environ Biophys 2002; 41:217–24.

14. Fratini E, Carbone C, Capece D, Esposito G, Simone G, Tabocchini MA, et al. Low-radiation environment affects the development of protection mechanisms in V79 cells. Radiat Environ Biophys 2015; 54:183–94.
15. Carbone MC, Pinto M, Antonelli F, Balata M. Effects of deprivation of background environmental radiation on cultured human cells. Il Nuovo Cimento B 2010; 125:469–77.
16. Antonelli F, Bell N, Sapora O, Simone G, Sorrentino E, Tabocchini MA, et al. PULEX. LNGS Annual Report 2007. Asergi, Italy: Laboratori Nazionali del Gran Sasso; 2008.
17. Gajendiran N, Jeevanram RK. Environmental radiation as the conditioning factor for the survival of yeast Saccharomyces cerevisiae. Indian J Exp Biol 2002; 40:95–100.
18. Carbone MC, Pinto M, Antonelli F, Amicarelli F, Balata M, Belli M, et al. The Cosmic Silence experiment: on the putative adaptive role of environmental ionizing radiation. Radiat Environ Biophys 2009; 48:189–96.
19. Satta L, Augusti-Tocco G, Ceccarelli R, Esposito A, Fiore M, Paggi P, et al. Low environmental radiation background impairs biological defence of the yeast Saccharomyces cerevisiae to chemical radiomimetic agents. Mutat Res 1995; 347:129–33.
20. Tixador R, Richoilley G, Monrozies E, Planel H, Tap G. Effects of very low doses of ionizing radiation on the clonal life-span in Paramecium tetraurelia. Int J Radiat Biol Relat Stud Phys Chem Med 1981; 39:47–54.
21. Antonelli F, Belli M, Pinto M, Sapora O, Sorrentino E, Simone G, et al. PULEX: Influence of environment radiation background on biochemistry and biology of cultured cells and on their response to genotoxic agents. Il Nuovo Cimento C 2008; 31:49–56.
22. Croute F, Soleilhavoup JP, Vidal S, Dupouy D, Planel H. Paramecium tetraurelia growth stimulation under low-level chronic irradiation: investigations on a possible mechanism. Radiat Res 1982; 92:560–7.
23. Boger J, Hahn RL, Rowley JK, Carter AL, Hollebone B, Kessler D, et al. The Sudbury Neutrino Observatory. Nucl Instr Meth Phys Res A 2000; 449:172–207.
24. Ahmad QR, Allen RC, Andersen TC, J DA, Barton JC, Beier EW, et al. Direct evidence for neutrino flavor transformation from neutral-current interactions in the Sudbury Neutrino Observatory. Phys Rev Lett 2002; 89:011301.
25. Smith NJT. The SNOLAB deep underground facility. Eur Phys J Plus 2012; 127:108.
26. Rindi A, Celani F, Lindozzi M, Miozzi S. Underground neutron flux measurement. Nucl Instr Meth Phys Res A 1988; 272:871–4.
27. Duncan F, Noble AJ, Sinclair D. The construction and anticipated science of SNOLAB. Annu Rev Nucl Part Sci 2010; 60:163–80.
28. Redpath JL, Sun C, Colman M, Stanbridge EJ. Neoplastic transformation of human hybrid cells by gamma radiation: a quantitative assay. Radiat Res 1987; 110:468–72.
29. Latham KM, Stanbridge EJ. Identification of the HeLa tumor-associated antigen, p75/150, as intestinal alkaline phosphatase and evidence for its transcriptional regulation. Proc Natl Acad Sci U S A 1990; 87:1263–7.
30. Mendonca MS, Antoniono RJ, Latham KM, Stanbridge EJ, Redpath JL. Characterization of intestinal alkaline phosphatase expression and the tumorigenic potential of gamma-irradiated HeLa × fibroblast cell hybrids. Cancer Res 1991; 51:4455–62.
31. Mendonca MS, Antoniono RJ, Sun C, Redpath JL. A simplified and rapid staining method for the HeLa × skin fibroblast human hybrid cell neoplastic transformation assay. Radiat Res 1992; 131:345–50.
32. Redpath JL, Antoniono RJ, Sun C, Gerstenberg HM, Blakely WF. Late mitosis/early G1 phase and mid-G1 phase are not hypersensitive cell cycle phases for neoplastic transformation of HeLa × skin fibroblast human hybrid cells induced by fission-spectrum neutrons. Radiat Res 1995; 141:37–43.
33. Lewis DA, Mayhugh BM, Qin Y, Trott K, Mendonca MS. Production of delayed death and neoplastic transformation in CGL1 cells by radiation-induced bystander effects. Radiat Res 2001; 156:251–8.
34. Pant MC, Liao XY, Lu Q, Molloi S, Elmore E, Redpath JL. Mechanisms of suppression of neoplastic transformation in vitro by low doses of low LET radiation. Carcinogenesis 2003; 24:1961–5.
35. Mitz C, Thome C, Cybulski ME, Laframboise L, Somers CM, Manzon RG, et al. A self-contained, controlled hatchery system for rearing lake whitefish embryos for experimental aquaculture. N Am J Aquacult 2014; 76:179–84.
36. Brooke LT. Effect of different constant incubation temperatures on egg survival and embryonic development in lake whitefish (Coregonus clupeaformis). Trans Am Fish Soc 1975; 104:555–9.
37. Mueller CA, Eme J, Manzon RG, Somers CM, Boreham DR, Wilson JY. Embryonic critical windows: changes in incubation temperature alter survival, hatchling phenotype, and cost of development in lake whitefish (Coregonus clupeaformis). J Comp Physiol B 2015; 185:315–31.
38. Sreetharan S, Thome C, Mitz C, Eme J, Mueller CA, Hulley EN, et al. Embryonic development of lake whitefish Coregonus clupeaformis: a staging series, analysis of growth and effects of fixation. J Fish Biol 2015; 87:539–58.
39. Phan N, De Lisio M, Parise G, Boreham DR. Biological effects and adaptive response from single and repeated computed tomography scans in reticulocytes and bone marrow of C57BL/6 mice. Radiat Res 2012; 177:164–75.
40. Pirkkanen J, Boreham DR, Mendonca MS. The CGL1 (HeLa × skin fibroblast) human hybrid cell line: a history of radiation induced effects and novel future directions. Radiat Res 2017; 188:
41. Thome C, Mitz C, Hulley EN, Somers CM., Manzon RG, Wilson JY, Boreham DR. Initial characterization of the growth stimulation and heat shock-induced adaptive response in developing lake whitefish embryos after ionizing radiation exposure. Radiat Res 2017; 188:
42. Mitz C, Thome C, Cybulski ME, Somers CM, Manzon RG, Wilson, JY, et al. Cost of hormesis: is there a trade-off between radiation stimulated growth and metabolic efficiency? Radiat Res 2017; 188:
43. Lemon JA, Phan N, Boreham, DR. Multiple CT scans extend lifespan by delaying cancer progression in cancer prone mice. Radiat Res 2017; 188:
44. Lemon JA, Phan N, Boreham DR. Single CT scan prolongs survival by extending cancer latency in Trp53 heterozygous mice. Radiat Res 2017; 188:
45. Khaper N, Puukila S, Lemon J, Lees S, Tia TC, Boreham D. Impact of ionizing radiation on the cardiovascular system: a review. Radiat Res 2017; 188:
46. Tharmalingam S, Sreetharan S, Kulesza AV, Boreham DR, Tai TC. Low-dose ionizing radiation exposure, oxidative stress and epigenetic programing of health and disease. Radiat Res 2017; 188:

RADIATION RESEARCH **188**, 475–485 (2017)
0033-7587/17 $15.00

DOI: 10.1667/RR14574.1

Initial Characterization of the Growth Stimulation and Heat-Shock-Induced Adaptive Response in Developing Lake Whitefish Embryos after Ionizing Radiation Exposure

Christopher Thome,[a,1] Charles Mitz,[a,1] Emily N. Hulley,[a,1] Christopher M. Somers,[c] Richard G. Manzon,[c] Joanna Y. Wilson[b] and Douglas R. Boreham[a,d,2]

Departments of [a] Medical Physics and Applied Radiation Sciences and [b] Biology, McMaster University, Hamilton, Canada; [c] Department of Biology, University of Regina, Regina, Canada; and [d] Northern Ontario School of Medicine, Sudbury, Canada

Thome, C., Mitz, C., Hulley, E. N., Somers, C. M., Manzon, R. G., Wilson, J. Y. and Boreham, D. R. Initial Characterization of the Growth Stimulation and Heat-Shock-Induced Adaptive Response in Developing Lake Whitefish Embryos after Ionizing Radiation Exposure. *Radiat. Res.* 188, 475–485 (2017).

Ionizing radiation is known to effect development during early life stages. Lake whitefish (*Coregonus clupeaformis*) represent a unique model organism for examining such effects. The purpose of this study was to examine how ionizing radiation affects development in lake whitefish embryos and to investigate the presence of an adaptive response induced by heat shock. Acute exposure to ^{137}Cs gamma rays was administered at five time points corresponding to major developmental stages, with doses ranging from 0.008 to 15.5 Gy. Chronic gamma-ray exposures were delivered throughout embryogenesis within a custom-built irradiator at dose rates between 0.06 and 4.4 mGy/day. Additionally, embryos were given a heat shock of 3, 6 or 9°C prior to a single acute exposure. Radiation effects were assessed based on survival, development rate, morphometric measurements and growth efficiency. Embryos showed high resistance to acute exposures with an $LD_{50/hatch}$ of 5.0 ± 0.7 Gy immediately after fertilization, increasing to 14.2 ± 0.1 Gy later in development. Chronic irradiation at all dose rates stimulated growth, with treated embryos up to 60% larger in body mass during development compared to unirradiated controls. Chronic irradiation also accelerated the time-to-hatch. A heat shock administered 6 h prior to irradiation reduced mortality by up to 25%. Overall, low-dose chronic irradiation caused growth stimulation in developing lake whitefish embryos and acute radiation mortality was reduced by a heat-shock-induced adaptive response.

INTRODUCTION

The type and significance of whole-organism effects from low-dose ionizing radiation exposure, generally defined as less than 100 mGy, remain poorly understood. Human epidemiological data from cohorts such as the atomic bomb survivors have not provided conclusive evidence regarding the levels of risk, if any, from these low-dose exposures. There is growing experimental data to suggest that linear extrapolation from higher doses overestimates risk and that dose-response curves follow a sublinear, threshold or hormetic response. The hormetic model had been demonstrated after chemical and radiological exposure, where low-dose exposures induce stimulatory effects such as increased growth, survival or fecundity, compared to the inhibitory effects at high doses (*1*). However, there is also evidence to suggest that initiation of a hormetic response may come at a cost to other physiological processes (*2–5*). Related to hormesis is the adaptive response, where a low-dose stress can protect cells or whole organisms from a subsequent high-dose exposure. A variety of different stressors have been shown to induce an adaptive response by reducing damage from high-dose ionizing radiation, including low-dose radiation (*6–8*), thermal stress (*9–11*) and oxidative chemical compounds (*12–14*). Similar cellular and molecular mechanisms have been implicated in both the adaptive response and radiation hormesis (*15*).

Early development is one of the most sensitive stages to ionizing radiation across a broad range of taxa. Data from both human and non-human biota have shown that developing embryos have a greater sensitivity to radiation compared to more advanced older life stages (*16–18*). The risk of prenatal mortality is highest close to fertilization, while sublethal exposures later in development can increase the probability of malformations (*16*). Embryogenesis in fish represents an excellent model for examining whole-organism developmental effects of ionizing radiation. The majority of bony fish are oviparous, whereby embryos are protected from their environment within an eggshell and all potential energy reserves are contained within their yolk. As

[1] Scholar-in-training, Radiation Research Society.

[2] Address for correspondence: Northern Ontario School of Medicine, Medical Sciences, 935 Ramsey Lake Road MSE 224, Sudbury, ON P3E 2C6, Canada; email: dboreham@nosm.ca.

ectotherms, a large proportion of yolk lipids and proteins are converted to growth as opposed to thermoregulation. Therefore, a direct measure of growth efficiency is possible through quantifying yolk utilization and body size. Lake whitefish (*Coregonus clupeaformis*) are a particularly good model species for examining the effects of radiation. They have a long embryonic development period, up to 200 days when raised at cold temperatures (*19–21*). This slow development rate allows for the accurate targeting of specific developmental stages for acute exposures as well as enabling extended exposure to low-dose chronic radiation. Additionally, the lake whitefish chorion is transparent, enabling accurate live staging of embryos (*22*). Lastly, embryos can easily be raised in large numbers using minimal space and resource requirements (*23*).

The objective of this study was to examine the effects of both acute and chronic irradiation on embryonic development in lake whitefish. Acute exposures were delivered over a range of low to high doses at five critical developmental time points. A chronic irradiator was designed specifically for exposing lake whitefish embryos to low-dose radiation throughout embryogenesis. In addition to survival, embryos were monitored for development rate and size, to provide insight into how both chronic and acute exposures affect embryonic growth and metabolic efficiency. The presence of an adaptive response was tested through exposure to a thermal stress prior to high-dose acute irradiation.

MATERIALS AND METHODS

Embryo Collection

Lake whitefish embryos were *in vitro* fertilized in the fall of three consecutive years (November 15, 2012, November 21, 2013 and November 30, 2014). Adult fish were gillnetted in Eastern Lake Huron (N 44.7094, W 81.3125, Ontario Ministry of Natural Resources scientific fishing permit to JYW). Eggs were stripped from multiple spawning females and combined with milt from multiple males. Eggs were dry fertilized for 5 min, then wet fertilized with lake water for 5 min, then transferred to 1.5-liter jars at a 50:50 ratio of embryos:lake water. Ovadine® (Syndel Laboratories Ltd., Nanaimo, Canada) was added to each jar for 30 min to disinfect embryos at a concentration of 5 ml Ovadine per 1 liter lake water. After 30 min, Ovadine was removed, and embryos were washed twice with lake water and transported to the laboratory on ice.

Embryo Rearing

Embryos were initially raised in upwelling hatching jars within a custom-designed recirculating filtered water system (*23*). Individual experiments were performed using petri dishes filled with dechlorinated municipal water. Petri dishes were housed on the shelves of the refrigeration units, above the upwelling hatching jars (*23*). Petri dish water was changed twice per week for the first month of development and then once per week after the majority of natural mortality had occurred. Dishes were checked daily and dead or hatched embryos were removed. Hatching jar and petri dish water temperature was continuously monitored using data loggers (Onset HOBO, Bourne, MA).

Embryos in hatching jars were incubated at 5.2 ± 0.1°C (mean ± SD), which was the lowest temperature that circulating water could maintain (*23*). Acutely irradiated embryos were incubated in the same refrigeration units as hatching jars, where static water temperature in petri dishes was 2.8 ± 0.3°C. Chronically irradiated embryos were incubated at approximately the same temperature as acutely irradiated embryos (2.8 ± 0.3°C for irradiated embryos, 2.7 ± 0.3°C for controls). Heat-shock experiments were performed in a separate refrigeration unit at 2.1 ± 0.3°C. A colder incubation temperature was used so that a 9°C heat shock could be administered, while preventing the absolute temperature from reaching lethal levels.

Acute Irradiation

Acutely irradiated embryos received a single 662 keV gamma-ray dose, using a cesium-137 (^{137}Cs) source. Irradiations were administered on day 1, 7, 15, 30 or 60 after fertilization, corresponding to cleavage, gastrulation, closure of the blastopore, organogenesis and fin flutter stages, respectively (*22*). Development stages were confirmed by light microscopy. Embryos were transferred from hatching jars to 12.5 cm^2 vented cap cell culture flasks and irradiated on an ice slurry. Radiation doses ranged from 0.008 ± 0.001 Gy to 15.5 ± 2.0 Gy, all at a dose rate of 0.39 ± 0.05 Gy/min. Doses were verified using thermoluminescent dosimeters (Mirion Technologies, Irvine, CA). At each dose point, 50 embryos were irradiated per flask, in duplicate or triplicate flasks. After irradiation, embryos were transferred to petri dishes until hatch.

Chronic Irradiation

Lake whitefish were chronically irradiated for the entirety of embryogenesis using a custom-built ^{137}Cs gamma irradiator designed to fit within a reinforced two-door refrigerator (Fig. 1). The containment unit was lined with 3 cm of lead to provide adequate shielding. A 37-MBq ^{137}Cs source (J. L. Shepherd & Associates, San Fernando, CA) was housed in the bottom of the unit, directed upwards towards a series of six shelves (Fig. 1A and B). The lowest shelf was loaded with one 15-cm petri dish, containing 100 embryos, due to the narrow beam window close to the source. The remaining five shelves were loaded with five 10-cm petri dishes, each containing 50 embryos. A 3-cm lead slide was used to block the beam window for when entry into the unit was required (Fig. 1C). Dose rates were calculated using thermoluminescent dosimeters (Table 1; Mirion Technologies, San Ramon, CA). Four dosimeters were placed on each shelf to record lateral spatial variation in dose rate. Five control dishes were placed outside of the lead box but within the same refrigerator. Embryos were loaded into the irradiator immediately upon their return to the laboratory, approximately 7 h after fertilization.

Heat Shock and Radiation

Embryos were exposed to a thermal shock prior to high-dose acute irradiation. On day 5 after fertilization (gastrulation), embryos were transferred from hatching jars to petri dishes at 2°C. After 48 h in dishes, embryos were exposed to a transient heat shock of magnitude 3, 6 or 9°C (absolute temperature of 5, 8 or 11°C) for 2 h. Water was removed from the dishes and fresh pre-heated water was added. After 2 h, dishes were transferred back to the 2°C refrigerator and water was allowed to gradually cool. At two different time points after heat shock, embryos were exposed to 7.75 Gy as described for acute irradiations. The dose of 7.75 Gy was selected based on the results from acute exposures to produce approximately 50% mortality. One set of embryos was irradiated 6 h after heat shock and a second set irradiated 24 h after heat shock. After irradiation, embryos were transferred back to petri dishes until hatch. All treatments (combined heat and radiation, and single exposure controls) were run in duplicate dishes with 50 embryos per dish.

Morphometric Measurements

All live hatches from chronic and acute exposures were fixed in 10% neutral buffered formalin for one week then transferred to 70% ethanol for long-term storage. A subset of chronically irradiated

FIG. 1. Design of chronic irradiator. Panel A: Containment unit with door open and six shelves to hold dishes containing embryos. Number 1 indicates the cover plate over source compartment. Panel B: Bottom of unit with source compartment cover plate removed. Number 2 indicates the lead pig containing 37 MBq ^{137}Cs source directed upwards. Panel C: Lead slide on right side of unit to block beam window during entry into unit. Slide is shown in ''open'' position.

embryos (25 per shelf) was fixed on day 76 and day 122 after fertilization (approximately 50 and 75% development). Hatched fish and dechorionated embryos were imaged and measured (Axio Zoom V16; Carl Zeiss, Oberkochen, Germany). Total body length was measured from a dorsal image. Yolk area was calculated based on two perpendicular yolk diameters measured from a lateral image. Images were also used to quantify morphological abnormalities (scoliosis, lordosis, fin defects).

Body and yolk mass were measured on fixed chronically irradiated embryos. After imaging, the embryo or hatched fish was dissected

TABLE 1
Chronic Irradiator Dose Measurements

		Cumulative exposure (mGy)		
Distance from source (cm)	Dose rate (mGy/day)	Day 76	Day 122	Hatch
81.4	0.06 ± 0.01	4.7 ± 1.0	7.6 ± 1.7	9.5 ± 2.2
67.2	0.11 ± 0.02	8.2 ± 1.3	13.2 ± 2.1	16.6 ± 2.8
52.9	0.19 ± 0.03	14.5 ± 2.6	23.3 ± 4.2	29.4 ± 5.8
38.6	0.39 ± 0.04	29.4 ± 3.1	47.1 ± 5.0	59.7 ± 7.5
24.3	1.05 ± 0.09	79.7 ± 7.1	128.0 ± 11.4	160.5 ± 17.3
10.0	4.40 ± 0.78	334.5 ± 59.4	537.0 ± 95.3	664.7 ± 117.9

Notes. Dose rates were measured on each shelf using thermoluminescent dosimeters. Cumulative exposure was calculated to day 75 and day 122, when embryos were fixed. Cumulative exposure at hatch was calculated using the median hatch date for embryos on each shelf. Error represents the range in dose rates based on measured lateral spatial variation on each shelf. Control dishes were housed in the same refrigeration unit but were not irradiated.

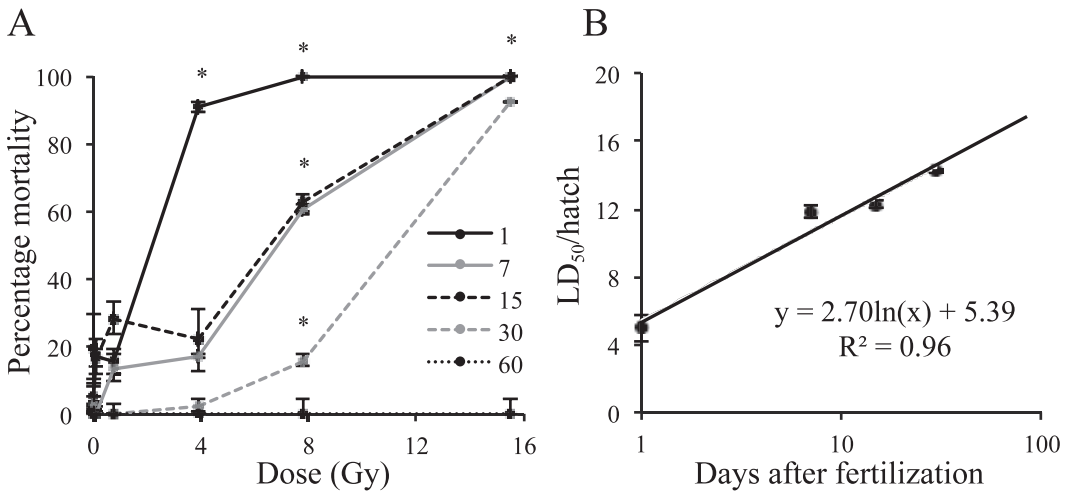

FIG. 2. Embryonic mortality after acute radiation exposure. Panel A: Cumulative percentage mortality was calculated at hatch after irradiation on day 1, 7, 15, 30 or 60 after fertilization. To eliminate differences in natural mortality rates, a correction factor based on control mortality was applied across all treatments. Percentage mortality was compared using one-way ANOVA. *Significant difference from same day controls based on Dunnett's post hoc test. Data points represent means ± SE. Panel B: The LD_{50} at hatch increased logarithmically with embryo age at irradiation. Data points represent the mean of replicate dishes. Error represents the SE in LD_{50} probit analysis.

from the yolk. Samples were dried overnight in a 70°C oven and a yolk-free body and yolk dry mass were measured (cat. no. XA105DU; Mettler-Toledo, Columbus, OH). A set of 25 embryos was also fixed and weighed on day 1 post fertilization (dpf), from which yolk conversion efficiency (YCE) was calculated according to the equation:

$$\text{YCE } (\%) = \frac{\text{yolk free body dry mass}}{(\text{1dpf yolk dry mass} - \text{yolk dry mass})} \times 100.$$

Statistical Analysis

Statistical analysis was performed using JMP® software version 12.1 (Cary, NC). Cumulative percentage mortality at hatch and time-to-hatch were compared between dishes using a one-way ANOVA. When the ANOVA was significant, percentage mortality in treatment dishes was compared to controls using Dunnett's post hoc test, and hatch timing was compared among all dishes using Tukey's honest significant difference (HSD) test. LD_{50} values were calculated based on probit analysis. Due to the high rate of natural mortality at early time points, a correction factor based on control mortality was applied across all treatments, using the Schneider-Orelli method (*24*). Body length and yolk area measurements were compared using a non-parametric Kruskal-Wallis one-way ANOVA on ranks followed by Dunn's test, because data were not normally distributed. Dry mass and YCE were compared using a one-way ANOVA followed by Tukey's HSD test. Mortality and hatch timing in combined heat shock and radiation experiments were analyzed using a two-way ANOVA followed by Tukey's HSD test.

RESULTS

Acute Irradiation

Embryos irradiated on day 1 had a significant reduction in survival-to-hatch with exposure to 3.88 Gy, and 100% mortality with exposure to 7.75 and 15.51 Gy [Fig. 2A: $F(6,14) = 40.81$, $P < 0.001$]. Mortality was elevated after irradiation on day 7, 15 and 30 with exposure to 7.75 Gy or greater [day 7: $F(6,7) = 91.00$, $P < 0.001$; day 15: $F(6,7) = 10.47$, $P = 0.0034$; and day 30: $F(6,7) = 790.78$, $P < 0.001$]. However, on day 60 there was no significant increase in mortality up to the highest tested dose [$F(5,6) = 0.91$, $P = 0.5312$]*. $LD_{50/hatch}$ values increased from 5.0 ± 0.8 Gy on day 1 up to 14.2 ± 0.1 Gy on day 30 (Fig. 2B). Increasing $LD_{50/hatch}$ values followed a logarithmic relationship up to 30 days after fertilization. Extrapolation to day 60 predicted an $LD_{50/hatch}$ of approximately 16 Gy; however, no increase in mortality occurred at that time point up to the highest tested dose of 15.51 Gy.

There was a dose-dependent latency period between irradiation and the timing of induced mortality. Soon after 7.75 and 15.51 Gy irradiation on day 1, mortality occurred, with a median time of 21 days. Mortality from 3.88 Gy, however, did not occur until day 129. On day 7, 15 and 30, the time to 50% mortality after 15.51 Gy irradiation was similar at all three time points (median of 87 days postirradiation) and occurred earlier than at 7.75 Gy (median of 114 days postirradiation).

Sublethal acute radiation exposure did not affect the timing or duration of hatching. Regardless of whether radiation exposure induced mortality, hatching among the surviving embryos began at the same time as controls and followed at a similar rate. However, at doses where there was a significant increase in mortality, the hatching window was shortened because there were fewer embryos surviving to hatch. A small, nonsignificant increase in developmental abnormalities was observed after 7.75 Gy on day 7, 15 and 30. The largest occurred after irradiation on day 30, but was still less than 10%. At all doses below 7.75 Gy, the rate of developmental abnormalities was less than 5%.

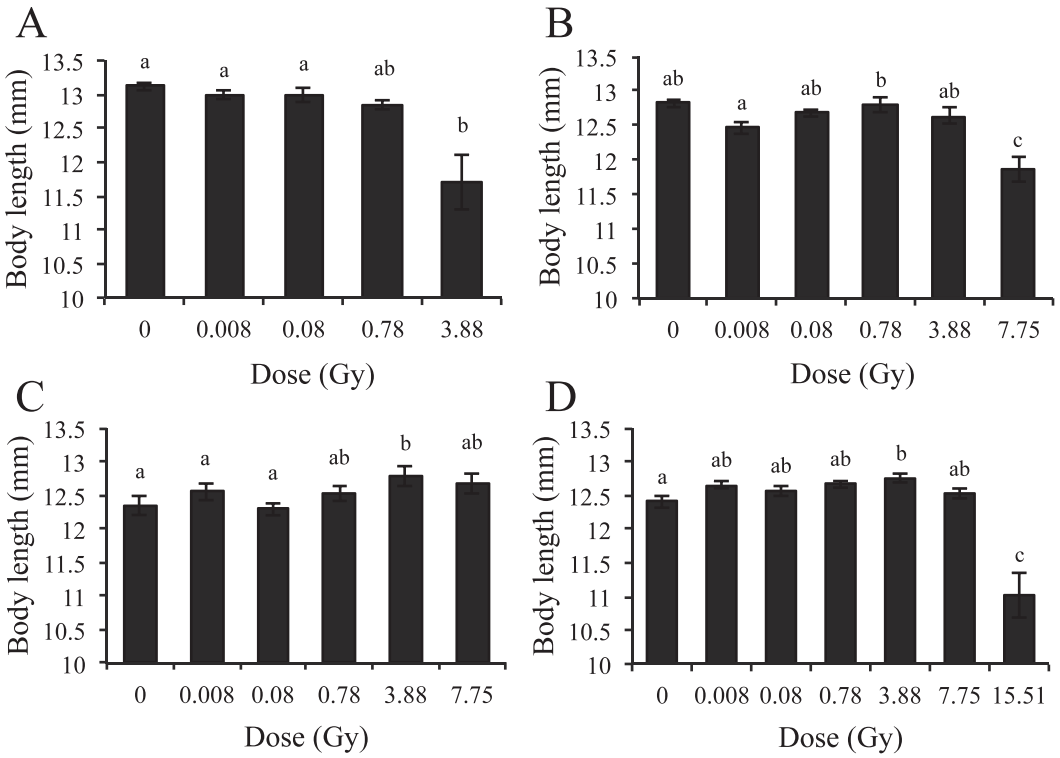

FIG. 3. Body length measurements at hatch after acute radiation exposure on day 1 (panel A), day 7 (panel B), day 15 (panel C) and day 30 (panel D) after fertilization. No embryos survived to hatch after 7.75 Gy on day 1 and 15.51 Gy on day 1, 7 and 15. Measurements were compared using a Kruskal-Wallis one-way ANOVA on ranks with Dunn's test. Letters indicate statistical differences. Bars represent means ± SE.

A reduction in size-at-hatch occurred, but only at doses where radiation-induced mortality was observed (Fig. 3). Body length at hatch was significantly smaller after 3.88 Gy on day 1 ($H = 17.71$, $df = 4$, $P = 0.0014$), 7.75 Gy on day 7 ($H = 34.17$, $df = 5$, $P < 0.001$) and 15.51 Gy on day 30 ($H = 39.69$, $df = 6$, $P < 0.001$). Interestingly, a significant increase in body length occurred after a dose of 3.88 Gy radiation on day 15 ($H = 22.33$, $df = 5$, $P < 0.001$) and day 30 (Fig. 3). No change in body length was observed when embryos were irradiated on day 60 ($H = 7.72$, $df = 5$, $P = 0.173$). The yolk area did not differ significantly from controls at any of the doses or time points tested (data not shown).

Chronic Irradiation

An unplanned transient temperature increase affected all chronically irradiated and control dishes on day 161 after fertilization, which was caused by a failure in the temperature sensor due to ice buildup on the compressor of the refrigeration unit. Temperature within the unit rose to 14°C which triggered hatch in all embryos that had not already hatched naturally. The temperature rise did not induce mortality.

No significant change in embryonic survival-to-hatch occurred at any of the six dose rates [Table 2; $F(6,23) = 0.97$, $P = 0.466$]. Chronic irradiation did result in a change in hatch dynamics. At the time of the compressor failure, more than 50% of the embryos in the irradiated dishes had already hatched and therefore, an accurate time to median hatch could still be calculated. At the same time, only a small percentage of embryos had hatched in the control dishes. A conservative comparison was made by using day 161 as the date of initial hatch or median hatch in dishes that had not reached that stage. Chronic irradiation resulted in an earlier first hatch [Table 2; $F(5,23) = 6.53$, $P = 0.0005$] and

TABLE 2
Percentage Mortality and Hatch Timing in Chronically Irradiated Embryos

Dose rate (mGy/day)	Percentage mortality	First hatch (dpf)	Median hatch (dpf)
0	14.3 ± 2.7	156 ± 3[a]	161[a]
0.06	11.2 ± 2.4	134 ± 3[b]	153 ± 1[b]
0.11	16.7 ± 1.5	137 ± 3[b]	153 ± 1[b]
0.19	16.2 ± 3.0	141 ± 3[b]	156 ± 1[b]
0.39	11.7 ± 1.4	141 ± 2[b]	155 ± 1[b]
1.05	15.4 ± 1.6	140 ± 1[b]	153 ± 1[b]
4.40	18.07	132[b]	151[b]

Notes. Cumulative percentage mortality was recorded at hatch. First hatch and median hatch were measured in days post fertilization (dpf). The first hatch and median hatch were advanced in control dishes due to refrigerator compressor failure. At the time of compressor failure, irradiated dishes had already reached the median hatch. Percentage mortality and hatch timing within each dish were compared using a one-way ANOVA with Tukey's HSD test.

[a,b] Letters indicate statistical differences. Values represent the means of individual replicate dishes ± SE.

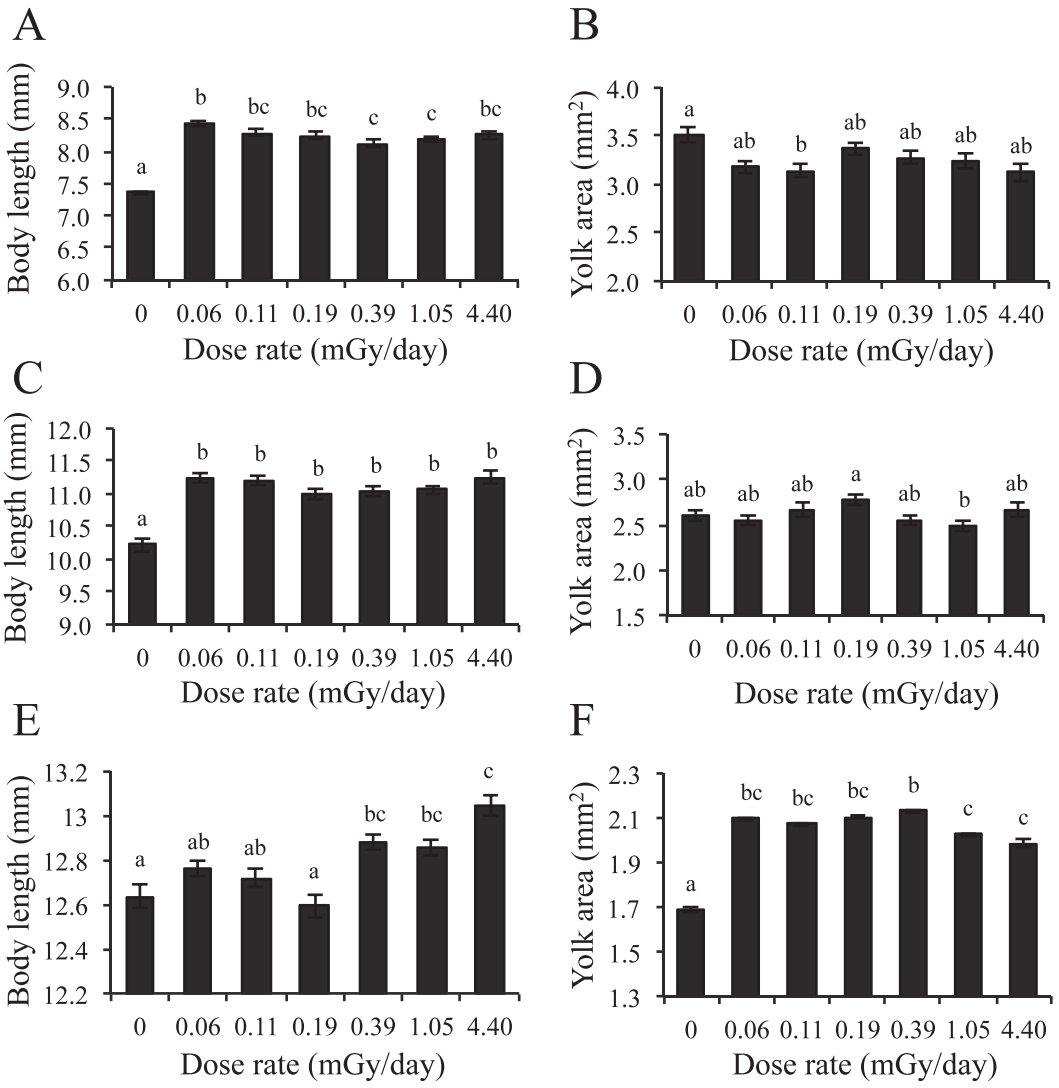

FIG. 4. Morphometric measurements after chronic radiation exposure. Body length and yolk area were measured on preserved embryos on day 76 (panels A and B), day 122 (panels C and D) and at hatch (panels E and F). Measurements were compared using a Kruskal-Wallis one-way ANOVA on ranks with Dunn's test. Letters indicate statistical differences. Bars represent means ± SE.

a shorter time to median hatch [$F(6,23) = 7.38$, $P = 0.0002$]. If the equipment failure had not occurred, then this difference would have been more pronounced.

The number of developmental abnormalities in embryos was low (less than 3%), and was consistent across all control and irradiated dishes. On day 76 and day 122, chronically irradiated embryos had a significantly greater body length (Fig. 4A and C. Day 76: $H = 65.93$, $df = 6$, $P < 0.001$; day 122: $H = 46.91$, $df = 6$, $P < 0.001$) and yolk-free body mass [Fig. 5A and C. Day 76: $F(6,140) = 18.39$, $P < 0.001$; day 122: $F(6,147) = 3.88$, $P = 0.0013$]. Yolk dry mass was correspondingly smaller in irradiated embryos [Fig. 5A and C. Day 76: $F(6,147) = 7.95$, $P < 0.001$; day 122: $F(6,146) = 4.90$, $P < 0.001$], although this was not reflected in yolk area measurements (Fig. 4B and D. Day 76: $H = 17.80$, $df = 6$, $P = 0.007$; day 122: $H = 15.13$, $df = 6$, $P = 0.019$). The increase in body mass was more pronounced on day 76, where mass was up to 60% greater relative to controls (Fig. 5A), compared to only 13% greater on day 122 (Fig. 5C). Similarly, embryo body length was up to 15% longer on day 76 compared to 10% longer on day 122 (Fig. 4A and C). Interestingly, the percentage increase in body mass (60%) was much greater than the increase in body length (15%). A significant increase in YCE was seen on day 76 [Fig. 5B: $F(6,135) = 7.85$, $P < 0.001$], but not on day 122 [Fig. 5D: $F(6,145) = 1.58$, $P = 0.157$]. No dose-response relationship was observed in embryo morphometric or dry mass measurements, although the highest dose rate of 4.40 mGy/day did have the most pronounced effect on several of the measurements (Figs. 4 and 5).

A different trend was observed at hatch. Irradiated embryos had a significantly smaller yolk-free body mass [Fig. 5E: $F(6,1074) = 21.71$, $P < 0.001$]. Embryo body length, however, was larger compared to unirradiated controls [Fig.

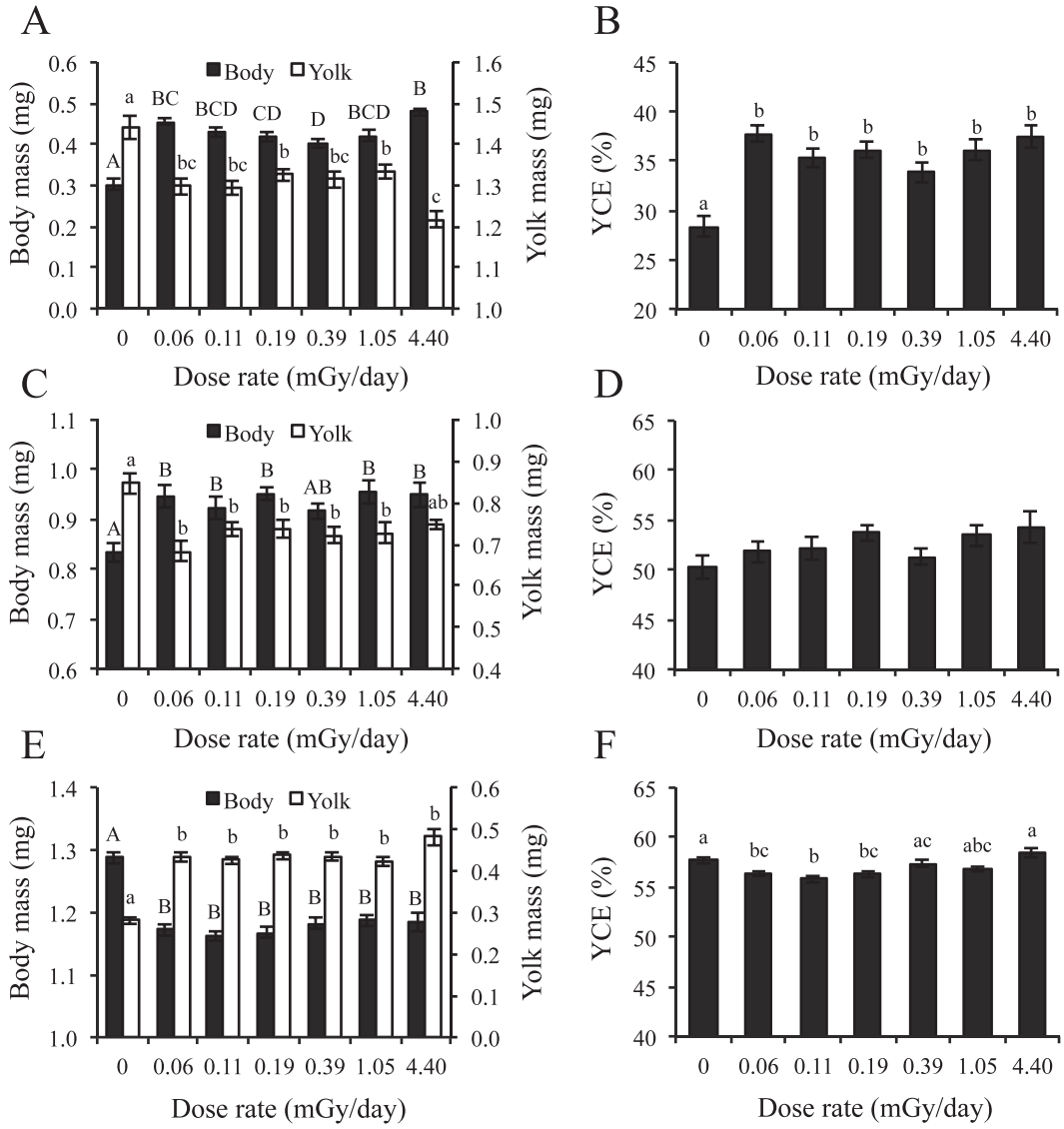

FIG. 5. Dry mass measurements after chronic radiation exposure. Yolk-free body mass, yolk mass and yolk conversion efficiency (YCE) were measured on preserved embryos on day 76 (panels A and B), day 122 (panels C and D) and at hatch (panels E and F). Dry mass and YCE were compared using a one-way ANOVA with Tukey's HSD test. Capital and lowercase letters indicate statistical differences from separately run tests. Bars represent means ± SE.

4E: H = 54.45, df = 6, $P < 0.001$]. Both yolk area and yolk mass were significantly greater after irradiation [Fig. 4F: H = 194.47, df = 6, $P < 0.001$; Fig. 5E: F(6,1074) = 27.99, $P < 0.001$]. No significant trend was observed in YCE at hatch [Fig. 5F: F(6,1038) = 6.45, $P < 0.001$].

Heat Shock and Radiation

Exposure to 7.75 Gy resulted in a significant increase in mortality compared to unirradiated embryos, regardless of heat-shock treatment [Fig. 6A and B. 6 h: F(1,8) = 148.10, $P < 0.001$; 24 h: F(1,8) = 201.25, $P < 0.001$]. Heat-shock treatment alone did not affect survival (6 h: F(3,8) = 1.85, $P = 0.22$; 24 h: F(3,8) = 0.26, $P = 0.85$). However, when combined with 7.75 Gy, 3 and 9°C heat shocks caused significant reductions in radiation-induced mortality when embryos were irradiated 6 h after heat shock [Fig. 6A: F(3,8) = 4.45, $P = 0.041$]. The largest reduction in mortality of approximately 25% occurred after a 3°C heat shock. However, a prior 6°C heat shock did not significantly reduce mortality. When irradiated 24 h after heat shock, none of the treatments significantly altered radiation-induced mortality [Fig. 6B: F(3,8) = 0.50, $P = 0.69$]. Heat shock did not affect the duration of development or the hatching dynamics (data not shown).

DISCUSSION

The effects of acute and chronic irradiation were examined during embryonic development in lake whitefish.

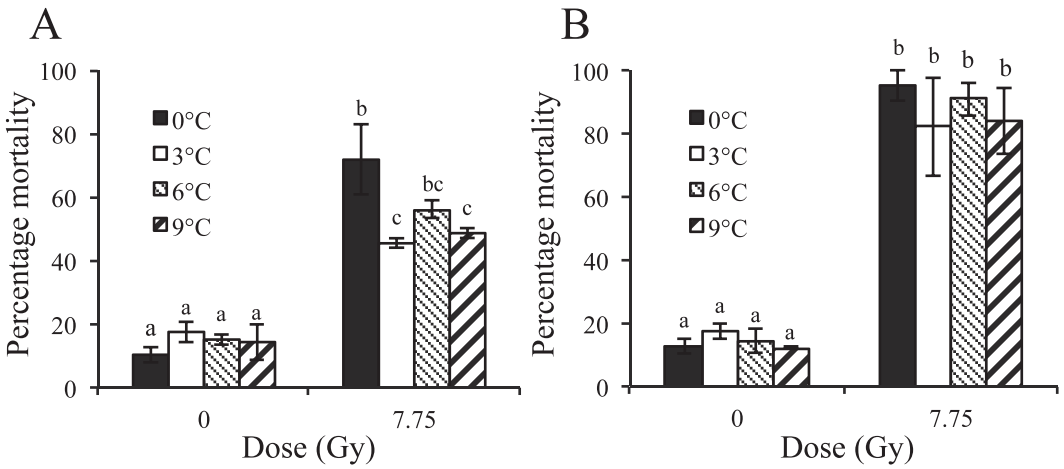

FIG. 6. Percentage mortality after combined heat shock and radiation exposure. Embryos were given a 2 h heat shock of 3, 6 or 9°C, then irradiated (panel A) 6 or (panel B) 24 h after heat shock. Percentage mortality in replicate dishes was compared using a two-way ANOVA with Tukey's HSD test. Letters indicate statistical differences. Bars represent means ± SE.

Growth stimulation was observed after low-dose chronic exposure. A slight growth enhancement also occurred after an acute sublethal dose of 3.88 Gy radiation delivered on day 15 or 30 post fertilization. Growth stimulation after low-dose exposure has not been previously observed in developing embryos, but has been shown in juvenile fish. Mothersill *et al*. (*25*) found increased growth performance in fathead minnows (*Pimephales promelas*) fed a radium diet of 10 and 100 mBq/g. Radiation-induced growth stimulation has also been demonstrated in other cell culture and whole organism models (*26–29*). Additional hormetic effects, apart from growth, have been observed in developing fish embryos. Zebrafish (*Danio rerio*) were reported to be more resistant to starvation post hatch when embryos were exposed throughout development to external gamma rays between 1 and 1,000 mGy/day (*30*). Chronic exposures of 4 mGy/day during embryogenesis in chinook salmon (*Oncorhynchus tshawytscha*) resulted in mature females producing more viable eggs (*31*). Multigenerational hormetic effects have been shown in mosquitofish (*Gambusia affinis*) where brood size was enhanced after exposure to radioisotope-contaminated water at a dose rate of 109 mGy/day (*32*).

Chronic Irradiation

The growth stimulation in chronically irradiated embryos was more pronounced earlier in development. On day 76, embryos were up to 60% larger in mass compared to only 13% on day 122. This suggests that radiation exposure has a greater effect earlier in development and diminishes near hatch. A similar effect was observed on hatch timing in zebrafish after low-dose X-ray irradiation. An acute dose given during the blastula period advanced hatch, however, radiation had no effect when delivered later in development during gastrulation or segmentation (*33*). The percentage change in body mass in lake whitefish was much greater than the percentage change in body length, suggesting that growth stimulation may be manifested more through an increase in lateral size compared to embryo length. The increase in body size coincided with a decrease in yolk mass, however, no change in yolk area was observed. This could be the result of differential consumption of yolk components between control and chronically irradiated embryos, leading to an altered ratio of lipids:protein:carbohydrates. Density differences between these energy sources could then result in a reduction in mass but no significant change in area. Mass and weight differences may also be the result of changes in water content. A full analysis of yolk constituents throughout development would be required to determine the cause of this discrepancy.

Multiple cellular and molecular events have been implicated in the hormetic response, including the upregulation of stress response proteins, DNA repair mechanisms, bystander effects and free radical scavenging (*34*). Specifically, growth stimulation after irradiation has been correlated with an activation of cell proliferation signaling pathways (*28, 35, 36*). Initiation of these mechanisms above constitutive baseline levels could be metabolically costly, and it has therefore been suggested that the hormetic response could come at a sacrifice to other physiological processes (*2–5*). Lake whitefish embryos represent a good model species for measuring both absolute growth and metabolic efficiency throughout development. In chronically irradiated embryos, the conversion efficiency of yolk potential energy into body mass was equal to or greater than unirradiated controls, indicating that the hormetic effects seen in lake whitefish may not come at a cost to metabolic efficiency.

Low-dose chronic-radiation exposure resulted in a shorter time-to-hatch. Unlike acute high doses, chronic irradiation did not affect survival, so changes in hatch timing are not an indirect effect of embryo mortality. The incubation

temperature between control and chronically irradiated embryos was almost identical (difference of 0.1°C); therefore, differences in hatch are not the result of temperature differences. An advanced hatch after irradiation has previously been observed in developing fish embryos of other species. Zebrafish embryos hatched earlier after both a single acute X-ray dose of 0.025 Gy delivered early in development (*33*) and after chronic exposure to gamma rays between 1 and 1,000 mGy/day throughout development (*30*). No dose response was observed after chronic irradiation in zebrafish, consistent with our findings for lake whitefish. Mammalian cell culture studies have also shown that the adaptive response in the low-dose region is not dose dependent (*37, 38*).

The advanced hatching is the likely reason that chronically irradiated embryos had a smaller body mass at hatch, despite demonstrating stimulated growth earlier in development. Earlier hatching embryos are generally smaller compared to those hatching later (*21, 39*). Although body mass was smaller at hatch compared to controls, irradiated embryos were slightly longer. Differences in hatch timing have a greater effect on body mass compared to length. Embryos grown at warmer temperatures will hatch earlier, and a rearing temperature of 8°C compared to 2°C results in lake whitefish embryos that are almost 50% smaller in body mass at hatch (*21*), but are less than 10% smaller in body length (*39*). The effect of early hatching after chronic irradiation was large enough to offset the growth stimulation in body mass seen earlier in development, but was not large enough to offset the trend in body length. Body length at hatch in irradiated embryos may have been smaller compared to controls if the compressor failure and premature hatch triggering had not occurred. At the time of the equipment failure most of the irradiated embryos had already hatched naturally, whereas the control embryos had not and were prematurely triggered to hatch. Had this temperature spike not occurred, the control embryos would have hatched later and would therefore have been larger in size. With respect to both the size at hatch and the timing of median hatch, the equipment failure likely only had an impact on the magnitude of the differences that were observed between control and irradiated embryos and did not impact the overall trend in the data.

Acute Irradiation

The mortality rate in control dishes was similar to what has previously been reported by others after laboratory rearing (*19, 39, 40*). An increase in mortality was observed after acute radiation exposure. Embryos were most sensitive immediately after fertilization and then became more resistant later in development. The specific time points for acute irradiation were chosen because they pertain to major developmental landmarks: newly fertilized/cleavage (day 1), gastrulation (day 7), closure of the blastopore (day 15), organogenesis (day 30) and post-organogenesis/fin flutter, where the majority of development had been completed and embryos were only undergoing growth [day 60 (*22*)]. Lake whitefish were more resistant compared to other related species. On day 1, lake whitefish had an $LD_{50/hatch}$ of approximately 5 Gy. Welander (*41*) found an LD_{50} for X rays in rainbow trout (*Oncorhynchus mykiss*) of 0.7 Gy when irradiated immediately after fertilization, increasing to 6 Gy at the germ ring stage (roughly equivalent to day 7 in lake whitefish). Additional LD_{50} values after irradiation at fertilization have been reported as 3 Gy in chinook salmon [*Oncorhynchus tshawytscha* (*42*)] and 0.9 Gy in plaice [*Pleuronectes platessa* (*43*)]. The increased radioresistance in lake whitefish might be attributable to their slow development rate. When incubated at cold temperature, the time from fertilization to hatch can be up to 200 days (*19*). This slower development would allow more time for repair of potentially lethal damage.

Mortality from acute irradiation was modified by a priming thermal stress. A 2 h heat shock reduced mortality when delivered 6 h prior to irradiation, but had no effect when delivered 24 h prior. A heat-induced adaptive response has previously been shown to protect against radiation-induced mortality in both cell culture and whole organism models (*9–11, 44, 45*). Heat-shock proteins (Hsp) are known to be involved in the response, in particular Hsp70 (*46, 47*). The increase in Hsp expression is transient and a return to baseline levels could explain why no change in survival was observed at 24 h. In lake whitefish, a similar 2 h heat shock of 3, 6 or 9°C has been shown to increase expression of *hsp70* mRNA as early as 2 h post heat shock (*48*). However, *hsp70* mRNA levels were elevated up to 48 h after heat shock, whereas the adaptive response in lake whitefish was absent by 24 h after heat shock. However, Stefanovic *et al*. (*48*) measured *hsp70* expression in lake whitefish on day 102 after fertilization, whereas embryos in this study were irradiated on day 7 after fertilization. The magnitude and timing of the stress response in fish is known to change throughout development (*49*), and the induction of *hsp70* may be shorter lived earlier in development. The differential response between the 6- and 24-h time points may also be due to other factors involved in the adaptive response, such as DNA repair pathways, reactive oxygen scavengers or immune modulation.

Acute exposure only affected hatch dynamics at doses where radiation increased mortality. After 7.75 and 15.51 Gy, the hatching rate was the same as controls but all surviving embryos were in the early portion of the natural hatching window. This early and shorter hatch window is partly the reason for body length differences. On average, surviving irradiated embryos hatched earlier and were therefore smaller at the point of hatching compared to the controls. Size differences are also likely due to the direct effects of high-dose radiation inducing cell death. A small increase in developmental abnormalities was observed in hatches after acute exposure, the highest percentage of which occurred in day 30-irradiated embryos. On day 30,

embryos are in organogenesis (*22*), which is known to be the most sensitive development stage for abnormalities (*16*). In aquatic species, developmental abnormalities have been observed after both acute and chronic irradiation (*32, 50*).

CONCLUSION

Overall, both chronic and acute ionizing radiation exposure produced measurable effects on lake whitefish embryo development rate, size and hatch dynamics. To our knowledge, this is the first published study to demonstrate, using a custom-designed irradiator, that chronic exposure can stimulate growth during embryogenesis in fish and that this hormetic response does not come at a measurable cost in metabolic efficiency. Chronic exposure also resulted in earlier hatching embryos compared to unirradiated controls. Embryos showed a high resistance to acute radiation exposure, particularly in the later stages of development. Mortality from acute exposures was modified by a priming thermal stress, which produced an adaptive response. However, this response was transient and was only observed shortly after heat shock.

ACKNOWLEDGMENTS

We thank John Eme, Casey Mueller, Mary Ellen Cybulski and Lisa Stoa for their assistance in collecting and raising lake whitefish embryos, as well as Kara Tsang for help with embryo analysis. Design and construction of the chronic irradiator was completed with assistance from Martin Wensveen and Clealand Berwick at the McMaster Engineering Machine Shop. Funding was provided through contracts from Bruce Power (CMS, RGM, JYW, DRB) and a Natural Sciences and Engineering Research Council of Canada Collaborative Research and Development Grant (CMS, RGM, JYW).

Received: July 14, 2016; accepted: April 27, 2017; published online: July 19, 2017

REFERENCES

1. Calabrese EJ, Baldwin LA. Tales of two similar hypotheses: the rise and fall of chemical and radiation hormesis. Hum Exp Toxicol 2000; 19:85–97.
2. Hercus M, Loeschcke V. Comments to paper by S. Rattan: applying hormesis in aging research and therapy–a perspective from evolutionary biology. Hum Exp Toxicol 2001; 20:305–8.
3. Saul N, Pietsch K, Sturzenbaum SR, Menzel R, Steinberg CE. Hormesis and longevity with tannins: free of charge or cost-intensive? Chemosphere 2013; 93:1005–8.
4. Costantini D, Monaghan P, Metcalfe NB. Prior hormetic priming is costly under environmental mismatch. Biol Lett 2014; 10:20131010.
5. Forbes VE. Is hormesis an evolutionary expectation? Funct Ecol 2000; 14:12–24.
6. Cassidy CL, Lemon JA, Boreham DR. Impacts of low-dose gamma-radiation on genotoxic risk in aquatic ecosystems. Dose Response 2007; 5:323–32.
7. Choi VW, Konishi T, Oikawa M, Iso H, Cheng SH, Yu KN. Adaptive response in zebrafish embryos induced using microbeam protons as priming dose and X-ray photons as challenging dose. J Radiat Res 2010; 51:657–64.
8. Schnarr K, Carter TF, Gillis D, Webber C, Lemon JA, Dayes I, et al. Biological response of positron emission tomography scan exposure and adaptive response in humans. Dose Response 2015; 13:1–9.
9. Shen RN, Hornback NB, Shidnia H, Wu B, Lu L, Broxmeyer HE. Whole body hyperthermia: a potent radioprotector in vivo. Int J Radiat Oncol Biol Phys 1991; 20:525–30.
10. Boreham DR, Mitchel RE. Regulation of heat and radiation stress responses in yeast by hsp-104. Radiat Res 1994; 137:190–5.
11. Boreham DR, Dolling JA, Maves SR, Miller S, Morrison DP, Mitchel RE. Heat-induced thermal tolerance and radiation resistance to apoptosis in human lymphocytes. Biochem Cell Biol 1997; 75:393–7.
12. Laval F. Pretreatment with oxygen species increases the resistance of mammalian cells to hydrogen peroxide and gamma-rays. Mutat Res 1988; 201:73–9.
13. Cortes F, Dominguez I, Flores MJ, Pinero J, Mateos JC. Differences in the adaptive response to radiation damage in G0 human lymphocytes conditioned with hydrogen peroxide or low-dose X-rays. Mutat Res 1994; 311:157–63.
14. Flores MJ, Pinero J, Ortiz T, Pastor N, Mateos JC, Cortes F. Both bovine and rabbit lymphocytes conditioned with hydrogen peroxide show an adaptive response to radiation damage. Mutat Res 1996; 372:9–15.
15. Tang FR, Loke WK. Molecular mechanisms of low dose ionizing radiation-induced hormesis, adaptive responses, radioresistance, bystander effects, and genomic instability. Int J Radiat Biol 2015; 91:13–27.
16. De Santis M, Cesari E, Nobili E, Straface G, Cavaliere AF, Caruso A. Radiation effects on development. Birth Defects Res C Embryo Today 2007; 81:177–82.
17. Michel C. Radiation embryology. Experientia 1989; 45:69–77.
18. Egami N, Ijiru KI. Effects of irradiation on germ cells and embryonic development in teleosts. Int Rev Cytol 1979; 59:195–248.
19. Griffiths JS. Potential effects of unstable thermal discharges on incubation of lake whitefish eggs. Biological Research Section CRD Report No. 79-521-K. Toronto: Ontario Hydro; 1979.
20. Eme J, Mueller CA, Manzon RG, Somers CM, Boreham DR, Wilson JY. Critical windows in embryonic development: Shifting incubation temperatures alter heart rate and oxygen consumption of lake whitefish (Coregonus clupeaformis) embryos and hatchlings. Comp Biochem Physiol A Mol Integr Physiol 2015; 179:71–80.
21. Mueller CA, Eme J, Manzon RG, Somers CM, Boreham DR, Wilson JY. Embryonic critical windows: changes in incubation temperature alter survival, hatchling phenotype, and cost of development in lake whitefish (Coregonus clupeaformis). J Comp Physiol B 2015; 185:315–31.
22. Sreetharan S, Thome C, Mitz C, Eme J, Mueller CA, Hulley EN, et al. Embryonic development of lake whitefish Coregonus clupeaformis: a staging series, analysis of growth and effects of fixation. J Fish Biol 2015; 87:539–58.
23. Mitz C, Thome C, Cybulski ME, Laframboise L, Somers CM, Manzon RG, et al. A Self-contained, controlled hatchery system for rearing lake whitefish embryos for experimental aquaculture. N Am J Aquacult 2014; 76:179–84.
24. Schneider-Orelli O. Entomologisches Praktikum-Einführung in die land- und forstwirtschaftliche Insektenkunde. Germany: Aarau: H.R. Sauerländer & Co.; 1947.
25. Mothersill C, Smith R, Lariviere D, Seymour C. Chronic exposure by ingestion of environmentally relevant doses of (226)Ra leads to transient growth perturbations in fathead minnow (Pimephales promelas, Rafinesque, 1820). Int J Radiat Biol 2013; 89:950–64.
26. Miller MW, Miller WM. Radiation hormesis in plants. Health Phys 1987; 52:607–16.
27. Li W, Wang G, Cui J, Xue L, Cai L. Low-dose radiation (LDR) induces hematopoietic hormesis: LDR-induced mobilization of

hematopoietic progenitor cells into peripheral blood circulation. Exp Hematol 2004; 32:1088–96.

28. Liang X, So YH, Cui J, Ma K, Xu X, Zhao Y, et al. The low-dose ionizing radiation stimulates cell proliferation via activation of the MAPK/ERK pathway in rat cultured mesenchymal stem cells. J Radiat Res 2011; 52:380–6.
29. Stark K, Scott DE, Tsyusko O, Coughlin DP, Hinton TG. Multi-level effects of low dose rate ionizing radiation on southern toad, Anaxyrus [Bufo] terrestris. PLoS One 2015; 10:e0125327.
30. Simon O, Massarin S, Coppin F, Hinton TG, Gilbin R. Investigating the embryo/larval toxic and genotoxic effects of gamma irradiation on zebrafish eggs. J Environ Radioact 2011; 102:1039–44.
31. Donaldson LR, Bonham K. Effects of chronic exposure of chinook salmon eggs and alevins to gamma irradiation. Trans Am Fish Soc 1970; 99:112–19.
32. Blaylock BG. The Fecundity of a Gambusia affinis affinis population exposed to chronic environmental radiation. Radiat Res 1969; 37:108–17.
33. Miyachi Y, Kanao T, Okamoto T. Marked depression of time interval between fertilization period and hatching period following exposure to low-dose X-rays in zebrafish. Environ Res 2003; 93:216–9.
34. Jolly D, Meyer J. A brief review of radiation hormesis. Australas Phys Eng Sci Med 2009; 32:180–7.
35. Suzuki K, Kodama S, Watanabe M. Extremely low-dose ionizing radiation causes activation of mitogen-activated protein kinase pathway and enhances proliferation of normal human diploid cells. Cancer Res 2001; 61:5396–401.
36. Kim CS, Kim JK, Nam SY, Yang KH, Jeong M, Kim HS, et al. Low-dose radiation stimulates the proliferation of normal human lung fibroblasts via a transient activation of Raf and Akt. Mol Cells 2007; 24:424–30.
37. Azzam EI, de Toledo SM, Raaphorst GP, Mitchel RE. Low-dose ionizing radiation decreases the frequency of neoplastic transformation to a level below the spontaneous rate in C3H 10T1/2 cells. Radiat Res 1996; 146:369–73.
38. Redpath JL, Liang D, Taylor TH, Christie C, Elmore E. The shape of the dose-response curve for radiation-induced neoplastic transformation in vitro: evidence for an adaptive response against neoplastic transformation at low doses of low-LET radiation. Radiat Res 2001; 156:700–7.
39. Brooke LT. Effect of Different Constant Incubation Temperatures on Egg Survival and Embryonic Development in Lake Whitefish (Coregonus clupeaformis). Trans Am Fish Soc 1975; 104:555–9.
40. Price JW. Time-temperature relations in the incubation of the whitefish, Coregonus clupeaformis (Mitchill). J Gen Physiol 1940; 23:449–68.
41. Welander AD. Some effects of x-irradiation of different embryonic stages of the trout (Salmo gairdnerii). Growth 1954; 18:227–55.
42. Wadley GW, Welander AD. X-rays and temperature: combined effects on mortality and growth of salmon embryos. Trans Am Fish Soc 1971; 100:267–75.
43. Ward E, Beach SA, Dyson ED. The effect of acute X-irradiation on the development of the plaice Pleuronectes platessa L. J Fish Biol 1971; 3:251–9.
44. Mitchel RE, Morrison DP. Heat-shock induction of ionizing radiation resistance in Saccharomyces cerevisiae, and correlation with stationary growth phase. Radiat Res 1982; 90:284–91.
45. Shimada Y. Heat-shock induction of radiation resistance in primordial germ cells of the fish Oryzias latipes. Int J Radiat Biol 1985; 48:189–96.
46. Park SH, Lee SJ, Chung HY, Kim TH, Cho CK, Yoo SY, et al. Inducible heat-shock protein 70 is involved in the radioadaptive response. Radiat Res 2000; 153:318–26.
47. Lee YJ, Park GH, Cho HN, Cho CK, Park YM, Lee SJ, et al. Induction of adaptive response by low-dose radiation in RIF cells transfected with Hspb1 (Hsp25) or inducible Hspa (Hsp70). Radiat Res 2002; 157:371–7.
48. Stefanovic DI, Manzon LA, McDougall CS, Boreham DR, Somers CM, Wilson JY, et al. Thermal stress and the heat shock response in embryonic and young of the year juvenile lake whitefish. Comp Biochem Physiol A Mol Integr Physiol 2016; 193:1–10.
49. Takle H, Baeverfjord G, Lunde M, Kolstad K, Andersen Ø. The effect of heat and cold exposure on HSP70 expression and development of deformities during embryogenesis of Atlantic salmon (Salmo salar). Aquacult 2005; 249:515–24.
50. Hyodo-Taguchi Y, Eto H, Egami N. RBE of fast neutrons for inhibition of hatchability in fish embryos irradiated at different developmental stages. Radiat Res 1973; 53:385–91.

RADIATION RESEARCH **188**, 486–494 (2017)
0033-7587/17 $15.00

DOI: 10.1667/RR14665.1

Is There a Trade-Off between Radiation-Stimulated Growth and Metabolic Efficiency?

Charles Mitz,[a,1] Christopher Thome,[a,1] Mary Ellen Cybulski,[a] Christopher M. Somers,[b] Richard G. Manzon,[b] Joanna Y. Wilson[c] and Douglas R. Boreham[a,2]

[a] *Department of Medical Physics and Applied Radiation Sciences, McMaster University, Hamilton, Ontario, Canada, L8S 4L8;* [b] *Department of Biology, University of Regina, Regina, Saskatchewan, Canada, S4S 0A2;* [c] *Department of Biology, McMaster University, Hamilton, Ontario, Canada, L8S 4K1; and* [d] *Northern Ontario School of Medicine, Sudbury, Ontario, Canada, P3E 2C6*

Mitz, C., Thome, C., Cybulski, M. E., Somers, C. M., Manzon, R. G., Wilson, J. Y. and Boreham, D. R. Is There a Trade-Off between Radiation-Stimulated Growth and Metabolic Efficiency? ***Radiat Res*** **188, 486–494 (2017).**

Beneficial protective effects may result from an adaptive respose to low dose radiation exposure. However, such benefits must be accompanied by some form of cost because the responsible biological mechanisms are not normally maintained in an upregulated state. It has been suggested that stimulation of adaptive response mechanisms could be metabolically costly, or that the adaptive response could come at a sacrifice to other physiological processes. We exposed developing lake whitefish embryos to a fractionated regime of gamma radiation (662 keV; 0.3 Gy min^{-1}) to determine whether radiation-stimulated growth was accompanied by a trade-off in metabolic efficiency. Developing embryos were exposed at the eyed stage to different radiation doses delivered in four fractions, ranging from 15 mGy to 8 Gy per fraction, with a 14 day separation between dose fractions. Dry weight and standard length measurements were taken 2–5 weeks after delivery of the final radiation exposure and yolk conversion efficiency was estimated by comparing the unpreserved dry weight of the yolk to the unpreserved yolk-free dry weight of the embryos and normalizing for size-related differences in somatic maintenance. Our results show that the irradiated embryos were 8–10% heavier than the controls but yolk conversion efficiency was slightly improved. This finding demonstrates that stimulated growth in developing lake whitefish embryos is not "paid for" by a trade-off in the efficiency of yolk conversion.

INTRODUCTION

Exposure to low levels of ionizing radiation is known to trigger an adaptive response that includes immune stimulation and the up-regulation of long-lasting protective effects that limit damage to DNA and stimulate its repair (*1, 2*), or confer protection against subsequent high-dose exposures (*3–5*). The response may also include stimulated growth (*6*), which has been widely reported in plants (*7*) and was first recognized more than a century ago (*8*). Radiation-enhanced growth has been less widely reported in animals although Mothersill *et al.* (*9*) reported a higher condition factor in fathead minnows (*Pimephales promelas*) fed a diet containing 100 mBq g^{-1} of ^{226}Ra. An enhanced condition factor has been reported following chronic external exposures to gamma radiation in juvenile clams (*Mercenaria mercenaria*) and scallops (*Argopecten irradians*) exposed to 0.007 to 0.008 mGy h^{-1} (*10*), and in juvenile blue crabs (*Callinectes sapidus*) exposed to 32 mGy h^{-1} (*11*). Enhanced growth has also been reported in Southern toad (*Anaxyrus terrestris*) larvae after exposure to low (0.13, 2.4, 21 and 222 mGy d^{-1}) doses of gamma radiation (*12*).

The mechanisms underlying radiation-induced growth stimulation remain poorly understood. Calabrese (*13*) has speculated that radiation may induce an overcompensation effect which may be analogous to compensatory growth observed after fasting-refeeding experiments (*14*). Alternate mechanisms include inactivation of inhibitory pathways (*15*) or even radiation as a direct input of energy (*16*). Calabrese and Baldwin (*17*) argue that hormetic effects, such as growth stimulation, may represent the rule rather than the exception in nature as they have been observed in plants, bacteria and vertebrates in response to more than 1,000 different chemical or environmental stressors (*18*).

The adaptive response poses an interesting problem from an evolutionary perspective. It is clear that the biological response to a mild stress increases fitness in the presence of an increased, repeated or sustained stress of similar character (*3–5*). An ecologically relevant example is the radiation-induced adaptive response, which is protective against other forms of stress such as heat shock and vice versa (*19, 20*). While near-lethal radiation levels would rarely be encountered in nature, the potential for heat stress

[1] Scholar-in-Training, Radiation Research Society.

[2] Address for correspondence: Northern Ontario School of Medicine, Sudbury, Ontario, Canada, P3E 2C6; email: dboreham@nosm.ca.

is ubiquitous and prior protection would be beneficial in most environments. The fact that the responsible mechanisms are not maintained in an upregulated state but rather require some form of sensitizing or priming exposure indicates that they cannot be free of cost. It has been suggested that stimulation of the adaptive response mechanisms could be metabolically costly (*21, 22*), or that the response could come at a sacrifice to other physiological processes (*23, 24*). Little work has been done to identify and quantify such costs and no direct measurement of the effects of the adaptive response on metabolic efficiency has previously been attempted.

This article presents a measurement of the metabolic efficiency of radiation-stimulated growth using normalized dry weight yolk conversion efficiency (YCE) measurements on developing lake whitefish (*Coregonus clupeaformis*) embryos irradiated with high-dose-rate gamma radiation. Radiation is a useful experimental stressor for such measurements because it avoids potential confounding effects found in certain chemical stressors that are simultaneously toxic (at high concentrations) and micronutrients. Embryonic development in fish also offers a suitable life-stage for examining metabolic effects of ionizing radiation because growth takes place under comparatively simple bioenergetic conditions where nutrition is supplied endogenously, active metabolism is minimal, and factors such as water quality, and oxygen availability may be controlled with reasonable accuracy in a laboratory setting. The lake whitefish offers further advantages as a test organism due to its low intraclutch variability in egg size (*25*), and lengthy development (*26–29*), which allows for the accurate targeting of specific developmental stages as well as enabling manual dechorionation and measurements to be completed at a consistent point in development.

METHODS

We exposed developing lake whitefish embryos to a fractionated regime of gamma radiation to determine whether radiation-stimulated growth in developing lake whitefish embryos was accompanied by a trade-off in metabolic efficiency. Because the differences in metabolic cost were expected to be small, we designed our experiment to maximize sensitivity to small changes in dry weight. Specific measures included the use of highly uniform eggs from a single female, and the timing of the irradiations during the eyed stage when natural mortality is particularly low. Dechorionated embryos were imaged live, and unpreserved dry weights were used exclusively to avoid confounding effects resulting from chemical preservation.

Egg Collection and Incubation

On November 26, 2014, Ontario Ministry of Natural Resources and Forestry (MNRF) provided us with whitefish eggs (mean dry weight 2.735 ± 0.081 mg) from a single female from Lake Simcoe fertilized earlier that day by pooled milt from different males. The fertilized embryos were transported in an ice bath to McMaster University where they were reared in refrigerated coolers using apparatus and methods described by Mitz *et al*. (*30*). Following initial development for 40 days in McDonald Bell hatching jars at 5°C, the embryos were transferred to petri dishes and held at a nominal 2°C (2.07 ± 0.004) for the experiments. Data loggers (Schlumberger Mini-Diver and Onset Hobo) were placed within the cooler units and set to record water temperature every 5 min. Photoperiod was ambient with natural lighting through the laboratory windows and was consistent across exposure groups.

The embryos were reared in 150-mm diameter petri dishes loaded with approximately 100 embryos per dish. Two duplicates were used for each of the treatment groups while three duplicates were used for the control. Additional control samples were used to determine the rate of yolk conversion to somatic tissue throughout development. The dishes were filled with dechlorinated municipal tap water, which was changed twice weekly. The position of the petri dishes was shuffled regularly throughout incubation to minimize any effect on growth from slight variations in temperature in different areas of the cooler shelves. Viable hatches were recorded and dead embryos removed daily. Embryo mortalities were recognized by the development of opacity on a significant portion of the egg or by the disintegration of the chorion and embryo.

Irradiations

Developing lake whitefish embryos were exposed to fractionated doses of 662 keV ^{137}Cs gamma radiation (0.3 Gy min^{-1}) ranging from 15 mGy to 8 Gy nominal dose per fraction. A total of four fractions were delivered per treatment beginning 41-days post-fertilization (dpf) in Development Stage 10 (*31*), at which time the eyes of embryos were fully pigmented and the major organs formed. For each exposure, the embryos (control and exposure groups) were transported to and from the irradiation facility in petri dishes placed on a bed of crushed ice in insulated coolers. Irradiations were carried out in petri dishes placed on an ice slurry. No absolute controls were possible as transportation of embryos on an ice slurry was part of the rearing protocol (*30*) and was used for all the embryos. Dose fractions were delivered at 14 day intervals followed by constant temperature incubation at 2°C for a further 14 days (97 dfp) before measuring and weighing a small subsample of embryos. A larger subsample was measured (dry weight and embryo dimensions) at 128 dpf at which time the embryos had reached hatching competence but before hatching had begun. Nominal doses were calculated based on previously generated calibration curves and verified using thermoluminescent dosimeters (Mirion Technologies, Irvine, CA). The dosimetry results showed a mean value ($n = 9$) of 0.944 ± 0.036 of the expected nominal dose.

Measurements

Small subsamples of 10 (treatment groups) and 20 embryos (control) were dechorionated and weighed individually at 97 dpf to determine the rate at which the embryos were growing and to determine the time required to complete the measurements on the unpreserved embryos. Larger (25–30 embryos per treatment group) samples were taken at 128 dpf and these provide most of the data presented in this article.

Dechorionated embryos were anesthetized using an approximately 0.5% solution of MS-222 (ethyl 3-aminobenzoate methanesulfonate, Sigma Aldrich) prior to being imaged live using an Axio Zoom V16 microscope (Carl Zeiss) equipped with a Canon EOS Rebel T1i camera. Measurements of standard length (SL) were made to the nearest 1 μm using Zeiss AxioVison digital image processing software.

Half the embryos from each treatment group were deyolked by tearing the yolk sac and manually removing the yolk contents using a fine needle followed by rinsing in fresh water to remove any yolk residue. The embryos were placed intact or deyolked on aluminum foil tares and dried to a constant weight overnight at a temperature of 70‡°C in a VWR Brand Model 1500EM drying oven. Anhydrous silica gel was placed in the drying oven along with the embryos and

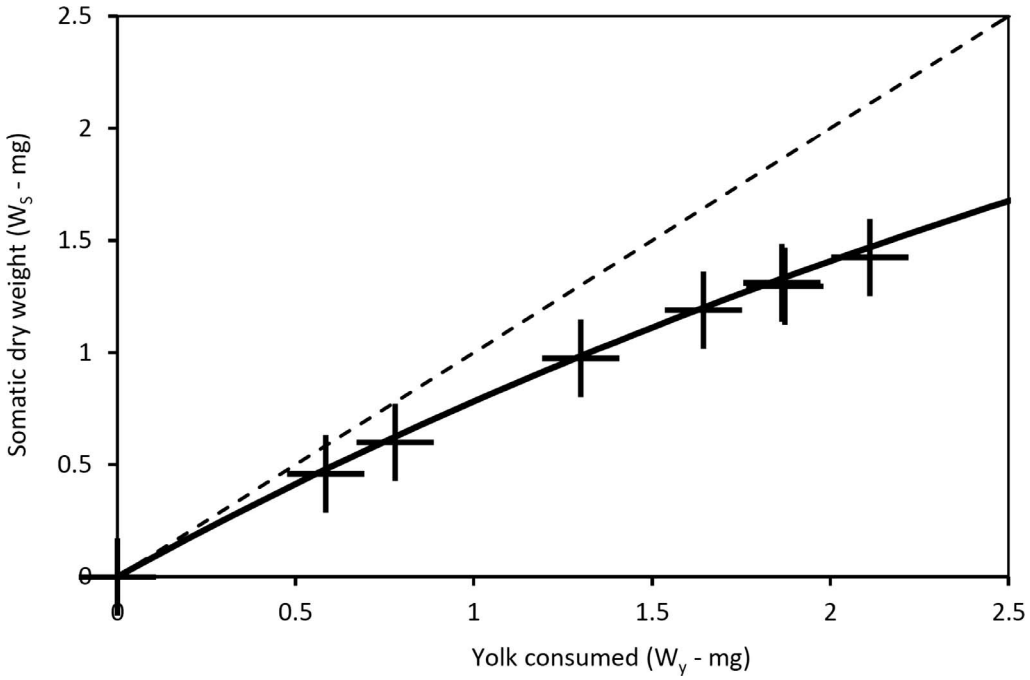

FIG. 1. Conversion of yolk dry weight to somatic dry weight for embryos reared at a constant 5°C. The dashed line represents 100% conversion efficiency. The solid line is fitted to measured data and deviates from 100% efficiency according to actual yolk conversion efficiency and the progressively greater proportion of energy devoted to somatic maintenance during later stages of embryonic development. The solid line represents a hyperbolic regression for the relationship $W_s = \varepsilon W_y((1 + aW_y)^{-1})$. The first derivative of this function provides an estimate of instantaneous yolk conversion efficiency. Data points (+) represent pooled data for yolked and deyolked embryos at different points in development.

placed beside the aluminum tares during weighing (Mettler-Toledo XA105DU, ±0.01 mg) to maintain low humidity. The order of weighing was random to reduce the potential for confounding effects resulting from humidity fluctuations during the weighing process. All measurements were taken using unpreserved embryos to avoid possible confounding effects resulting from chemical preservation (*32, 33*).

The relationship between embryo dry weight and somatic (i.e., yolk-free) dry weight was calculated using individual and pooled embryo weights. Individual measurements were taken for 25 yolked and 25 deyolked embryos per treatment group except for the 8 Gy dose fractions for which high mortality limited the number of embryos to 8 yolked and 10 deyolked. The dry weight of the yolk was estimated by subtracting the pooled yolk-free dry weight from the pooled total embryo weight. The initial dry weight was determined by subtracting the mean chorion dry weight (0.316 ± 0.00424 mg, n = 40) from the total egg dry weight (2.735 ± 0.081 mg, n = 90). The relationship between somatic dry weight, SL and yolk consumption was developed using a time series of pooled yolked and deyolked dry weights to establish the rate of change in dry weight and SL experienced in the absence of irradiation.

Normalized YCE

The efficiency of yolk conversion[3] was calculated by determining a nominal value defined by the yolk-free dry weight of the embryos divided by the amount of yolk consumed. This value was then normalized to correct for size differences between exposure groups vs. the control. Normalization was necessary to account for maintenance metabolism which scales with body weight, W_S, according to W_S^b where b is generally taken to be in the range of 0.75 (*34, 35*). The fraction of yolk energy allocated to maintenance per unit time therefore increases with increasing values of W_S but at progressively decreasing rate for all values of b less than unity. In addition to normalizing YCE to take into account the greater somatic maintenance requirements associated with a larger body size, it is necessary to account for the fact that larger embryos have spent less time at each weight than the control.

From the time series of embryo and yolk weights, we determined that the relationship between W_S somatic (yolk-free) dry weight and W_y (total yolk consumed) at time t, can be approximated using an empirically-derived hyperbolic relationship in the form $W_s = \varepsilon W_y((1 + aW_y)^{-1})$ (Fig. 1) where a is experimentally determined and ε represents the limiting efficiency of yolk conversion as the maintenance allocation approaches zero. Size-related differences in metabolic maintenance allocation may be addressed by determining the difference in somatic dry weight (ΔW_S) between a given experimental group and the control, and calculating the additional yolk mass ΔW_y required to produce ΔW_S in the absence of any maintenance allocation (since all measurements were made at the same point in time):

$$\Delta W_y = \frac{\Delta W_y}{\varepsilon} \tag{1}$$

Now we can normalize for each treatment group by transforming the control YCE according to:

$$\underset{YCE}{n} = \frac{W_S + \Delta W_S}{W_y + \left(\frac{\Delta W_S}{\varepsilon}\right)} \tag{2}$$

This transformation corrects for differences in somatic maintenance between groups and reduces the apparent differences obtained using nominal YCE.

[3] We have ignored any differences in the specific energy content of the yolk and somatic tissue so ''efficiency'' is simply a dry weight approximation.

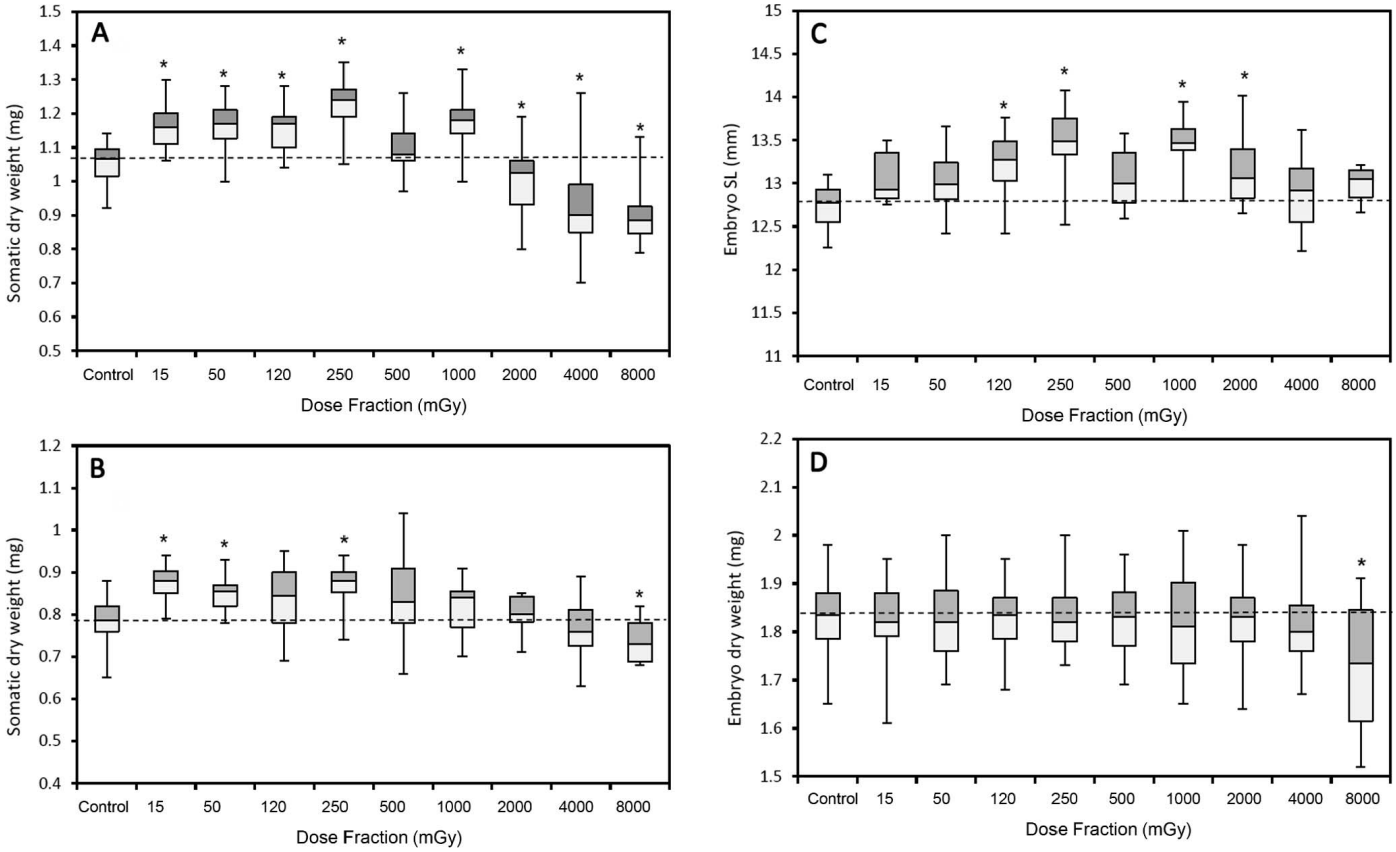

FIG. 2. Panels A and B: Relationship between somatic dry weight and radiation dose for whitefish embryos sampled at 128 dpf (panel A) and at 97 dpf (panel B) The absence of statistical significance at 97 dpf reflects the smaller number of embryos (n = 9–20 per dose fraction compared to 25–36 for 128 dpf, except for the 8 Gy dose fractions where high mortality resulted in only 8 embryos). Panels C and D: Relationship between embryo standard length (SL) and total embryo dry weight (i.e., including yolk) and radiation dose for whitefish embryos. Panel C: SL vs. radiation dose for whitefish embryos sampled at 128 dpf. Panel D: Total embryo weight and radiation dose for embryos sampled at 128 dpf. *Statistically significant relative to the control.

Statistical Analysis

Statistical analysis was conducted using Sigmaplot V11.0. Morphometric measurements and dry weights were compared using a one-way ANOVA followed by Tukey's HSD test. Differences in condition factor (dry weight normalized to SL) were compared to the control using separate ANOVAs on SL and on condition factor. Differences were considered statistically significant at $P \leq 0.05$.

RESULTS

The 4 × 4 Gy and 4 × 8 Gy embryos experienced high (>50%) mortality during the experiment. Mortality was uniformly low (<5%) for the control and all other dose fractions. Embryos were not reared to the normal hatching stage but a number of the 4 × 4 and 4 × 8 Gy embryos spontaneously hatched prior to the termination of the experiment.

There was a significant effect of radiation dose on the dry weight of the embryos ($F_{9,300} = 43.1$, $P < 0.001$). Embryos receiving less than 2 Gy per dose fraction (i.e., less than 8 Gy total dose) were heavier than the control by an average of 10.3 ± 2.7% (Fig. 2A). The difference in dry weight was significant for all trials except the 4 × 500 mGy group ($P = 0.093$). Between 4 × 15 mGy and 4 × 1 Gy there was no significant difference in size, but a nonsignificant peak in the 4 × 250 mGy fractions was noted in both the early (97 dpf) and late (128 dpf) measurements (Fig. 2A and B). From 4 × 2 Gy to 4 × 8 Gy the embryos became lighter with increasing dose and both groups were significantly different from the control. Growth stimulation was similar for both the 97 and 128 dpf measurements (8.5 ± 4.0% and 10.3 ± 2.7%).

Standard length varied significantly with radiation exposure ($F_{9,191} = 11.1$, $P < 0.001$) although the differences between treatment groups were small and fewer trials were statistically different from the control (Fig. 2C). The relationship between radiation dose and total embryo weight (Fig. 2D) showed only subtle and nonsignificant differences except for the 4 × 8 Gy group.

Differences in condition factor (dry weight normalized to SL) were observed between the different exposure groups (Fig. 3). The 4 × 15 mGy group was significantly heavier for a given length than the control while the difference for the 4 × 50 mGy group was near-significant. The relationship between dry weight and SL was not significantly different from the control for the intermediate

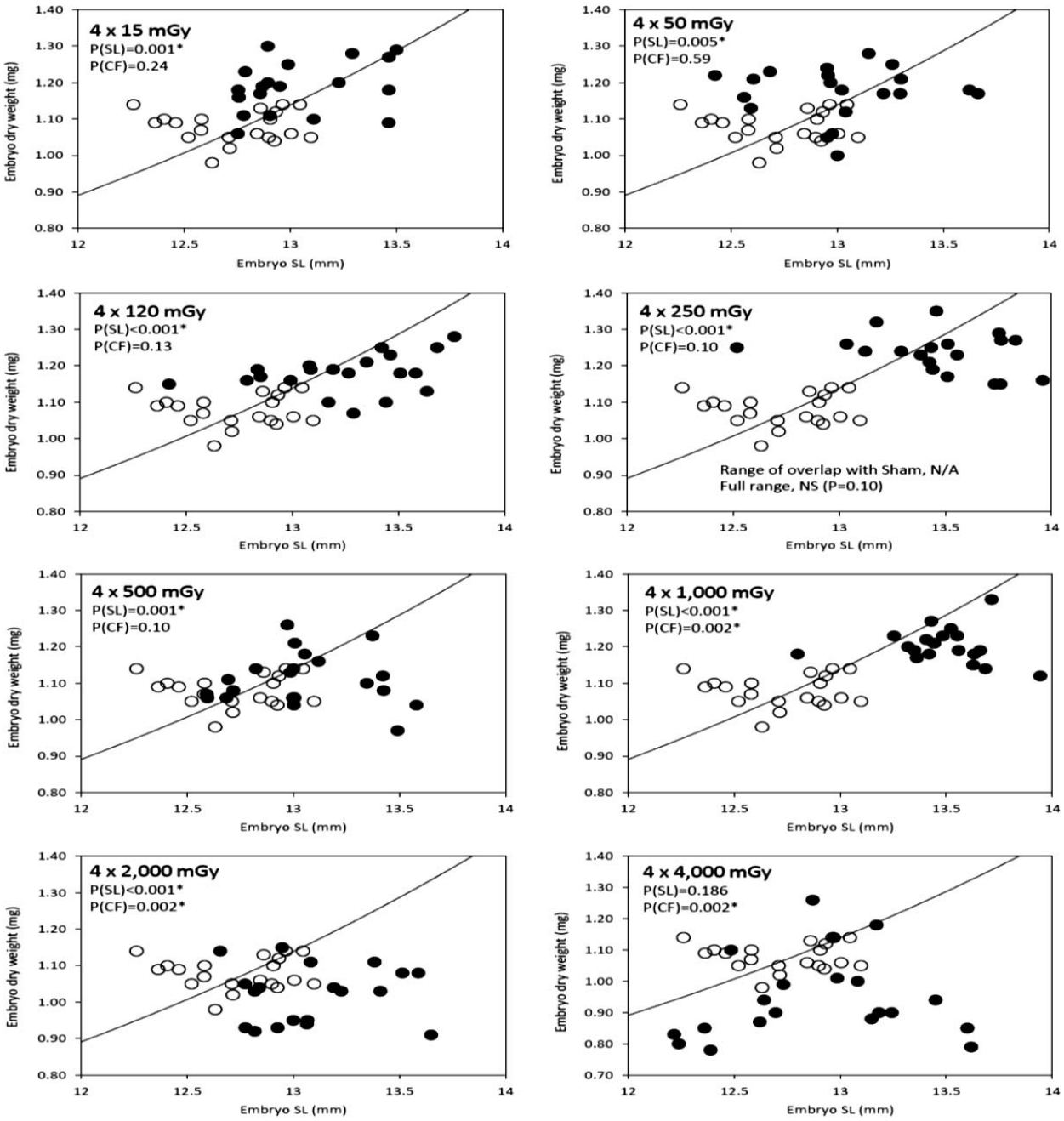

FIG. 3. Relationship between somatic dry weight and SL for different irradiation groups (●) vs the control group (○). The solid line is a regression relationship relating standard length (SL) to somatic dry weight (DW = 0.047exp0.245SL) for 2°C incubation (i.e., this curve represents the DW-SL trajectory that the control is expected to follow over time). The first *P* value refers to difference in SL, relative to the control, the second to difference in condition factor (i.e., the relationship between SL and DW) relative to the control.

exposures (120, 250 and 500 mGy) but the 4 × 1 to 4 × 8 Gy groups were significantly lighter for a given SL. In the intermediate dose range (120 mGy to 1 Gy) the greater somatic weight appears to result solely from increased length. Thus, the results show two aspects of stimulation where the greater length occurs even at dose ranges where the condition factor is negatively affected. This association is particularly strong for the highest dose (4 × 4 Gy) for which we have reliable morphological measurements (the 4 × 8 Gy group suffered high mortality and contained a high proportion of deformed embryos). For this group, SL was statistically indistinguishable from the control but the condition factor was significantly and substantially lower.

The nominal yolk conversion efficiency for the control was calculated to be 62.3 ± 0.52% compared to values ranging between 62.5 and 65.7% for dose fractions between 15 mGy and 1 Gy. With higher (i.e., >1 Gy) dose fractions, nominal YCE declined to a low of approximately 55% for the 4 × 8 Gy trial. Normalized YCE was more tightly constrained (Fig. 4) with all values for dose fractions less

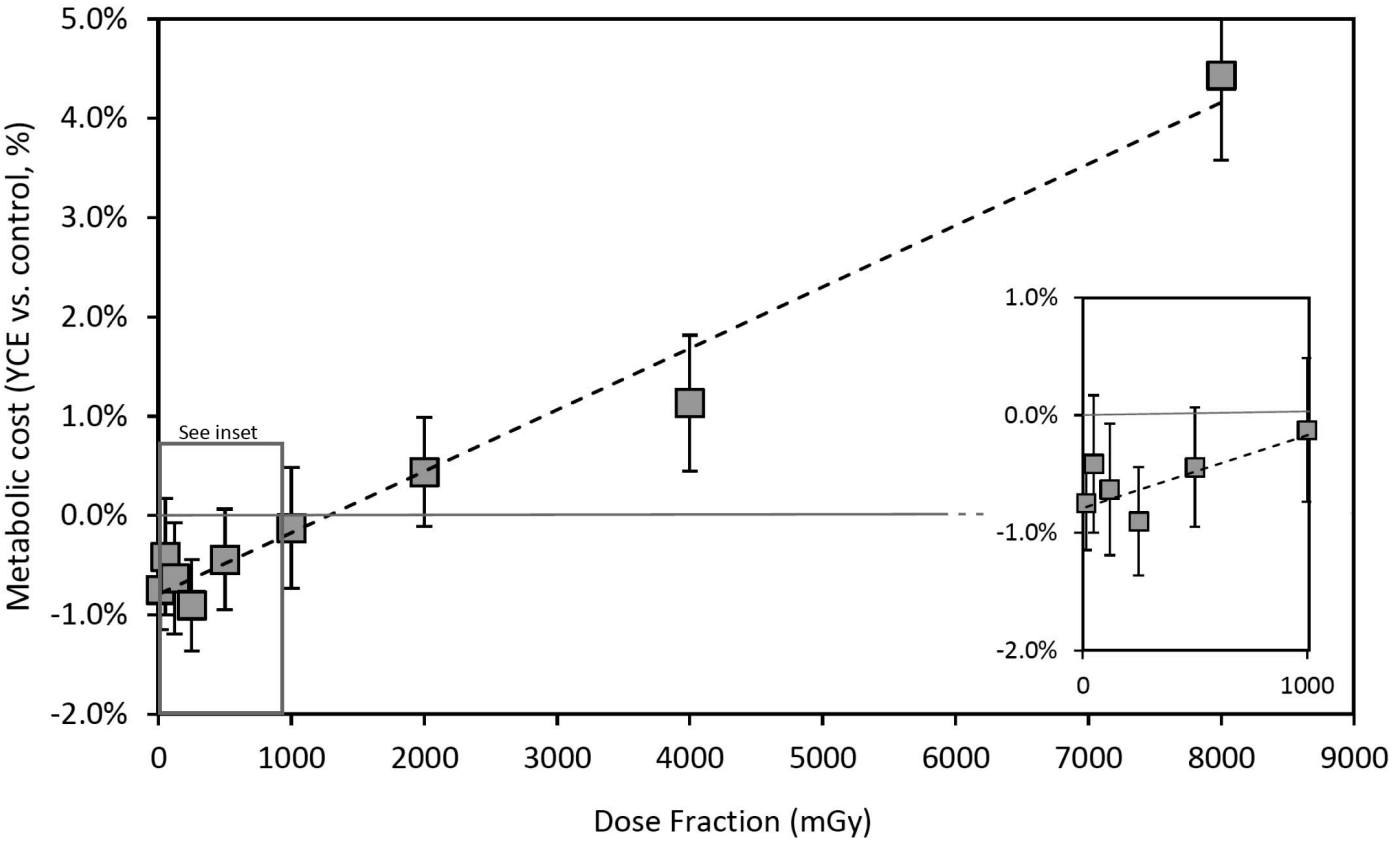

FIG. 4. Metabolic cost for different radiation exposures, presented as a percent change in yolk conversion efficiency compared to the control embryos, normalized for differences in somatic maintenance resulting from differences in specific growth rate. The dashed line represents the best fit relationship (excluding the control) determined by linear regression.

than 2 Gy being higher than the control. For the 15 mGy to 1 Gy dose fractions, the cost in metabolic efficiency (relative to the control) ranged from –0.13% for the 4 × 1 Gy group to –0.90% for the 4 × 250 mGy group.

We found a relationship between the calculated metabolic cost and degree of growth stimulation (Fig. 5). When the 4 × 8 Gy group is excluded (this dose group is clearly in the lethal range and contained numerous deformed embryos) the relationship between growth stimulation and metabolic cost appears linear although the 4 × 1 Gy point is an outlier combining significant growth stimulation with a near-zero rather than negative metabolic cost. This point indicates that the relationship between calculated metabolic cost and growth stimulation is likely to take the form of a sharply elliptical curve where high-exposure groups may experience reduced but still positive growth stimulation combined with reduced metabolic efficiency as seen in the 4 × 2 Gy and higher dose groups.

Limitations and Uncertainty

Taken in aggregate, the growth stimulation we observed was both significant and substantial. However, the 4 × 500 mGy group appears to be an outlier with SL and mean somatic weight only marginally higher than that of the control. This might simply be the result of chance or it might reflect the presence of some unrecognized factor affecting size in this treatment group as the early time point (i.e., the 97 dpf measurements) for this dose fraction showed growth stimulation consistent with the other exposure groups. We investigated the dry weight distribution for this group for a size difference between replicates recognizable from bimodality in the dry weight measurements. No such bimodality was observed in the histogram (data not shown).

The absence of a significant dose-response relationship between the different low-dose groups (Fig. 2A and C) means that our estimation of growth stimulation is dependent on the difference between the irradiated embryos as a group and the control. The distribution of dry weights for the control did not meet normality criteria (Shapiro-Wilk, $W = 0.937$, $P = 0.041$) however the early time weights were normally distributed ($P = 0.408$) and the substitution of median or modal dry weights for the 128 dpf control group did not meaningfully affect the calculated growth stimulation. We note that growth stimulation of generally similar magnitude was found in a parallel study (*36*) using chronic irradiation with a different whitefish population raised in a different laboratory.

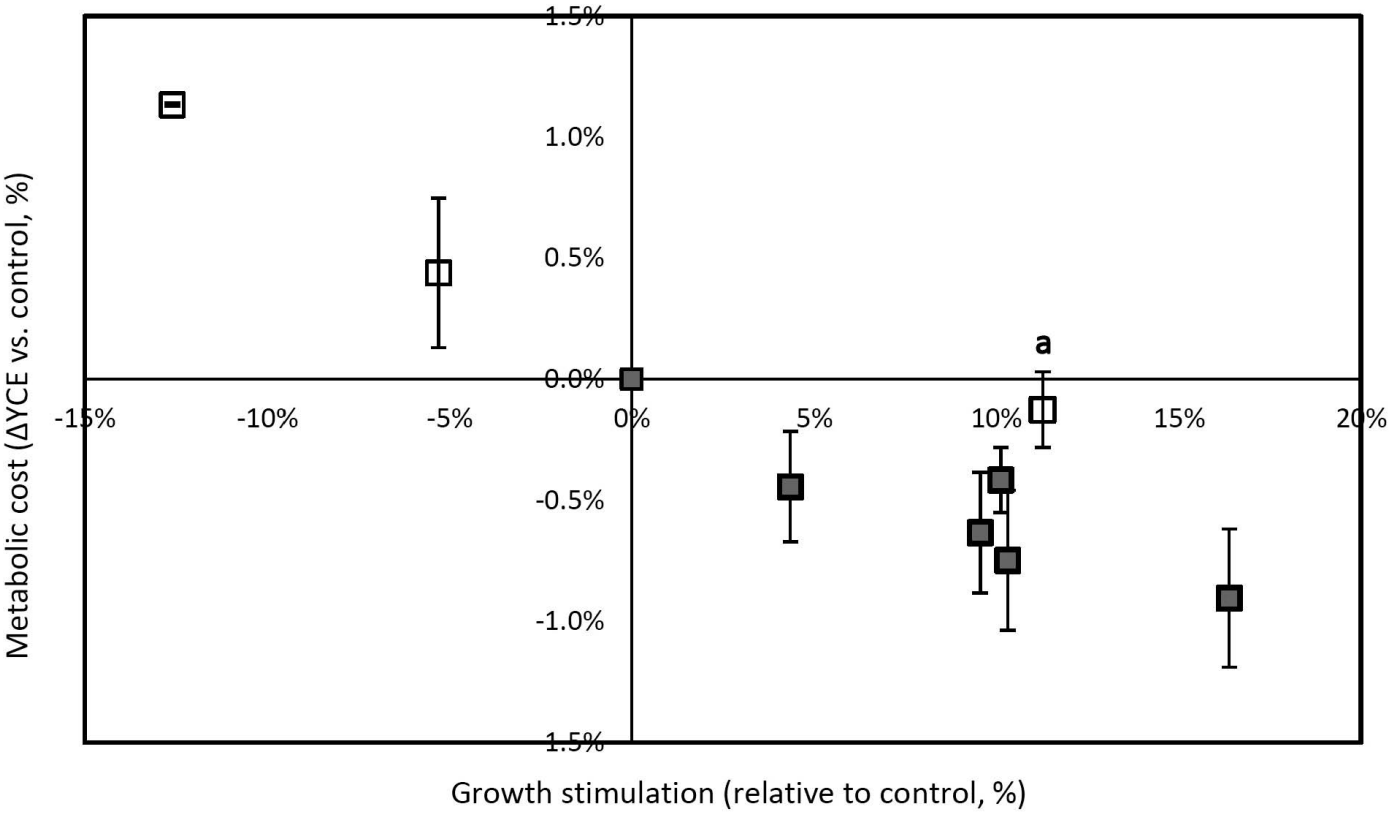

FIG. 5. Relationship between calculated metabolic cost and growth stimulation. Within the lower dose fractions (i.e., less than 1 Gy per dose fraction, denoted above by the shaded markers) the relationship between growth stimulation and metabolic cost is approximately linear suggesting that the cost may truly be slightly negative. The outlier (denoted a) is the 4×1 Gy trial which may reflect the deterioration in condition factor observed for the higher dose groups. Error bars denote confidence intervals (i.e., $2 \times$ SEM).

Our calculated values for normalized YCE suggest that the treatment groups experiencing stimulated growth converted yolk to somatic mass more efficiently than the control (i.e., the metabolic efficiency cost is negative). Calculation of normalized YCE is sensitive to small variations in the measured total embryo weight, the confidence intervals for which are sufficiently large to shift the entire linear YCE-dose relationship (Fig. 4) upward so that it crosses the Y axis at zero. Our normalization procedure also assumes a constant value for the limiting yolk conversion efficiency ε. We cannot exclude the possibility of small variations in the value for ε between the control and irradiated groups, although sensitivity testing shows that small variations in ε do not significantly affect the results. The relationship between growth stimulation/retardation and calculated metabolic cost (Fig. 5) follows a roughly linear relationship for the lower dose fractions (i.e., less than 1 Gy per dose fraction). While the metabolic cost of the stimulated growth is sensitive to variations in the control, the near-linear relationship between growth stimulation and metabolic cost appears to be robust for the lower dose fractions, persisting when we substituted median and modal values for somatic and whole embryo dry weights in place of the mean.

DISCUSSION

Conservation of elements of the adaptive response through deep geologic time (*37*) provides evidence that they increase fitness in the presence of an environmental stress. In the absence of any trade-off, at least some components of the adaptive response would also be expected to increase fitness under normal environmental conditions. A response that provided an organism with stress resistance would be expected to increase fitness over time even if that resistance conferred no advantage other than protection against a possible future event. The need for a sensitizing or priming exposure implies that the adaptive response cannot be free of cost.

Our experimental results demonstrate that radiation-stimulated growth in developing lake whitefish embryos is not ''paid for'' by a trade-off in the efficiency of yolk conversion. To the extent to which we may extrapolate from a single hormetic response in a single model organism, the absence of a trade-off in metabolic efficiency suggests that such a trade-off may not function as a generalized cost accompanying the adaptive response. However, the stimulated growth itself represents a substantial investment of energy that might decrease fitness if the energy invested in growth is diverted from other physiological processes, or if it results in an embryo hatching with insufficient yolk

reserves to sustain itself during the transition to exogenous feeding. This later possibility is an example of phenological mismatch (*38, 39*) which has been identified as a specific concern for lake whitefish (*27*).

Under natural conditions lake whitefish spawn in the fall when water temperatures drop below about 10°C (*40, 41*). Hatching takes place in spring, typically in April or May, and coincides with the spring break-up of ice cover. Growth stimulation would result in an embryo with lower yolk reserves and greater somatic maintenance demands than its unaffected siblings. Dostatni *et al*. (*42*) reported that the caloric quantity of zooplankton (the main food source for whitefish hatchlings) increased approximately fourfold in the first three weeks following ice out with a peak in early May approximately 20-fold higher. Embryos hatching asynchronously to this natural increase in food supply may therefore experience low survival. Under typical incubation temperatures of between 0.5 and 1.5°C, growth stimulation in the range of the 8–10% we observed would be equivalent to hatching several weeks early (*31*), a meaningful difference given the vulnerability of lake whitefish hatchlings to starvation (*43–45*).

While mismatch between yolk reserves and seasonal changes in prey availability adequately accounts for an evolutionarily-relevant cost specific to stimulated growth in developing whitefish embryos, it is harder to imagine it as a generalized cost across different taxa. More plausible is a form of energetic mismatch resulting from an increased metabolic rate (implied by growth stimulation without a trade-off in growth efficiency). Such an increase, if sustained, would increase future energetic demands when resources might be scarce thereby increasing the vulnerability to starvation. An increased metabolic rate in times of food scarcity could also lead to trade-offs in immunity (*46*) or a nonadaptive allocation of limited resources amongst different physiological processes as postulated by Saul *et al*. (*23*) and Costantini *et al*. (*24*). Therefore the energetic mismatch and allocation hypotheses should be seen as complementary rather than alternative explanations. Other potential trade-offs include the possibility that maintaining a degree of reserve immune capacity or ''safety factor'' could confer some form of selective advantage (*47*). In fully mobilizing the constituent pathways of the adaptive response an organism may achieve certain transient benefits but will have simultaneously expended this reserve capacity.

Our results are limited to a single effect caused by a single stressor experienced by a single species at a single life-stage, but the absence of any direct trade-off in metabolic efficiency points to the absolute energetic requirements of stimulated growth as a possible candidate for a general cost. This would suggest that stimulated growth is not intrinsically beneficial but rather an energy demand capable of altering naturally evolved growth trajectories, or requiring the diversion of resources from other physiological processes leading to a longer term decrease in fitness. It would also imply the persistence of effects beyond the transient availability of excess food under natural conditions.

The adaptive response to low-dose ionizing radiation exposure may modify risk by conferring protective effects not present at baseline levels. However, natural selection assures the existence of an accompanying cost. The nature of such cost remains unknown but any risk model incorporating an adaptive response is necessarily incomplete without its inclusion.

ACKNOWLEDGMENTS

The authors wish to thank Lisa Stoa, Emily Hulley and Shayenthrian Sreetharan for assistance with the experimental work and the Ontario Ministry of Natural Resources and Forestry who made our experiment possible by providing us whitefish embryos. We are grateful to Bruce Power for its support of this work, both financially and technically, and for funding through a Natural Sciences and Engineering Research Council of Canada (NSERC) Collaborative Research and Development Grant.

Received: October 26, 2016; accepted: August 14, 2017; published online: September 6, 2017

REFERENCES

1. Ludwików G, Xiao Y, Hoebe RA, Franken NA, Darroudi F, Stap J, et al. Induction of chromosome aberrations in unirradiated chromatin after partial irradiation of a cell nucleus. Int J Radiat Biol 2002; 78:239–247.
2. Feinendegen LE, Pollycove M, Neumann RD. Low-dose cancer risk modeling must recognize up-regulation of protection. Dose Response 2009; 8:227–252.
3. Boreham DR, Mitchel REJ. DNA lesions that signal the induction of radioresistance and DNA repair in yeast. Radiat Res 1991; 28:19–28.
4. Azzam E, de Toledo S, Gooding T, Little JB. Intercellular communication is involved in the bystander regulation of gene expression in human cells exposed to very low fluences of alpha particles. Radiat Res 1998; 150:497–504.
5. Broome EJ, Brown DL, Mitchel REJ. Dose responses for adaption to low doses of 60 Co γ rays and 3 H β particles in normal human fibroblasts. Radiat Res 1999; 158:181–186.
6. Tang FR, Loke WK. Molecular mechanisms of low dose ionizing radiation-induced hormesis, adaptive responses, radioresistance, bystander effects, and genomic instability. Int J Radiat Biol 2015; 91:13–27.
7. Breslavets LB. Plants and X-rays. Moscow; Acad. Sci. USSR Press 1946, (Translation: American Institute of Biological Sciences 1960)
8. Russell EJ. The effect of radium on the growth of plants. Nature 1915; 96:147–148.
9. Mothersill C, Smith R, Lariviere D, Seymour C. Chronic exposure by ingestion of environmentally relevant doses of 226 Ra leads to transient growth perturbations in Fathead Minnow (Pimephales Promelas, Rafinesque, 1820). Int J Radiat Biol 2013; 89:950–964.
10. Baptist JP, Wolfe DA, Colby DR. Effects of chronic gamma radiation on the growth and survival of juvenile clams (Mercenaria Mercenaria) and scallops (Argopecten Irradians). Health Phys 1976; 30:79–83.
11. Engel DW. Effect of single and continuous exposures of gamma radiation on the survival and growth of the Blue Crab, Callinectes sapidus. Radiat Res 1967; 32:685–691.
12. Stark K, Scott DE, Tsyusko O, Coughlin DP, Hinton TG. Multi-

level effects of low dose rate ionizing radiation on Southern Toad, Anaxyrus [Bufo] terrestris. PLoS One 2015; 10:e0125327.

13. Calabrese EJ. Evidence that hormesis represents an ''overcompensation'' response to a disruption in homeostasis. Ecotoxicol Environ Saf 1999; 42:135–137.
14. Johnston IA, Bower NI, Macqueen, DJ. Growth and the regulation of myotomal muscle mass in Teleost fish. J Exp Biol 2011; 214:1617–1628.
15. Miller MW, Miller WM. Radiation hormesis in plants. Health Phys 1987; 52:607–616.
16. Dadachova E, Casadevall A. Ionizing radiation: How fungi cope, adapt, and exploit with the help of melanin. Curr Opin Microbiol 2008; 11:525–531.
17. Calabrese EJ, Baldwin LA. Toxicology rethinks its central belief. Nature 2003; 421:691–692.
18. Costantini D, Metcalfe NB, Monaghan P. Ecological processes in a hormetic framework. Ecol Lett 2010; 13:1435–1447.
19. Boreham DR, Trivedi A, Weinberger P, Mitchel REJ. The involvement of topoisomerases and DNA polymerase 1 in the mechanism of induced thermal and radiation resistance in yeast. Radiat Res 1990; 123:203–212.
20. Boreham DR, Mitchel REJ. Regulation of heat and radiation stress responses in yeast by HSP-104. Radiat Res 1994; 137:190–195.
21. Forbes VE. Is hormesis an evolutionary expectation? Funct Ecol 2000; 14:12–24.
22. Zhang Q, Pi J, Woods CG, Jarabek AM, Clewell HJ, Andersen ME. Hormesis and adaptive cellular control systems. Dose-Response 2008; 6:196–208.
23. Saul N, Pietsch K, Stürzenbaum SR, Menzel R, Steinberg CE. Hormesis and longevity with tannins: free of charge or cost-intensive? Chemosphere 2013; 93:1005–1008.
24. Costantini D, Monaghan P, Metcalfe NB. Prior hormetic priming is costly under environmental mismatch; Biol Lett 2014; 10: 20131010.
25. Muir AM, Arts MT, Koops MA, Johnson TB, Krueger CC, Sutton TM. Reproductive life-history strategies in lake whitefish (Coregonus clupeaformis) from the Laurentian Great Lakes. Can J Fish Aquat Sci 2014; 71:1256–1269.
26. Brooke LT. Effect of different constant incubation temperatures on egg survival and embryonic development in lake whitefish (Coregonus clupeaformis). Trans Am Fish Soc 1975; 104:555–559.
27. Patrick, P., Chen E, Parks J, Powell, Poulton JS, Fietsch C-L.Effects of fixed and fluctuating temperature on hatch of Round Whitefish and Lake Whitefish eggs. N Am J Fish Manage 2013; 33:1091–1099.
28. Eme J, Mueller CA, Manzon RG, Somers CM, Boreham DR, et al. Critical windows in embryonic development: Shifting incubation temperatures alter heart rate and oxygen consumption of Lake Whitefish (Coregonus clupeaformis) embryos and hatchlings. Comp Biochem Physiol A Mol Integr Physiol 2015; 179:71–80.
29. Mueller CA, Eme J, Manzon RG, Somers CM, Boreham DR, Wilson JY. Embryonic critical windows: Changes in incubation temperature alter survival, hatchling phenotype and cost of development in lake whitefish (Coregonus clupeaformis). J Comp Physiol B 2015; 185:315–331.
30. Mitz C, Thome C, Cybulski ME, Laframboise L, Somers CM, Manzon RG, Wilson JY, et al. A self-contained, controlled hatchery system for rearing lake whitefish embryos for experimental aquaculture. N Am J Aquacult 2014; 76:179–184.
31. Sreetharan S, Thome C, Mitz C, Eme J, Mueller CA, Hulley EN. Manzon RG, et al. Embryonic development of lake whitefish (Coregonus clupeaformis): a staging series, analysis of growth and impacts of fixation. J Fish Biol 2015; 87:539–558.
32. Smith BB, Walker KF. Shrinkage of 0+ carp (Cyprinus carpio L.) after preservation in ethanol. Mar Freshwater Res 2003; 54:113–116.
33. Melo MT, Saturnino C, Santos JNS, Vasconcellos RM, Cruz-Filho AG, Araujo FG. Correction of the weight and length for juveniles Atherinella brasilliensis (actinopterygii: atherinopsidae) after fixation in formalin and preservation in ethanol. Zoologia 2010; 27:892–896.
34. West GB, Brown JH, Enquist BJ. The fourth dimension of life: Fractal geometry and allometric scaling of organisms. Science 1999; 284:1677–1679.
35. Gillooly JF, Charnov EL, West GB, Savage VM, Brown JH. Effects of size and temperature on developmental time. Nature 2002; 1417:70–73.
36. Thome C, Mitz C, Hulley EN, Somers CM, Manzon RG, Wilson JY, Boreham DR. Initial characterization of the growth stimulation and heat-shock-induced adaptive response in developing lake whitefish embryos after ionizing radiation exposure. Radiat Res 2017; 188:
37. Wang W, Vinocur B, Shoseyov O, Altman A. Role of plant heat-shock proteins and molecular chaperones in the abiotic stress response. Trends Plant Sci 2004; 9:244–252.
38. Cushing DH. The regularity of the spawning season of some fishes. ICES J Mar Sci 1969; 33:81–92.
39. Genner MJ, Halliday NC, Simpson SD, Southward AJ, Hawkins SJ, Sims DW. Temperature-driven phenological changes within a marine larval fish assemblage. J Plankton Res 2009; 32:699–708.
40. Hart JL. The spawning and early life history of the whitefish, Coregonus clupeaformis (Mitchill), in the Bay of Quinte, Ontario. Cont Can Biol Fish 1931; 6:165–214.
41. Scott WB, Crossman EJ. Freshwater fishes of Canada. Fish Research Board of Canada Bulletin 184, 1973.
42. Dostatni D, Mamcarz A, Poczyczyński P. Feeding of early- and late-hatched whitefish in illuminated cages. Arch Pol Fish 1999; 7:281–295.
43. Taylor WW, Freeberg MH. Effect of food abundance on larva1 Lake whitefish, Coregonus clupeaformis growth and survival. J Fish Biol 1984; 25:733–741.
44. Reshetnikov YS, Bogdanov VD. Features of reproduction of whitefishes. J Ichthyol 2011; 51:432–456.
45. Meyer S, Caldarone EM, Chícharo MA, Clemmesen C, Faria AM, Faulk C, Folkvord A, Holt GJ, Hoie H, Kanstinger P, Malzahn A, Moran D, Petereit C, Stottrup JG, Peck MA. On the edge of death: Rates of decline and lower thresholds of biochemical condition in food-deprived fish larvae and juveniles. J Mar Syst 2012; 93:11–24.
46. McClure CD, Zhong W, Hunt VL, Chapman FM, Hill FV, Priest NK. Hormesis results in trade-offs with immunity. Evolution 2014; 68:2225–2233.
47. Diamond J. Quantitative evolutionary design. J Physiol 2002; 542:337–345.

RADIATION RESEARCH **188**, 495–504 (2017)
0033-7587/17 $15.00

DOI: 10.1667/RR14575.1

Multiple CT Scans Extend Lifespan by Delaying Cancer Progression in Cancer-Prone Mice

Jennifer A. Lemon,[a,1] Nghi Phan[b] and Douglas R. Boreham[a]

[a] *Medical Sciences, Northern Ontario School of Medicine, Sudbury, Canada, P3E 2C6;* [b] *Medical Physics and Applied Radiation Sciences, McMaster University, Hamilton, Canada, L8S 4K1*

Lemon, J. A., Phan, N. and Boreham, D. R. Multiple CT Scans Extend Lifespan by Delaying Cancer Progression in Cancer-Prone Mice. ***Radiat. Res.*** **188, 495–504 (2017).**

Computed tomography (CT) scans are a routine diagnostic imaging technique that utilize low-energy X rays with an average absorbed dose of approximately 10 mGy per clinical whole-body CT scan. The growing use of CT scans in the clinic has raised concern of increased carcinogenic risk in patients exposed to ionizing radiation from diagnostic procedures. The goal of this study was to better understand cancer risk associated with low-dose exposures from CT scans. Historically, low-dose exposure preceding a larger challenge dose increases tumor latency, but does little to impact tumor frequency in *Trp*53$^{+/-}$ mice. To assess the effects of CT scans specifically on tumor progression, whole-body CT scans (10 mGy/scan, 75 kVp) were started at four weeks after 4 Gy irradiation, to allow for completion of tumor initiation. The mice were exposed to weekly CT scans for ten consecutive weeks. In this study, we show that CT scans modify cellular end points commonly associated with carcinogenesis in cancer-prone *Trp*53$^{+/-}$ heterozygous mice. At five days after completion of CT scan treatment, the multiple CT scans did not cause detectable differences in bone marrow genomic instability, as measured by the formation of micronucleated reticulocytes and H2AX phosphorylation in lymphoid-type cells, and significantly lowered constitutive and radiation induced levels of apoptosis. The overall lifespan of 4 Gy exposed cancer-initiated mice treated with multiple CT scans was increased by approximately 8% compared to mice exposed to 4 Gy alone ($P < 0.017$). Increased latency periods for lymphoma and sarcoma ($P < 0.040$) progression contributed to the overall increase in lifespan. However, repeated CT scans did not affect carcinoma latency. To our knowledge, this is the first reported study to show that repeated CT scans, when administered after tumor initiation, can improve cancer morbidity by delaying the progression of specific types of radiation-induced cancers in *Trp*53$^{+/-}$ mice.

[1] Address for correspondence: Medical Sciences, Northern Ontario School of Medicine, 935 Ramsey Lake Road, Sudbury, Canada, P3E 2C6; email: jlemon@nosm.ca.

INTRODUCTION

The number of computed tomography (CT) scans performed annually have nearly tripled in the last 15 years (*1*). The average dose from a clinical whole-body CT scan is approximately 12 mSv (*2*). This increased exposure of the public to low-dose ionizing radiation has raised considerable concern in both the scientific and medical communities over the potential for increased risk of carcinogenesis (*3–5*). Due to the difficulty in obtaining direct, empirical data from human populations, the estimation of risk relies on the extrapolation models developed largely from high-dose radiation exposures, the predominant one being the linear no-threshold (LNT) model. Basing calculations on the assumptions that form the LNT model, a number of studies have concluded there is an increased risk of carcinogenesis that is proportional to the dose received from CT scans (*6–8*). Despite the inherent flaws that have invalidated the LNT as a viable hypothesis for predicting biological responses to low-dose radiation, the theory persists as a simplistic model on which modern radiation safety guidelines are based (*9*).

Alternative to the LNT model of risk assessment, considerable experimental evidence has accumulated that indicates biological responses to low-dose radiation are not linear, and can, in some instances, induce protective responses that reduce the cellular damage from an array of genotoxic agents, including high doses of ionizing radiation (*10–15*). The protective mechanisms induced as a result of low-dose irradiation include increased cellular antioxidants (*16*), induction of error-free DNA repair mechanisms (*17*), upregulation of anti-inflammatory responses (*16, 18, 19*) and increased immune surveillance (*19, 20*). There are numerous reported studies of acute and chronic low-dose exposures reducing cancer incidence (*20–22*), increasing cancer latency (*23–25*) and extending overall survival in numerous animal models (*20, 21, 23, 26, 27*). These studies and many others demonstrate radiation-induced adaptive response at the whole-animal level, however, the key feature in these studies has been that the low, adapting dose always preceded the large challenge radiation dose. Consequently, whether the low dose was affecting the initiation and/or progression stages of carcinogenesis was unclear. We have

TABLE 1
Treatment Groups

Group	Treatment
Acute biological end point study	
Control (n = 5)	Nonirradiated (sham-irradiated group, 7–8 weeks old)
CT (n = 5)	Weekly CT scans for 10 weeks (starting at 11–12 weeks old)
4 Gy (n = 5)	4 Gy acute exposure (7–8 weeks old)
4 Gy + CT (n = 10)	4 Gy acute exposure (7–8 weeks old) + 10 weekly CT scans (starting at 11–12 weeks old)
Lifetime cancer study	
Control (n = 199)	Nonirradiated (sham-irradiated group, 7–8 weeks old)
4 Gy (n = 203)	4 Gy acute exposure (7–8 weeks old)
4 Gy + CTs (n = 198)	4 Gy acute exposure (7–8 weeks old) + 10 weekly CT scans (starting at 11–12 weeks old)

Notes. With the exception of the lifetime study groups, all groups were age matched at time of respective treatments and at the time of tissue collection (22–23 weeks old). Tissue collection (and *in vitro* irradiation where applicable) occurred five days after the last CT scan.

demonstrated that single and multiple CT scans preceding a large cancer-initiating dose can reduce cancer risk by inducing protective cellular responses (*28*) and prolonging cancer latency (*29*). The wealth of human and animal data point to clear thresholds for carcinogenesis, meaning that doses falling below the threshold have no clinically relevant risks for carcinogenesis. It follows that the studies basing cancer risk predictions on invalidated hypotheses are unethical, and the fear of low-dose radiation exposure (i.e., CT scans) that they propagate negatively impacts the ability of physicians to perform necessary medical tests for fear of malpractice (*9, 30*).

There are no reported studies on the biological effects of multiple low-dose exposures after the neoplastic process has been fully initiated by a high-dose exposure. In this study, we investigated the potential modifying effects of low-dose diagnostic exposures delivered after an acute cancer-inducing *in vivo* high-dose radiation exposure. Low-dose exposures were delivered weekly for ten consecutive weeks, four weeks after high-dose (4 Gy) gamma irradiation. In *Trp*53$^{+/-}$ mice, radiation-induced tumorigenesis is associated with the loss of p53 function, and there is reported evidence that it occurs within weeks of a high-dose exposure. Donehower and colleagues (*31*) showed that inactivation of p53 two weeks after high-dose irradiation led to the promotion of lymphoma development. Reporting complementary results, Evans and colleagues (*32*) found that activating p53 function two weeks after a high-dose radiation exposure suppressed lymphoma development in mice. Presuming that high-dose exposure abrogates p53 function (*33*), we postulated that a four-week period after an acute 4 Gy exposure was sufficient to complete initiation of events required for tumorigenesis in cancer-prone *Trp*53$^{+/-}$ mice. The goal of this work was to determine whether low-dose fractionated exposures via repeated CT scans during the promotion phase of carcinogenesis could modify the frequency and latency of tumorigenesis. To gain insight into the biological mechanisms involved in radiation-induced tumorigenesis and the modifying effects of low-dose CT scans, biological end points associated with persistent unstable chromosomal aberrations, residual DNA damage, DNA oxidative stress damage and apoptosis were examined. Therefore, in this study, we endeavored to assess the risk associated with diagnostic radiation exposure, specifically on the progression stage of carcinogenesis, by investigating the ability of CT scans to alter the frequency and latency of radiation-induced carcinogenesis in *Trp*53$^{+/-}$ cancer-prone mice.

MATERIALS AND METHODS

Animal Breeding and Genotyping

Male *Trp*53 heterozygous (B6.129S2-*Trp*53$^{tm1Tyj/+}$) mice and female *Trp*53 homozygous (129X1/SvJ *Trp*53$^{+/+}$) (Jackson Laboratory, Bar Harbor, MA) were bred to obtain F1 *Trp*53$^{+/-}$ (heterozygous) progeny. The F1 mice were genotyped by PCR (Mouse Genotype Inc.; Carlsbad, CA) and *Trp*53$^{+/-}$ female mice were randomly assigned to experimental groups.

Animal Housing

Mice were maintained in specific-pathogen-free (SPF) housing on a 12:12-h light:dark photoperiod (23 ± 2°C and 40–80% humidity). Animals had access to food and water *ad libitum*. All housing, handling and experimental procedures were approved by the Animal Research Ethics Board at McMaster University (Hamilton, Canada) and conducted in accordance to the guidelines of the Canadian Council on Animal Care (Ottawa, Canada).

In Vivo Irradiation

There were four treatment groups (see Table 1) for short-term (acute biological end point) studies and two groups for lifetime studies (4 Gy and 4 Gy + CT scans). Cohorts of mice (7–8 weeks old) were placed into a customized polycarbonate tube and received a challenge dose of 4 Gy whole-body gamma irradiation (662 keV, ^{137}Cs; dose rate of 0.349 Gy/min). Control and CT scan-only groups were handled identically, except without the challenge dose. After 4 Gy irradiation, mice assigned to the lifetime studies were returned to SPF housing. Mice assigned to the lifetime groups were monitored daily until end point and euthanization, when required. End point for euthanasia was determined *a priori* in accordance with McMaster ethics policies and previous lifetime mouse studies (*23–25*).

Computed Tomography Protocols

Four weeks after the 4 Gy *in vivo* challenge dose, one group was given weekly whole-body CT scans for ten consecutive weeks. CT scans were performed on the X-SPECT small animal imaging system (Gamma Medica, Northridge, CA) at the McMaster Pre-clinical and Translational Imaging Facility. Mice were placed into polycarbonate tubes and given a CT scan (75 kVp, 255 μA, 1 mm aluminum filter,

half-value layer 4.28 mm aluminum, 185 projections) with a whole-body absorbed dose of approximately 10 mGy. Mice were not anaesthetized during the CT scanning procedure, since immobilization for image analysis was not required.

Computed Tomography Dosimetry

Whole-body dose measurements were obtained using thermoluminescent dosimeter (TLD) chips (Harshaw TLD-100™ LiF Chips). Whole-body absorbed dose in mice was measured by surgically implanting TLD chips in five locations in a mouse carcass: head, chest, abdomen, above the skin and under the skin. Measurements were performed on two individual carcasses during the study. TLD chip analyses were performed by K & S Associates, Inc. (Nashville, TN). The overall uncertainty of the TLD measurement process is 5% at the 95% confidence interval for a single TLD chip at the measurement location. Consistent dosimetry was confirmed and validated repeatedly throughout the study using a 0.6 cc ionization chamber [PTW Farmer® Dose-meter (model no. 2570A) and PTW Freiburg Ion Chamber (model no. TN30010); PTW, Freiburg, Germany]. The calculated average whole-body dose for a CT scan at the aforementioned specifications was 10.3 ± 1.1 mGy, with a dose rate of 18.6 mGy/min.

In Vitro Irradiation Challenge

Tissues from mice assigned to the acute biological end point investigation were harvested five days after the final CT scan time point. Blood and bone marrow were collected and separated into three aliquots (1×10^6 cells/ml) for *in vitro* exposures of either 0, 1 or 2 Gy at a dose rate of 0.188 Gy/min (662 keV, Cs^{137}). All samples were held at 0°C in ice-water slurry during the *in vitro* irradiation challenges.

Sample Collection and Cell Preparation

Blood. Blood was collected via cardiac puncture from mice anaesthetized with 3% isoflurane. Approximately 500 μl of blood was collected in heparinized syringes, of which 50 μl was immediately aliquoted into 1.5-ml microcentrifuge tubes containing 350-μl heparin solution (VWR International, Mississauga, Canada) for micronucleated reticulocyte (MN-RET) analysis. The remaining blood sample was kept in ice-water slurry for apoptosis analyses. Heparinized blood for the MN-RET assay was maintained at room temperature until fixation. After blood collection, mice were euthanized by cervical dislocation.

Bone marrow. Bone marrow samples were collected by flushing both femurs with 1-ml heparinized RPMI 1640 media (Lonza Inc., Allendale, NJ). The disaggregated bone marrow cell suspension was transferred to a 1.5-ml microcentrifuge tube and filtered using a 30-μm filter to remove stromal elements. The resulting cell suspension was held at 0°C on ice slurry until processing. Bone marrow cells were counted using a Z2 Coulter Particle Count and Size Analyzer (Beckman Coulter® Inc., Miami, FL). The samples were adjusted to a final concentration of 1×10^6 cells/ml in ice-cold RPMI 1640 supplemented with 10% fetal bovine serum (FBS; PAA Laboratories Inc., Toronto, Canada), 1% penicillin/streptomycin and 1% L-glutamine (Lonza, Inc.). Three 1.5-ml replicate aliquots of the cell sample suspension were made for *in vitro* irradiations at 0, 1 and 2 Gy.

Micronucleated Reticulocyte Assay

All reagents used for the micronucleated reticulocyte (MN-RET) assay were included in the Mouse MicroFlowPLUS® kit (Litron Laboratories, Rochester, NY). Cells were fixed in absolute methanol (Sigma-Aldrich®, Mississauga, Canada) at –80°C and stored at –80°C for a minimum of 24 h before staining and flow cytometric analysis. The fixed blood samples were washed and labeled for flow cytometric analysis according to the Mouse MicoFlowPLUS Kit manufacturer's procedure and previously described by Dertinger *et al*. (*34*). Briefly, fixed blood cells were washed with 12-ml buffer solution and cell pellets were maintained at 0°C until staining. After the wash, 80 μl of reagent mixture containing anti-CD71-FITC, anti-CD61-PE, RNase and buffer solution was added to 20 μl aliquot of each fixed blood sample in duplicate. The cells were incubated on ice for 30 min followed by 30 min at room temperature and then returned to ice. Immediately prior to flow cytometry analysis, 1 ml of 4°C propidium iodide (PI; 1.25 μg/ml in buffer solution) was added to each tube. Data acquisition was performed using the EPICS XL flow cytometer (Beckman Coulter, Brea, CA) equipped with a 488-nm argon laser. The gating logic used to quantitatively analyze the erythrocyte subpopulations has been described elsewhere (*34*). Analysis windows were set to quantify the number of reticulocytes (RETs) and MN-RETs for each sample. Representative bivariate graphs illustrating the resolution of the various erythrocyte populations have been previously published (*34, 35*). Initially, the number of RETs was determined in 2×10^5 erythrocytes. Samples were subsequently run to determine the number of MN-RETs in a total of 2×10^4 total RETs per sample.

Gamma-H2AX Fluorescence Assay

Bone marrow cells were adjusted to 1×10^6 cells/ml and transferred to 15-ml conical tubes (BD Biosciences, Mississauga, Canada) and irradiated as described above. After irradiations, 500-μl aliquots were removed from irradiated cell samples and incubated for either 30 or 120 min in a 37°C water bath. After incubation, 3 ml of 70% ethanol at 0°C was immediately added to each tube. Tubes were maintained at 0°C for 1 h prior to storage at –20°C until analysis. For analysis, the fixed bone marrow samples were centrifuged at 5°C (250*g*, 8 min) and the supernatant was discarded. Cells were then washed in 3-ml Tris-buffered saline (1× TBS; Trizma base with NaCl; Sigma-Aldrich), centrifuged (250*g*, 8 min), resuspended in 1 ml of Tris-saline-Triton™ [TST; TBS with 4% FBS and 0.1% Triton X-100 (Sigma-Aldrich)] and incubated on ice for 10 min to permeabilize cells. The cells were again centrifuged at 250*g* for 8 min, the supernatant was discarded and cells were resuspended in 200 μl of a 1:400 dilution of anti-phospho-H2A.X (ser139) antibody (γ-H2AX; Upstate Cell Signaling, Charlottesville, VA). The cell samples containing the primary antibodies were incubated on a tube rocker at room temperature for 2 h in the dark. The cells were then washed with 3 ml of TST, resuspended in 200 μl of a 1:500 dilution of Alexa Fluor™ 488-conjugated goat anti-rabbit IgG F(ab')2 antibody (γ-H2AX), and incubated at room temperature for 1 h in the dark. The cells were then washed in 3 ml of TBS and resuspended in 300 μl TBS with 5 μl PI (1 mg/ml; Sigma-Aldrich). Samples were placed on ice and promptly analyzed by flow cytometry. Analysis was based on 5×10^4 cells from the lymphocyte-rich cell population, as determined by flow cytometric scattering patterns. The levels of γ-H2AX fluorescence were determined by measuring the mean fluorescence intensity of the respective cell populations. Each sample was analyzed in duplicate.

Apoptosis Assay

The proportion of apoptotic cell death was determined by flow cytometry using Annexin V with 7-amino actinomycin D (7AAD), as previously described elsewhere (*36*). The reagents were purchased as a commercial kit (Annexin V-FITC-7-AAD, cat. no. IM3614; Beckman Coulter, Mississauga, Canada). Additionally, anti-CD61-PE (Beckman Coulter) and anti-CD45-PETR (Invitrogen Canada/Life Technologies Inc., Burlington, Canada) antibodies were used to peripheral blood lymphocytes ($CD45^+$) with the platelet ($CD61^+$) population gated out. Apoptotic lymphocytes were identified as being $CD45^+$, Annexin V^+, $7AAD^+$ and $CD61^-$. Briefly, each mouse blood sample was adjusted to 1×10^6 cells/ml and divided into three aliquots in 5-ml polypropylene assay tubes (Sarstedt, Montreal, Canada) for *in vitro* irradiations. Samples were held at 0°C for irradiation at 0, 1 or 2 Gy, after which they were incubated at 37°C, 5% CO_2 for 8 h. Red blood

cells were lysed by adding 2 ml of 37°C 1× NH_4Cl and incubated at room temperature for 10 min. The samples were then centrifuged (5°C, 250*g*, 5 min), the supernatant discarded and the sample tubes were vortexed gently. The samples were then washed with 2 ml of cold Hank's Buffered Salt Solution (HBSS; 5°C; Invitrogen Canada) and resuspended in 250 µl of supplied 1× binding buffer. A 100-µl antibody cocktail was added to each sample containing 1× binding buffer (Annexin V solution, anti-$CD45^+$, anti-$CD61^+$, 7AAD). Cells were maintained at 0°C and analyzed within 30 min by flow cytometry. The percentage of apoptotic cells was determined from an analysis of 5×10^4 lymphocytes.

Overall Lifetime Health Assessment

After treatment, mice were returned to the housing room and examined daily for abnormal indications. Objective criteria were set *a priori* to determine end point for euthanasia when it was clear that death was imminent and consistent with previous studies performed with *Trp*$53^{+/-}$ mice (*23–25*). Lymphoma and osteosarcoma are the most frequent cancer types in *Trp*$53^{+/-}$ mice (*23, 37*). After euthanasia at end point, mice complete necropsy and histological assessment were performed. Standard tissues (sternum, thymus, heart, lungs, liver, spleen, kidneys, thoracic spine, lumbar spine and brain) and any abnormalities (tumors, enlarged organs or lymph nodes, etc.) were collected. All tissues were fixed in 10% buffered formalin. Vertebrae and other mineralized tissues were further demineralized. Trimmed fixed tissue sections were embedded in paraffin and sectioned on a Leica RM 2165 microtome at 3-µm thickness and stained with hematoxylin and eosin for histological examination. The presence of any pathology was diagnosed by an experienced animal pathologist based on slide examination and necropsy reports. Blinded repeat samples were resubmitted for quality assurance with 100% reproducibility. If two of the same type of cancer were found in a mouse, this was counted as a single cancer, since it was not possible to distinguish an independent primary cancer from a metastasis. If a mouse had multiple different cancer types, these were counted as individual independent cancers. Both survival and cancer latency were defined as the time between treatment (7–8 weeks of age) and euthanasia at end point. Although this definition of latency does not follow the strict conditions for determining cancer latency (i.e., time between exposure and clinical onset of cancer), it permits the determination of the days at risk of developing cancer following radiation exposure.

Statistical Analyses

Data are presented as mean ± standard error (SE) with $P \leq 0.05$ deemed statistically significant at a 95% confidence interval. Dose-response significance testing was performed with multiple linear regression analysis. Student's *t* tests were performed to determine if significant differences existed between groups for MN-RET data. Two-way ANOVA with Bonferroni's post hoc test was used to determine significance between groups for γ-H2AX, 8-OHdG and apoptosis data. The frequencies of different cancer types in the lifetime groups were tested for statistical significance using Fisher's Exact test or Chi-squared test. Survival curve probabilities were analyzed using Kaplan-Meier analysis. Differences in overall lifespan and cancer latency (calculated as days at risk after 4 Gy irradiation) were analyzed with the log-rank test. All statistical tests were corrected for multiple comparisons. Survival analyses, except for all-cause mortalities, accounted for competing causes of death via competing risk censoring.

RESULTS

Micronucleated Reticulocytes

MN-RETs were measured in mouse peripheral blood 15 weeks after a single acute 4 Gy irradiation to assess genomic stability in hematopoietic progenitor cells. To determine if fractionated low-dose exposures could modify the effects of the large acute dose, mice were exposed to 10 weekly 10 mGy CT scans (Fig. 1A). Exposure to 4 Gy did not significantly alter the level of MN-RET formation over control levels. Repeated CT scans did not alter either control or 4 Gy irradiated MN-RET frequency compared to control animals ($P > 0.30$).

Gamma-H2AX

Five days after the final CT scan, the constitutive γ-H2AX fluorescence levels in bone marrow lymphocytes did not differ significantly among any of the treatment groups ($P > 0.42$; Fig. 1B). However, when the harvested bone marrow samples were exposed to a 1 or 2 Gy *in vitro* challenge dose, the samples from mice that had repeated CT scans had significantly lower γ-H2AX fluorescence levels (2.08 ± 0.02 and 2.56 ± 0.02, respectively) than those of non-CT canned mice, at 2.28 ± 0.06 and 2.82 ± 0.08, respectively ($P < 0.015$). Repeated CT scans after 4 Gy irradiation did not produce the same reduction, relative to 4 Gy alone ($P > 0.87$; Fig. 1B).

Apoptosis

Apoptotic cell death in peripheral blood $CD45^+$ lymphocytes was measured to assess persistent cytotoxicity after 4 Gy irradiation *in vivo* and subsequent repeated CT scans. Mice exposed to 4 Gy alone at 7–8 weeks old did not exhibit differences in apoptotic response, relative to control mice, when measured at 22–23 weeks old ($P > 0.05$; Fig. 1C). Mice treated with weekly CT scans exhibited a significant 20% reduction in spontaneous apoptosis levels, compared to non-CT scanned mice ($P < 0.038$). When their peripheral blood received a 1 and 2 Gy challenge dose *in vitro*, the same reduction in apoptosis was observed, relative to non-CT scanned mice ($P < 0.05$). The reduction in apoptosis levels induced by repeated CT scans was not different between the CT only and the 4 Gy + CT groups at all doses (*P* value). There was a significant positive correlation between apoptosis levels and challenge doses *in vitro* up to 2 Gy ($P < 0.010$; Fig. 1C).

Effects of Repeated CT Scans on Overall Survival and Cancer Frequency after 4 Gy Exposure

Considering all-cause mortalities, *Trp*$53^{+/-}$ mice exposed to 4 Gy at 7–8 weeks old had a median lifespan of 246 ± 6.1 days. The median lifespan of mice given ten weekly CT scans after 4 Gy irradiation was significantly prolonged to 256 ± 5.2 days ($P < 0.023$; Fig. 2). The total number of cancers in the 4 Gy irradiated group and the 4 Gy + CT group were not statistically different, at 256 and 268 cancers, respectively. The average total number of cancers per mouse was more than 1 for both treatment groups, with multiple different cancers often developing in the same

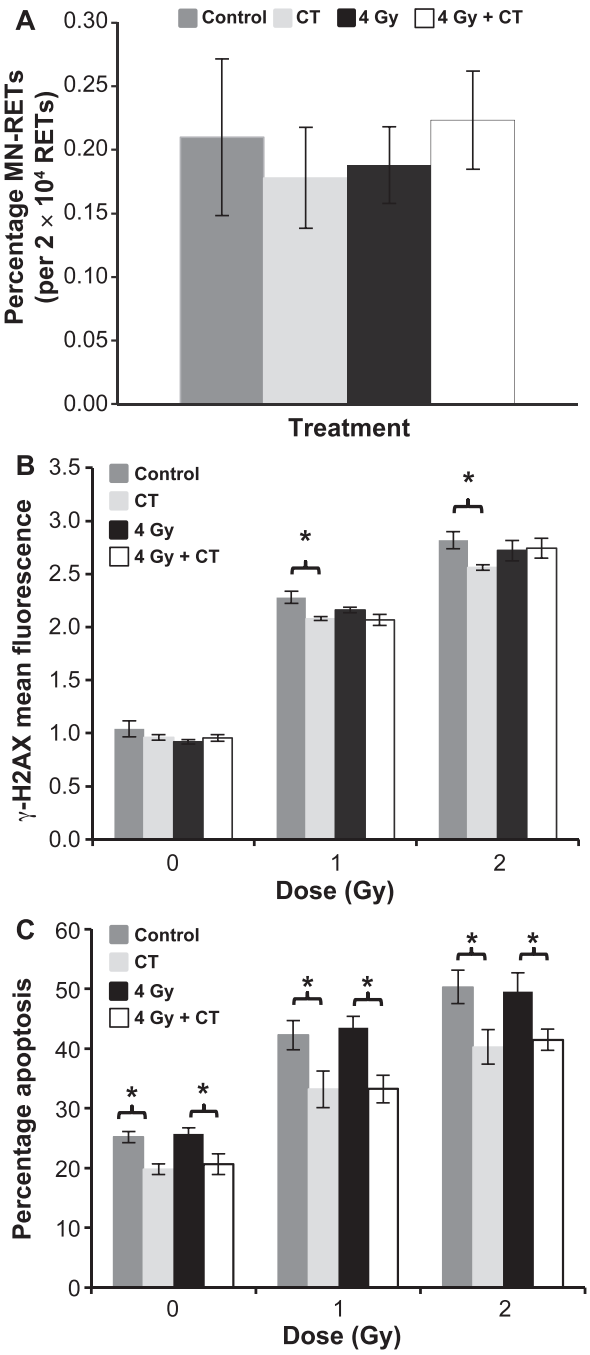

FIG. 1. Acute biological end points assessed five days after the final CT scan. Results represent the mean ± SEM (samples analyzed in duplicate); *$P < 0.05$. Panel A: Spontaneous MN-RET frequencies in peripheral blood. Panel B: Mean γ-H2AX levels in lymphocyte-rich populations of bone marrow cells. Panel C: Apoptosis (Annexin V^+, $7AAD^+$) levels in $CD45^+$ peripheral blood lymphocytes. n = 5 animals for all analyses.

*Trp*53$^{+/-}$ mouse, especially sarcoma and carcinoma subtypes (Table 2). In the 4 Gy alone group there were 122 mice with lymphoma, 78 mice with one or more sarcomas and 24 mice with one or more carcinomas. Comparatively, the 4 Gy + CT group had 109 mice diagnosed with lymphoma, 84 mice

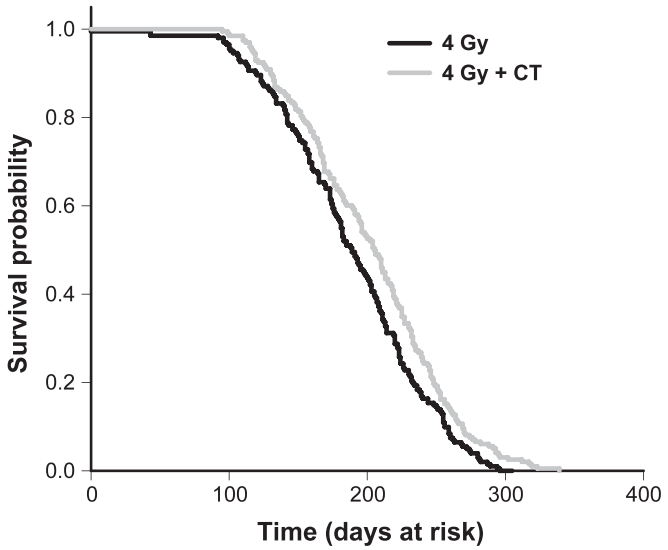

FIG. 2. Comparison of overall survival (all-cause mortality) of mice exposed to either 4 Gy alone (n = 203) or 4 Gy + CT (n = 198).

with one or more sarcomas and 28 mice with one or more carcinomas. The differences in cancer frequencies between the 4 Gy alone and 4 Gy + CT groups were not significant ($P > 0.32$). However, within the treatment groups there was a significant difference in the types of cancer that mice developed. In both treatment groups, multiple tumor types can exist in a single animal; however, lymphomas were the most prevalent and comprised 60% of lesions, followed by sarcomas with approximately 40% of lesions and carcinomas at 10% ($P < 0.014$). Pooled across both treatment groups and uncorrected for competing risks, after 4 Gy irradiation the median survival of mice diagnosed with lymphoma was 171 ± 4.1 days, significantly shorter than the median survival of mice with either sarcoma (232 ± 4.7 days) or carcinoma (225 ± 8.7 days; $P < 0.001$). There was no difference in median survival between the sarcoma- and carcinoma-diagnosed mice ($P > 0.515$).

Effects of Repeated CT Scans on Lymphoma Frequency and Latency after 4 Gy Irradiation

Repeated CT scans after receiving 4 Gy irradiation did alter the frequency of mice developing either T-cell or B-cell lymphoma, relative to the 4 Gy-alone group ($P > 0.747$; Table 2). In both groups, the incidence of T-cell lymphoma was three times greater than that of B-cell lymphoma ($P < 0.05$). After accounting for competing causes of death, repeated CT scans given after 4 Gy irradiation significantly increased lymphoma latency, compared to mice exposed to 4 Gy alone ($P < 0.040$; Fig. 3A). CT scanned mice diagnosed with lymphoma had a significant extension in median cancer latency of approximately 30 days (~16%) compared to non-CT scanned mice with lymphoma (233 ± 8.0 days vs. 203 ± 6.3 days, $P < 0.05$).

TABLE 2
Frequency of Malignant Cancers in *Trp53*$^{+/-}$ Mice Exposed to High-Dose Ionizing Radiation

Group	Median ± SE survival[a]	Lymphoma T cell:B cell	Sarcoma				Carcinoma					Total cancers (per animal)[c]
			Osteo	Hemangio	Fibro	Others	Adeno	Squam	Basal	Basosquam	Other	
Control (n = 199)	484 ± 7.4	11:25	104	23	10	16	12	2	2	4	2	211 (1.06)
4 Gy (n = 203)	246 ± 6.1	97:26	36	21	26	11	7	4	4	5	14	256 (1.26)
4 Gy + CT (n = 198)	258 ± 5.2 [b]	84:25	41	33	27	9	8	8	8	10	18	268 (1.35)

[a] For all-causes of death, no correction required for competing risks.
[b] Statistically significant relative to 4 Gy only ($P < 0.023$).
[c] No significant differences in cancer frequencies and proportions were detected between the 4 Gy and 4 Gy + CT groups ($P > 0.05$).

Effects of Repeated CT Scans on Sarcoma Frequency and Latency after 4 Gy Irradiation

The frequencies of any sarcoma subtypes were not altered in the mice that were repeatedly CT scaned after receiving 4 Gy irradiation. The CT scan group did not differ significantly from the 4 Gy irradiation alone group in the proportion of mice developing one, two or three sarcoma subtypes. In both treatment groups the most prevalent sarcoma subtypes were osteosarcoma with 50% of lesions, hemangiosarcoma at 34% and fibrosarcoma at 33% of lesions. Correcting for competing risks, mice given repeated CT scans after 4 Gy irradiation did not show any alterations in median sarcoma latency, relative to the 4 Gy irradiation alone group, at 236 ± 4.8 days and 232 ± 4.7 days, respectively ($P > 0.286$). There were no significant differences in cancer latency between the treatment groups when stratification analyses were performed on the various sarcoma subtypes.

Effects of Repeated CT Scans on Carcinoma Frequency and Latency after 4 Gy Irradiation

The frequency of total carcinoma and its subtypes did not differ appreciably between animals receiving repeat CT scans after 4 Gy irradiation and the 4 Gy irradiation alone group. When corrected for competing causes of death, there was a significant increase in latency of carcinoma for CT scanned mice ($P < 0.029$). The median latency for CT scanned mice with carcinoma was 248 ± 8.2 days, compared to 225 ± 8.4 days for non-CT scanned mice with carcinoma (Fig. 3B).

DISCUSSION

The increasing frequency in the use of CT scans in diagnostic medicine has contributed to the growing concern of increased cancer risk from exposure to low-dose ionizing radiation. At acute doses of ionizing radiation above 500 mGy there is convincing evidence to support that carcinogenesis risk is proportional to dose (*40–43*). However, the biological and health consequences of doses ≤100 mGy are the most critical with respect to occupational and medical exposures, and have a preponderance of evidence that supports a nonlinear dose response. The induction of protective responses after low-dose or low-dose-rate exposures has been reported at the molecular, cellular and organismal level (*22, 26, 44–48*). Although there have also been several studies investigating the frequency and latency of tumorigenic effects of *in vivo* exposure to different radiation doses and qualities in both wild-type and cancer-prone strains (*49–57*), the design of these studies does not differentiate whether these effects are

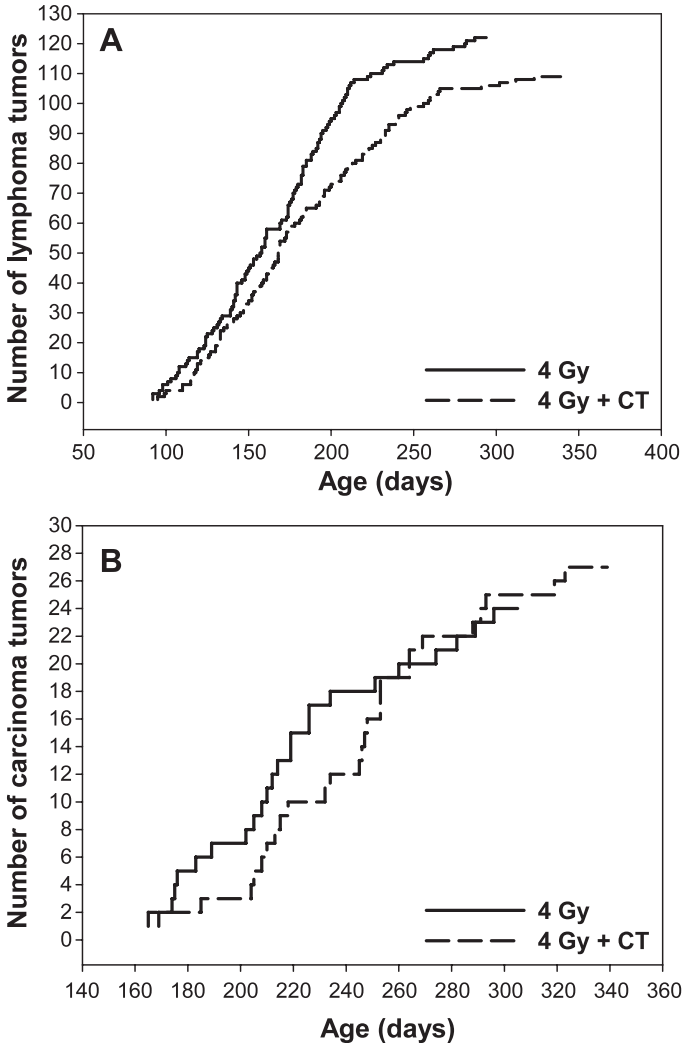

FIG. 3. Comparisons of cancer type-specific tumor number and latency in *Trp53*$^{+/-}$ mice exposed to either 4 Gy alone (n = 203) or 4 Gy + CT scans (n = 198). Panel A: Number of animals developing lymphoma. Panel B: Number of animals developing carcinoma.

the result of modifying effects on the initiation or progression stages of carcinogenesis. To determine whether low-dose radiation exposure specifically has an effect on the progression stage of carcinogenesis, our experimental design allowed the initiation phase to have completed prior to the introduction of the low-dose CT scans. In the current study, we explored the modifying effects of repeated low-dose CT scans in acute biological responses and the mechanisms associated with the progression phase of tumorigenesis after high-dose γ irradiation (4 Gy) using *Trp*53$^{+/-}$ cancer-prone mice. By examining biological end points associated with unstable chromosomal aberrations, persistent genomic instability and apoptosis, we sought to gain insight into the mechanistic developments associated with radiation-induced tumorigenesis and the possible modifying effects of fractionated low-dose exposure via repeated CT scans.

Acute Biological Responses

The biological effects of repeated CT scans after an acute high-dose exposure were determined using commonly investigated end points of carcinogenesis. We chose to focus only on cancer-prone mice, since we have previously examined these same end points in wild-type and *Trp*53$^{+/-}$ mice, comparing the influence of Trp53 status (*58*). Radiation-induced genomic instability, genotoxicity and cytotoxicity were investigated via micronucleated reticulocyte (MN-RET) formation, H2AX phosphorylation and apoptosis, respectively. Micronucleated reticulocytes are an indicator of unstable chromosomal aberrations in hematopoietic stem cells. They are an extremely sensitive biomarker used to enumerate acute genotoxicity or induced genomic instability (*34, 35*). The average lifespan of reticulocytes *in vivo* is only a few days (*59, 60*), thus examining MN-RET frequency in peripheral blood five days after the last CT scan (at 15 weeks after 4 Gy irradiation) allowed for the assessment of indirect damage resulting from on-going radiation-induced genomic instability in precursor stem cells. In the current study, *Trp*53$^{+/-}$ mice irradiated with 4 Gy alone or with 4 Gy followed by repeated CT scans did not have differing MN-RET frequencies relative to age-matched unirradiated controls, suggesting none of the treatment groups experienced prolonged radiation-induced genomic instability in hematopoietic stem cells. This observation contrasts a study performed by Hamasaki *et al*. (*60*) in which it was reported that one year after a single 2.5 Gy X-ray exposure, BALB/c and C57BL/6 mice had significantly elevated MN-RET frequencies. The elevated MN-RET levels in BALB/c and C57Bl/6 were statistically different, which suggests that the discrepancy with the current study is associated with strain and age differences in mouse models (*61*). Phosphorylated H2AX (γ-H2AX) was used as a surrogate biomarker for DNA double-strand breaks (DSBs) (*62, 63*). H2AX histones around DNA DSB sites rapidly phosphorylate early in DNA repair, acting as a scaffold for building DNA repair complexes. Although γ-H2AX is typically a transient measure of DSB repair, protracted expression of γ-H2AX levels can reveal aberrant DNA repair mechanisms and ongoing genomic instability typical of carcinogenesis (*38, 64–66*). After acute γ irradiation, peak levels of γ-H2AX formation occur at approximately 30 min postirradiation, typically decreasing to background levels within 48 h (*67, 68*). In the current study, γ-H2AX levels were measured in lymphocyte-rich bone marrow cell populations five days after the last CT scan. Elevated levels of γ-H2AX fluorescence at this time point correlate with residual DNA DSBs and act as a biomarker of ongoing genomic instability, instead of initial radiation damage (*69*). Constitutive levels of γ-H2AX did not differ between the treatment and control groups, further showing that mice exposed to 4 Gy at 7–8 weeks of age did not develop genomic instability by 15 weeks. Rube *et al*. reported that residual DNA damage depends decisively on the underlying cell ability to repair DNA DSBs (*70*). The absence of increased levels of γ-H2AX may be due to the relatively young age of the mice at the time of irradiation, suggesting they still had sufficient repair capacity to remove radiation-induced DNA damage and mitigate radiation-induced genomic instability. However, some caution should be applied when interpreting these results, since the minimum reported dose detection limit for flow cytometry-based γ-H2AX assay is approximately 100 mGy (*39, 71–74*). To support the mechanistic aspect of adaptive response induction, mouse bone marrow cells harvested at the same time point were challenged *in vitro* with 1 and 2 Gy γ irradiation. There was a significant reduction in γ-H2AX fluorescence levels in mice that received only repeated CT scans, indicating that this CT scan regimen was able to induce an adaptive response. Further investigation into the latent effect of a 4 Gy irradiation on DNA repair mechanisms and ROS/RNS cycles, which are commonly observed after acute irradiation, are required to elucidate this phenomenon.

Radiation-Induced Cancer Late Effects

In the current study, *in vivo* 4 Gy whole-body irradiation was performed on young cancer-prone *Trp*53$^{+/-}$ mice to initiate tumorigenic events. There was a four-week delay before starting the CT scan regimen to allow for the initiation stage of neoplastic transformation to be completed prior to treatment. The goal of this work was to determine if repeated low-dose CT scans could alter cancer risk in the progression stage of tumorigenesis. The hypothesis, based on low-dose literature, was that repeated CT exposures may delay the onset of cancer by altering the progression stage of tumorigenesis. Low-dose exposures have been shown to protect cells against neoplastic transformation when given prior to a subsequent large acute challenge dose (*45, 75*). Acute and chronic low-dose exposures have also been

reported to increase cancer latency and overall lifespan in cancer-prone (*24*), radiation-challenged (*76–78*) and immune-compromised mice (*20, 21, 26*). Moreover, low-dose radiation exposures (<150 mGy per fraction) have been successfully used in clinical trials to treat cancers (*79*).

To our knowledge, this is the first reported study to show that repeated CT scans, when administered specifically during the progression phase of carcinogenesis (i.e., after a high-dose exposure to ionizing radiation), were able to significantly extend the overall lifespan of cancer-prone *Trp*53$^{+/-}$ mice. The main effect was driven by a significant delay in cancer latency of mice with lymphoma and carcinoma. The increase in cancer latency, however, did not extend to sarcoma malignancies. This observation was possibly due to the exceeding of an upper-dose threshold for protective effects that is dependent on tissue type. Mitchel *et al*. (*15*) found that 100 mGy alone was able to significantly extend lymphoma latency but not the latency of osteosarcoma, whereas 10 mGy alone was able to extend both cancer subtype latencies (*23, 80*). Thus, it is arguable that the total dose of repeated CT scans (100 mGy) is beyond the protective upper dose threshold for sarcoma malignancies. We hypothesize that early-onset cancers like radiation-induced lymphoma have a greater potential to benefit from the protective biological modifications induced by the current CT scan regimen than late-onset cancers. Additionally, the intrinsic late development of sarcoma relative to lymphoma may limit the potential of the current low-dose radiation treatment regimen (*25*). However, as carcinoma is also classed as a late-onset cancer, it may be that inborn features of sarcoma development make it less responsive to low-dose radiation treatment. An extended CT scan treatment regimen will need to be examined to determine if it can provide additional benefits to later-onset cancers.

Contrary to concerns raised with the LNT model, the CT regimen in this study did not increase the total frequency of malignancies or the frequencies of the cancer subtypes common to this mouse strain. This observation supports the postulate that low-dose CT exposures do not influence the initiation phase of radiation-induced tumorigenesis, but rather mitigate the progression stage. This finding is in agreement with published literature that has demonstrated low-dose radiation exposure results in significant extensions in cancer latency, with no significant alteration in the frequency of cancer subtypes in *Trp*53$^{+/-}$ mice (*25*). The data from our study provides acute biological evidence to support the hypothesis that low-dose exposures can modify mechanisms associated with genomic instability, consequently altering the progression rate of cells transforming into a fully malignant phenotype.

CONCLUSION

To our knowledge, this is the first reported study to demonstrate that repeated low-dose CT scans given four weeks after high-dose (4 Gy) irradiation increased latency of both early- and late-onset cancers, and reduced biomarkers associated with cancer risk in radiation-challenged, cancer-prone *Trp*53$^{+/-}$ mice. This protective effect is likely associated with anti-oncogenic mechanisms induced by the low-dose exposure, including increased DNA damage surveillance, induction of error-free DNA repair mechanisms and antioxidant upregulation (*17*). Assessment of key biological end points revealed that mice treated with repeated CT scans demonstrated: 1. No observable changes of genomic instability; 2. Resistance to radiation-induced chromosomal aberrations; and 3. Decreased cytotoxicity.

ACKNOWLEDGMENTS

This work was supported by U.S. Department of Energy, Low-dose Research Program (grant no. DE-FG02-07ER64343), Bruce Power and the National Sciences and Engineering Research Council of Canada. Expert technical support was provided by Mary Ellen Cybulski, Lisa Laframboise, Nicole McFarlane and Jackie Ferreira. Chantal Saab and Rod Rhem from the McMaster Center for Preclinical and Translational Imaging provided technical assistance with the computed tomography aspects of the study. Dr. Dean Percy provided expert histopathological analysis of samples.

Received: July 14, 2016; accepted: May 10, 2017; published online: July 25, 2017

REFERENCES

1. Smith-Bindman R, Miglioretti DL, Johnson E, Lee C, Feigelson HS, Flynn, M, et al. Use of diagnostic imaging studies and associated radiation exposure for patients enrolled in large integrated health care systems, 1996–2010. JAMA 2012; 307:2400–9.
2. Brenner DJ, Elliston CD. Estimated radiation risks potentially associated with full-body CT screening. Radiology 2004; 232:735–8.
3. Beyan C, Kaptan K, Ifran A, Ocal R, Ulutin C, Ozturk B. The effect of radiologic imaging studies on the risk of secondary malignancy development in patients with Hodgkin lymphoma. Clin Lymphom Myelom 2007; 7:467–9.
4. Pierobon J, Webber CE, Nayiager T, Barr RD, Moran GR, Gulenchyn KY. Radiation doses originating from diagnostic procedures during the treatment and follow-up of children and adolescents with malignant lymphoma. J Radiolog Prot 2011; 31:83–93.
5. Lin C, Loberiza FR Jr. Low-dose radiation and secondary malignancy: Is there a causal relationship? Clin Lymphom Myelom 2007; 7:450.
6. Brenner DJ. Radiation risks potentially associated with low-dose CT screening of adult smokers for lung cancer. Radiology 2004; 231:440–5.
7. Kim KP, Einstein AJ, Berrington de González A. Coronary artery calcification screening: estimated radiation dose and cancer risk. Arch Intern Med 2009; 169:1188–94.
8. Faletra FF, D'Angeli I, Klersy C, Averaimo M, Klimusina J, Pasotti E, et al. Estimates of lifetime attributable risk of cancer after a single radiation exposure from 64-slice computed tomographic coronary angiography. Heart 2010; 96:927–32.
9. Mossman KL. The LNT Debate in Radiation Protection: Science vs. Policy. Dose Response 2012; 10:190–202.
10. Leonard BE, Leonard VF. Mammogram and diagnostic X-rays–evidence of protective bystander, adaptive response (AR) radio-

protection and AR retention at high dose levels. Int J Radiat Biol 2008; 84:885–99.

11. Feinendegen LE, Pollycove M, Neumann RD. Whole-body responses to low-level radiation exposure: New concepts in mammalian radiobiology. Exp Hematol 2007; 35:37–46.
12. Schollnberger H, Stewart RD, Mitchel RE. Low-let-induced radioprotective mechanisms within a stochastic two-stage cancer model. Dose Response 2006; 3:508–18.
13. Calabrese EJ, Baldwin LA. Tales of two similar hypotheses: the rise and fall of chemical and radiation hormesis. Human Exp Toxicol 2000; 19:85–97.
14. Cramers P, Atanasova P, Vrolijk H, Darroudi F, van Zeeland AA, Huiskamp R, et al. Pre-exposure to low doses: modulation of X-ray-induced DNA damage and repair? Radiat Res 2005; 164:383–90.
15. Mitchel RE. The dose window for radiation-induced protective adaptive responses. Dose Response 2009; 8:192–208.
16. Kataoka T. Study of antioxidative effects and anti-inflammatory effects in mice due to low-dose X-irradiation or radon inhalation. J Radiat Res 2013; 54:587–96.
17. Tang FR, Loke WK. Molecular mechanisms of low dose ionizing radiation-induced hormesis, adaptive responses, radioresistance, bystander effects, and genomic instability. Int J Radiat Biol 2014; 21:1–15.
18. Hildebrant G, Seed MP, Freemantle CN, Alam CA, Colville-Nash PR, Trott KR. Mechanisms of the anti-inflammatory activity of low-dose radiation therapy. Int J Radiat Biol 1998; 74:367–78.
19. Nakatsukasa H, Tsukimoto M, Tokunaga A, Kojima S. Repeated gamma irradiation attenuates collagen-induced arthritis via up-regulation of regulatory T cells but not by damaging lymphocytes directly. Radiat Res 2010; 174:313–24.
20. Ina Y, Tanooka H, Yamada T, Sakai K. Suppression of thymic lymphoma induction by life-long low-dose-rate irradiation accompanied by immune activation in C57BL/6 mice. Radiat Res 2005; 163:153–8.
21. Shin SC, Kang YM, Kim HS. Life span and thymic lymphoma incidence in high- and low-dose-rate irradiated AKR/J mice and commonly expressed genes. Radiat Res 2010: 174: 341–6.
22. Ishii K, Hosoi Y, Yamada S, Ono T, Sakamoto K. Decreased incidence of thymic lymphoma in AKR mice as a result of chronic, fractionated low-dose total-body X irradiation. Radiat Res 1996; 146:582–5.
23. Mitchel REJ, Jackson JS, Morrison DP, Carlisle SM. Low doses of radiation increase the latency of spontaneous lymphomas and spinal osteosarcomas in cancer-prone, radiation-sensitive Trp53 heterozygous mice. Radiat Res 2003; 159:320–7.
24. Mitchel REJ, Jackson JS, McCann RA, Boreham DR. The adaptive response modifies latency for radiation-induced myeloid leukemia in CBA/H mice. Radiat Res 1999; 152:273–9.
25. Mitchel RE, Jackson JS, Carlisle SM. Upper dose thresholds for radiation-induced adaptive response against cancer in high-dose-exposed, cancer-prone, radiation-sensitive Trp53 heterozygous mice. Radiat Res 2004; 162:20–30.
26. Ina Y, Sakai K. Prolongation of life span associated with immunological modification by chronic low-dose-rate irradiation in MRL-lpr/lpr mice. Radiat Res 2004; 161:168–73.
27. Nomura T, Sakai K, Ogata H. Magae J. Prolongation of life span in the accelerated aging klotho mouse model, by low-dose-rate continuous gamma irradiation. Radiat Res 2013; 179:717–24.
28. Phan N, De Lisio M, Parise G, Boreham DR. Biological effects and adaptive response from single and repeated computed tomography scans in reticulocytes and bone marrow of C57BL/6 mice. Radiat Res 2012; 177:164–75.
29. Lemon JA, Phan N, Boreham DR. Single CT scan prolongs survival by extending cancer latency in Trp53 heterozygous mice. Radiat Res 2017; 188:.
30. Tubiana M, Feinendegen LE, Yang C, Kaminski JM. The linear no-threshold relationship is inconsistent with radiation biologic and experimental data. Radiology 2009; 251:13–22.
31. Hinkal G, Parikh N, Donehower LA. Timed somatic deletion of p53 in mice reveals age-associated differences in tumor progression. PLoS One 2009; 4:e6654.
32. Christophorou MA, Ringshausen I, Finch AJ, Swigart LB, Evan GI. The pathological response to DNA damage does not contribute to p53-mediated tumour suppression. Nature 2006; 443:214–7.
33. Marusyk A, Porter CC, Zaberezhnyy V, DeGregori J. Irradiation selects for p53-deficient hematopoietic progenitors. PLoS Biol 2010; 8:e1000324.
34. Dertinger SD, Tsai Y, Nowak I, Hyrien O, Sun H, Bemis JC, et al. Reticulocyte and micronucleated reticulocyte responses to gamma irradiation: dose-response and time-course profiles measured by flow cytometry. Mutat Res 2007; 634:119–25.
35. Dertinger SD, Camphausen K, Macgregor JT, Bishop ME, Torous DK, Avlasevich S, et al. Three-color labeling method for flow cytometric measurement of cytogenetic damage in rodent and human blood. Environ Mol Mutagen 2004; 44:427–35.
36. Lemon JA, Rollo CD, McFarlane NM, Boreham DR. Radiation-induced apoptosis in mouse lymphocytes is modified by a complex dietary supplement: the effect of genotype and gender. Mutagen 2008; 23:465–72.
37. Donehower LA. The p53-deficient mouse: A model for basic and applied cancer studies. Semin Cancer Biol 1996; 7:269–78.
38. Redon CE, Nakamura AJ, Martin OA, Parekh PR, Weyemi US, Bonner WM. Recent developments in the use of gamma-H2AX as a quantitative DNA double-strand break biomarker. Aging 2011; 3:168–74.
39. Rothkamm K, Horn S. Gamma-H2AX as protein biomarker for radiation exposure. Ann Ist Super Sanita 2009; 45:265–71.
40. Little MP. Cancer and non-cancer effects in Japanese atomic bomb survivors. J Radiolog Prot 2009; 29:A43–59.
41. Hendry JH, Simon SL, Wojcik A, Sohrabi M, Burkart W, Cardis E, et al. Human exposure to high natural background radiation: what can it teach us about radiation risks? J Radiolog Prot 2009; 29:A29–42.
42. Preston DL, Cullings H, Suyama A, Funamoto S, Nishi N, Soda M, et al. Solid cancer incidence in atomic bomb survivors exposed in utero or as young children. J Nat Cancer Inst 2008; 100:428–36.
43. Pollycove M, Feinendegen LE. Radiation-induced versus endogenous DNA damage: possible effect of inducible protective responses in mitigating endogenous damage. Human Exp Toxicol 2003; 22:290–323.
44. Ma S, Liu X, Jiao B, Yang Y, Liu X. Low-dose radiation-induced responses: Focusing on epigenetic regulation. Int J Radiat Biol 2010; 86:517–28.
45. Azzam EI, De Toledo SM, Raaphorst GP, Mitchel REJ. Low-dose ionizing radiation decreases the frequency of neoplastic transformation to a level below the spontaneous rate in C3H 10T1/2 cells. Radiat Res 1996; 146:369–73.
46. de Toledo SM, Asaad N, Venkatachalam P, Li L, Howell RW, Spitz DR, Azzam EI. Adaptive responses to low-dose/low-dose-rate gamma rays in normal human fibroblasts: The role of growth architecture and oxidative metabolism. Radiat Res 2006; 166:849–57.
47. Shin SC, Lee KM, Kang YM, Kim K, Lim SA, Yang KH, Kim JY, Nam SY, Kim HS. Differential expression of immune-associated cancer regulatory genes in low-versus high-dose-rate irradiated AKR/J mice. Genomics 2011; 97:358–63.
48. Day TK, Zeng G, Hooker AM, Bhat M, Scott BR, Turner DR, Sykes PJ. Extremely low priming doses of X radiation induce an adaptive response for chromosomal inversions in pKZ1 mouse prostate. Radiat Res 2006; 166:757–66.
49. Maisin JR, Wambersie A, Gerber GB, Mattelin G, Lambiet-Collier M, De Coster B, et al. Life-shortening and disease incidence in

C57Bl mice after single and fractionated gamma and high-energy neutron exposure. Radiat Res 1988; 113:300–17.

50. Fujikawa K, Hasegawa Y, Matsuzawa S, Fukunaga A, Itoh T, Kondo S. Dose and dose-rate effects of X rays and fission neutrons on lymphocyte apoptosis in p53(+/+) and p53(–/–) mice. J Radiat Res 2004; 41:113–27.

51. Ullrich RL, Jernigan MC, Satterfield LC, Bowles ND. Radiation carcinogenesis: Time-dose relationships. Radiat Res 1987; 111:179–84.

52. Storer JB, Ullrich RL. Life shortening in BALB/c mice following brief, protracted, or fractionated exposures to neutrons. Radiat Res 1983; 96:335–47.

53. Grahn D, Lombard LS, Carnes BA. The comparative tumorigenic effects of fission neutrons and cobalt-60 gamma rays in the B6CF1 mouse. Radiat Res 1992; 129:19–36.

54. Maisin JR, Gerber GB, Vankerkom J, Wambersie A. Survival and diseases in C57BL mice exposed to X rays or 3.1 MeV neutrons at an age of 7 or 21 days. Radiat Res 1996; 146:453–60.

55. Thomson JF, Grahn D. Life shortening in mice exposed to fission neutrons and gamma rays. VIII. Exposures to continuous gamma radiation. Radiat Res 1989; 118:151–60.

56. Storer JB, Mitchell TJ. Limiting values for the RBE of fission neutrons at low doses for life shortening in mice. Radiat Res 1984; 97:396–406.

57. Thomson JF, Williamson FS, Grahn D. Life shortening in mice exposed to fission neutrons and gamma rays. V. Further studies with single low doses. Radiat Res 1985; 104:420–8.

58. Lemon JA, Taylor K, Verdecchia K, Phan N, Boreham DR. The influence of Trp53 in the dose response of radiation-induced apoptosis, dna repair and genomic stability in murine haematopoietic cells. Dose Response 2014; 12:365–385.

59. Krzyzanski W, Perez-Ruixo JJ. An assessment of recombinant human erythropoietin effect on reticulocyte production rate and lifespan distribution in healthy subjects. Pharma Res 2007; 24:758–72.

60. Hamasaki K, Imai K, Hayashi T, Nakachi K, Kusunoki Y. Radiation sensitivity and genomic instability in the hematopoietic system: Frequencies of micronucleated reticulocytes in whole-body X-irradiated BALB/c and C57BL/6 mice. Cancer Sci 2007: 98:1840–4.

61. Dertinger SD, Bemis JC, Phonethepswath S, Tsai Y, Nowak I, Hyrien O, et al. Reticulocyte and micronucleated reticulocyte responses to gamma irradiation: Effect of age. Mutat Res 2009; 675:77–80.

62. Samper E, Morgado L, Estrada JC, Bernad A, Hubbard A, Cadenas S, et al. Increase in mitochondrial biogenesis, oxidative stress, and glycolysis in murine lymphomas. Free Rad Biol Med 2009; 46:387–96.

63. Schmielau J, Finn OJ. Activated granulocytes and granulocyte-derived hydrogen peroxide are the underlying mechanism of suppression of T-cell function in advanced cancer patients. Cancer Res 2001; 61:4756–60.

64. Bourton EC, Plowman PN, Smith D, Arlett CF, Parris CN. Prolonged expression of the gamma-H2AX DNA repair biomarker correlates with excess acute and chronic toxicity from radiotherapy treatment. Int J Cancer 2011; 129:2928–34.

65. Nagelkerke A, van Kuijk SJ, Sweep FC, Nagtegaal ID, Hoogerbrugge N, Martens JW, et al. Constitutive expression of gamma-H2AX has prognostic relevance in triple negative breast cancer. Radiother Oncol 2011; 101:39–45.

66. Brunner AH, Hinterholzer S, Riss P, Heinze G, Weiss K, Brustmann H. Expression of gamma-H2AX in endometrial carcinomas: an immunohistochemical study with p53. Gynecolog Oncol 2011; 121:206–11.

67. Beels L, Werbrouck J, Thierens H. Dose response and repair kinetics of gamma-H2AX foci induced by in vitro irradiation of whole blood and T-lymphocytes with X-and gamma-radiation. Int J Radiat Biol 2010; 86:760–8.

68. Groesser T, Chang H, Fontenay G, Chen J, Costes SV, Barcellos-Hoff MH, et al. Persistence of gamma-H2AX and 53BP1 foci in proliferating and non-proliferating human mammary epithelial cells after exposure to gamma-rays or iron ions. Int J Radiat Biol 2011; 87:696–710.

69. Yu T, MacPhail SH, Banath JP, Klokov D, Olive PL. Endogenous expression of phosphorylated histone H2AX in tumors in relation to DNA double-strand breaks and genomic instability. DNA Repair 2006; 5:935–46.

70. Rube CE, Fricke A, Wendorf J, Stutzel A, Kuhne M, Ong MF, Lipp P, Rübe C. Accumulation of DNA double-strand breaks in normal tissues after fractionated irradiation. Int J Radiat Oncol Biol Phys 2010; 76:1206–13.

71. Redon CE, Dickey JS, Nakamura AJ, Kareva IG, Naf D, Nowsheen S, et al. Tumors induce complex DNA damage in distant proliferative tissues in vivo. PNAS 2010; 107:17992–7.

72. MacPhail SH, Banath JP, Yu TY, Chu EH, Lambur H, Olive PL. Expression of phosphorylated histone H2AX in cultured cell lines following exposure to X-rays. Int J Radiat Biol 2003; 79:351–8.

73. MacPhail SH, Banath JP, Yu Y, Chu E, Olive PL. Cell cycle-dependent expression of phosphorylated histone H2AX: Reduced expression in unirradiated but not X-irradiated G1-phase cells. Radiat Res 2003; 159:759–67.

74. Andrievski A, Wilkins RC. The response of gamma-H2AX in human lymphocytes and lymphocytes subsets measured in whole blood cultures. Int J Radiat Biol 2009; 85:369–76.

75. Redpath JL, Antoniono RJ. Induction of an adaptive response against spontaneous neoplastic transformation in vitro by low-dose gamma radiation. Radiat Res 1998; 149:517–20.

76. Elmore E, Lao XY, Kapadia R, Redpath JL. The effect of dose rate on radiation-induced neoplastic transformation in vitro by low doses of low-LET radiation. Radiat Res 2006; 166:832–8.

77. Yonezawa M. Induction of radio-resistance by low dose X-irradiation. Yakugaku Zasshi 2006; 126:833–40.

78. Yonezawa M, Misonoh J, Hosokawa Y. Two types of X-ray-induced radioresistance in mice: Presence of 4 dose ranges with distinct biological effects. Mutat Res 1996; 358:237–43.

79. Sakamoto K. Radiobiological basis for cancer therapy by total or half-body irradiation. Nonlinearity Biol Toxicol Med 2004; 2:293–316.

80. Mitchel REJ, Burchart P, Wyatt H. A Lower Dose Threshold for the in vivo protective adaptive response to radiation. Tumorigenesis in chronically exposed normal and Trp53 heterozygous C57BL/6 mice. Radiat Res 2008; 170:765–75.

RADIATION RESEARCH **188**, 505–511 (2017)
0033-7587/17 $15.00

DOI: 10.1667/RR14576.1

Single CT Scan Prolongs Survival by Extending Cancer Latency in *Trp53* Heterozygous Mice

Jennifer A. Lemon,[a,1] Nghi Phan[b] and Douglas R. Boreham[a]

[a] *Medical Sciences Division, Northern Ontario School of Medicine, Sudbury, Canada, P3E 2C6* [b] *Department of Medical Physics and Applied Radiation Sciences, McMaster University, Hamilton, Canada, L8S 4K1*

Lemon, J. A., Phan, N. and Boreham, D. R. Single CT Scan Prolongs Survival by Extending Cancer Latency in *Trp53* Heterozygous Mice *Radiat. Res.* 188, 505–511 (2017).

There is growing concern over the effects of medical diagnostic procedures on cancer risk. Although numerous studies have demonstrated that low doses of ionizing radiation can have protective effects including reduced cancer risk and increasing lifespan, the hypothesis that any radiation exposure increases cancer risk still predominates. In this study, we investigated cancer development and longevity of cancer-prone *Trp53*$^{+/-}$ mice exposed at 7–8 weeks of age to a single 10 mGy dose from either a diagnostic CT scan or gamma radiation. Mice were monitored daily for adverse health conditions until they reached end point. Although the median lifespan of irradiated mice was extended compared to control animals, only CT scanned mice lived significantly longer than control mice ($P < 0.004$). There were no differences in the frequency of malignant cancers between the irradiated and control groups. Exposure to a single CT scan caused a significant increase in the latency of sarcoma and carcinoma ($P < 0.05$), accounting for the increased lifespan. This study demonstrates that low-dose exposure, specifically a single 10 mGy CT scan, can prolong lifespan by increasing cancer latency in cancer-prone *Trp53*$^{+/-}$ mice. The data from this investigation add to the large body of evidence, which shows that risk does not increase linearly with radiation dose in the low-dose range.

INTRODUCTION

Diagnostic imaging has become an integral part of patient health assessment, providing noninvasive routes to diagnose injury and disease. The use of diagnostic imaging modalities, including computed tomography (CT) scans, has increased exponentially in North America, from 3 million CT procedures in 1980 to greater than 85 million in 2014 (*1*). This increase has raised concern in both the medical and scientific communities regarding the carcinogenic risk associated with the increased exposure to ionizing radiation from these diagnostic procedures (*2–4*). The foundation of radiation risk study calculations is based on the linear no-threshold (LNT) hypothesis, a linear extrapolation of data from high doses that asserts that exposure to any radiation dose, no matter how low, increases cancer risk (*5*, *6*). While it has been established that exposure to large doses of ionizing radiation decreases survival in many organisms (*7–10*), the LNT hypothesis has been invalidated as viable model to predict biological effects of radiation doses below 500 mGy (*11, 12*). At low-dose and low-dose-rate exposures, the biological response to low-dose radiation is not linear, primarily because of the induction of protective mechanisms, which increase high-fidelity DNA repair (*13–15*), improve immune surveillance (*16, 17*) and increase endogenous antioxidant systems (*18–21*). At the whole-organism level, these mechanisms act to reduce the risk of both cancer and non-cancer diseases and prolong survival (*22–30*). The average dose range for a single CT scan (10–30 mGy) falls within the low-dose exposure range (*31–34*). We have previously shown that CT scans reduce markers of DNA damage, increase apoptosis and induce cell cycle arrest when exposed to a large challenge dose of gamma radiation (*35*). Numerous published studies have shown the phenomenon of radiation-induced lifespan extension. In the majority of these studies, the effects of X-ray and γ-ray exposures on tumorigenesis and immune function have been investigated (*11, 27–29, 36, 37*). Mice exposed to a single 100 mGy radiation dose exhibited increased latency for myeloid leukemia induced by a 1 Gy challenge dose (*37*). Immune-compromised mice irradiated at a chronic low-dose rate were shown to live longer than unirradiated mice (*29*). Although the mechanisms associated with the anti-cancer effects of low-dose radiation are unclear, enhanced cellular protection through increased damage surveillance and repair, alterations in apoptosis and augmentation of both innate and adaptive immunity appear to have significant merit (*26, 27, 29, 38–41*). We recently showed that multiple CT scans increased cancer latency in *Trp53*$^{+/-}$ mice by altering mechanisms associated with tumor progression (*51*).

[1] Address for correspondence: Medical Sciences, Northern Ontario School of Medicine, 935 Ramsey Lake Road, Sudbury, Canada, P3E 2C6; email: jlemon@nosm.ca.

Here, we investigate the effects of a single whole-body 10 mGy CT scan on cancer latency and frequency in cancer-prone *Trp*53$^{+/-}$ mice. This cancer-prone mouse model was used to potentiate effects of low-dose radiation and simulate the effects on the radiosensitive subset of the population. We postulate that exposure to a whole-body CT scan induces protective mechanisms known to be stimulated by low-dose irradiation, thereby increasing cancer latency and prolonging lifespan.

MATERIALS AND METHODS

Animal Breeding and Genotyping

Male *Trp*53 heterozygous (B6.129S2-*Trp*53$^{tm1Tyj/+}$) mice and female *Trp*53 homozygous (129X1/SvJ *Trp*53$^{+/+}$), both obtained from Jackson Laboratory (Bar Harbor, ME), were bred to yield F1 *Trp*53$^{+/-}$ (heterozygous) offspring. Offspring were genotyped by PCR (Mouse Genotype Inc., Carlsbad, CA), and approximately 575 *Trp*53$^{+/-}$ F1 female mice were randomly assigned into the experimental groups.

Animal Housing

Mice were maintained in specific-pathogen-free (SPF) housing on a 12 h light:dark photoperiod (23 $\pm$ 2°C). Animals were group housed with no more than five mice per cage; food and water were provided *ad libitum*. All housing, handling and experimental procedures were approved by the Animal Research Ethics Board at McMaster University (Hamilton, Canada) and conducted in accordance to the guidelines of the Canadian Council on Animal Care (Ottawa, Canada). Mice assigned to the lifetime groups were kept to end point and euthanized as required, according to *a priori* criteria in agreement with McMaster ethics policies and previous lifetime mouse studies (*11, 36, 37*).

In Vivo 10 mGy Irradiation

At 7–8 weeks old, *Trp*53$^{+/-}$ female mice were assigned to one of three treatment groups: control (sham irradiated), single 10 mGy CT scan or single 10 mGy γ irradiation (662 keV Cs^{137}). CT scans were performed in the McMaster Centre for Pre-Clinical and Translational Imaging facility, using an X-SPECT animal imaging system (Gamma Medica, Northridge, CA). CT scans were performed at the following settings: 75 kVp, 215 μA, 1 mm aluminum filter, half-value layer 4.28 mm aluminum. For both the CT scan and γ-radiation treatments, pairs of mice were irradiated in a customized polycarbonate tube at 18.6 mGy/min. The mice were irradiated in batches in the first half of the photoperiod and not anaesthetized during irradiation. The control group was handled identically as treatment groups, with the exception of irradiation. After irradiation, mice were returned to SPF housing and monitored until end point.

Computed Tomography Dosimetry

Whole-body irradiation measurements were obtained using thermoluminescence dosimeter (TLD) chips (Harshaw TLD-100™ LiF Chips). TLD chip analyses were performed by a third party specializing in clinical diagnostic radiation measurements (K & S Associates Inc., Nashville, TN). To measure the whole-body absorbed dose in mice, TLD chips were surgically implanted in five locations in a mouse carcass: head, chest, abdomen, above the skin and under the skin. Measurements were performed on six individual carcasses on two separate occasions (before and during the study). The overall uncertainty of the TLD measurement process is 5% at the 95% confidence interval for a single TLD chip at the measurement location. This uncertainty does not take into account minor variations in the placement of the TLD chips among different mouse carcasses. Consistent dosimetry was confirmed and validated repeatedly throughout the study using a 0.6-cc ionizing chamber [PTW Farmer® Dose-meter (model no. 2570A) and PTW Freiburg Ion Chamber (model no. TN30010); PTW, Freiburg, Germany]. Lower energy 75 kVp X rays are less effective at penetrating tissue, resulting in a less uniform dose through tissue thickness relative to 662 keV γ rays. Consequently, mice were exposed to an average whole-body dose as calculated from the TLD data.

Animal Health Assessment

Mice were monitored daily for indications of abnormalities. Objective criteria in accordance with the guidelines of the Canadian Council on Animal Care were set *a priori* to determine the health status and end points for euthanasia. In all cases, treatment status was blinded by the use of coding with respect to animal identification, necropsy reports and histological submissions. For all mice, specific tissues were harvested and fixed in 10% neutral buffered formalin. Vertebrae and heavily mineralized tissues were further processed in an EDTA (145 g/l) solution to allow for proper paraffin embedding. The paraffin blocks were sectioned on a Leica RM 2165 microtome at 3-μm thickness and stained with hematoxylin and eosin for histological examination. All pathologies were diagnosed by an experienced veterinarian pathologist using information from monitoring tags, necropsy reports and histopathological examinations. Blinded repeat histological samples were resubmitted to the pathologist for quality assurance, which demonstrated 100% accuracy. Multiple cancers of the same type found within a mouse were classified as a single observation of that cancer type, since not all primary cancers and metastases can be uniquely distinguished. Conversely, if a mouse had multiple types of cancer, each cancer type was classified separately. In mice with histologically confirmed cancers, the measure of cancer latency in this study was defined as the time immediately after treatment to the time of death/euthanasia (days at risk). In animal studies, obtaining accurate measures of cancer latency is often difficult; internal cancers are diagnosed post-mortem, and may or may not have been the cause of death. The definition of cancer latency in this study permits the evaluation of cancer risk by measuring the days postirradiation that mice have to develop cancer.

Statistical Analyses

Statistical analyses were performed using SigmaPlot™ version 11.0 (Systat® Software Inc., Chicago, IL). Data is presented as median $\pm$ standard error (SE) with $P \leq 0.05$ considered statistically significant. The frequencies of different cancer types in the treatment groups were tested for statistical significance using Fisher's exact test or Chi-squared test. Survival curve probabilities were analyzed using Kaplan-Meier analysis. Differences in overall lifespan and cancer latency (calculated as ''days at risk'' after treatment) were analyzed with the log-rank test. All statistical tests were corrected for multiple comparisons. Survival analyses, except for all-cause mortalities, accounted for competing causes of death via competing risk censoring.

RESULTS

Effects of Single CT Scan and Single Gamma Irradiation on Survival and Cancer Frequency

*Trp*53$^{+/-}$ mice exposed to either a single CT scan or dose of γ radiation had nominally greater lifespans than control mice for all-cause mortalities (Table 1), however, only the median lifespan of CT-scanned mice was significantly extended ($P < 0.004$). At 50% survival, CT scanned mice (502 $\pm$ 11.2 days) lived 18 days longer than control mice

TABLE 1
Longevity of Treatment Groups Based on All-Cause Mortality

Group	Survival (days)					
	Minimum longevity	Maximum longevity	25th Quartile	Median ± SE	Mean ± SE	75th Quartile
Control (n = 99)	134	673	543 ± 7.5	484 ± 7.4	471 ± 7.2	410 ± 9.9
10 mGy CT scanned (n = 188)	171	714	577 ± 7.7, ($P < 0.001$)[a]	502 ± 11.2, ($P < 0.004$)[a]	494 ± 7.5	420 ± 10.0
10 mGy γ irradiated (n = 187)	103	736	545 ± 6.2	499 ± 8.9	478 ± 7.8	420 ± 12.8

Note. No correction required for competing risks.
[a] Statistically significant relative to control group.

(484 ± 7.4 days). This difference increased below the 50% survival level, with CT-scanned mice living 34 days longer than control mice at the 25% survival level (Table 1, Fig. 1; $P < 0.001$). The longevity extension in the γ-irradiated group only reached significance at 5% survival (Fig. 1), with this group obtaining a maximal longevity of 736 days, which was 22 and 63 days longer than CT scanned and control mice, respectively (Table 1). The frequency of total malignant cancers did not differ significantly among any of the treatment groups ($P > 0.140$; Table 2). The proportions of lymphoma and sarcoma cancers between the treatment groups were not significantly different ($P > 0.451$), however, the incidence of carcinoma in the CT scanned group was significantly reduced compared to the other groups ($P < 0.013$). Lymphoma and osteosarcoma are the cancer types most often observed in *Trp*53$^{+/-}$ mice (*42*). All treatment groups developed cancers consistent with this strain of mouse; sarcomas were by far the most prevalent (~70%), followed by lymphomas (~20%) and carcinomas (~10%). Pooled across the groups and uncorrected for competing risks, the median post-treatment lifespans of mice diagnosed with lymphoma, sarcoma and carcinoma did not differ at 469 ± 11.7 days, 461 ± 4.6 days and 471.5 ± 11.3 days, respectively ($P > 0.681$).

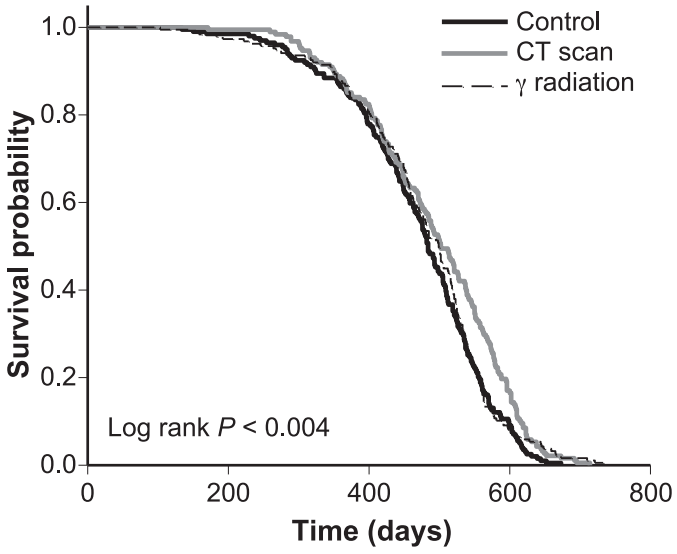

FIG. 1. Comparison of overall survival (all-cause mortality) in control mice relative to mice exposed to 10 mGy CT scan or 10 mGy γ radiation dose.

Effects of Single CT Scan and Single Gamma Irradiation on Lymphoma Frequency and Latency

Although CT scan or γ irradiation did not significantly alter the frequency of lymphoma, relative to the control group ($P < 0.077$; Table 2), there was a trend towards a reduction in both irradiated groups. When accounting for competing causes of death, neither CT scans nor γ irradiations significantly altered the latency of lymphoma development ($P > 0.429$; Fig. 2A).

Effects of Single CT Scan and Single Gamma Irradiation on Sarcoma Frequency and Latency

The frequency of sarcoma subtypes was not altered significantly by either the CT scan or γ radiation ($P > 0.647$). Relative to the control group, treatment with a single 10 mGy CT scan increased the latency of sarcoma development ($P < 0.010$; Fig. 2B). Correcting for competing risks, the median latency of sarcoma in the CT scan treatment group increased by 30 days over the control group (495 ± 10.1 days and 465 ± 7.5 days, respectively), equivalent to a gain of approximately 5 human years (*43*). At the 25% survival level, the difference in sarcoma latency remained greater than 30 days between the CT-scanned group and control group. There was no significant difference in total sarcoma latency between the control and γ-irradiated groups ($P > 0.497$).

Effects of Single CT Scan and Single Gamma Irradiation on Carcinoma Frequency and Latency

The frequency of total carcinomas or its subtypes did not differ between control and γ-irradiated mice ($P > 0.141$; Table 2). Mice treated with a single CT scan had a significantly lower incidence of adenocarcinoma relative to the control and γ-irradiated groups (3, 12 and 14, respectively; $P < 0.046$). When corrected for competing causes of death, CT scans significantly increased the latency of carcinoma, relative to all other groups ($P < 0.016$; Fig. 2C).

TABLE 2
Frequency of Malignant Cancers in *Trp*53$^{+/-}$ Mice: Quantification of Common Cancer Subtypes

Group	Cancer frequency											
	Lymphoma		Sarcoma				Carcinoma					Total cancers (per mouse)[a]
	T-cell	B-cell	Osteo	Hemangio	Fibro	Others	Adeno	Squamous	Basal	Basosquamous	Others	
Control (n = 199)	11	25	104	23	10	16	12	2	2	4	2	211 (1.06)
10 mGy CT scanned (n = 188)	8	37	113	23	10	14	3	4	1	4	2	219 (1.16)
10 mGy γ irradiated (n = 187)	8	35	92	23	14	16	14	2	1	0	3	208 (1.11)

[a] No significant differences in cancer frequencies or number of total cancers among groups ($P > 0.05$).S

DISCUSSION

Although the LNT hypothesis is currently used as the basis for radiation protection policies, significant data has accrued that invalidates this hypothesis at radiation doses below 200 mGy (*6, 17, 18, 22–30*). Numerous radiation exposure and longevity studies involving both animals and humans have been published, which support the notion of beneficial effects of low-dose radiation for cancer and other disease end points (*12, 22*). Recently, it has been reported that in *Trp*53$^{+/-}$ female mice, the life-shortening effect of acute radiation exposure is 38.9 ± 1.9 days per Gy (*10*). Applying the LNT hypothesis, the life-shortening effect from a 10 mGy exposure would be less than a day. Although the statistical power in this study was not sufficient to detect such a small reduction, a reduction was expected based on this extrapolation. Our study showed there was no evidence of lifespan reduction in either CT scanned or γ-irradiated groups. On the contrary, both radiation treatments demonstrated increased lifespan, with only CT scanned mice reaching statistical significance. Currently, the most viable alternative to the LNT is the radiation hormesis model. Although it too has limitations, this hypothesis supports the concept that low-dose radiation could be used to reduce cancer incidence (*22, 23, 44*). Numerous published studies, including this one, support the radiation hormesis model (*39, 40, 44–46*). We have shown that a single whole-body 10 mGy CT scan at 7–8 weeks of age significantly increased the median lifespan in cancer-prone female *Trp*53$^{+/-}$ mice. A similar nonsignificant prolongation of lifespan, relative to control mice, was observed for the 10 mGy γ-irradiated mice. In the same mouse model, Mitchel *et al*. (*11*) also reported a nonsignificant increase in lifespan after 10 mGy γ irradiation. Analysis of cancer latency, as a surrogate measure for cancer risk, in these *Trp*53$^{+/-}$ mice revealed that the observed lifespan extension is due to increased cancer latency, specifically increased sarcoma and carcinoma latency. Mitchel *et al*. have reported similar findings in this *Trp*53$^{+/-}$ mouse model (*11*). They showed that receiving a 10 mGy γ dose reduced cancer risk by increasing the latencies of lymphoma and spinal osteosarcoma. Although 10 mGy γ irradiation in our study did not replicate these results, the discrepancy is likely due to differences in the energy and/or dose rate of the γ exposures. The nonuniform dose of 75 kVp X rays result in higher peripheral doses than the homogeneous γ-ray exposure. This, combined with the significantly lower dose rate than the Mitchel *et al*. study (*11*), are probable explanations for the lack of gamma-radiation-induced effect in this study. The effects of radiation energy and dose rate on longevity have been documented, demonstrating significant moderating effects on the biological impact of absorbed dose (*45, 47–50*).

In the current study, the mechanisms responsible for lifespan extension in CT scanned *Trp*53$^{+/-}$ mice were not elucidated, however, parallel studies indicate that CT scans induce low-level DNA damage, initiating adaptive response mechanisms, increasing apoptosis and presumably eliminating genetically unstable cells (*35*), particularly during the progression stage of tumorigenesis (*51*). Although this study focused on young female *Trp*53$^{+/-}$ mice to maintain consistency with earlier research (*11*), studies related to the current one have been done to examine the effects of CT scans on both sexes and a range of ages of cancer-prone mice, all of which demonstrate similar responses to CT scans (*35, 51, 52*). It is generally assumed that young animals are more radiosensitive than adults (*53, 54*), suggesting lower doses may be required to initiate carcinogenesis, however, it follows that cellular repair and elimination mechanisms should also be more robust at lower doses in young animals. If this is the case, older mice may require higher dose CT scans to achieve similar benefits on cancer latency. Further studies are required, however, to clarify this assumption.

There is a great deal of evidence supporting the upregulation of mechanisms behind the lifespan extension after both acute (*28, 29, 55*) and chronic exposure (*22, 27, 29, 38, 45*) to low doses of radiation. Two key mechanisms that have been highlighted are radiation-induced stimulation of immune functions and radiation-induced protective effects against neoplastic diseases. It has been demonstrated that radiation-enhanced immune responses heighten surveillance, improving elimination of oncogenic cells, thereby restricting the development of neoplastic diseases (*39, 40, 44, 45*). Nowosielska *et al*. demonstrated that BALB/c mice irradiated *in vivo* with a single 100 mGy X-ray dose displayed enhanced anti-tumor reactions mediated by natural killer cells and cytotoxic macrophages when intravenously injected with L1 tumor cells (*44*). Other researchers have shown similar upregulation in immune-mediated anti-neoplastic effects after exposures to X-ray doses as low as 10 mGy (*40, 46*). Low-

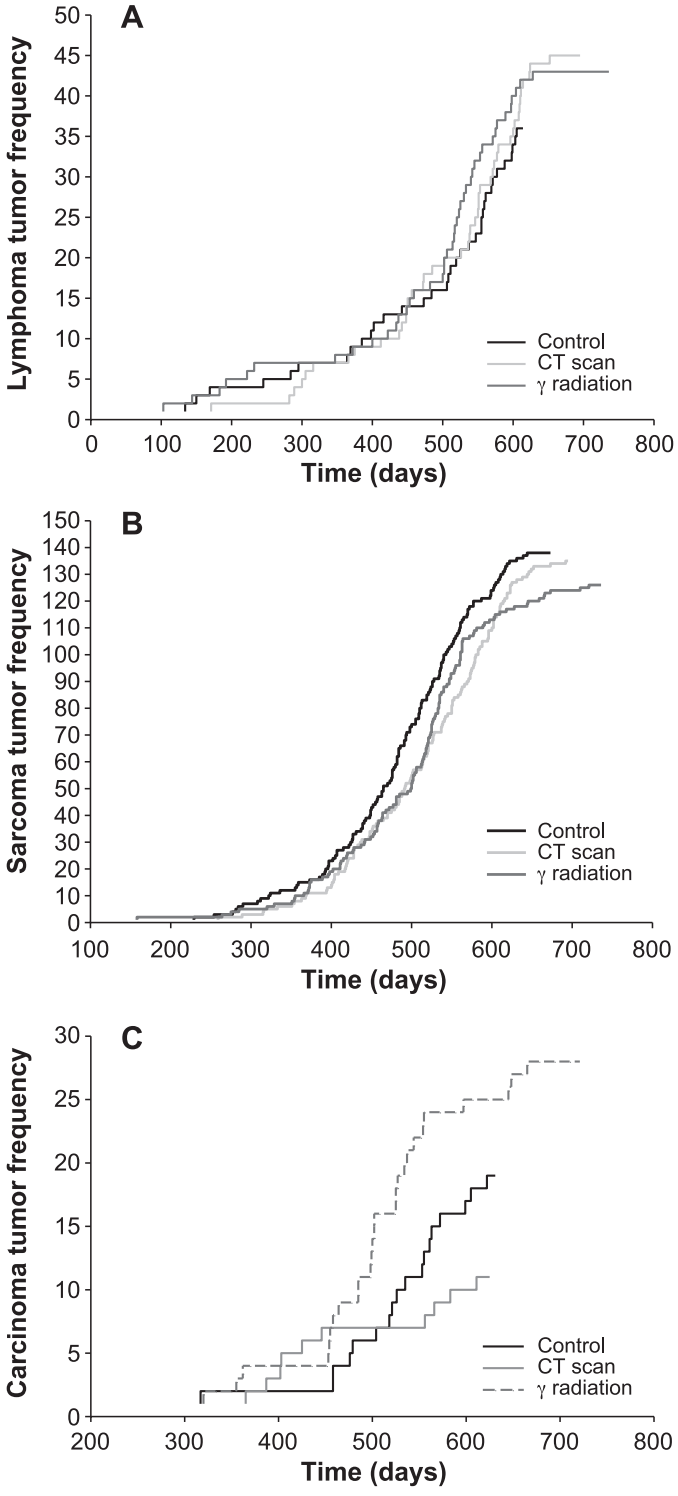

FIG. 2. Comparisons of type-specific tumor frequency in *Trp*53$^{+/-}$ mice. Comparison of control mice and mice exposed to either a single 10 mGy CT scan or a single 10 mGy γ radiation dose. Survival probabilities were corrected for competing causes of death. Panel A: Latency of mice developing lymphoma. Panel B: Latency of mice developing sarcoma. Panel C: Latency of mice developing carcinoma.

dose irradiation of nontransformed cells has been shown to stimulate anti-cancer mechanisms that selectively remove precancerous cells (*39*). At low doses and/or low dose rates, there is evidence that both innate and adaptive immune responses are improved (*38, 41, 45, 50*). Liu *et al.* observed that mice exposed to 75 mGy of X rays had an increase in T-cell function by 212%, relative to unirradiated controls (*38, 41, 56*). James *et al.* reported that mice exposed to doses between 5 and 40 mGy/day increased proliferation of splenic T cells (*57*). More recently, Ina *et al.* demonstrated that chronic lifetime exposure to γ radiation in immune-compromised MRL-*lpr/lpr* mice significantly increased life-span, relative to unirradiated controls (*10*). The prolongation in lifespan was associated with radiation-induced immunological modifications that ameliorated the ensuing autoimmune diseases (*27, 29*). In a follow-up study, the same group reported that low-dose-rate irradiation in various wild-type mouse strains (C57BL/6, BALB/c, C3H/He, DBA/1, DBA/2 and CBA) stimulated an increase in CD4$^+$ T cells and CD8 expression, and improved response to immunization (*38*). In the current study, a single 10 mGy CT scan increased lifespan by delaying the onset of some types of cancer. Others have reported similar delay in cancer latency for radiation-induced myeloid leukemia in CBA/H mice (*37*), and both spontaneous and radiation-induced lymphoma and osteosarcoma in *Trp*53$^{+/-}$ mice (*11, 36*). In the cancer-prone AKR mouse strain, mice irradiated with 50 or 150 mGy three or two times per week, respectively, had greater survival than unirradiated controls due to a reduction in lymphoma incidence (*58*). In the same mouse strain, Shin *et al.* found that mice irradiated with a chronic low-dose rate of 0.7 mGy/h lived significantly longer than unirradiated mice (*45*). Additionally, the incidence of lymphoma was 10% lower in the irradiated mice than unirradiated mice (*59*). Similarly, C57BL/6 mice exposed to continuous whole-body γ radiation for 450 days, starting 35 days before challenging with cancer-inducing exposures totaling 7.2 Gy, had nearly 50% less lymphoma than challenge-only mice (*42*). Despite the differences in experimental design, there appear to be many types of low-dose and/or low-dose-rate exposure regimens that extend longevity in rodent models with cancer end points. This begs the question of whether the same cellular mechanisms were initiated by these diverse modalities. In our study with *Trp*53$^{+/-}$ mice, there were no differences in the frequency and proportions of the cancers that developed among the irradiated and control groups. The lack of effect on cancer frequency, but a delay in cancer latency, is corroborated by previous investigations of the same mouse strain (*11, 36, 51*). Developing upon the idea proposed by Mitchel *et al.* (*36*), and confirmed in our parallel study (*51*), the major effect of a single low-dose radiation exposure in *Trp*53$^{+/-}$ mice is likely due to a delay in the progression, not elimination, of genomic instability associated with endogenous or exogenous cancer-initiating events. Working in concert with the immune-stimulatory effects of low-dose irradiation are the induction of DNA repair processes (*59–61*)

and upregulation of endogenous antioxidants (*62, 63*). Activation of several cellular signal transduction pathways has been associated with radiation-induced adaptive response and low-dose radiation hormesis, including extracellular signal-related kinase (ERK), mitogen-activated protein kinase (MAPK), phospho-c-Jun NH_2-terminal kinase (JNK), protein 53 (Trp53) and ataxia telangiectasia-mutated (ATM) pathways (*24, 64*, *65*). Activation of these signaling pathways induce a diverse range of stress response functions including DNA repair, cell cycle arrest, apoptosis and upregulation of cellular protective mechanisms (*66–68*).

Here we have shown that a low-dose radiation exposure, specifically a single 10 mGy CT scan, can prolong lifespan by reducing cancer risk in radiosensitive, cancer-prone *Trp*$53^{+/-}$ mice. The data from this investigation add to the large body of evidence, which demonstrates that although damage increases linearly with dose, cellular biological responses to radiation-induced damage results in a non-linear risk response to dose in the low-dose range.

ACKNOWLEDGMENTS

This research was supported by U.S. Department of Energy, Low Dose Research Program (grant no. DE-FG02-07ER64343) Bruce Power and the National Sciences and Engineering Research Council of Canada. Expert technical support was provided by Mary Ellen Cybulski, Lisa Laframboise, Nicole McFarlane and Jackie Ferreira. Chantal Saab and Rod Rhem from the McMaster Center for Preclinical and Translational Imaging provided technical assistance with the computed tomography aspects of the study. Dr. Dean Percy provided expert histopathological analysis of samples.

Received: July 14, 2016; accepted: June 2, 2017; published online: July 25, 2017

REFERENCES

1. Health care utilization: diagnostic exams 2014. Paris: The Organisation for Economic Co-operation and Development. (http://bit.ly/1qtVKpJ)
2. Miglioretti DL, Johnson E, Williams A, Greenlee RT, Weinmann S, Solberg LI, et al. The use of computed tomography in pediatrics and the associated radiation exposure and estimated cancer risk. JAMA Pediatr 2013; 167:700–7.
3. Mathews JD, Forsythe AV, Brady Z, Butler MW, Goergen SK, Byrnes GB, et al. Cancer risk in 680,000 people exposed to computed tomography scans in childhood or adolescence: data linkage study of 11 million Australians. BMJ 2013; 346:f2360.
4. Blecher CM. Alarm about computed tomography scans is unjustified. Med J Aust 2010; 192:723–4.
5. Brenner DJ, Sachs RK. Estimating radiation-induced cancer risks at very low doses: Rationale for using a linear no-threshold approach. Radiat Environ Biophys 2006; 44:253–6.
6. Preston RJ. Update on linear non-threshold dose-response model and implications for diagnostic radiology procedures. Health Phys 2008; 95:541–6.
7. Thomson JF, Williamson FS, Grahn D, Ainsworth EJ. Life shortening in mice exposed to fission neutrons and gamma rays I. single and short-term fractionated exposures. Radiat Res 1981; 86:559–72.
8. Thomson JF, Grahn D. Life shortening in mice exposed to fission neutrons and gamma rays. VIII. exposures to continuous gamma radiation. Radiat Res 1989; 118:151–60.
9. Grahn D, Lombard LS, Carnes BA. The comparative tumorigenic effects of fission neutrons and cobalt-60 gamma rays in the B6CF1 mouse. Radiat Res 1992; 129:19–36.
10. Carlisle SM, Burchart PA, Mitchel RE. Cancer and non-cancer risks in normal and cancer-prone Trp53 heterozygous mice exposed to high-dose radiation. Radiat Res 2010; 173:40–8.
11. Mitchel REJ, Jackson JS, Morrison DP, Carlisle SM. Low doses of radiation increase the latency of spontaneous lymphomas and spinal osteosarcomas in cancer-prone, radiation-sensitive Trp53 heterozygous mice. Radiat Res 2003; 159:320–7.
12. Calabrese EJ, Baldwin LA. The effects of gamma rays on longevity. Biogerontol 2000; 1:309–19.
13. Osipov AN, Buleeva G, Arkhangelskaya E, Klokov D. In vivo gamma-irradiation low dose threshold for suppression of DNA double strand breaks below the spontaneous level in mouse blood and spleen cells. Mutat Res 2013; 756:141–5.
14. Shin SC, Kang YM, Kim HS. Life span and thymic lymphoma incidence in high- and low-dose-rate irradiated AKR/J mice and commonly expressed genes. Radiat Res 2010; 174:341–6.
15. Yu L, Bruesewitz MR, Thomas KB, Fletcher JG, Kofler JM, McCollough CH. Optimal tube potential for radiation dose reduction in pediatric CT: principles, clinical implementations, and pitfalls. Radiographics 2011; 31:835–48.
16. Manda K, Glasow A, Paape D, Hildebrandt G. Effects of ionizing radiation on the immune system with special emphasis on the interaction of dendritic and T cells. Front Oncol 2012; 2:102.
17. Arenas M, Sabater S, Hernández V, Rovirosa A, Lara PC, Biete A, et al. Anti-inflammatory effects of low-dose radiotherapy. Indications, dose, and radiobiological mechanisms involved. Strahlenther Onkol 2012; 188:975–81
18. Eldridge A, Fan M, Woloschak G, Grdina DJ, Chromy BA, Li JJ. Manganese superoxide dismutase interacts with a large scale of cellular and mitochondrial proteins in low-dose radiation-induced adaptive radioprotection. Free Radic Biol Med 2012; 53:1838–47.
19. Avti PK, Pathak CM, Kumar S, Kaushik G, Kaushik T, Farooque A, et al. Low dose gamma-irradiation differentially modulates antioxidant defense in liver and lungs of Balb/c mice. Int J Radiat Biol 2005; 81:901–10.
20. Yamaoka K, Kojima S, Nomura T. Changes of SOD-like substances in mouse organs after low-dose X-ray irradiation. Physiol Chem Phys Med NMR 1999; 31:23–8.
21. Kojima S, Matsuki O, Nomura T, Yamaoka K, Takahashi M, Niki E. Elevation of antioxidant potency in the brain of mice by low-dose gamma-ray irradiation and its effect on 1-methyl-4-phenyl-1,2,3,6-tetrahydropyridine (MPTP)-induced brain damage. Free Radic Biol Med 1999; 26:388–95.
22. Vaiserman AM. Radiation hormesis: historical perspective and implications for low-dose cancer risk assessment. Dose-Response 2010; 8:172–191.
23. Doss M. Linear no-threshold model vs. radiation hormesis. Dose Response 2013; 11:480–97.
24. Tang FR, Loke WK. Molecular mechanisms of low dose ionizing radiation induced hormesis, adaptive responses, radioresistance, bystander effects, and genomic instability. Int J Radiat Biol 2014; 30:1–68.
25. Caratero A, Courtade M, Bonnet L, Planel H, Caratero C. Effect of a continuous gamma irradiation at a very low dose on the life span of mice. Gerontology 1998; 44:272–6.
26. Courtade M, Caratero A, Jozan S, Pipy B, Caratero C. Influence of continuous, very low-dose gamma-irradiation on the mouse immune system. Int J Radiat Biol 2001; 77:587–92.
27. Ina Y, Sakai K. Prolongation of life span associated with immunological modification by chronic low-dose-rate irradiation in MRL-lpr/lpr mice. Radiat Res 2004; 161:168–73.
28. Ina Y, Tanooka H, Yamada T, Sakai K. Suppression of thymic lymphoma induction by life-long low-dose-rate irradiation accompanied by immune activation in C57BL/6 mice. Radiat Res 2005; 163:153–8.

29. Ina Y, Sakai K. Further study of prolongation of life span associated with immunological modification by chronic low-dose-rate irradiation in MRL-lpr/lpr mice: effects of whole-life irradiation. Radiat Res 2005; 163:418–23.
30. Spalding JF, Thomas RG, Tietjen GL. Life span of C57 mice as influenced by radiation dose, dose rate, and age at exposure. INIS 1982; 14:1–56.
31. Mettler FA, Jr, Wiest PW, Locken JA, Kelsey CA. CT scanning: patterns of use and dose. J Radiol Prot 2000; 20:353–9.
32. Frush DP, Applegate K. Computed tomography and radiation: Understanding the issues. J Am Coll Radiol 2004; 1:113–9.
33. Fujii K, Aoyama T, Yamauchi-Kawaura C, Koyama S, Yamauchi M, Ko S, Akahane K, Nishizawa K. Radiation dose evaluation in 64-slice CT examinations with adult and paediatric anthropomorphic phantoms. Br J Radiol 2009; 82:1010–8.
34. Shrimpton PC, Hillier MC, Lewis MA, Dunn M. National survey of doses from CT in the UK: 2003. Br J Radiol 2006; 79:968–80.
35. Phan N, De Lisio M, Parise G, Boreham DR. Biological effects and adaptive response from single and repeated computed tomography scans in reticulocytes and bone marrow of C57BL/6 mice. Radiat Res 2012; 177:164–75
36. Mitchel RE, Jackson JS, Carlisle SM. Upper dose thresholds for radiation-induced adaptive response against cancer in high-dose-exposed, cancer-prone, radiation-sensitive Trp53 heterozygous mice. Radiat Res 2004; 162:20–30.
37. Mitchel REJ, Jackson JS, McCann RA, Boreham DR. The adaptive response modifies latency for radiation-induced myeloid leukemia in CBA/H mice. Radiat Res 1999; 152:273–9.
38. Ina Y, Sakai K. Activation of immunological network by chronic low-dose-rate irradiation in wild-type mouse strains: Analysis of immune cell populations and surface molecules. Int J Radiat Biol 2005; 81:721–9.
39. Portess DI, Bauer G, Hill MA, O'Neill P. Low-dose irradiation of non-transformed cells stimulates the selective removal of precancerous cells via intercellular induction of apoptosis. Cancer Res 2007; 67:1246–3.
40. Cheda A, Wrembel-Wargocka J, Lisiak E, Nowosielska EM, Marciniak M, Janiak MK. Single low doses of X rays inhibit the development of experimental tumor metastases and trigger the activities of NK cells in mice. Radiat Res 2004; 161:335–40.
41. Lacoste-Collin L, Jozan S, Cances-Lauwers V, Pipy B, Gasset G, Caratero C, et al. Effect of continuous irradiation with a very low dose of gamma rays on life span and the immune system in SJL mice prone to B-cell lymphoma. Radiat Res 2007; 168:725–32.
42. Jacks T, Remington L, Williams BO, Schmitt EM, Halachmi S, Bronson RT, et al. Tumor spectrum analysis in p53-mutant mice. Curr Biol 1994; 4:1–7.
43. Demetrius L. Aging in mouse and human systems a comparative study. Ann NY Acad Sci 2006;1067: 66–82.
44. Nowosielska EM, Wrembel-Wargocka J, Cheda A, Lisiak E, Janiak MK. Enhanced cytotoxic activity of macrophages and suppressed tumor metastases in mice irradiated with low doses of X-rays. J Radiat Res 2006; 47:229–36.
45. Shin SC, Kang YM, Kim HS. 2010 Life span and thymic lymphoma incidence in high- and low-dose rate irradiated AKR/J mice and commonly expressed genes. Radiat Res 2010; 174:341–6.
46. Cheda A, Nowosielska EM, Wrembel-Wargocka J, Janiak MK. Production of cytokines by peritoneal macrophages and splenocytes after exposures of mice to low doses of X-rays. Radiat Environ Biophys 2008; 47:275–83.
47. Maisin JR, Wambersie A, Gerber GB, Mattelin G, Lambiet-Collier M, De Coster B, et al. Life shortening and disease incidence in C57Bl mice after single and fractionated gamma and high energy neutron exposure. Radiat Res 1988; 113:300–17.
48. Maisin JR, Gerber GB, Vankerkom J, Wambersie A. Survival and diseases in C57BL mice exposed to X-rays or 3.1 MeV neutrons at an age of 7 or 21 days. Radiat Res 1996; 146:453–60.
49. Thomson JF, Williamson FS, Grahn D. Life shortening in mice exposed to fission neutrons and gamma rays. V. Further studies with single low doses. Radiat Res 1985; 104:420–8.
50. Shin SC, Lee KM, Kang YM, Kim K, Lim SA, Yang KH, et al. Differential expression of immune-associated cancer regulatory genes in low- versus high-dose-rate irradiated AKR/J mice. Genomics 2011; 97:358–63.
51. Lemon JA, Phan N, Boreham DR. Multiple CT scans extend lifespan by delaying cancer progression in cancer prone mice. Radiat Res 2017; 188:.
52. Lemon JA, Taylor K, Verdecchia K, Phan N, Boreham DR. The influence of Trp53 in the dose response of radiation-induced apoptosis, dna repair and genomic stability in murine haematopoietic cells. Dose Response 20–14; 12:365–85.
53. Stojkovic R, Fucic A, Ivankovic D, Jukic Z, Radulovic P, Grah J, et al. Age and sex differences in genome damage between prepubertal and adult mice after exposure to ionising radiation. Arh Hig Rada Toksikol 2016; 67:297–303.
54. Casciati A, Dobos K, Antonelli F, Benedek A, Kempf SJ, Belles M, et al. Age-related effects of X-ray irradiation on mouse hippocampus. Oncotarget 2016; 7:28040–58.
55. Calabrese EJ. Overcompensation stimulation: a mechanism for hormetic effects. Crit Rev Toxicol 2001; 31:425–70.
56. Liu SZ, Liu WH, Sun JB. Radiation hormesis: its expression in the immune system. Health Phys 1987; 52:579–83.
57. James SJ, Makinodan T. T cell potentiation in normal and autoimmune-prone mice after extended exposure to low doses of ionizing radiation and/or caloric restriction. Int J Radiat Biol Relat Stud Phys Chem Med 1988; 53:137–52.
58. Ishii K, Hosoi Y, Yamada S, Ono T, Sakamoto K. Decreased incidence of thymic lymphoma in AKR mice as a result of chronic, fractionated low-dose total-body X irradiation. Radiat Res 1996; 146:582–5.
59. Tapio S, Jacob V. Radioadaptive response revisited. Radiat Environ Biophys 2007; 46:1–12.
60. Feinendegen LE, Pollycove M, Neumann RD. Whole-body responses to low-level radiation exposure: New concepts in mammalian radiobiology. Exp Hematol 2007; 35:S37–46.
61. Otsuka K, Koana T, Tauchi H, Sakai K. Activation of antioxidative enzymes induced by low dose-rate whole-body gamma irradiation: Adaptive response in terms of initial DNA damage. Radiat Res 2006; 166:474–8.
62. Pollycove M, Feinendegen LE. Radiation-induced versus endogenous DNA damage: possible effect of inducible protective responses in mitigating endogenous damage. Hum Exp Toxicol 2003; 22:290–323.
63. Feinendegen LE, Pollycove M, Sondhaus CA. Responses to low doses of ionizing radiation in biological systems. Nonlinearity Biol Toxicol Med 2004; 2:143–71.
64. Sasakia MS, Ejimaa Y, Tachibanaa A, Yamadaa T, Ishizakib K, Shimizuc T, et al. DNA damage response pathway in radioadaptive response. Mutat Res Fund Mol Mech Mutagen 2002; 504:101–18
65. Liang X, So YH, Cui J, Ma K, Xu X, Zhao Y, Cai L, Li W. The low-dose ionizing radiation stimulates cell proliferation via activation of the MAPK/ERK pathway in rat cultured mesenchymal stem cells. J Radiat Res 2011; 52:380–6.
66. Feinendegen LE, Pollycove M, Neumann RD. Whole-body responses to low-level radiation exposure: New concepts in mammalian radiobiology. Exp Hematol 2007; 35:37–46.
67. Cramers P, Atanasova P, Vrolijk H, Darroudi F, van Zeeland AA, Huiskamp R, et al. Pre-exposure to low doses: modulation of X-ray-induced dna damage and repair? Radiat Res 2005; 164:383–90.
68. Mitchel REJ. Low doses of radiation are protective in vitro and in vivo: evolutionary origins. Dose Response 2006; 4:75–90.

RADIATION RESEARCH **188**, 512–524 (2017)
0033-7587/17 $15.00

DOI: 10.1667/RR14911.1

REVIEW

The CGL1 (HeLa × Normal Skin Fibroblast) Human Hybrid Cell Line: A History of Ionizing Radiation Induced Effects on Neoplastic Transformation and Novel Future Directions in SNOLAB

Jake S. Pirkkanen,[a,1] Douglas R. Boreham[a,b,c] and Marc S. Mendonca[d,2]

[a] *Department of Biology, Laurentian University, Sudbury, Ontario, Canada, P3E 2C6;* [b] *Northern Ontario School of Medicine, Sudbury, Ontario, Canada, P3E 2C6;* [c] *Bruce Power, Tiverton, Ontario, Canada, N0G 2T0; and* [d] *Department of Radiation Oncology, Radiation and Cancer Biology Laboratories, and Department of Medical & Molecular Genetics, Indiana University School of Medicine, Indianapolis, Indiana 46202*

Pirkkanen, J. S., Boreham, D. R. and Mendonca, M. S. The CGL1 (HeLa × Normal Skin Fibroblast) Human Hybrid Cell Line: A History of Ionizing Radiation Induced Effects on Neoplastic Transformation and Novel Future Directions in SNOLAB. *Radiat. Res*. 188, 512–524 (2017).

Cellular transformation assays have been utilized for many years as powerful *in vitro* methods for examining neoplastic transformation potential/frequency and mechanisms of carcinogenesis for both chemical and radiological carcinogens. These mouse and human cell based assays are labor intensive but do provide quantitative information on the numbers of neoplastically transformed foci produced after carcinogenic exposure and potential molecular mechanisms involved. Several mouse and human cell systems have been generated to undertake these studies, and they vary in experimental length and endpoint assessment. The CGL1 human cell hybrid neoplastic model is a non-tumorigenic pre-neoplastic cell that was derived from the fusion of HeLa cervical cancer cells and a normal human skin fibroblast. It has been utilized for the several decades to study the carcinogenic/neoplastic transformation potential of a variety of ionizing radiation doses, dose rates and radiation types, including UV, X ray, gamma ray, neutrons, protons and alpha particles. It is unique in that the CGL1 assay has a relatively short assay time of 18–21 days, and rather than relying on morphological endpoints to detect neoplastic transformation utilizes a simple staining method that detects the tumorigenic marker alkaline phosphatase on the neoplastically transformed cells cell surface. In addition to being of human origin, the CGL1 assay is able to detect and quantify the carcinogenic potential of very low doses of ionizing radiation (in the mGy range), and utilizes a neoplastic endpoint (re-expression of alkaline phosphatase) that can be detected on both viable and paraformaldehyde fixed cells. In this article, we review the history of the CGL1 neoplastic transformation model system from its initial development through the wide variety of studies examining the effects of all types of ionizing radiation on neoplastic transformation. In addition, we discuss the potential of the CGL1 model system to investigate the effects of near zero background radiation levels available within the radiation biology lab we have established in SNOLAB.

INTRODUCTION

The creation of somatic whole cell hybrids involves the *in vitro* fusion of two different parental eukaryotic cell types to form a karyotypically unique hybrid cell line, which can have significantly different genetic and phenotypic properties from the initial two parental cell types. At the chromosomal and gene levels, the fusion and selection of stable hybrid cell lines frequently involves loss and occasionally gain of chromosomes from one or the other original parental cell genomes. For mammalian cell applications, immortalized rat, mouse, hamster and human hybrids have been developed and utilized since the 1960s (*1–4*). These hybrid eukaryotic cell lines have been useful scientific tools for chromosomal and genomic mapping of many genes including tumor suppressor genes and also important for monoclonal antibody production (*5, 6*). In some of these hybrids, the presence of a selection marker (i.e., antibiotic resistance genes) on a specific human chromosome allowed for preferential loss of a majority of the other human chromosomes in the hybrid and the retention of marked human chromosome. In addition, these various hybrids have allowed investigation of genomic instability after exposure to chemical mutagens or ionizing radiation but were also useful for studying neoplastic transformation or carcinogenicity induced by either chemicals or ionizing radiation (*7–13*). However, over time investigators observed that the rodent intraspecies or

[1] Scholar-in-Training, Radiation Research Society.

[2] Address for correspondence: Department of Radiation Oncology, Radiation and Cancer Biology Laboratories, 541 Clinical Drive, CL-500A, Indiana University School of Medicine, Indianapolis, IN 46202; e-mail: mmendonc@iupui.edu.

interspecies human rodent cellular hybrids, presented numerous challenges including constitutive genomic instability and high spontaneous rates of chromosomal loss after exposure to chemical carcinogens or X rays. Interestingly, several of these original reports suggested that the malignant properties of a neoplastic and normal mouse cellular hybrid were oncogene driven and dominant (*14, 15*), as these cells would produce tumors if introduced into a host. However, other investigators showed evidence of suppression or partial suppression of malignancy in some cell hybrids (*16–21*), suggesting a recessive phenotype indicative of tumor suppressor gene activity (*22–24*). In these experiments some of these hybrid cells would only form tumors when the hybrid cells were injected into mice at very high cell numbers versus their original cancer cell parent. In retrospect, this was probably not clear evidence of complete tumor suppression, because tumors eventually did appear however data strongly suggest that chromosomal loss was likely the causative factor. Indeed, later studies of tumor growth performed with cross species hybrid cells indicated that complete versus partial suppression was due to either the absence or presence of chromosomal instability that over time lead to loss of putative tumor suppressor genes (*22*).

The above referenced studies were critical for setting the standards for the development of human cell based systems to investigate the chromosomal and molecular basis of chemical of radiation-induced neoplastic transformation/carcinogenesis. However, the development of these human cell based neoplastic transformation assays turned out to be technically very difficult because human cells in general are very resistant to chemical and ionizing radiation-induced transformation; and even when transformation did occur the frequency of transformation in human cells as compared to those of rodent origin is reduced by orders of magnitude to 1 in 1 million or 1 in 10 million cells analyzed (*25, 26*). Despite these difficulties, human bronchial and breast epithelial cell based transformation systems were developed to investigate mechanisms of neoplastic transformation after high-LET alpha-particles exposure. These cell systems identified chromosomal changes, allelic imbalances, and candidate tumor suppressor genes such Betaig-H3, integrin $\alpha5\beta1$, p16 and p21(cip1), but *in vitro* quantitative assays for neoplastic transformation with these systems after radiation exposure were simply not technically possible (*27–35*). It was only after the development of the stable human hybrid cell line called CGL1, a fusion of malignant and nonmalignant human cells, were both highly quantitative measurements of ionizing radiation-induced neoplastic transformation frequency and investigation of the cellular and molecular mechanisms involved in radiation-induced neoplastic transformation possible. A summary of some of the major developments in hybrid cells and in the CGL1 human hybrid neoplastic transformation assay are shown in Tables 1 and 2.

CGL1

The CGL1 cell line is a pre-neoplastic nontumorigenic hybrid cell. Stanbridge and colleagues first created the original hybrid cell line called ESH5 from a fusion of the cervical cancer cell line HeLa D98/AH.2 (a $HGPRT^-$ variant) and a normal proliferating diploid male skin fibroblast (GM0077) of human origin in HAT selective medium (*36–38*). After the third subclone, CGL1 was isolated from the ESH5 cells after growth in methycellulose. Genetic and chromosomal analyses revealed that CGL1 was very chromosomally stable with a mode of 96–100 chromosomes on average, and essentially has four copies of each chromosome, i.e., two copies of each chromosome from both the HeLa and the fibroblast parent cells, plus HeLa marker chromosomes (*38*). When injected subcutaneously into nude mice CGL1 is nontumorigenic and remains genetically stable (*38–40*). As opposed to rodent or a non-mammalian source, CGL1 was shown to be stable in tissue culture for that could therefore potentially be used to quantitatively assess neoplastic transformation *in vitro* (*41–46*). Stanbridge *et al*. initial reports of the creation of stable human hybrid cells was subsequently confirmed by others (*36, 47, 48*). The CGL1 hybrid cell failed to grow tumors in nude mice even when injected at cell densities as high as 1×10^7 and provided clear evidence of complete tumor growth suppression, as opposed to partial growth suppression that had been observed by others (*36, 48, 49*). It was initially unclear whether this suppression was due to specific chromosomal or gene loss, but these mechanisms were proposed to likely be contributing factors. The subsequent fusion of a senescent fibroblast cell with an immortal cancer cell resulting in a hybrid with indefinite proliferative capacity was also of great interest because it suggested that the limited ability of normal cells to proliferate indefinitely was a recessive trait (*50, 51*). The characteristics of chromosomal stability, suppression of tumorigenicity, and yet retention of phenotypic properties of transformed cells in culture, made CGL1 potentially advantageous for studying what factors influenced the spontaneous or experimentally induced rates of neoplastic transformation in CGL1 cells.

CHARACTARIZATION OF NONTUMORIGENIC CGL1 AND SPONTANEOUS TUMORIGENIC SEGREGANTS CGL3 AND CGL4

In addition to CGL1, two spontaneously transformed hybrid cell lines were isolated from the original ESH5 hybrid fusion (*38, 52*). Two of these spontaneous tumorigenic hybrid lines named CGL3 and CGL4 displayed unique characteristics including altered cellular morphology that more resembled the epithelial HeLa tumorigenic parental cell than the more fibroblast like CGL1 hybrid. These tumorigenic CGL3 and CGL4 segregants were determined to consistently express a p75/150 antigen

TABLE 1
A Summary of Various Major Developments in Hybrid Cells and CGL1 Human Hybrid Neoplastic Transformation Assays

Year	First author	Event
1962	Barski (14)	Hybridization of somatic mouse cell lines
1965	Harris (1)	Established human × mouse hybrid cell lines
1968	Silagi (128)	Hybridization of two human cell lines
1969	Harris (24)	Fusion of mouse cells to study suppression of malignancy
1969	Chen (129)	First to report mouse cells for studies of malignant transformation
1973	Reznikoff (130)	Establishment of the C3H/10T1/2 assay
1976	Stanbridge (36)	Used two HeLa cells variants (D98/AH-2 and HBU) to study suppression of malignancy.
1980	Stanbridge (52)	Obtained CGL1, CGL2, CGL3 and CGL4 from ESH5 (D98/AH-2 × GM0077 hybrid)
1981	Stanbridge (38)	Studied chromosome stability of human cells hybrids. Identified two chromosomes (11 and 14) that are linked to control of tumorigenic expression
1981	Der (37)	Identified p75-150 as membrane phosphoprotein marker in human hybrid cells
1982	Stanbridge (49)	Analyzed tumorigenicity and transformation of different hybrid human cell lines
1987	Redpath (45)	Developed a quantitative assay for neoplastic transformation with the nontumorigenic human hybrid CGL1 cell line using gamma radiation and established first a dose-response relationship with CGL1
1988	Colman (131)	Compared the radiation sensitives of non-tumorigenic and tumorigenic human hybrid cells lines
1988	Sun (62)	Further characterized the radiation-induced immunoperoxidase based neoplastic transformation assay in CGL1 hybrid cells. Investigated influence of cell density
1989	Mendonca (78)	Defined persistently lower plating efficiency postirradiation and delayed expression of lethal mutations in irradiated CGL1 hybrid cells
1989	Mendonca (70)	Isolated HeLa × normal fibroblasts cells that expressed radiation-induced tumor-associated antigen from irradiated CGL1 hybrid cells
1990	Mendonca (59)	Demonstrated long-term incubation at low extracellular pH lowers radiation-induced neoplastic transformation
1990	Latham (54)	Cloned p75/150 cDNA identifying it as IAP
1991	Mendonca (58)	Isolated CONs and GIMs. Characterization of cells lines, including IAP
1992	Mendonca (57)	Developed Western blue as a staining method for HeLa × normal fibroblast cells
1993	Mendonca (72)	Demonstrated that the induction of the neoplastically transformed foci by radiation was delayed and correlated with the onset of genomic instability and delayed death in the CGL1 hybrid cells
1994	Redpath (132)	Studied the effects of temperature (22°C) on the repair of potentially lethal and potentially transforming damage
1995	Mendonca (133)	Loss of tumor suppressor loci on fibroblast chromosomes 11 is associated with radiation-induced neoplastic transformation of CGL1 hybrid human cells

associated with epithelial morphology, which was determined after subsequent studies to be intestinal alkaline phosphatase (IAP) (*37, 38, 53, 54*). Abnormal regulation of alkaline phosphatases had been previously observed in tumorigenic cell lines and is commonly observed in human tumors (*55, 56*) but IAP was found to be the exclusive isozyme expressed in CGL1 (*57*). The expression of IAP, which was only detected in the HeLa parent cells and the tumorigenic CGL3 and CGL4 hybrids suggested that IAP was a potentially more reliable tumorigenic marker that could potentially be utilized to detect radiation-induced neoplastic transformation of nontumorigenic CGL1 cells since morphological endpoints in this system eventually were determined to be inadequate indicators of neoplastic transformation (*45, 58*).

IAP DETECTION

A major step forward in the utilization of CGL1 in the quantitative assessment of neoplastic transformation frequency was the development of neoplastic transformation assay that used a primary p75 antibody and a secondary immunoperoxidase antibody to detect neoplastically transformed foci among the nontransformed CGL1 cells in T-75 cell culture flasks (*43, 45, 59–62*). However, it was the eventual use of the ''Western Blue'' (WB) method that repurposed the WB dye that contains 5-bromo-4-chloro-3-indolyl-phosphate (BCIP) and nitro blue tetrazolium (NBT) (normally used for Western blots) to directly detect the p75/IAP cellular foci in the transformation flasks, which both greatly simplified and reduced cost of the neoplastically transformed foci detection procedure (*57*). The WB staining method was possible because intestinal alkaline phosphatase, which is expressed in the neoplastically transformed cells enzymatically cleaves the phosphate group of BCIP and the subsequent contact with NBT results in a colored precipitant which can be detected stereo-microscopically. Viable as well as fixed neoplastic transformation cultures of CGL1 cells can be stained and rapidly assessed for neoplastically transformed colonies (*57*). The p75 immunoperoxidase antibody and WB staining procedures have been successfully utilized to quantitatively assess transformation frequency induced by a variety of radiation types, including UV, X ray, gamma ray, neutrons, protons and alpha particles (*44, 45, 58, 62–65*). As stated above, over time it has been demonstrated that the WB method is not only faster and considerably less expensive compared to immunohistochemical and flow cytometry based methods,

TABLE 2
A Summary of Various Major Developments in Hybrid Cells and CGL1 Human Hybrid Neoplastic Transformation Assays

Year	First author	Event
1997	Bettaga (131)	Alpha-particle-induced neoplastic transformation of synchronized CGL1 hybrid human cells
1998	Mendonca (40)	Loss of putative tumor suppressor loci on fibroblast chromosomes 11 and 14 may be required for radiation-induced neoplastic transformation of CGL1 hybrid human cells
1999	Mendonca (75)	Previous loss of fibroblast chromosomes 11 increases radiosensitivity and radiation-induced neoplastic transformation frequency of CGL1 hybrid human cells
1998	Feijter-Rupp (134)	Studied the changes in gap junctional intercellular communication in Human hybrid cell lines. Absence of gap junctions and gap messages was noted and might be related to loss of specific chromosomes
1999	Suzuki (135)	Showed an enhanced expression of glucose transporter GLUT3 in human hybrid cells
1999	Tsujimoto (136)	Studied different gene expression in human hybrid cells
1999	Mendonca (137)	Delayed apoptosis associated with radiation-induced neoplastic transformation of human hybrid cells
2000	Mendonca (138)	Previous loss of fibroblast chromosomes 14 increases radiosensitivity but lowers CGL1 susceptibility to radiation-induced neoplastic transformation frequency
2001	Lewis (77)	Bystander killing induced by medium transfer is cytotoxic and neoplastically transforming to CGL1 human hybrid cells
2002	Frankenberg (139)	Studied neoplastic transformation of CGL1 hybrid cells after irradiation with mammography X rays
2002	Srivatsan (140)	Identified a deletion location of 300Kb interval in chromosome 11q13 in HeLa cells
2004	Mendonca (106)	Detection of homozygous deletions within the 11q13 cervical cancer tumor suppressor locus in radiation-induced, neoplastic transformed CGL1 human hybrid cells
2005	Mendonca (79)	A radiation-induced acute apoptosis precedes the delayed apoptosis and neoplastic transformation of CGL1 hybrid cells
2005	Elmore (103)	Studied neoplastic transformation by low doses of protons in human CGL1 hybrid cells
2007	Mendonca (141)	Inhibition of NF-kB increases radiation sensitivity of CGL1 human hybrid cells
2008	Veena (142)	Inactivation of the Cystatin E/M tumor suppressor gene in cervical cancer
2009	Bettega (143)	Studied neoplastic transformation by carbon ions in human CGL1 hybrid cells

because the WB method does not require large amounts of expensive primary and secondary antibodies, but data also strongly suggests that the higher rates of transformation observed utilizing the WB staining method is due to an increase in the sensitivity of the method to detect low levels of IAP expression (*57*).

THE CGL1 NEOPLASTIC TRANSFORMATION ASSAY

The quantitative assay for studying radiation-induced neoplastic transformation with CGL1 cells was developed by Redpath, Sun, Stanbridge, Colman and Mendonca at the University of California, Irvine, from the mid to late 1980s through early 1990s (*41–46, 57–61, 64, 66–71*). From the outset, the CGL1 assay was meticulously characterized for variables such as: initial CGL1 cell plating densities, serum types and serum concentration, transformation flask refeeding schedules, ionizing radiation dose ranges, time of replating after irradiation into the T-75 transformation flasks, total overall length of incubation to allow foci development, as well as the influence of pH and temperature on foci formation (*41–46, 57–61, 64, 66–71*).

The influence of each of these variables on the frequency of neoplastic transformation observed after various types of radiation exposure is of critical importance and will be summarized here. CGL1 stocks are grown in a standard MEM supplemented with 5% calf serum supplemented with glutamine and antibiotics and an antifungal. It is critical that the cell culture growth media is maintained at pH 7.2, since it was shown that lower acidic pH in the range 6.6–6.8 during the 21-day incubation period to allow foci formation, greatly suppressed the observed radiation-induced neoplastic transformation frequency (*44, 59, 62*). For a standard X-ray or gamma-ray neoplastic transformation assay, subconfluent monolayers of CGL1 cells are irradiated with source and dose of radiation being determined by the investigator. For many of the initial ionizing radiation experiments a range of doses between 0 and 7 Gy of gamma or X ray were utilized to determine dose response. However, many later studies frequently utilized 0 and 7 Gy because higher radiation doses did not result in higher neoplastic transformation frequencies, i.e., a plateau was observed (*43, 45, 59–62*). The irradiated CGL1 cells are incubated for 6 h postirradiation to allow for PLD repair as this was shown to also maximize the observed number of neoplastically foci/transformation frequency per Gy (*43, 45, 59–62*). After 6 h, the cells are harvested by standard cell culture methods, counted and then seeded into T-25 flasks for survival assays and into T-75 tissue culture flasks for the neoplastic transformation assays containing their regular cell culture media. The T-25 flasks are plated separately to determine the plating efficiencies (PEs) of irradiated and unirradiated cells (*44, 58, 62*) by plating 100–1,000 cells in T-25 flasks depending on survival levels after irradiation. Cell numbers seeded will vary depending on dose received and expected cell survival, but in general are plated at 50 cells per square centimeter for the transformation assay and 5 cells per square centimeter for the plating efficiencies (*69, 72*). After seven days, the flasks are fed (growth media is replaced) twice a week leading up to 21 days (*44, 62*). The

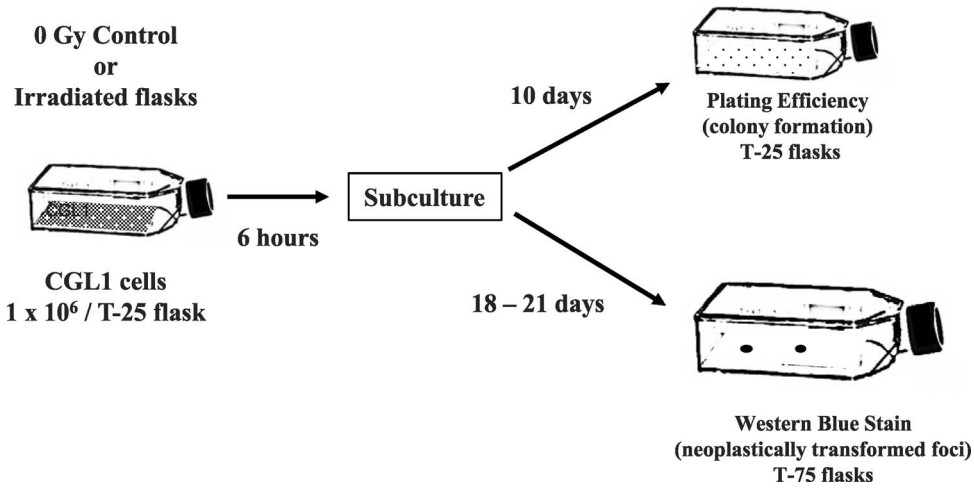

FIG. 1. A general timeline of the CGL1 neoplastic transformation assay.

cells are then fixed in paraformaldehyde, rinsed with PBS and then stained with Western Blue to detect the neoplastically transformed IAP positive colonies (stained foci) via stereomicroscopy. A general timeline of the CGL1 neoplastic transformation assay is shown in Fig. 1. Neoplastic transformation frequency is calculated by counting the number of stained IAP positive foci within each flask and the number of surviving cells in the T-75 transformation flasks calculated from the plating efficiencies. The neoplastic transformation efficiency is calculated by two methods. In the first method, the neoplastic transformation frequency (TF) is calculated by dividing the total number of neoplastically IAP positive foci observed in all the transformation flasks at each radiation dose by the number of total surviving CGL1 cells at that radiation dose (*43, 59*). In the second method, the fraction of transformation flasks containing foci at each radiation dose are calculated by simply diving the number of flasks with foci by the total number of flasks plated at each radiation dose (*43, 59, 73*).

SUMMARIES OF CGL1 RADIATION-INDUCED TRANSFORMATION (TF) ASSAYS GAMMA-RAY DATA

The initial studies of radiation-induced neoplastic transformation of CGL1 were performed with Cs-137 gamma rays. Redpath and colleagues demonstrated that the spontaneous background neoplastic transformation frequencies for the 21-day neoplastic transformation assay with CGL1 cells *in vitro* was variable but in the range of 0.1 to 1 $\times 10^{-5}$ (*44, 57, 62*). Gamma-ray dose response studies at 2, 4, 7 and 10 Gy showed increasing radiation-induced neoplastic transformation frequencies from 1×10^{-4} at 2 Gy, up to 6 to 8 $\times 10^{-4}$ at 7 and 10 Gy. Both the spontaneous and radiation-induced neoplastic transformation frequencies were found to be strongly dependent on initial cell density plated into the transformation flasks, pH of the growth medium, length of incubation period after irradiation before replating for the transformation assay and the total length of the neoplastic transformation assay (*43, 45, 59–62*). In general, the optimal conditions that produced the most consistent results in terms of induction of radiation-induced neoplastic transformation frequency per Gy of ionizing radiation are: 1. wait 6 h postirradiation subconfluent monolayers of CGL1 cells before plating the cells in T-25 flasks for cell survival and into T75 flasks for the neoplastic transformation assay; 2. adjust the plating density of the CGL1 cells in the neoplastic transformation T-75 flasks to 50 cells per cm^2 for the controls at 0 Gy and for each ionizing radiation dose level being investigated; 3. beginning on day 7 or 8 post-plating feed all the transformation flasks two times per week to maintain the pH between 7.2 and 7.4 in the transformation flasks; 4. on day 9 or 10 post-plating fix and stain the T-25 survival flasks with 70% ethanol and crystal violet and count colonies and determine survival at 0 Gy and the various X-ray doses be investigated; 4. on days 19–21 post-plating fix the cell monolayers in the T-75 transformation flasks with paraformaldehyde in PBS and stain with Western Blue to detect the neoplastically transformed IAP positive foci; 5. gently rinse the transformation flasks several times with PBS at pH 7.2 and leave the last PBS rinse in the flasks; 6. visually score each transformation flask for blue neoplastically transformed foci by eye and with a stereomicroscope; 7. calculate transformation frequency by dividing the number of foci detected at the 0 Gy and the various X-ray doses being investigated by the number of total viable cells at risk for the 0 Gy and X-rays doses tested.

KINETICS OF FOCI DEVELOPMENT, DELAYED DEATH AND APOPTOSIS

For several decades, research has been done to investigate the delayed expression/appearance of ionizing radiation-

induced neoplastically transformed foci in CGL1 cell cultures (*69, 72, 74–77*). It was initially proposed that the observed delay in foci formation was due to insensitivity of the detection method, however as previously mentioned, with the advent of the WB staining method this was no longer a plausible explanation. However, during the initial characterization it was shown that plating efficiency in irradiated cells never reaches the same levels as unirradiated cells during the 21-day assay, but reaches a plateau at a lower plating efficiency level at day 9 or 10 and then surprisingly the PE began to significantly decrease for the next 10 days (*72, 74, 78*). A decrease in plating efficiency of unirradiated CGL1 cells in the transformation flasks does not occur during the 21-day assay period. It was eventually shown that this reduction of PE was due to the onset of delayed death or lethal mutations in the progeny of the irradiated CGL1 cells due to the onset of genomic instability(72, 74, 78). Further studies demonstrated that this expression of delayed death and reduction in PE was due to the induction of a novel form of delayed apoptosis involving p53 transcriptional upregulation and induction of the pro-apoptotic BAX mRNA and protein (*74*). It was subsequently shown that that this delay apoptosis was not due to an aberrant acute apoptosis as this was clearly detected in later studies with the CGL1 assay (*79*).

ADAPTIVE RESPONSE AND BYSTANDER EFFECT STUDIES WITH CGL1

The above data with the CGL1 system was focused on relatively high doses of X rays and gamma rays, however there was also strong interest in understanding the radiation biology of very low doses of ionizing radiation and any potential role for bystander or adaptive and protective responses that may be important at lower radiation doses. Adaptive responses are defined to be altered responses that are observed when cells are first exposed to a low dose of radiation and subsequently challenged with a higher dose versus the response observed with the higher radiation dose alone. The first studies into adaptive response in the context of neoplastic transformation showed that a priming low dose radiation exposure changed the efficacy of a challenge dose to induce damage and led to suppression of neoplastic transformation in mouse cell line C3H10T1/2 (*80, 81*). Interestingly, these data also indicated that very low doses of radiation reduced to levels of neoplastic transformation frequency below that of the unirradiated spontaneous controls. Several studies have explored these very low-dose adaptive responses in CGL1 cells (*77, 82–87*). In one of the initial studies, CGL1 cells were irradiated with 1 cGy of gamma radiation and incubated for 24 h (*88*). The transformation frequency was found to be significantly reduced in cultures that had been held for 24 h after receiving a priming dose of 1 cGy as compared to unirradiated controls or cells that had received 1 cGy but had been plated immediately. A later experiment looked at the use of 0.1, 0.5, 5 and 10 cGy of gamma radiation on the effect of neoplastic transformation in CGL1 cells that had similarly been held prior to plating (*82*). It was observed in pooled data that transformation frequency was reduced for the low-dose-irradiated CGL1 cells when compared to sham-irradiated CGL1 cells (*82*). The transfer of cell culture medium from irradiated cell cultures has been shown to reduce survival in to unirradiated cell cultures (*89–91*). This bystander effect has been proposed to occur via cellular gap junction interactions, or excreted cell signal/cytokine based mechanisms (*92–95*). It has been shown in studies that media transfer from irradiated CGL1 cell cultures was able to effect plating efficiencies significantly when transferred to unirradiated CGL1 cells and significantly increased the neoplastic transformation frequency above the CGL1 spontaneous neoplastic transformation frequency (*77*). In addition, the CGL1 bystander study demonstrated that bystander effects were not only cytotoxic but also carcinogenic (*77*).

LOW-DOSE AND DOSE-RATE RADIATION STUDIES

Dose and dose rate as well as radiation type and quality play a crucial role in the biological effects of ionizing radiation. There has long been a scientific interest in the biological effects of ionizing radiation at very low-dose (i.e., $<$100 cGy) and dose-rate exposures for a variety of radiation types. Furthermore, elucidating the effects this has on neoplastic transformation and any potential hormetic response is of significant importance. Some of the first initial low-dose studies utilized the C3H10T1/2 neoplastic transformation model. Investigation of these subtle low-dose effects, that were undetectable in normal cell cultures, were now possible with C3H10T1/2 cells (*81, 96, 97*). These initial low-dose C3H10T1/2 studies (80, 81) explored low dose and adaptive responses with an assortment of doses and dose rates as well as types of radiation, often with nonlinear results. It was shown that a single ionizing radiation (γ ray) dose of 1–100 mGy at a dose rate of 2.4 mGy min^{-1} lowered the frequency of neoplastic transformation below the spontaneous level (*81*). It was also shown that chronic doses (0.1, 0.65 or 1.5 Gy at a dose rate of 0.0024 Gy min^{-1} of γ rays) protected against an acute challenge dose of 4 Gy (X rays). In these studies it was noted that protective level from acute challenge was not dependent on the size of the initial adaptive dose, potentially indicative of a no threshold switch based mechanism (*80*). Analogous studies into these low-dose effects were continued in the CGL1 human hybrid cell system after its development. Similar to C3H10T1/2 model, the CGL1 neoplastic transformation model was found to be an appropriately sensitive system for the detection of very low-radiation-dose effects (*82, 83, 88*), that have not been observed in other tissue culture models (*44, 57*). A range of radiation types, dose rates and doses have been investigated with CGL1 and, as has been reported with the C3H10T1/2

assays, the data demonstrate interesting nonlinear results at low dose and dose rates. For example, in one study, CGL1 cells were exposed to fission spectrum neutrons at two dose rates, 0.22 cGy min^{-1} and 10.7 cGy min^{-1} to achieve a total dose of 45 cGy (*98*). The low-dose rate was determined to be more effective at inducing re-expression of IAP and neoplastic transformation of CGL1 cells without any evidence of increasing cell death. Using the Western Blue detection method, this study showed an inverse dose-rate effect on rates of neoplastic transformation as had been shown previously with fission spectrum neutrons using the older immunohistochemical detection method (*64, 99*). This effect had been originally shown in C3H10T1/2 cells also using fission spectrum neutrons (*100, 101*). In another study, 60kVp X rays at doses of 0, 0.04, 0.1, 0.4, 4.0, 9.0, 18.0 and 36.0 cGy were used to assess neoplastic transformation frequency in CGL1 cells. A significant decrease in transformation frequency was observed at 0.04, 0.1 and 0.4 cGy, as well as at 4.0 and 9.0 cGy (though not significantly) as compared to 0 cGy controls. In an analogous study using the CGL1 model system, gamma radiation (667 KeV photons) from a Cs-137 source showed a similar trend (*82, 88*). Taken together the data indicate that at these very low-radiation doses there is a ''U'' or ''J'' shaped dose-response curve for radiation-induced neoplastic transformation. This suggests that at very low doses of ionizing radiation, the initial decrease in neoplastic transformation frequency investigators have observed may be due to induction of an adaptive/protective hermetic response to very low-dose-radiation exposure, which disappears as the dose of radiation increases. A study of diagnostically and medically relevant levels of X rays (28 kVp) showed suppression of transformation frequency in a dose range of 0.05–10 cGy to levels below that of no dose control exposures (*102*). A study utilizing doses of 0–600 mGy protons (232 MeV) in CGL1 (*103*) further showed evidence of neoplastic transformation suppression at doses up to 50mGy. Interestingly these low-dose and dose-rate U-shaped dose-response curves for neoplastic transformation do not support a linear nonthreshold model. Rather, these data suggest that there appears to be a threshold for which low-dose and dose-rate ionizing radiation in a variety of qualities can suppress transformation.

MECHANISMS OF IR INDUCED NEOPLASTIC TRANSFORMATION OF CGL1 CELLS

Gamma-radiation-induced mutants (GIMs) and control (CON) cell lines were isolated from CGL1 neoplastic transformation assays (58, 70). These GIMS were selected for radiation-induced re-expression of the tumorigenic marker intestinal alkaline phosphatase to further investigation the correlation between IAP expression, tumorigenicity and the molecular mechanisms involved in the radiation-induced expression of CGL1 cells. The GIMS were found to be quite morphologically distinct from CGL1 and while the isolated cell lines all had variable levels of IAP expression, all were found to be tumorigenic when subcutaneously injected into nu/nu nude mice (*58*). The CON cell lines are morphologically quite similar to CGL1 as well as IAP negative and nontumorigenic, but were isolated from 7 Gy gamma-irradiated CGL1 cells. These data indicated that exposure to radiation and any random subsequent chromosomal or genomic changes alone were not sufficient for malignancy, but that re-expression of IAP and the specific underlying chromosomal, genomic, and molecular changes associated with IAP re-expression appeared to be involved. The initial experimental analysis of CGL1 and the subsequent isolated GIM variants suggested that the loss of a single copy of chromosomes 11 and 14 correlated with both IAP re-expression as well as malignancy determined by subcutaneous injection in nu/nu mice (*38, 53, 104, 105*). Previous investigators had shown the microcell mediated transfer of fibroblast chromosome 11 back into the spontaneously arising tumorigenic CGL3 hybrid cells caused a suppression of IAP expression as well as tumorigenicity (*105*). Later work by Mendonca *et al*. found that late-passage subclones of CON1 (*39, 40*) lost one copy of the fibroblast chromosome 11, but were still negative for IAP expression. Analysis of GIM and CON cell lines by RFLP and chromosome painting suggested that both copies of fibroblast chromosome 11 contained a putative tumor suppressor locus, and that the loss or inactivation of both tumor suppressor loci would result in radiation induced neoplastic transformation *in vitro* (*39*). Fine mapping with PCR based markers confirmed loss of one copy of the fibroblast chromosome 11 in the radiation-induced tumorigenic GIMs and evidence of a small 5–20 kB deletion in the remaining copy of the fibroblast chromosome 11 (*106*). These deletion mapping studies identified PACS-1, FRA-1, GAL3ST2 and SF3B2 and RAB1B as candidate tumor suppressor genes (*106*).

FUTURE DIRECTIONS: SNOLAB – AN ULTRA-LOW-DOSE RESEARCH ENVIRONMENT

Life has evolved in the ubiquitous presence of ionizing radiation, from natural sources both terrestrial and cosmic. Terrestrial sources of radiation are radioactive elements found in rocks, soil, water and air. This includes isotopes of uranium, thorium and potassium, as well as their daughter products, predominantly radon gas. Galactic cosmic radiation (GCR) in space largely consists of high-energy particles, positively charged ions and larger nuclei. These cosmic particles produce secondary radiation in the Earth's atmosphere, which can reach the surface of the planet and interact with organisms. This natural background radiation (NBR) pervades the Earth's surface and, as such, is a normal component of biological life. However, NBR levels are dependent on several factors, including altitude, terrestrial geology and geomagnetic field. Annual doses from NBR can range from 2–260 mSv depending on

location, with some evidence suggesting that even within this range of NBR levels biological effects are observable (*107–112*).

Many current radiobiological studies investigate responses to low doses and dose rates of ionizing radiation and these data yield important models for the associated health risks of these exposures. The hypersensitivity model suggests that there is a greater biological risk at lower doses of radiation (*113*). The linear no threshold model proposes that cancer risk increases with radiation dose in a linear relationship while the threshold model infers that below a certain dose there is no increased risk (*114*). The hormetic model suggests that below a given dose, instead of increased risk, the health effects may be prophylactic (*115*). However, all of these models inherently include NBR exposure and consequently there is a deficit in our understanding of the biological effects of ionizing radiation exposure at levels sub-NBR.

Over the last four decades, little has been elucidated about the biological effects of ultra-low NBR environments, although some interesting observations have been published. Work with *Paramecium caudatum* involved cultures grown within lead-shielded chambers designed to minimize GCR (*116*). An inhibition of cellular division and subsequent decrease in growth rate in the cultures was observed as compared to those grown in a basal NBR environment. Furthermore, the attenuated growth rates returned to normal levels when exposed to externally generated radiation at levels and rates analogous to NBR. This work was recently replicated (*117*) and comparable results have also been observed in *Synechococcus lividus* (*118*). These experiments presented an important initial case for the significant stimulatory effect of terrestrial and cosmic NBR on cellular proliferation, with a potential role of ROS considered (*119, 120*). There has been limited use of subterranean laboratory facilities to shield cultures from GCR including work with the extremely radiation-resistant bacteria *Deinococcus radiodurans* (*121*) and diploid yeast *Saccharomyces cerevisiae* (*122*). These cultures were grown underground in the Waste Isolation Pilot Plant (WIPP) in New Mexico, U.S. and the Gran Sasso National Laboratory (LNGS) in Abruzzo, Italy, respectively. The trend among these different model systems grown in sub-NBR environments is of negative biological effects in terms of growth rate and susceptibility to challenge with chemical and radiological stressors (*123*). One of the most significant gaps in these limited data is the insufficient amount of experimentation with mammalian cells, though a few preliminary experiments have been performed. Chinese hamster V79 and Human lymphoblastoid TK6 cells grown underground in LNGS and WIPP were shown to have decreased cell density, lowered ROS scavenging, increased background and induced mutation rate, increased apoptotic sensitivity, greater micronuclei formation and increased expression of certain heat shock proteins (*122, 124–126*).

Although these findings are important to begin to understand the biological effects of sub-NBR exposure, there is significant variation between research groups in terms of the model organism used, type of shielding and level below NBR achieved experimentally. One of the most significant factors behind the dearth of empirical data is simply the scarcity of facilities that can accommodate this type of research. However, it is unquestionable that the ideal location to perform this type of research is underground, rather than at the surface of the planet where GCR contamination is intrinsic. Located approximately 30 km from Laurentian University and The Northern Ontario School of Medicine (NOSM) in Sudbury, ON, Canada, there exists a world-class Canadian research facility that has been specifically engineered and constructed to effectively eradicate GCR. The Sudbury Neutrino Observatory (SNOLAB) is a Nobel Prize winning astroparticle physics laboratory located in Vale's active Creighton Nickel Mine and has the deepest and lowest NBR biological research laboratory environment in the world. Situated 2 km (6,800 ft.) underground, it is incomparable to any other facility in terms of depth and proximity to Laurentian University and NOSM. The facility is comprised of 5,000 m^2 of Class 2000 clean room (maximum 2×10^3 particles ≥ 0.5 μm/ft^3) located within norite rock, which consists of 1% stable K^{39} (~0.001% radioactive K^{40}), 0.13 ppm uranium and 5.56 ppm thorium (*126*). The 2,070 m of rock overburden above SNOLAB provides within the facility an attenuated muon flux of 3×10^{-6} m^{-2} s^{-1}, a thermal neutron flux of 4.7×10^{-2} m^{-2} s^{-1} and a fast neutron flux of 4.6×10^{-2} m^{-2} s^{-1} (*126*). This translates to approximately 50 million times less GCR than would be measured at the surface. Radon gas (Rn^{222}) is the most profuse and challenging radiological issue facing sub-NBR experiments underground and is present within SNOLAB at an average level of approximately 130 Bq m^{-3}. Attempts to keep radiological contamination of terrestrial origin are a major priority within the facility, as the ore dust in the active mine located outside of the facility contains approximately 60 mg g^{-1} Fe, 1.1 μg g^{-1} U and about 5.6 μg g^{-1} Th (*127*). This is achieved, in part, by 10 full HEPA filtered air exchanges h^{-1} within SNOLAB. This air is scrubbed and recirculated to help reduce increased radon emanation (*126*). Additionally, there is an 8.0-mm thick polymer coating over the rock walls within SNOLAB to further address this issue (*126*). Low levels of neutrons and gamma rays still infiltrate via this polymer coating through spontaneous fission of elements radioactive decay, but remain at levels still far below surface NBR.

FUTURE DIRECTIONS: CGL1 ULTRA-LOW-DOSE STUDIES

We propose to utilize the exceptional ultra-low ionizing sub-NBR environment that SNOLAB offers to quantitatively assess biological effects in an established human

tissue culture model. The working hypothesis is that ionizing NBR promotes and maintains genomic stability through highly conserved adaptive response mechanisms and that the absence of which will lead to reduced cell growth, increased neoplastic transformation rates, sensitivity to oxidative stress and higher baseline levels of DNA damage. The CGL1 cell line is an ideal tissue culture system for quantitatively investigating the biological effects of an ultra-low-dose radiation environment. We propose to use CGL1 cells to whether growth in the ultra-low-background radiation available in SNOLAB influences CGL1 population doubling time, plating efficiency, spontaneous levels of DNA damage repair by micronucleus formation and γH2AX formation assays and spontaneous levels of neoplastic transformation in CGL1 cells grown underground in SNOLAB compared to CGL1 cells kept at the surface control laboratory space. If we observe differences in the CGL1 cells grown at ultra-low-dose radiation levels down in SNOLAB versus CGL1 cells grown natural background radiation (NBR) levels at the surface lab, we will evaluate gene expression differences by cDNA microarray and quantitative RT-qPCR assays to observe regulatory changes that may occur as culture time in the sub-NBR increases analyses and determine the genetic and epigenetic mechanisms driving these changes and will provide important mechanistic information in the evaluation of how ultra-low doses of radiation alter CGL1 cells. The Western Blue based CGL1 cell neoplastic transformation assay is highly sensitive and has been used to detect very small changes spontaneous transformation frequency when the cells are irradiated with a few mGy of ionizing radiation (*82, 83, 85, 87, 88, 103*). Therefore, we propose that in the ultra-low radiation environment that SNOLAB provides, the CGL1 based transformation assay is ideal to detect small changes in spontaneous background neoplastic transformation frequency.

SNOLAB's ultra-low-dose sub-NBR environment and close proximity to both Laurentian University and Northern Ontario School of Medicine provide the ideal environment for the recently established ''Researching the Effects of the Presence and Absence of Ionizing Radiation'' (REPAIR) project. These facilities will allow us to test whether CGL1 cells, adapted to the ultra-low-dose NBR environment underground, will alter either the spontaneous, X ray and/or radon-induced levels of neoplastic transformation and the cellular and molecular mechanisms involved. CGL1 cell growth rate, micronucleus and γ-H2AX, changes in gene expression, rates of neoplastic transformation and capacity to react to changes in oxidative stress levels will be assessed in sub-NBR adapted CGL1 cells grown underground in SNOLAB versus the CGL1 cells kept at surface NBR doses. We strongly believe that the resulting SNOLAB data will be of high scientific value and will contribute to a better understanding of ultra-low-dose radiation biology.

ACKNOWLEGDMENTS

The REPAIR project is financially supported through an industrial research grant from Bruce Power, the Mitacs Accelerate program and the Natural Sciences and Research Council of Canada.

Received: August 8, 2017; accepted: August 17, 2017; published online: September 5, 2017

REFERENCES

1. Harris H, Watkins JF. Hybrid cells derived from mouse and man: artificial heterokaryons of mammalian cells from different species. Nature 1965; 205:640–6.
2. Harris H, Watkins JF, Ford CE, Schoefl GI. Artificial heterokaryons of animal cells from different species. J Cell Sci 1966; 1(1):1–30.
3. Weiss MC, Green H. Human-mouse hybrid cell lines containing partial complements of human chromosomes and functioning human genes. Proc Natl Acad Sci U S A 1967; 58(3):1104–11.
4. Matsuya Y, Green H, Basilico C. Properties and uses of human-mouse hybrid cell lines. Nature 1968; 220(5173):1199–202.
5. Yagami H, Kato H, Tsumoto K, Tomita M. Monoclonal antibodies based on hybridoma technology. Pharmaceutical Patent Analyst 2013; 2(2):249–63.
6. Zhang C. Hybridoma technology for the generation of monoclonal antibodies. Meth Mol Biol 2012; 901:117–35.
7. Kim GJ, Chandrasekaran K, Morgan WF. Mitochondrial dysfunction, persistently elevated levels of reactive oxygen species and radiation-induced genomic instability: a review. Mutagenesis 2006; 21(6):361–7.
8. Smith LE, Nagar S, Kim GJ, Morgan WF. Radiation-induced genomic instability: radiation quality and dose response. Health Phys 2003; 85(1):23–9.
9. Limoli CL, Giedzinski E, Morgan WF, Swarts SG, Jones GD, Hyun W. Persistent oxidative stress in chromosomally unstable cells. Cancer Res 2003; 63(12):3107–11.
10. Limoli CL, Ponnaiya B, Corcoran JJ, Giedzinski E, Kaplan MI, Hartmann A, et al. Genomic instability induced by high and low LET ionizing radiation. Adv Space Res 2000; 25(10):2107–17.
11. Morgan WF, Day JP, Kaplan MI, McGhee EM, Limoli CL. Genomic instability induced by ionizing radiation. Radiat Res 1996; 146(3):247–58.
12. Morgan WF, Murname JP. A role for genomic instabiltiy in cellular radioresistance? Cancer Metastasis Rev 1995; 14(1): 49–58.
13. Marder BA, Morgan WF. Delayed chromosomal instabiltiy induced by DNA damage. Mol Cell Biol 1993; 13(11):6667–77.
14. Barski G, Cornefert F. Characteristics of ''hybrid''-type clonal cell lines obtained from mixed cultures in vitro. J Natl Cancer Inst 1962; 28:801–21.
15. Scaletta LJ, Ephrussi B. Hybridization of normal and neoplastic cells in vitro. Nature 1965; 205(4977):1169.
16. Harris H. Suppression of malignancy by cell fusion. Nature 1969; 223:363–8.
17. Bregula U, Klein G, Harris H. The analysis of malignancy by cell fusion. II. Hybrids between Ehrlich cells and normal diploid cells. J Cell Sci 1971; 8:673–80.
18. Wiener F, Klein G, Harris H. The analysis of malignancy by cell fusion. 3. Hybrids between diploid fibroblasts and other tumour cells. J Cell Sci 1971; 8:681–92.
19. Klein G, Friberg S, Wiener F, Harris H. Hybrid cells derived from fusion of TA3-Ha ascites carcinoma with normal fibroblasts. 1. Malignancy, karyotype, and formation of isoantigenic variants. J Natn Cancer Inst 1973; 50:1259–68.
20. Wiener F, Klein G, Harris H. The analysis of malignancy by cell

fusion. IV. Hybrid between tumour cells and a malignant L cell derivative. J Cell Sci 1973; 12:253–61.

21. Wiener F, Klein G, Harris H. The analysis of malignancy by cell fusion. V. Further evidence of the ability of normal diploid cells to suppress malignancy. J Cell Sci 1974; 15:177–83.

22. Sabin AB. Suppression of malignancy in human cancer cells: issues and challenges. Proc Natl Acad Sci U S A 1981; 78(11): 7129–33.

23. Ephrussi B, Davidson RL, Weiss MC, Harris H, Klein G. Malignancy of somatic cell hybrids. Nature 1969; 224(5226): 1314–6.

24. Harris H, Miller OJ, Klein G, Worst P, Tachibana T. Suppression of malignancy by cell fusion. Nature 1969; 223(5204):363–8.

25. Borek C. X-ray induced in vitro neoplastic transformation of human diploid cells. Nature 1980; 283(5749):776–8.

26. Borek C. Cellular and molecular mechanisms in malignant transformation of diploid rodent and human cells by radiation. Carcinog Compr Surv 1985; 9:365–78.

27. Li H, Gu Y, Miki J, Hukku B, McLeod DG, Hei TK, et al. Malignant transformation of human benign prostate epithelial cells by high linear energy transfer alpha-particles. Int J Oncol 2007; 31(3):537–44.

28. Roy D, Calaf G, Hei TK. Role of vitamin D receptor gene in radiation-induced neoplastic transformation of human breast epithelial cell. Steroid 2003; 68(7-8):621–7.

29. Zhao YL, Piao CQ, Hei TK. Overexpression of Betaig-h3 gene downregulates integrin alpha5beta1 and suppresses tumorigenicity in radiation-induced tumorigenic human bronchial epithelial cells. Br J Cancer 2002; 86(12):1923–8.

30. Zhao YL, Piao CQ, Hall EJ, Hei TK. Mechanisms of radiation-induced neoplastic transformation of human bronchial epithelial cells. Radiat Res 2001; 155(1 Pt 2):230–4.

31. Suzuki M, Piao CQ, Zhao YL, Hei TK. Karyotype analysis of tumorigenic human bronchial epithelial cells transformed by chrysolite asbestos using chemically induced premature chromosome condensation technique. Int J Mol Med 2001; 8(1):43–7.

32. Roy D, Calaf G, Hei TK. Frequent allelic imbalance on chromosome 6 and 17 correlate with radiation-induced neoplastic transformation of human breast epithelial cells. Carcinogenesis 2001; 22(10):1685–92.

33. Piao CQ, Zhao YL, Hei TK. Analysis of p16 and p21(Cip1) expression in tumorigenic human bronchial epithelial cells induced by asbestos. Oncogene 2001; 20(50):7301–6.

34. Hei TK, Zhao YL, Roy D, Piao CQ, Calaf G, Hall EJ. Molecular alterations in tumorigenic human bronchial and breast epithelial cells induced by high LET radiation. Adv Space Res 2001; 27(2): 411–9.

35. Willey JC, Hei TK, Piao CQ, Madrid L, Willey JJ, Apostolakos MJ, et al. Radiation-induced deletion of chromosomal regions containing tumor suppressor genes in human bronchial epithelial cells. Carcinogenesis 1993; 14(6):1181–8.

36. Stanbridge EJ. Suppression of malignancy in human cells. Nature 1976; 260:17–20.

37. Der CJ, Stanbridge EJ. A tumor-specific membrane phosphoprotein marker in human cell hybrids. Cell 1981; 26:429–38.

38. Stanbridge EJ, Flandermeyer RR, Daniels DW, Nelson-Rees WA. Specific chromosome loss associated with the expression of tumorigenicity in human cell hybrids. Somatic Cell Genetics 1981; 7(6):699–712.

39. Mendonca MS, Fasching CL, Srivatsan ES, Stanbridge EJ, Redpath JL. Loss of a putative tumor suppressor locus after gamma-ray-induced neoplastic transformation of HeLa x skin fibroblast human cell hybrids. Radiat Res 1995; 143(1):34–44.

40. Mendonca MS, Howard K, Fasching CL, Farrington DL, Desmond LA, Stanbridge EJ, et al. Loss of suppressor loci on chromosomes 11 and 14 may be required for radiation-induced neoplastic transformation of HeLa x skin fibroblast human cell hybrids. Radiat Res 1998; 149(3):246–55.

41. Redpath JL, Sun C, Colman M, Stanbridge EJ. Radiobiological studies of human hybrid cells (skin fibroblasts x HeLa) and their tumorigenic segregants. Int J Radiat Biol 1985; 48(4):479–83.

42. Sun C, Redpath JL, Colman M, Stanbridge EJ. Repair of potentially lethal radiation damage in confluent and non-confluent cultures of human hybrid cells. Int J Radiat Biol 1986; 49(3):395–402.

43. Redpath JL. Radiation-induced neoplastic transformation of human cell hybrids. In: Cerutti PA, Nygaard OF, Simic MG, editors. Anticarcinogenesis and Radiation Protection. New York: Plenum Press; 1987. p. 335–40.

44. Redpath JL, Sun C, Colman M, Stanbridge EJ. Neoplastic transformation of human hybrid cells by gamma radiation: a quantitative assay. Radiat Res 1987; 110(3):468–72.

45. Redpath JL. Radiation-Induced Neoplastic Transformation of Human Cell Hybrids. In: Cerutti PA, Nygaard OF, Simic MG, editors. Anticarcinogenesis and Radiat Protection. Boston, MA: Springer US; 1988. p. 335–40.

46. Sun C, Redpath JL, Colman M, Stanbridge EJ. Further studies on the radiation-induced expression of a tumor-specific antigen in human cell hybrids. Radiat Res 1988; 114:84–93.

47. Klinger HP, Baim AS, Eun CK, Shows TB, Ruddle FH. Human chromosomes which affect tumorigenicity in hybrids of diploid human with heteroploid human or rodent cells. Cytogenetics Cell Genetics 1978; 22(1-6):245–9.

48. Klinger HP. Suppression of tumorigenicity in somatic cell hybrids. I. Suppression and reexpression of tumorigenicity in diploid human X D98AH2 hybrids and independent segregation of tumorigenicity from other cell phenotypes. Cytogenetics Cell Genetics 1980; 27(4):254–66.

49. Stanbridge EJ, Der CJ, Doersen CJ, Nishimi RY, Peehl DM, Weissman BE, et al. Human cell hybrids: analysis of transformation and tumorigenicity. Science 1982; 215(4530):252–9.

50. Schneider JA. Somatic cell hybridization as a tool for studying the metabolic disease cystinosis. Birth Defects 1973; 9:160–8.

51. Norwood TH, Pendergrass WR, Sprague CA, Martin GM. Proc natn Acad Sci USA 1974; 71:2231–5.

52. Stanbridge EJ, Wilkinson J. Dissociation of anchorage independence form tumorigenicity in human cell hybrids. Int J Cancer 1980; 26(1):1–8.

53. Srivatsan ES, Benedict WF, Stanbridge EJ. Implication of chromosome 11 in the suppression of neoplastic expression in human cell hybrids. Cancer Res 1986; 46:6174–9.

54. Latham KM, Stanbridge EJ. Identification of the HeLa tumor-associated antigen, p75/150, as intestinal alkaline phosphatase and evidence for its transcriptional regulation. Proc Natl Acad Sci U S A 1990; 87:1263–7.

55. Millan JL. Oncodevelopmental expression and structure of alkaline phosphatase genes. Anticancer Res 1988; 8(5A): 995–1004.

56. Harris H. The human alkaline phosphatases: what we know and what we don't know. Int J Clin Chem 1990; 186(2):133–50.

57. Mendonca MS, Antoniono RJ, Sun C, Redpath JL. A simplified and rapid staining method for the HeLa x skin fibroblast human hybrid cell neoplastic transformation assay. Radiat Res 1992; 131(3):345–50.

58. Mendonca MS, Antoniono RJ, Latham KM, Stanbridge EJ, Redpath JL. Characterization of intestinal alkaline phosphatase expression and the tumorigenic potential of gamma-irradiated HeLa x fibroblast cell hybrids. Cancer Res 1991; 51(16): 4455–62.

59. Mendonca MS, Sun C, Redpath JL. Suppression of radiation-induced neoplastic transformation of human cell hybrids by long term incubation at low extracellular pH. Cancer Res 1990; 50(7): 2123–7.

60. Redpath JL, Sun C, Mendonca MS, Colman M, Stanbridge EJ, editors. The application of a human hybrid cell system to studies of radiation induced neoplastic cell transformation: quantitative, cellular, and molecular aspects. Proceedings of Workshop on Cell Transformation Systems Relevant to Radiation Induced Cancer in Man. 1989 April; Dublin.

61. Sun C, Colman M, Redpath JL. Suppression of the radiation-induced expression of a tumor-associated antigen in human cell hybrids by the protease inhibitor antipain. Carcinogenesis 1988; 9(12):2333–5.

62. Sun C, Redpath JL, Colman M, Stanbridge EJ. Further studies on the radiation-induced expression of a tumor-specific antigen in human cell hybrids. Radiat Res 1988; 114(1):84–93.

63. Redpath JL, Sun C. UVC-induced expression of a tumor-associated antigen in human cell hybrids (HeLa X skin fibroblasts): repair of potentially lethal and potentially transforming damage. Carcinogenesis 1989; 10(4):723–6.

64. Redpath JL, Hill CK, Jones CA, Sun C. Fission-neutron-induced expression of a tumour-associated antigen in human cell hybrids (HeLa x skin fibroblasts): evidence for increased expression at low dose rate. Int J Radiat Biol 1990; 58(4):673–80.

65. Pant MC, Liao XY, Lu Q, Molloi S, Elmore E, Redpath JL. Mechanisms of suppression of neoplastic transformation in vitro by low doses of low LET radiation. Carcinogenesis. 2003; 24(12):1961–5.

66. Redpath JL, Sun C, Colman M, Stanbridge EJ. Neoplastic transformation of human hybrid cells by irradiation: A quantitiative assay. Radiat Res 1987; 110:468–72.

67. Colman M, Bahtt S, Candelaria M, Sun C, Redpath JL. A comparison of the radiation sensitivities of non-tumorigenic and tumorigenic human hybrid cell lines. Int J Radiat Biol 1988; 53(4):609–16.

68. Sun C, Redpath JL. Application of a freeze-thaw technique to studies of radiation-induced cell transformation. Int J Radiat Biol 1988; 54:825–7.

69. Mendonca MS, Kurohara W, Antoniono R, Redpath JL. Plating efficiency as a function of time post-irradiation: Evidence for the delayed expression of lethal mutations. Radiat Res 1989; 119:389–93.

70. Mendonca MS, Redpath JL. Isolation of human cell hybrids (HeLa x skin fibroblast) expressing a radiation-induced tumour-associated antigen. Br J Cancer 1989; 60(3):324–6.

71. Redpath JL, Sun C, Blakely WF. Effect of fission-neutron dose rate on th induction of a tumor associated antigen in human cell hybrids (HeLa X skin fibroblasts). Radiat Res 1991; 128:S71.

72. Mendonca MS, Antoniono RJ, Redpath JL. Delayed heritable damage and epigenetics in radiation-induced neoplastic transformation of human hybrid cells. Radiat Res 1993; 134(2):209–16.

73. Kennedy AR, Cairns J, Little JB. Timing of steps in transformation of C3H10 T1/2 cells by X-irradiation. Nature 1984; 307:85–6.

74. Mendonca MS, Temples TM, Farrington DL, Bloch C. Evidence for a role of delayed death and genomic instability in radiation-induced neoplastic transformation of human hybrid cells. Int J Radiat Biol 1998; 74(6):755–64.

75. Mendonca MS, Howard K, Desmond LA, Derrow CW. Previous loss of chromosome 11 containing a suppressor locus increases radiosensitivity, neoplastic transformation frequency and delayed death in HeLa x fibroblast human hybrid cells. Mutagenesis 1999; 14(5):483–90.

76. Mendonca MS, Howard KL, Farrington DL, Desmond LA, Temples TM, Mayhugh BM, et al. Delayed apoptotic responses associated with radiation-induced neoplastic transformation of human hybrid cells. Cancer Res 1999; 59(16):3972–9.

77. Lewis DA, Mayhugh BM, Qin Y, Trott K, Mendonca MS. Production of delayed death and neoplastic transformation in CGL1 cells by radiation-induced bystander effects. Radiat Res 2001; 156(3):251–8.

78. Mendonca MS, Kurohara W, Antoniono R, Redpath JL. Plating efficiency as a function of time postirradiation: evidence for the delayed expression of lethal mutations. Radiat Res 1989; 119(2): 387–93.

79. Mendonca MS, Mayhugh BM, McDowell B, Chin-Sinex H, Smith ML, Dynlacht JR, et al. A radiation-induced acute apoptosis involving TP53 and BAX precedes the delayed apoptosis and neoplastic transformation of CGL1 human hybrid cells. Radiat Res 2005; 163(6):614–22.

80. Azzam EI, Raaphorst GP, Mitchel RE. Radiation-induced adaptive response for protection against micronucleus formation and neoplastic transformation in C3H 10T1/2 mouse embryo cells. Radiat Res 1994; 138(1 Suppl):S28–31.

81. Azzam EI, de Toledo SM, Raaphorst GP, Mitchel RE. Low-dose ionizing radiation decreases the frequency of neoplastic transformation to a level below the spontaneous rate in C3H 10T1/2 cells. Radiat Res 1996; 146(4):369–73.

82. Redpath JL, Liang D, Taylor TH, Christie C, Elmore E. The shape of the dose-response curve for radiation-induced neoplastic transformation in vitro: evidence for an adaptive response against neoplastic transformation at low doses of low-LET radiation. Radiat Res 2001; 156(6):700–7.

83. Redpath JL, Lu Q, Lao X, Molloi S, Elmore E. Low doses of diagnostic energy X-rays protect against neoplastic transformation in vitro. Int J Radiat Biol 2003; 79(4):235–40.

84. Redpath JL. Radiation-induced neoplastic transformation in vitro: evidence for a protective effect at low doses of low LET radiation. Cancer Metastasis Rev 2004; 23(3-4):333–9.

85. Ko M, Lao XY, Kapadia R, Elmore E, Redpath JL. Neoplastic transformation in vitro by low doses of ionizing radiation: role of adaptive response and bystander effects. Mutat Res 2006; 597(1-2):11–7.

86. Redpath JL, Elmore E. Radiation-induced neoplastic transformation in vitro, hormesis and risk assessment. Dose Response 2007; 5(2):123–30.

87. Elmore E, Lao XY, Kapadia R, Giedzinski E, Limoli C, Redpath JL. Low doses of very low-dose-rate low-LET radiation suppress radiation-induced neoplastic transformation in vitro and induce an adaptive response. Radiat Res 2008; 169(3):311–8.

88. Redpath JL, Antoniono RJ. Induction of an adaptive response against spontaneous neoplastic transformation in vitro by low-dose gamma radiation. Radiat Res 1998; 149(5):517–20.

89. Seymour CM, C. Medium from irradiated human epithelial cells but not human fibroblasts reduces the clonogenic survival of unirradiated cells. Int J Radiat Biol 1997; 71(4):421–7.

90. Mothersill C, Seymour CB. Cell-cell contact during gamma irradiation is not required to induce a bystander effect in normal human keratinocytes: evidence for release during irradiation of a signal controlling survival into the medium. Radiat Res 1998; 149(3):256–62.

91. Seymour CB, Mothersill C. Relative contribution of bystander and targeted cell killing to the low-dose region of the radiation dose-response curve. Radiat Res 2000; 153:508–11.

92. Azzam EI, de Toledo SM, Gooding T, Little JB. Intercellular communication is involved in the bystander regulation of gene expression in human cells exposed to very low fluences of alpha particles. Radiat Res 1998; 150(5):497–504.

93. Prise KM, Belyakov OV, Folkard M, Michael BD. Studies of bystander effects in human fibroblasts using a charged particle microbeam. Int J Radiat Biol 1998; 74(6):793–8.

94. Grosovsky AJ. Radiation-induced mutations in unirradiated DNA. Proc Natl Acad Sci U S A 1999; 96:5346–7.

95. Zhou H, Randers-Pehrson G, Waldren CA, Vannais D, Hall EJ, Hei TK. Induction of a bystander mutagenic effect of alpha particles in mammalian cells. Proc Natl Acad Sci U S A 2000; 97(5):2099–104.

96. Reznikoff CA, Brankow DW, Heidelberger C. Establishment and

characterization of a cloned line of C3H mouse embryo cells sensitive to postconfluence inhibition of division. Cancer research. 1973; 33(12):3231–8.

97. Raaphorst GP, Azzam EI, Borsa J, Sargent MD. In vitro transformation by bromodeoxyuridine and X irradiation in C3H 10T1/2 cells. Radiat Res 1985; 101(2):279–91.

98. Redpath JL, Antoniono RJ, Sun C, Gerstenberg HM, Blakely WF. Late mitosis/early G1 phase and mid-G1 phase are not hypersensitive cell cycle phases for neoplastic transformation of HeLa x skin fibroblast human hybrid cells induced by fission-spectrum neutrons. Radiat Res 1995; 141(1):37–43.

99. Redpath JL, Sun C, Blakely WF. Effect of fission-neutron dose rate on the induction of a tumor-associated antigen in human cell hybrids (HeLa X skin fibroblasts). Radiat Res 1991; 128(1 Suppl):S71–4.

100. Hill CK, Buonaguro FM, Myers CP, Han A, Elkind MM. Fission-spectrum neutrons at reduced dose rates enhance neoplastic transformation. Nature 1982; 298(5869):67–9.

101. Hill CK, Han A, Elkind MM. Fission-spectrum neutrons at a low dose rate enhance neoplastic transformation in the linear, low dose region (0-10 cGy). Int J Radiat Biol Studi Phys Chem Med 1984; 46(1):11–5.

102. Ko SJ, Liao XY, Molloi S, Elmore E, Redpath JL. Neoplastic transformation in vitro after exposure to low doses of mammographic-energy X rays: quantitative and mechanistic aspects. Radiat Res 2004; 162(6):646–54.

103. Elmore E, Lao XY, Ko M, Rightnar S, Nelson G, Redpath J. Neoplastic transformation in vitro induced by low doses of 232 MeV protons. Int J Radiat Biol 2005; 81(4):291–7.

104. Kaelbling M, Klinger HP. Suppression of tumorigenicity in somatic cell hybrids. III. Cosegregation of human chromosome 11 of a normal cell and suppression of tumorigenicity in intraspecies hybrids of normal diploid x malignant cells. Cytogenetics Cell Genetics 1986; 41(2):65–70.

105. Saxon PJ, Srivatsan ES, Stanbridge EJ. Introduction of human chromosome 11 via microcell transfer controls tumorigenic expression of HeLa cells. EMBO J 1986; 5(13):3461–6.

106. Mendonca MS, Farrington DL, Mayhugh BM, Qin Y, Temples T, Comerford K, et al. Homozygous deletions within the 11q13 cervical cancer tumor-suppressor locus in radiation-induced, neoplastically transformed human hybrid cells. Genes Chromosomes Cancer 2004; 39(4):277–87.

107. Ghiassi-nejad M, Mortazavi SM, Cameron JR, Niroomand-rad A, Karam PA. Very high background radiation areas of Ramsar, Iran: preliminary biological studies. Health Phys 2002; 82(1): 87–93.

108. Ghiassi-Nejad M, Zakeri F, Assaei RG, Kariminia A. Long-term immune and cytogenetic effects of high level natural radiation on Ramsar inhabitants in Iran. J Environ Radioact 2004; 74(1-3): 107–16.

109. Masoomi JR, Mohammadi S, Amini M, Ghiassi-Nejad M. High background radiation areas of Ramsar in Iran: evaluation of DNA damage by alkaline single cell gel electrophoresis (SCGE). J Environ Radioact 2006; 86(2):176–86.

110. Attar M, Molaie Kondolousy Y, Khansari N. Effect of high dose natural ionizing radiation on the immune system of the exposed residents of Ramsar Town, Iran. Iran J Allergy, Asthma Immunol 2007; 6(2):73–8.

111. Yazdani M, Naderi-Manesh H, Khajeh K, Soudi MR, Asghari SM, Sharifzadeh M. Isolation and characterization of a novel gamma-radiation-resistant bacterium from hot spring in Iran. J Basic Microbiol 2009; 49(1):119–27.

112. Zakeri F, Rajabpour MR, Haeri SA, Kanda R, Hayata I, Nakamura S, et al. Chromosome aberrations in peripheral blood lymphocytes of individuals living in high background radiation areas of Ramsar, Iran. Radiat Environ Biophys 2011; 50(4): 571–8.

113. Joiner MC, Marples B, Lambin P, Short SC, Turesson I. Low-dose hypersensitivity: current status and possible mechanisms. Int J Radiat Oncol Biol Phys 2001; 49(2):379–89.

114. Martin CJ. The LNT model provides the best approach for practical implementation of radiation protection. Br J Radiol 2005; 78(925):14–6.

115. Scott BR. Radiation-hormesis phenotypes, the related mechanisms and implications for disease prevention and therapy. J Cell Commun Signal 2014; 8(4):341–52.

116. Planel G, Soleilhavoup JP, Tixador R, Croute F, Richoilley G. Demonstration of a stimulating effect of natural ionizing radiation and of very low radiation doses on cell multiplication. Biological and environmental effects of low-level radiation: proceedings of a symposium1976. p. 127–40.

117. Kawanishi M, Okuyama K, Shiraishi K, Matsuda Y, Taniguchi R, Shiomi N, et al. Growth retardation of Paramecium and mouse cells by shielding them from background radiation. J Radiat Res 2012; 53(3):404–10.

118. Conter A, Dupouy D, Planel H. Demonstration of a biological effect of natural ionizing radiations. Int J radiat Biol Relat Stud In Phys Chem Med 1983; 43(4):421–32.

119. Croute F, Soleilhavoup JP, Vidal S, Dupouy D, Planel H. Paramecium tetraurelia Growth Stimulation under Low-Level Chronic Irradiation: Investigations on a Possible Mechanism. Radiat Res 1982; 92(3):8.

120. Planel H, Soleilhavoup JP, Tixador R, Richoilley G, Conter A, Croute F, et al. Influence on cell proliferation of background radiation or exposure to very low, chronic gamma radiation. Health Phys 1987; 52(5):8.

121. Castillo H, Schoderbek D, Dulal S, Escobar G, Wood J, Nelson R, et al. Stress induction in the bacteria Shewanella oneidensis and Deinococcus radiodurans in response to below-background ionizing radiation. Int J Radiat Biol 2015; 91(9):749–56.

122. Satta L, Antonelli F, Belli M, Sapora O, Simone G, Sorrentino E, et al. Influence of a low background radiation environment on biochemical and biological responses in V79 cells. Radiat Environ Biophys 2002; 41(3):8.

123. Gajendiran N, Jeevanram RK. Environmental radiation as the conditioning factor for the survival of yeast Saccharomyces cerevisiae. Indian J Exp Biol 2002; 40(1):6.

124. Carbone MC, Pinto M, Antonelli F, Amicarelli F, Balata M, Belli M, et al. The Cosmic Silence experiment: on the putative adaptive role of environmental ionizing radiation. Radiat Environ Biophys 2009; 48(2):189–96.

125. Carbone MC, Pinto M, Antonelli F, Balata M, Belli M, Devirgiliis LC, et al. Effects of deprivation of background environmental radiation on cultured human cells. Il Nuovo Cimento 2010; 125(4):9.

126. Smith NJT. The SNOLAB deep underground facility. The European J Physics Plus 2011; 127:9.

127. Boger J, Hahn RL, Rowley JK, Carter AL, Hollebone B, Kessler D, et al. The Sudbury Neutrino Observatory. Nuclear Instruments Meth Phys Res 2000; 449(1–2):172–207.

128. Silagi S, Darlington G, Bruce SA. Hybridization of two biochemically marked human cell lines. Proc Natl Acad Sci U S A 1969; 62(4):1085–92.

129. Chen TT, Heidelberger C. Quantitative studies on the malignant transformation of mouse prostate cells by carcinogenic hydrocarbons in vitro. Int J Cancer 1969; 4(2):166–78.

130. Reznikoff CA, Bertram JS, Brankow DW, Heidelberger C. Quantitative and qualitative studies of chemical transformation of cloned C3H mouse embryo cells sensitive to postconfluence inhibition of cell division. Cancer Res 1973; 33(12):3239–49.

131. Colman M, Bhatt S, Candelaria M, Sun C, Redpath JL. A comparison of the radiation sensitivities of non-tumorigenic and tumorigenic human hybrid cell lines. Int J radiat Biol Relat Stud Phys Chem Med 1988; 53(4):609–16.

132. Redpath JL, Antoniono RJ, Mendonca MS, Sun C. The effect of

postirradiation holding at 22 degrees C on the repair of sublethal, potentially lethal and potentially neoplastic transforming damage in gamma-irradiated HeLa x skin fibroblast human hybrid cells. Radiat Res 1994; 137(3):323–9.

133. Mendonca MS, Fasching CL, Srivatsan ES, Stanbridge EJ, Redpath JL. Loss of a putative chromosome 11 tumor suppresor locus after gamma ray-induced neoplastic transformation of HeLa X fibroblast human cell hybrids. Radiat Res 1995; 143:34–44.

134. de Feijter-Rupp HL, Hayashi T, Kalimi GH, Edwards P, Redpath JL, Chang CC, et al. Restored gap junctional communication in non-tumorigenic HeLa-normal human fibroblast hybrids. Carcinogenesis 1998; 19(5):747–54.

135. Suzuki T, Iwazaki A, Katagiri H, Oka Y, Redpath JL, Stanbridge EJ, et al. Enhanced expression of glucose transporter GLUT3 in tumorigenic HeLa cell hybrids associated with tumor suppressor dysfunction. Europ J Biochem/FEBS. 1999; 262(2):534–40.

136. Tsujimoto H, Nishizuka S, Redpath JL, Stanbridge EJ. Differential gene expression in tumorigenic and nontumorigenic HeLa x normal human fibroblast hybrid cells. Mol Carcinog 1999; 26(4):298–304.

137. Mendonca MS, Howard K, Farrington DL, Desmond LA, Temples TM, Mayhugh BM, et al. Delayed apoptotic responses associated with radiation-induced neoplastic transformation of human hybrid cells. Cancer Res 1999; 59:3972–9.

138. Mendonca MS, Desmond LA, Temples TM, Farrington DL, Mayhugh BM. Loss of chromosome 14 increases the radiosensitivity of CGL1 human hybrid cells but lowers their susceptibility to radiation-induced neoplastic transformation. Mutagenesis 2000; 15(3):187–93.

139. Frankenberg D, Kelnhofer K, Garg I, Bar K, Frankenberg-Schwager M. Enhanced mutation and neoplastic transformation in human cells by 29 kVp relative to 200 kVp X rays indicating a strong dependence of RBE on photon energy. Radiat Prot Dos 2002; 99(1-4):261–4.

140. Srivatsan ES, Chakrabarti R, Zainabadi K, Pack SD, Benyamini P, Mendonca MS, et al. Localization of deletion to a 300 Kb interval of chromosome 11q13 in cervical cancer. Oncogene 2002; 21(36):5631–42.

141. Mendonca MS, Chin-Sinex H, Gomez-Millan J, Datzman N, Hardacre M, Comerford K, et al. Parthenolide sensitizes cells to X-ray-induced cell killing through inhibition of NF-kappaB and split-dose repair. Radiat Res 2007; 168(6):689–97.

142. Veena MS, Lee G, Keppler D, Mendonca MS, Redpath JL, Stanbridge EJ, et al. Inactivation of the cystatin E/M tumor suppressor gene in cervical cancer. Genes Chromosomes Cancer 2008; 47(9):740–54.

143. Bettega D, Calzolari P, Hessel P, Stucchi CG, Weyrather WK. Neoplastic transformation induced by carbon ions. Int J Radiat Oncol Biol Phys 2009; 73(3):861–8.

RADIATION RESEARCH **188**, 525–538 (2017)
0033-7587/17 $15.00

DOI: 10.1667/RR14587.1

REVIEW

Low-Dose Ionizing Radiation Exposure, Oxidative Stress and Epigenetic Programing of Health and Disease

Sujeenthar Tharmalingam,[a] Shayenthiran Sreetharan,[b] Adomas V. Kulesza,[b] Douglas R. Boreham[a,c] and T. C. Tai[a,1]

[a] *Northern Ontario School of Medicine, Laurentian University, Sudbury, Canada, P3E 2C6; and Departments of* [b] *Biology and* [c] *Medical Physics and Applied Radiation Sciences, McMaster University, Hamilton, Canada, L8S 4K1*

Tharmalingam, S., Sreetharan, S., Kulesza, A. V., Boreham, D. R. and Tai, T. C. Low-Dose Ionizing Radiation Exposure, Oxidative Stress and Epigenetic Programing of Health and Disease. *Radiat. Res.* 188, 525–538 (2017).

Ionizing radiation exposure from medical diagnostic imaging has greatly increased over the last few decades. Approximately 80% of patients who undergo medical imaging are exposed to low-dose ionizing radiation (LDIR). Although there is widespread consensus regarding the harmful effects of high doses of radiation, the biological effects of low-linear energy transfer (LET) LDIR is not well understood. LDIR is known to promote oxidative stress, however, these levels may not be large enough to result in genomic mutations. There is emerging evidence that oxidative stress causes heritable modifications via epigenetic mechanisms (DNA methylation, histone modification, noncoding RNA regulation). These epigenetic modifications result in permanent cellular transformations without altering the underlying DNA nucleotide sequence. This review summarizes the major concepts in the field of epigenetics with a focus on the effects of low-LET LDIR (<100 mGy) and oxidative stress on epigenetic gene modification. In this review, we show evidence that suggests that LDIR-induced oxidative stress provides a mechanistic link between LDIR and epigenetic gene regulation. We also discuss the potential implication of LDIR exposure during pregnancy where intrauterine fetal development is highly susceptible to oxidative stress-induced epigenetic programing.

INTRODUCTION

The use of medical diagnostic imaging has increased greatly over the last 20 years. A large portion of these medical diagnostic techniques involve ionizing radiation, including radiography, fluoroscopy, computed tomography (CT) and nuclear medicine. Annually, there are more than 3.6 billion X-ray examinations, 37 million nuclear medicine applications and 7.5 million radiotherapy procedures worldwide (*1, 2*). In the U.S. alone, in 2006 the number of individual exposures to diagnostic medical radiation had increased to more than seven times that of the early 1980s (*3*). Specifically, the number of CT and nuclear medicine examinations had increased 2.7-fold and 1.6-fold, respectively, from 1998 to 2008 (*4*).

An average individual has an annual radiation exposure of approximately 6.2 mSv, with roughly half from medical imaging, while the other half comes from background sources (*4*). Approximately 80% of patients who undergo medical imaging are exposed to low doses of ionizing radiation, with mean effective dose at 2.4 ± 6.0 mSv per person per year (*5*). The term ''low-dose ionizing radiation'' (LDIR) can be used in a variety of contexts. For the purpose of this review we define LDIR to be less than or equal to 0.1 Gy (or 100 mGy) unless otherwise stated. Furthermore, only low-linear energy transfer (LET) radiation types such as X or gamma rays will be discussed. Although there is widespread consensus regarding the harmful effects of high doses of radiation and mechanisms of cell injury, the biological effects and mechanism of action of low-LET LDIR (which encompasses the majority of exposures from medical diagnostics) is not very well understood.

LOW-DOSE IONIZING RADIATION AND OXIDATIVE STRESS

Ionizing radiation can be classified as directly or indirectly ionizing (*6*). Positively charged particles are described as directly ionizing, as they contain sufficient energy to disrupt the atomic structure of the absorbing material. These charged particles are relatively large and thus deposit energy over short distances resulting in harmful biological effects. Indirectly ionizing radiation such as gamma radiation donates a portion or the entirety of its

[1] Address for correspondence: Northern Ontario School of Medicine, Medical Sciences Division, 935 Ramsey Lake Rd., Sudbury, Ontario P3E 2C6, Canada; e-mail: tc.tai@nosm.ca.

energy to produce fast-moving charged particles, such as electrons (*6*). These fast-moving species result in direct cellular damage to bio-molecules such as DNA, or form highly reactive free radical species known as reactive oxygen species (ROS).

The majority of observed biological effects mediated by LDIR occur due to the generation of ROS via indirect radiolysis of water molecules (*7*). Ionizing radiation also stimulates ROS production by promoting inducible nitric oxide synthase (NOS) activity resulting in nitric oxide ($^{\bullet}NO$) formation (*8*). $^{\bullet}NO$ reacts with superoxide radical (O_2^-) generating peroxynitrite ($ONOO^-$). $ONOO^-$ is a strong oxidant radical that reacts with a wide range of biomolecules including DNA bases, proteins and lipids.

Another major source of cellular ROS production includes nicotinamide adenosine dinucleotide phosphate (NADPH) oxidase. NADPH oxidase is a multi-subunit enzyme complex that assembles on the cell membrane of phagocytic and non-phagocytic cells when activated. NADPH oxidase generates superoxide anion by transferring electrons from cytosolic NADPH across the cell membrane to extracellular molecular oxygen (*9*). Weyemi *et al.,* demonstrated that LDIR promotes DNA damage via activation of NADPH oxidase family members NOX4 and NOX5 (*10*). Indeed, knockdown of NOX4 and NOX5 in human primary fibroblasts resulted in reduced levels of DNA damage, indicating that NADPH oxidase is a significant source of LDIR mediated ROS production (*10*).

LDIR further contributes to ROS production by altering mitochondrial electron transport chain (ETC) activity. The mitochondrial matrix contains a series of enzymatic machinery that serves as electron donors and acceptors required for reduction of molecular oxygen to water to produce energy. However, this process also results in the generation of free radical byproducts due to leakage of electrons from the mitochondria. The leaked electrons contribute to basal levels of superoxide production (*11*). Radiation promotes electron release from the mitochondria, therefore resulting in excess superoxide generation (*12*). Ionizing radiation further disrupts mitochondrial function by inhibiting mitochondrial protein import and activity of key ETC enzymes including aconitase (*13*). These LDIR-mediated mitochondrial effects exacerbate basal oxidative stress levels resulting in elevated ROS signaling.

Free radicals damage various biological macromolecules including DNA, resulting in the formation of single-strand or double-strand breaks. Single-strand breaks are more easily repaired by the cell, which uses the complementary strand of DNA as a template (*6*). Double-strand breaks (DSBs) undergo repair through homologous or non-homologous recombination pathways. In addition to radiation-induced two-ended breaks, DSBs can also occur from single-strand breaks when a replication fork encounters a DNA lesion resulting in replication-induced DSBs (*14*). These DSBs produce various chromosome and chromatid aberrations including chromosome ring formation, dicentric chromosome establishment or anaphase bridge development (*6*). Radiation-induced DNA damage also results in apoptosis or ''programed cell death'' when cellular damage exceeds adequate repair mechanisms. Within the context of radiation damage, apoptosis is critical to ensure normal functioning of tissue by removing aberrant cells. It is important to note that under resting conditions, background steady state ROS levels in cells result in 10^3–10^4 DNA damage sites per cell per day (*15*). In addition to maintaining basal DNA damage events, DNA repair mechanisms must adapt to increased DNA damage rates during irradiation to maintain adequate DNA protection. This demonstrates that dose rate (radiation dose absorbed in unit time) is an important variable in determining radiation induced DNA mutation rates.

The production of free radicals and cellular oxidative stress has been well defined and characterized as a mechanism of ionizing radiation-induced cellular damage. There is emerging evidence that oxidative stress causes heritable modifications to the genomic structure while the underlying DNA nucleotide sequence remains unchanged. These structural genome changes are referred to as epigenetic modifications, and control stable gene expression patterns allowing for heritable phenotypic modifications without altering the genotype. Recent studies also demonstrate that LDIR modulates epigenetic mechanisms. Therefore, we propose the following mechanism for LDIR induced cellular effects: 1. LDIR triggers free radical production resulting in increased cellular oxidative stress; 2. oxidative stress targets epigenetic regulators, thus altering gene regulation patterns; and 3. gene dysregulation causes cellular phenotypic changes that translate into altered physiological health outcomes (Fig. 1). In this review, we discuss the field of epigenetics and critically summarize the current state of knowledge regarding LDIR ($\geq$100 mGy), oxidative stress and epigenetic changes as a mechanism for understanding the biological effects mediated by LDIR.

EPIGENETICS

Introduction to Epigenetics

Developmental and environmental factors shape the repertoire of genes that are expressed at a given spatial and temporal state of a cell. Each differentiated cell has its own gene expression signature that reflects the genotype and environmental influences (*16*). The establishment and maintenance of the metastable transcriptional state is therefore fundamental for the cell's ability to remember and ''memorize'' developmental events such as changes in external environment and developmental cues (*17*).

Epigenetics was coined by Conrad Waddington to describe stably heritable changes in the structure and function of the genome, which are acquired as the single-cell zygote differentiates into various cell types (*18–20*). Developing and fully differentiated cells must faithfully

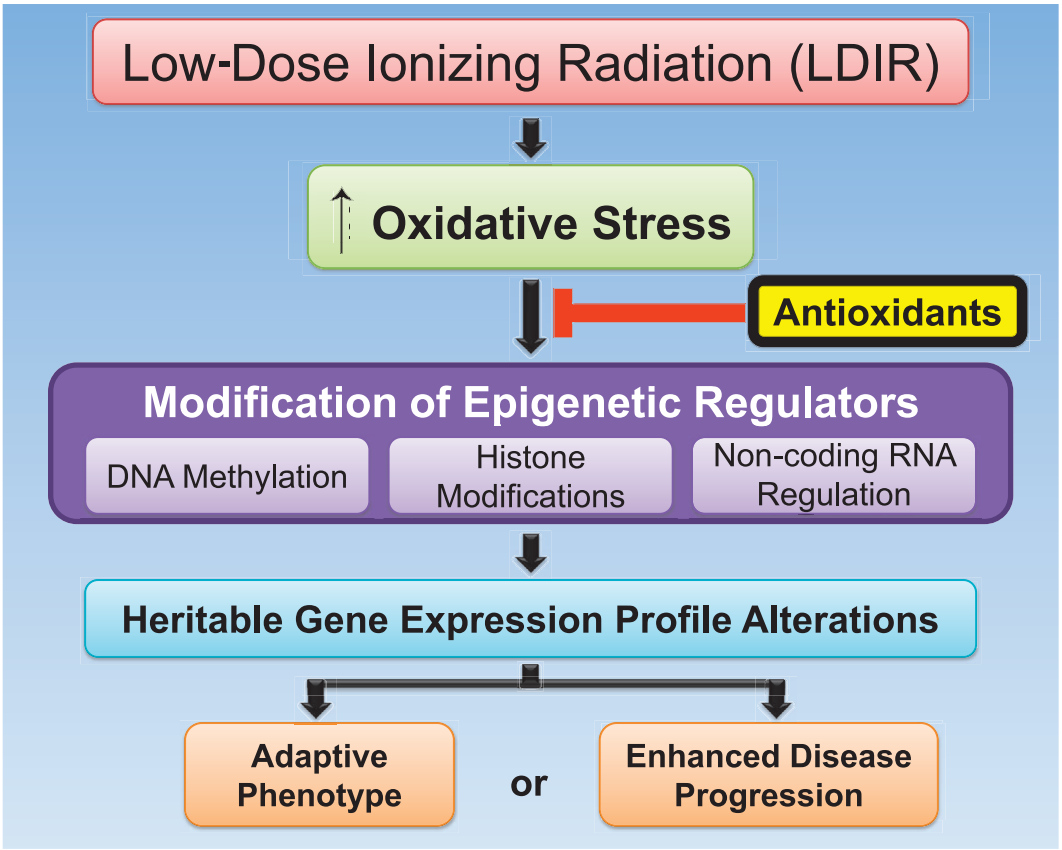

FIG. 1. Proposed mechanism for low-dose ionizing radiation (LDIR)-induced cellular effects. 1. LDIR triggers free radical production, resulting in increased cellular oxidative stress. 2. Oxidative stress targets epigenetic regulators, thus altering gene regulation patterns. 3. Gene dysregulation causes cellular phenotypic changes that translate into altered physiological health outcomes.

transmit the acquired gene expression patterns during cell division without producing changes in the underlying DNA sequence (*16*). Thus, the transmission of gene expression memory that occurs in the absence of changes in the DNA sequence is known as epigenetic inheritance (*19*). The epigenome is dynamic and responds to environmental perturbations to ensure proper cell function. Once the epigenetic modifications have taken place, these marks are maintained in all subsequent cell divisions. There is clear evidence that exposure to pathophysiological conditions evokes epigenetic changes resulting in numerous diseases (*16*).

Epigenetic Mechanisms

Epigenetic information is preserved and inherited through specific signals (described in detail below). These include covalent modifications to DNA, modifications to histone proteins or noncoding RNAs.

DNA modifications. Genomic DNA is organized in arrays of chromatin that are comprised of DNA and histones. The basic chromatin unit, known as the nucleosome, is composed of 147 bp of DNA wrapped around eight core histone octomers (two subunits each of histones H2A, H2B, H3 and H4) (*21*). Chromatin keeps DNA tightly packaged, preventing chromosome breakage, and controls gene expression and DNA replication. The highly condensed and transcriptionally silent form of chromatin is known as heterochromatin, and also includes telomeres, pericentric regions and areas rich in repetitive sequences. In contrast, euchromatin is less condensed and contains actively transcribing genes. Thus, factors that control access to gene binding by transcription factors determine gene expression levels.

The most widely studied epigenetic DNA modification mechanism is cytosine methylation of DNA at the carbon 5 residue to form 5-methyl-cytosine (5meC) (*22*). The methyl group protrudes from the cytosine nucleotide into the major grove of the DNA and has two main effects: 1. displacement of transcription factors that normally bind DNA; and 2. attraction of methyl binding proteins, which are in turn associated with gene silencing and chromatin compaction (*23–25*).

It is estimated that 3% of cytosine in human DNA are methylated. Methylation is restricted to cytosine (C) nucleotides in the sequence CG (annotated CpG) (*16, 26*). Although the CpG nucleotide frequency in the vertebrate genome is low, small stretches of DNA have CpG dinucleotides that extend for hundreds of bases, known as

CpG islands. Approximately half of transcribed genes contain CpG islands near their promoter region (*26*). However, CpG islands are generally hypomethylated or have very low levels of methylation under resting conditions.

Regulation of proper DNA methylation is vital for proper cell proliferation, cell differentiation and genomic stability. Pathological conditions, which cause global DNA hypomethylation, activate transposable elements, resulting in elevated chromosome breakage, aneuploidy, increased mutation rates and overall genomic instability (*22, 27–29*). Furthermore, altered global DNA methylation is a well-known characteristic of cancer progression.

DNA methyltransferases (DNMTs) are enzymes responsible for DNA methylation. DNMT3a and DNMT3b are responsible for establishing cytosine methylation at previously unmethylated CpG sites (*30*). DNMT3L is an isoform of DNMT3a that lacks methylation activity, but helps *de novo* DNA methylation of transposons in the germline. DNMT1 maintains pre-existing methylation patterns by having an increased propensity for hemimethylated DNA substrates (only one of two complementary strands is methylated). Thus, heritable gene expression patterns of CpG methylation imposed on the genome by defined developmental time points in precursor cells are maintained by DNMT1 and subsequently transmitted to descendants of the cell lineage (*30–33*).

DNA methylation of CpG islands is associated with transcriptional silencing and repression of gene expression (*16*). Methylated DNA is recognized by a family of methyl CpG-binding domain proteins. These proteins include MeCP2 and MBD1–MBD4. MeCP2 recruits chromatin-remodeling co-repressor complexes to regions of DNA that specifically bind the MeCP2 protein (*34*). Mutations in MeCP2 have been reported to result in Rett syndrome (*35*). Rett syndrome is an example of genetic mutation causing a shift in the epigenome expression profile.

Histone modifications. Histone proteins are comprised of long chains of amino acids. Modification of these amino acid residues alters chromatin fiber compaction, resulting in changes in the accessibility and recruitment of transcription regulatory factors to promoter sequences on DNA (*16, 21*). Chromatin remodeling complexes are proteins that modulate the interaction between nucleosome and DNA by adding post-translational modifications to histone. Nine different histone modifications have been described: 1. lysine acetylation; 2. lysine methylation; 3. arginine methylation; 4. serine/threonine tyrosine phosphorylation; 5. serine/threonine ubiquitylation; 6. GlcNAcylation; 7. citrullination; 8. krotonilation; and 9. proline isomerization (*21*). The histone code refers to the set of modifications to the histone tail of the nucleosome (*25*).

Histone acetylation on lysine residues by histone acetyltransferases (HAT) induces chromatin structure relaxation and a marked increase in gene expression. This is achieved by neutralizing the positive amine group present in lysine with amide conversion, thus reducing the interaction between the negatively charged DNA with the histone. Acetylation allows increased access to gene regulatory proteins and transcription factors leading to enhanced gene expression (*36, 37*). HAT preferentially targets lysine residues within histones H3 and H4. Histone acetylation promotes chromatin relaxation allowing for greater access to promoter regions (*38*). Conversely histone deacetylases (HDAC) result in chromatin compaction and reduced gene expression.

Unlike histone acetylation, histone methylation does not alter the charge of the modified residue (*39*). Thus, histone methylation can either repress or activate transcription depending on the site of methylation. Arginine methylation of H3 and H4 promotes transcriptional activity, whereas lysine methylation of H3 and H4 can both activate or repress transcription depending on the site of methylation (*40*). In addition, lysine residues can be methylated several times, providing mono-, di- or tri-methylation (*41*). Enzymes responsible for histone methylation include histone methyltransferases such as lysine-specific histone methyltransferases and arginine-specific histone methyltransferases.

All core histones are phosphorylated, which is a critical step in chromosome condensation during mitosis/meiosis, transcription regulation and DNA damage repair (*42*). Histone phosphorylation functions by establishing interactions between other histone-modifying enzymes and effector proteins, leading to further downstream events. Furthermore, histone ubiquitylation of H2A and H2B are monoubiquilated by Polycomb and RNF20/40 ubiquitin ligases, leading to gene silencing and gene activation, respectively (*43*).

Histone modifications demonstrate intense cross talk: modification of the same histone (cis); between different histones with the same nucleosome (trans); and across different nucleosomes (*44*). This brings vast complexity to the control of gene expression, since each modification exerts its effect differently, and this is further complicated since the effect is determined on the extent of methylation, whether it is mono-, di- or tri-methylation. Histone modification and DNA methylation act together to control the structure of the chromatin and ultimately, gene expression levels (*22*). Thus, gene expression is a complex process, which is dependent on the DNA sequence itself, the histone-modifying proteins and the methylation state of the gene. These genetic and epigenetic patterns are interlinked and interdependent (*16*).

Noncoding RNA-mediated epigenetic modulation. Numerous studies indicate that approximately 90% of eukaryotic genome is transcribed, however, only 1–2 % of these transcripts encode for proteins (*45*). Thus, the majority of transcribed genes act as noncoding RNAs, which perform infrastructural (housekeeping role in translation and splicing including ribosomal, transfer and small nuclear RNAs) and

regulatory roles (modification of other RNAs by miRNAs, piRNAs, siRNAs, IncRNAs) (*46*).

miRNAs are small (21–25 nt) single-stranded noncoding RNAs that regulate gene expression at the post-transcriptional level by repressing specific mRNAs targets (*22, 47, 48*). miRNAs are derived from distinctive hairpin stem loop structures called pre-miRNA. Drosha, a RNAase III enzyme, cleaves pre-miRNA into a 70-nt-long miRNA in the nucleus and allows the miRNA to enter the cytoplasm, where it associates with another RNAse III enzyme (DICER) to be cleaved into 21–25-nt-long dsRNA. The dsRNA is separated into two strands, one of which is incorporated with AGO2 (Argonaute protein family) to form the RNA-induced silencing complex (RISC). RISC binds to 3′UTR or target mRNAs and represses target mRNA translation. miRNAs are transcribed independently, in clusters, or as polycistron transcripts (*22, 48*).

Similar to miRNAs, small interfering RNAs (siRNAs) are linear double-stranded RNA that is processed by DICER into mature 20–24 nt transcripts. siRNA silences gene expression by forming complementary nucleotide sequence with target mRNA (*49*). Similarly, long noncoding RNAs (IncRNAs), which form the majority of noncoding RNAs, are characterized by transcripts >200 nt in length (*50*). IncRNAs are also involved in gene silencing.

Piwi-interacting RNAs (piRNAs) consist of short single-stranded (24–31 nt) noncoding RNA characterized by a uridine at the 5′ and 2′-O-methyl modification at the 3′ end (*51*). piRNA transcripts form complexes with Piwi proteins of the Argonaute protein family. piRNA and Piwi protein expression is restricted to germ cells and involved in silencing of transposable elements during germ line development (*52*). Piwi proteins are required for production of piRNA, and are involved in spermatogenesis, germ cell self-renewal and transposon splicing. The most common function of piRNA pathway is to maintain genomic stability by suppressing transposable elements by transcriptional repression (*53*). piRNA allows for methylation of regulatory regions or retrotransposons in embryonic germ cells. Mutation in Piwi genes is characterized by increased DNA damage at γ-H2AX foci, linking it to DNA damage repair (*22, 54*). Human cells transfected with Piwi resulted in histone H3K9 methylation and significant downregulation of p16 gene expression (*55*). The mouse genome encodes three Piwi genes, all involved in spermatogenesis (*22*). Piwi complexes using the piRNA can guide active DNA methyltransferases to target sequence for DNA methylation. piRNAs and other RNAs provide epigenetic mechanisms by recruiting proteins that will affect the chromatin structure (*17*).

Biological Effects of Epigenetic Modulation

Cytosine methylation, histone modifications and noncoding RNA transcripts form the core epigenetic mechanisms that contribute to the unique expression profile of an individual cell despite all cells of the individual having an identical genomic code (*25*). Epigenetic mechanisms therefore regulate gene expression by altering the genomic structure to allow specific transcription factors to recognize consensus control sequences within the genome and initiate transcription.

The epigenome is most susceptible to dysregulation during gestation, neonatal development, puberty and old age (*16*). During embryogenesis, the epigenome is especially vulnerable to environmental factors since the rate of DNA synthesis is high, and elaborate DNA methylation patterning and chromatin modifications are established for normal tissue development.

Epigenetic imprinting during fertilization. Genomes of mature sperm and egg in mammals are highly methylated compared to somatic cells (*33*). However, during the first phase of fertilization, there is genome-wide demethylation. The paternal genome undergoes significant transformation in the egg cytoplasm, where sperm chromatin is remodeled by removal of protamines and replaced by acetylated histones, followed by demethylation (*33, 56, 57*). This rapid paternal-specific asymmetric loss of methylation occurs in a process termed active demethylation, which has been confirmed by methylcytosine-specific antibodies and bisulphite sequencing (*19*). Here, the whole paternal genome was demethylated except at paternally imprinted genes, heterochromatin centromeres and various repetitive elements (*58*). After this stage, there is a stepwise decline in methylation up to the morula stage known as passive demethylation (*59, 60*), which is due to the absence of methylation maintenance proteins that occurs during DNA replication (*61*). Therefore, the newly replicated strand fails to be methylated and the level of methyl cytosines per nucleus declines (*30*).

The initiation of *de novo* methylation occurs after the fifth cycle, which coincides with the time of the first differentiation event (*16, 59, 60*). Here, two cell lineages result: the inner cell mass (ICM) and the trophoectoderm. The cells of ICM are hypermethylated and give rise to adult tissues, while the trophoectoderm, which forms the placenta, is largely hypomethylated.

During the early differentiation phase, primordial germ cells are methylated (*62*). There is a rapid decline in DNA methylation as these cells migrate to the genital ridge (*63*). This is essential for resetting parent-of-origin-specific methylation marks, which must match the sex of the developing embryo (*16*). Once the germ cells have been demethylated, the cells enter mitotic (male) or meiotic (female) arrest. This occurs during the prospermatogonia stage in males (*33*), where the methylation level of the oocyte and sperm genome remains low and unchanged (*64*). Only during the growth phase is the imprinting laid down on the genome. Re-methylation of female germ cells occurs during the growth of oocytes (*33, 61*). Epigenetic reprograming is vital for the resetting of the imprints.

Epigenetics in X-chromosome inactivation. In mammals, females with two X chromosomes achieve X-linked gene

dosage parity with the single X chromosome of males through epigenetic inactivation of one X chromosome (*65*). Random X-chromosome inactivation occurs at the late blastocyst stage (*66*). For each cell that gives rise to the female fetus, one of two X chromosomes is randomly inactivated. Thus, female mammals are mosaics, comprised of mixtures of cell lines in which either the maternal or paternal X chromosome is inactivated. X chromosome inactivation occurs when the X chromosome destined for inactivation is coated by a noncoding RNA (*67*). This is followed by recruitment of histone-modifying protein complexes, which leads to loss of acetylation, gain of methylation and ubiquitination of various histone proteins (*68, 69*). The cumulative epigenetic modifications transform the X chromosome into a transcriptionally inactive heterochromatin structure.

Transgenerational epigenetic inheritance. Epigenetic modifications demonstrate transgenerational inheritance. However, DNA methylation-associated phenotypes inherited from one generation to the next in mammals are rare due to genome-wide DNA demethylation and chromatin remodeling that occurs in the primordial germ cells of the developing embryo (*70, 71*). However, some retrotransposons, especially the intracisternal A-type particles (IAP), remain methylated and are resistant to DNA demethylation reprograming (*72*). Similarly, in a more detailed study, using DNA immunoprecipitation techniques followed by promoter array hybridization, over 100 genes that had no change in DNA methylation during fertilization were identified (*19, 73, 74*). One example of germline-resistant demethylation that results in transgenerational inheritance is the epigenetic hypermethylation of mismatch repair genes MLH1 and MSH2 in the spermatozoa of individuals affected by colorectal cancer (*75, 76*). These individuals demonstrate mismatch repair deficiency and multiple tumor formation without changes to the underlying nucleotide sequence of the mismatch repair genes.

The identification of DNA methylation effects in transgenerational studies has been underrepresented due to current knowledge that cytosines can be methylated at non-CpG sites, unlike previous beliefs (*19*). Therefore, newer studies are needed to reanalyze sequences to account for this difference. For example, in human embryonic stem cells, approximately 25% of methylated cytosine residues are found at CHG or CHH, where H is A, T or C. Cytosines can be additionally hydroxymethylated, formylated and carboxylated, bringing more complexity (*77*). Furthermore, in previously published studies, investigators initially believed that histones were cleared from DNA in mature sperm and replaced by protamines. However, approximately 4% of genes in sperm are packaged in the nucleosome (*78–80*). Therefore, the molecular basis of transgenerational epigenetic inheritance remains unclear, but is increasingly pointing towards diffusible factors, such as RNA, in addition to DNA methylation and chromatin remodeling (*81*).

MECHANISM: LDIR, OXIDATIVE STRESS AND EPIGENETIC GENE REGULATION

Effects of LDIR on Epigenetic Gene Regulation

Programed cellular changes manifest in the unexposed progeny of irradiated cells for many cell divisions after the initial exposure. The increased prevalence of LDIR-induced genomic instability, and non-Mendelian mode-of-inheritance-based mechanisms suggests that LDIR acts via epigenetic-based mechanisms (*82*). The sections below contain discussions on the effects of LDIR on DNA methylation, histone modification and noncoding RNA expression. Although studies have predominantly used cancer models to determine the effects of radiation-induced cellular changes, the molecular and mechanistic knowledge gained from these studies is broadly applicable to most biological cellular systems.

LDIR and DNA methylation. Recently published studies indicate that LDIR exposure affects DNA methylation patterns. Using mouse model systems, LDIR exposure has been shown to demonstrate dose-dependent, sex and tissue-specific effects on global hypomethylation (*83*). For example, breast cancer cells treated with fractionated doses demonstrated locus-specific DNA hypomethylation at TRAPC1, FOXC1 and LINE1 genes (*20, 84*). These hypomethylation patterns were paralleled by a decrease in expression levels of DNA methylatransferases such as DNMT1, DNMT3A and DNMT3B, and methyl CpG-binding proteins such as MeCP2. Similarly, Luzhna *et al.,* demonstrated that LDIR causes hypomethylation and activation of ''long interspersed element-1'' (LINE-1) ORF, causing increased LINE-1 protein levels and increased LINE-1 mobilization resulting in increased genomic instability (*85*). The effects of LDIR in global DNA hypomethylation levels were also evident in irradiated workers compared to controls. Here, LINE-1 methylation levels were higher in irradiated workers than controls. The global demethylation in these irradiated workers resulted in significantly higher chromosome aberrations (*86*). Therefore, the global hypomethylation patterns induced by LDIR provide a mechanistic link between radiation exposure and increased genomic instability.

Although LDIR exposure induces global hypomethylation, recent studies show that LDIR promotes gene-specific promoter hypermethylation (69). In fact, promoter hypermethylation rather than global hypomethylation was more stable, since acute LDIR induced transient genomic hypomethylation in blood 2 h postirradiation, but was not evident at one month. Similarly, DNMT1 and MBD2 were downregulated in a tissue-specific manner, but these changes did not persist. Analysis of chronic LDIR revealed gene-specific hypermethylation at 811 regions, which encompassed almost all important biological systems as indicated by GO and KEGG pathway analysis. These included numerous hypermethylated genes such as Rad23b and Ddit3, which displayed tissue-specific methylation and

downregulation that were persistent one month postirradiation (*69*). Another study revealed that long-term LDIR-induced adaptive response resulted in global genomic DNA hypermethylation accompanied by increases in DNMT1 and MeCP2 expression, and heterochromatin formation (*87*). This study demonstrates that the epigenome adapts to the initial LDIR exposure by overcompensating for the decrease in DNMT1 and MeCP2, by increasing DNA hypermethylation and enhancing expression of DNMT1 and MeCP2.

Also, the severity of the epigenome shift depends on the radiation dose. For example, Newman *et al*., demonstrated that a single radiation dose in a mouse model comparable to human diagnostic radiation exposure did not result in significant long- or short-term changes to repeat elements or global DNA methylation patterns (*88*). Conversely, Kovalchuk *et al*., showed that chronic low-dose exposure proved to be a more potent inducer of epigenetic effects than the acute exposure. This supports previous findings that chronic exposure leads to greater genome destabilization than acute exposure (*89*). Therefore, further research is needed to fully elucidate the role of radiation dosage and DNA methylation status.

LDIR and histone modification. LDIR results in a wide variety of histone modifications. For example, LDIR exposure inhibited H4 lysine tri-methylation, a similar phenomenon seen in aggressive breast cancers (*90*). Similarly, low-dose X-ray irradiation in a mouse model resulted in decreased tri-methylation of histone H4-Lys20 in the thymus and overall reduction in chromatin compaction structure (*91*). The loss of histone H4-Lys20 tri-methylation was accompanied by a significant increase in global DNA hypomethylation as well as the accumulation of DNA damage. The altered DNA methylation status was associated with reduced expression of maintenance DNMT1 and *de novo* DNA methyltransferase DNMT3a in irradiated animals. Interestingly, expression of DNMT3b was decreased only in males. In addition, LDIR resulted in approximately 20% reduction in the levels of methyl-binding proteins MeCP2 and MBD2 (*91*). These studies demonstrate that changes in DNA methylation and histone modification mediated by LDIR results in overall genomic instability.

LDIR and noncoding RNA. Numerous studies have demonstrated that LDIR exposure alters miRNA levels, which ultimately leads to modified protein expression profiles. miRNAs such as miR-21, miR-34a, miR-29c, miR-16, miR-202, miR-303 and miR-572 are all LDIR-responsive miRNAs implicated in radiation-induced altered gene regulation (*92–95*). Interestingly, LDIR-mediated miRNA alterations demonstrate temporal regulation. For example, Bae *et al.,* identified numerous LDIR-responsive miRNAs that differed depending on the postirradiation time point (*92*). At 6 h after LDIR exposure, expression levels of miR-3656, miR-3125 and miR-940 were significantly increased while expression levels of miR-328, miR-885-5p and let-7d-3p were downregulated. At 24 h postirradiation miR-3937, miR-1825 and miR-369-3p were significantly upregulated while miR-634 was downregulated (*92*). Therefore, LDIR-induced miRNA expression patterns are temporally unique. Taken together, these studies demonstrate that LDIR modulates miRNA levels leading to altered gene expression patterns.

Mechanism: Link between Oxidative Stress and Epigenetic Gene Regulation

Recently reported studies suggest that elevated radical species and oxidative stress alters epigenetic gene regulation mechanisms (*96–98*). Stressors, such as ionizing radiation, generate increased ROS production. When cellular antioxidant defense mechanisms are unable to counteract the formation of ROS, the excess free radicals damage biological macromolecules, including lipids, proteins and nucleic acids. We propose that cells adapt to ionizing radiation-induced oxidative insult by modifying epigenetic gene regulation.

Oxidative stressors mediate epigenetic modifications by: 1. inhibiting macromolecules involved in maintaining epigenetic regulation by forming protein adducts; 2. altering genomic DNA methylation status; 3. modifying post-translational histone interactions leading to changes in chromatin compaction; and 4. activating signaling pathways that control transcription factor expression (*99, 100*). Oxidative stress also contributes to epigenetic changes by altering the action of small noncoding RNAs. Analysis of ROS-mediated miRNA expression patterns revealed that epigenetic changes at gene location corresponded to fragile sites known to be targets of oxidative damage. The sections below contain further discussion on the mechanisms by which oxidative stress modulates epigenetic gene regulation.

ROS-mediated protein adduct formation. ROS generated from ionizing radiation mediates epigenetic changes by directly interacting with macromolecules involved in epigenetic maintenance, such as DNA methyltransferases and DNA histones, thereby inhibiting their function. For example, oxidation of cellular lipids results in the generation of unsaturated alkenal electrophiles such as 4-hydroxy-2-nonenal (4-HNE) or 4-oxo-2- nonenal (4-ONE) (*101*). These electrophilic molecules bind to lysine and histidine residues present in biological macromolecules via ketoamide adduct formation. Since histones are lysine-rich proteins, they are targets for ketoamide adduct formation and offer a novel link between oxidative stress and gene expression. Treatment of cells with alkynyl-4-HNE or alkynyl-4-ONE resulted in lysine modification in all four histone subtypes (*101*). In particular, adduct formation on specific lysine residues correlated with numerous studies demonstrating that acetylation or methylation of the same lysine residues resulted in cancer progression via epigenetic mechanisms (*102–104*). Galligan *et al.,* (*101*) robustly tested this mechanism by inducing oxidative stress in

RAW264.7 macrophages by lipopolysaccharide treatment. Analysis of treated cells revealed 4-ketoamide adduct formation at lysine 27 in histone 3B compared to no adduct formation in untreated cells. The ketoamide adduct formation interferes with histone acetylation and methylation sites, thus providing a mechanistic link between oxidative stress and epigenetic patterning.

ROS-mediated DNA methylation changes. ROS-directed DNA damage increases gene methylation at the site of injury resulting in gene silencing (*105*). DNA lesions are rapidly restored by DNA repair enzymes. However, studies have shown that the process of homology-directed DNA repair is routinely associated with DNA methylation at the site of injury (*106*). The selective methylation of distal segments of repaired DNA is achieved by DNA damage response genes such as GADD45A and nuclear protein 95 (Np95) (*107*). GADD45A has high affinity for hemimethylated DNA intermediates, which recruit Np95. Np95 then directs histone H3 methyltransferase to the site of damaged DNA, followed by recruitment of *de novo* methyltransferases Dnmt3a and Dnmt3b, resulting in DNA methylation (*106*). Here, ROS indirectly mediates epigenetic methylation alterations in the genome by inducing DNA breaks, which are then repaired and methylated by DNMTs.

Hypermethylation of the Pax3 gene provides a good example of oxidative stress-mediated developmental epigenetic changes due to intrauterine stress. Pax3 is a transcription factor and its expression controls neural tube closure during embryogenesis. Pax3 activity is inhibited during embryonic development in diabetic mice, resulting in developmental defects. Gestational diabetes exposes the fetus to hyperglycemia-induced oxidative stress resulting in increased Pax3 CpG island methylation by promoting DNMT3b activity (*108*). Similarly, cholangiocarcinoma liver cancer cells achieved resistance to oxidative stress by increasing expression levels of epigenetics-related genes such as DNMT1 (*109*). These results indicate that oxidative stress downregulates expression of specific genes by promoting DNMT activity, thereby providing a molecular link between oxidative stress and epigenetic gene regulation.

Although numerous studies have shown gene-specific hypermethylation due to ROS-directed DNA damage, overall global methylation status of the genome is significantly decreased during oxidative stress. Ionizing radiation generates ROS production predominantly via mitochondrial electron transport chain and NADPH oxidases present in the cytoplasm. Elevated mitochondrial ROS production causes global nuclear DNA hypomethylation due to accumulation of methyltransferases to the mitochondria to aid in the repair of mitochondrial DNA repair, leaving the nucleus devoid of methyltransferases (*110*). The global nuclear DNA hypomethylation that results from increased mitochondrial ROS production is epigenetically preserved, leading to numerous gene expression changes.

Another mechanism of oxidative stress-induced global hypomethylation revolves around inappropriate inhibition of epigenetic regulators. Oxidization of reduced glutathione (GSH) to GSSH inhibits S-adenosyl methionine synthetase, the enzyme responsible for synthesizing S-adenosyl methionine (SAM). SAM is utilized by DNMTs and histone methyltransferases and therefore, oxidative stress-mediated inhibition of SAM results in genomic hypomethylation (*111*). Similarly, LINE-1 methylation was shown to significantly decreased in H_2O_2 treated HK-2 kidney cells (*112*). This study demonstrated that exposure of cells to ROS leads to homocysteine deficiency, which consequently causes SAM depletion and eventual hypomethylation of LINE-1 (*112*).

ROS-mediated post-translational histone modifications. Oxidative stress can also modulate epigenetic gene regulation at the DNA lesion site by altering the state of the chromatin structure. DSBs are predominantly repaired under fast kinetics using poly ADP ribose (PAR) polymerases, which utilize NAD^+ to catalyze the formation of PAR at the site of DNA damage (*113*). The accumulation of PAR at the site of injury activates chromatin remodeling protein ALC1, which causes nucleosome relaxation resulting in epigenetic gene upregulation (*114*). Similarly, approximately 15% of DSBs are repaired with slow kinetics via a process that requires ataxia telangiectasia mutated (ATM), a serine/threonine kinase that is activated and recruited during DSB signaling response. ATM modifies the heterochromatin structure near the DSB by phosphorylation of KAP-1, a heterochromatin formation factor that is essential for opening tightly packed heterochromatin regions to allow for DSB repair (*113*). There are numerous reports linking DNA-damaging chemicals known to increase ROS production to DNA hypomethylation via this type of chromatin remodeling. Therefore, oxidative stress alters epigenetic gene regulation by controlling the chromatin structure near the site of DNA damage.

ROS-mediated DNA oxidization of deoxyguanosine into 8-hydroxydeoxyguanosine (8-OHdG) also results in histone modifications. Gene promoters with 8-OHdG adduct formation have been reported to change the chromatin status from active chromatin with trimethyl-H3K4 and acetylated-H4K16 to a repressive form expressing trimethyl-H3K27 (*115*). The change in chromatin status was associated with gene methylation. An example of oxidative stress-mediated hypermethylation due to histone modifications is evident in the DMA-mismatch repair gene (MSH2) promoter. Chronic oxidative stress resulted in enhanced histone H3K27 acetylation, reduced HDAC1 expression, and hypermethylation of the DNA-mismatch repair (MMR) transcription (*116*). This epigenetic hypermethylation of the MSH2 promoter resulted in loss of MMR-mediated cell apoptosis. Similarly, transglutaminases (TGs) are calcium-dependent enzymes implicated in cell death but can also control chromatin remodeling via sirtuin 1 (SIRT1)-mediated histone deacetylation. During oxidative stress,

TGs enter the nucleus and bind to chromatin structures, resulting in transcriptional repression of genes involved in metabolic or oxidative adaptation (*117*). Oxidative stress also causes changes in oxidized and reduced forms of nicotinamide adenine dinucleotide (NAD^+/NADH ratio). A reduced NAD^+/NADH ratio due to cellular oxidative stress inhibits the activity of histone deacetylases and poly-ADP ribosyltransferases. These examples demonstrate that oxidative stress translates into inappropriate epigenetic gene regulation via histone modification and alteration in chromatin compaction. This type of epigenetic gene suppression is prevalent in tumor suppressor genes, leading to cancer progression.

There are numerous transcription factors, which are epigenetically regulated by oxidative stress signals that target histones. For example, inflammation-mediated oxidative stress induces histone acetylation followed by chromatin remodeling, leading to increased AP-1, forkhead box O and NF-κB activation (*118*). These elevated transcription factors enhance expression and release of pro-inflammatory cytokines. Conversely, induction of mitochondrial oxidative stress via n-succinimidyl n-methylcarbamate exposure resulted in hypermethylation of p16 and smad4 gene promoters and subsequent reduction in respective gene products (*119*). Hypermethylation of these promoters was produced by histone modifications, which included hypermethylation of histone 3 and histone 4, hypoacetylation of histone 3 and histone 4 and increased γ-H2AX phosphorylation. Therefore, oxidative stress-mediated epigenetic changes in transcription factor expression are dependent on the type of histone modifications, with hypoacetylation suppressing expression while enhanced histone acetylation promoting expression.

Various drugs and toxins that elevate oxidative stress also mediate epigenetic changes by targeting histones. Khanal *et al*., demonstrated that benzo(a)pyrene-induced oxidative stress modulates the epigenetic status of the estrogen receptor α promoter by transforming the transcriptionally active histone modification status into a repressive state (*120*). Similarly, hypoxia mimetic deferoxamine induced expression of histone deacetylase 9 (HDAC9) and suppressed expression of lysine acetyltransferase 5 (KAT5) and DNA methyltransferase 3A (DNMT3A), demonstrating that expression of genes encoding epigenetic chromatin-modifying enzymes could be influenced by hypoxia mimetics (*121*). Furthermore, using bisulfite genomic DNA sequencing and methylated DNA immunoprecipitation, Paredes-Gonzalez *et al.,* demonstrated that the anti-cancer drug apigenin protects against oxidative damage by demethylation coupled with attenuating DNMT and HDAC activity (*122*).

ROS-mediated loss of epigenetic imprinting. Oxidative stress causes loss of genomic imprinting via NF-κB signaling, resulting in expression of numerous genes that would normally be imprinted and thus repressed. NF-κB is a transcription factor that regulates cellular stress responses to oxidative stress. Under resting conditions, NF-κB associates with the IκB family of inhibitory proteins. During oxidative stress, IκB is degraded, which allows NF-κB to translocate into the nucleus to bind specific response elements to initiate cellular responses to protect from oxidative stress. Studies in malignant and non-cancerous human prostate cell lines revealed that exposure to oxidative stress resulted in loss of imprinting in insulin-like growth factor 2 (IGF2) imprint control regions (*123*)

Under normal conditions, enhancer-blocking element CCCTC-binding factor (CTCF) binds to the imprint control region of IGF2, preventing access to enhancers. This inhibits gene expression and promotes IGF2 gene silencing. Under oxidative stress, NF-κB binds to the CTCF promoter region with the co-repressor HDAC1 resulting in decreased expression. Reduced CTCF expression results in impaired binding to the IGF2 imprint control regions. Removal of CTCF allows IGF2 enhancers to bind to the gene resulting in loss of imprinting and biallelic IGF2 expression (*123*). Therefore, oxidative stress results in loss of imprinting and inappropriate gene regulation through upregulation of NF-κB activation.

ROS-mediated induction of bystander effects. The radiation-induced bystander effect occurs when nonirradiated cells display phenotypes and molecular gene expression signatures similar to neighboring irradiated cells. Irradiated cells utilize a wide variety of intercellular mechanisms to transmit signals to neighboring nonirradiated cells, including calcium signaling, intercellular communication machinery such as gap junctional proteins, and potent growth factors like TGFβ1 (*124–127*). There are numerous published studies, which also implicate ROS in the induction of radiation-induced bystander effects (*128, 129*). It will be interesting to elucidate whether epigenetic mechanisms play a role in ROS-mediated bystander effects. Further studies are needed to determine this link at the low-dose range.

FETAL AND DEVELOPMENTAL RADIATION CONCERNS

The concept of LDIR-related increased oxidative stress production and modified epigenetic regulation is most relevant in terms of understanding the cellular events that occur in the fetus when pregnant women undergo diagnostic imaging or radiation therapy. The intrauterine period of life provides a critical window during development in which the fetus is very sensitive to environmental perturbations (*130*). The epigenome of the developing fetus is vulnerable to oxidative stress, which can lead to aberrant epigenetic modifications that can persist into adulthood and induce numerous diseases. Exposure to radiation during pregnancy is often in the low-dose range and may potentially lead to long-term effects to the unborn child. Estimated fetal doses received during diagnostic treatments include 1.4 and 1.1 mGy for abdominal and pelvic X rays, respectively, and 8 and 25 mGy for abdominal and pelvic CT scans, respectively (*131*).

Studies have shown that maternal stress or adversity during gestation provides an unfavorable fetal environment (*132*). The developing organs and systems in the fetus adapt to the altered uterine environment by permanently modifying cellular and physiological states, which has lasting effects throughout an individual's lifespan. This concept of ''developmental programing'' is based on numerous epidemiological, clinical, animal and molecular studies, which suggest that adverse conditions during embryonic and fetal development can predispose or alter health outcomes in adulthood (*133, 134*). Embryonic organogenesis in particular is known to be a sensitive period for ionizing radiation-induced malformations. This is likely due to the high rates of cell proliferation and development of major organ systems, with ionizing radiation known to interfere with high rates of cell proliferation (*135, 136*).

The various triggers of fetal programing predominantly result in elevated oxidative stress and ROS formation in the intrauterine environment. Numerous epidemiological studies support the role of oxidative stress as a mechanistic basis for fetal programing (*137–139*). For example, low birth weight is often associated with elevated oxidative stress during intrauterine development, resulting in cardiovascular disease and type 2 diabetes in adulthood (*140*). Published studies have demonstrated elevated levels of lipid peroxidation and pronounced indices for antioxidant enzymes in the placenta of stressed mothers, while their growth-restricted children continued to exhibit increased serum levels of lipid peroxidation and DNA damage (*141–143*). Similar results were observed in studies of animals treated with dexamethasone (a chemical glucocorticoid), which resulted in elevated ROS levels in the coronary circulation and mitochondria of hearts (*144*). Thus, oxidative stress provides a mechanistic link between intrauterine stress and developmental programing. Therefore, we propose that LDIR exposure may cause developmental programing in the fetus via oxidative stress-mediated epigenetic modifications. Epigenetic modulation may explain some of the observed long-term developmental programing health outcomes that result from LDIR and oxidative stress.

The effects of LDIR on epigenetic modulation during fetal programing are best studied using the metastable epiallele in Agouti Yellow Viable (A^{vy}) mice (*70, 145*). Metastable epialleles serve as environmental biosensors (*146*). These genes are variably expressed in individuals due to epigenetic modifications that were established during early development. In the A^{vy} mice, the Agouti locus is comprised of an upstream intracisternal A-particle (IAP) retrotransposon (*70*). Under normal environmental conditions, CpG methylation of IAP occurs during embryonic development, and the subsequent silencing of Agouti expression results in a brown coat color (*72*). When the retrotransposon is unmethylated due to environment-induced epigenetic modulation, the Agouti gene is hypomethylated and aberrantly expressed, leading to a yellow coat color, as well as obesity and diabetes (*147*). Interestingly, Bernal *et al*., demonstrated that LDIR in pregnant A^{vy} mice increased DNA methylation in the offspring, resulting in hypomethylation of the Agouti gene and increased frequency of mice with pseudoagouti (brown) coat color similar to control. The effects of LDIR on DNA methylation and coat color change were negated by maternal dietary antioxidant supplementation (*148*). In this example, LDIR provided a positive adaptive phenotype through oxidative stress-mediated epigenetic alterations. Further, similar studies of LDIR-mediated epigenetic gene-specific analysis are required to establish the role of LDIR in fetal programing.

CONCLUDING REMARKS

While the use of diagnostic imaging and radiation therapy has profoundly increased over the last few decades, the effects of LDIR on health outcomes have not been fully elucidated. Furthermore, with increased patient survival rates due to modern cancer radiation therapy, the risk of treatment-related deleterious effects, including secondary cancers, is becoming an increasing clinical problem (*22*). Delayed effects can manifest in the unexposed progeny of irradiated cells for many cell divisions after the initial insult. The increased prevalence of LDIR-induced genomic instability, and non-Mendelian mode-of-inheritance-based mechanisms, suggests that LDIR acts via epigenetic-based mechanisms (*82*). These heritable cellular effects can either provide a positively adaptive phenotype or result in enhanced disease progression (Fig. 1).

This review summarizes recent studies, which present compelling evidence that oxidative stress generated from sources such as low-LET ionizing radiation provides a mechanistic link between LDIR and epigenetic gene regulation (Fig. 1). Epigenetic changes mediated by oxidative stress are faithfully preserved, resulting in permanent cellular transformations. Numerous studies have demonstrated that ROS scavengers such as n-acetylcysteine and tempol prevent epigenetic DNA methylation changes induced by oxidative stress (*149–151*). Similarly, oxidative stress mediated by intrauterine hypoxia was shown to be protected by administering DNMT inhibitors (*137*) or methyl donors such as genistein (*152, 153*). Taken together, these studies demonstrate that exogenous application of antioxidant supplements protects the biological system by preventing aberrant epigenetic transformations.

LDIR-mediated epigenetic modifications may also provide supporting evidence for hormetic or beneficial effects of low doses of radiation. Very-low-dose radiation may be beneficial when minimal cellular damage provides a stimulus for establishment of enhanced repair mechanisms. If the radiation exposure level is low, not only is the cell able to repair the damage, but this slightly elevated level of repair/regulatory proteins may infer the cell a protective effect. This theory has been reported in numerous studies in an ''adaptive response'' model. In this view, low doses of radiation primes

the system, and when challenged by a large and acute dose of radiation the biological system performs better than a system that is given only the acute dose (*154–157*).

This review brings to light the need for improved evaluation of LDIR-induced epigenetic gene regulation. Currently, there are no epidemiological studies that have been done to determine the effects of LDIR on epigenetic gene regulation. This review emphasizes the need to conduct such studies to better elucidate the role of LDIR on health outcomes. Although ROS and upregulated DNA repair mechanisms have been well characterized as a mechanism of ionizing radiation-induced cellular damage, these changes result in phenotypic modifications only when the underlying DNA nucleotide sequence is altered. More importantly, these genomic mutational changes may not fully explain the subtle gene expression alterations that occur with LDIR. Therefore, future studies are needed to explore both the genetic and epigenetic makeup of the biological system and fully elucidate the effects of ionizing radiation on health and disease.

ACKNOWLEDGEMENTS

Funding provided by Bruce Power and the Natural Science and Engineering Council of Canada.

Received: July 22, 2016; accepted: April 21, 2017; published online: July 28, 2017

REFERENCES

1. Smith-Bindman R, Miglioretti DL, Johnson E, Lee C, Feigelson HS, Flynn M, et al. Use of diagnostic imaging studies and associated radiation exposure for patients enrolled in large integrated health care systems, 1996–2010. JAMA 2012; 307:2400–9.
2. Lau L, Perez M. Global initiative on radiation safety in healthcare settings. Geneva: World Health Organization; 2008.
3. Schauer DA, Linton OW. National Council on Radiation Protection and Measurements report shows substantial medical exposure increase. Radiology 2009; 253:293–6.
4. Schauer DA, Linton OW. NCRP report no. 160, Ionizing radiation exposure of the population of the United States, medical exposure–are we doing less with more, and is there a role for health physicists? Health Phys 2009; 97:1–5.
5. Fazel R, Krumholz HM, Wang Y, Ross JS, Chen J, Ting HH, et al. Exposure to low-dose ionizing radiation from medical imaging procedures. N Engl J Med 2009; 361:849–57.
6. Hall EJ. Radiation, the two-edged sword: cancer risks at high and low doses. Cancer J 2000; 6:343–50.
7. Azzam EI, Jay-Gerin JP, Pain D. Ionizing radiation-induced metabolic oxidative stress and prolonged cell injury. Cancer Lett 2012; 327:48–60.
8. Mikkelsen RB, Wardman P. Biological chemistry of reactive oxygen and nitrogen and radiation-induced signal transduction mechanisms. Oncogene 2003; 22:5734–54.
9. Babior BM. NADPH oxidase: an update. Blood 1999; 93:1464–76.
10. Weyemi U, Redon CE, Aziz T, Choudhuri R, Maeda D, Parekh PR, et al. Inactivation of NADPH oxidases NOX4 and NOX5 protects human primary fibroblasts from ionizing radiation-induced DNA damage. Radiat Res 2015; 183:262–70.
11. Nohl H, Jordan W. The mitochondrial site of superoxide formation. Biochem Biophys Res Commun 1986; 138:533–9.
12. Droge W. Free radicals in the physiological control of cell function. Physiol Rev 2002; 82:47–95.
13. Bulteau AL, Ikeda-Saito M, Szweda LI. Redox-dependent modulation of aconitase activity in intact mitochondria. Biochemistry 2003; 42:14846–55.
14. Bidnenko V, Ehrlich SD, Michel B. Replication fork collapse at replication terminator sequences. EMBO J 2002; 21:3898–907.
15. Lindahl T. Instability and decay of the primary structure of DNA. Nature 1993; 362:709–15.
16. Nafee TM, Farrell WE, Carroll WD, Fryer AA, Ismail KM. Epigenetic control of fetal gene expression. BJOG 2008; 115:158–68.
17. Bonasio R, Tu S, Reinberg D. Molecular signals of epigenetic states. Science 2010; 330:612–6.
18. Van Speybroeck L. From epigenesis to epigenetics: the case of C. H. Waddington. Ann N Y Acad Sci 2002; 981:61–81.
19. Daxinger L, Whitelaw E. Understanding transgenerational epigenetic inheritance via the gametes in mammals. Nat Rev Genet 2012; 13:153–62.
20. Kim JG, Park MT, Heo K, Yang KM, Yi JM. Epigenetics meets radiation biology as a new approach in cancer treatment. Int J Mol Sci 2013; 14:15059–73.
21. Rothbart SB, Strahl BD. Interpreting the language of histone and DNA modifications. Acta Biochim Biophys 2014; 1839:627–43.
22. Merrifield M, Kovalchuk O. Epigenetics in radiation biology: a new research frontier. Front Genet 2013; 4:40.
23. Bird AP, Wolffe AP. Methylation-induced repression–belts, braces, and chromatin. Cell 1999; 99:451–4.
24. Hark AT, Schoenherr CJ, Katz DJ, Ingram RS, Levorse JM, Tilghman SM. CTCF mediates methylation-sensitive enhancer-blocking activity at the H19/Igf2 locus. Nature 2000; 405:486–9.
25. Fazzari MJ, Greally JM. Epigenomics: beyond CpG islands. Nat Rev Genet 2004; 5:446–55.
26. Trasler JM. Gamete imprinting: setting epigenetic patterns for the next generation. Reprod Fertil Dev 2006; 18:63–9.
27. Ehrlich M. DNA methylation in cancer: too much, but also too little. Oncogene 2002; 21:5400–13.
28. Robertson KD. DNA methylation and chromatin - unraveling the tangled web. Oncogene 2002; 21:5361–79.
29. Jaenisch R, Bird A. Epigenetic regulation of gene expression: how the genome integrates intrinsic and environmental signals. Nat Genet 2003; 33:S245–54.
30. Goll MG, Bestor TH. Eukaryotic cytosine methyltransferases. Annu Rev Biochem 2005; 74:481–514.
31. Robertson KD. DNA methylation, methyltransferases, and cancer. Oncogene 2001; 20:3139–55.
32. Rountree MR, Bachman KE, Herman JG, Baylin SB. DNA methylation, chromatin inheritance, and cancer. Oncogene 2001; 20:3156–65.
33. Reik W, Dean W, Walter J. Epigenetic reprogramming in mammalian development. Science 2001; 293:1089–93.
34. Nan X, Campoy FJ, Bird A. MeCP2 is a transcriptional repressor with abundant binding sites in genomic chromatin. Cell 1997; 88:471–81.
35. Amir RE, Zoghbi HY. Rett syndrome: methyl-CpG-binding protein 2 mutations and phenotype-genotype correlations. Am J Med Genet 2000; 97:147–52.
36. Goldberg AD, Allis CD, Bernstein E. Epigenetics: a landscape takes shape. Cell 2007; 128:635–8.
37. Campos EI, Stafford JM, Reinberg D. Epigenetic inheritance: histone bookmarks across generations. Trends Cell Biol 2014; 24:664–74.

38. Nightingale KP, Baumann M, Eberharter A, Mamais A, Becker PB, Boyes J. Acetylation increases access of remodelling complexes to their nucleosome targets to enhance initiation of V(D)J recombination. Nucleic Acids Res 2007; 35:6311–21.

39. Tessarz P, Kouzarides T. Histone core modifications regulating nucleosome structure and dynamics. Nat Rev Mol Cell Biol 2014; 15:703–8.

40. Bedford MT, Richard S. Arginine methylation an emerging regulator of protein function. Mol Cell 2005; 18:263–72.

41. Rice JC, Briggs SD, Ueberheide B, Barber CM, Shabanowitz J, Hunt DF, et al. Histone methyltransferases direct different degrees of methylation to define distinct chromatin domains. Mol Cell 2003; 12:1591–8.

42. Sawicka A, Seiser C. Sensing core histone phosphorylation - a matter of perfect timing. Acta Biochim Biophys 2014; 1839:711–8.

43. Weake VM, Workman JL. Histone ubiquitination: triggering gene activity. Mol Cell 2008; 29:653–63.

44. Lee JS, Smith E, Shilatifard A. The language of histone crosstalk. Cell 2010; 142:682–5.

45. Struhl K. Transcriptional noise and the fidelity of initiation by RNA polymerase II. Nat Struct Mol Biol 2007; 14:103–5.

46. Mattick JS, Makunin IV. Non-coding RNA. Hum Mol Genet 2006; 15 Spec No 1:R17–29.

47. Cai Y, Yu X, Hu S, Yu J. A brief review on the mechanisms of miRNA regulation. Genomics Proteomics Bioinformatics 2009; 7:147–54.

48. Stroynowska-Czerwinska A, Fiszer A, Krzyzosiak WJ. The panorama of miRNA-mediated mechanisms in mammalian cells. Cell Mol Life Sci 2014; 71:2253–70.

49. Xu C, Tian J, Mo B. siRNA-mediated DNA methylation and H3K9 dimethylation in plants. Protein Cell 2013.

50. Fatica A, Bozzoni I. Long non-coding RNAs: new players in cell differentiation and development. Nat Rev Genet 2014; 15:7–21.

51. Iwasaki YW, Siomi MC, Siomi H. PIWI-interacting RNA: its biogenesis and functions. Annu Rev Biochem 2015; 84:405–33.

52. Luteijn MJ, Ketting RF. PIWI-interacting RNAs: from generation to transgenerational epigenetics. Nat Rev Genet 2013; 14:523–34.

53. Castel SE, Martienssen RA. RNA interference in the nucleus: roles for small RNAs in transcription, epigenetics and beyond. Nat Rev Genet 2013; 14:100–12.

54. *54*. d'Adda di Fagagna F. A direct role for small non-coding RNAs in DNA damage response. Trends Cell Biol 2014; 24:171–8.

55. Sugimoto K, Kage H, Aki N, Sano A, Kitagawa H, Nagase T, et al. The induction of H3K9 methylation by PIWIL4 at the p16Ink4a locus. Biochem Biophys Res Commun 2007; 359:497–502.

56. Oswald J, Engemann S, Lane N, Mayer W, Olek A, Fundele R, et al. Active demethylation of the paternal genome in the mouse zygote. Curr Biol 2000; 10:475–8.

57. Mayer W, Niveleau A, Walter J, Fundele R, Haaf T. Demethylation of the zygotic paternal genome. Nature 2000; 403:501–2.

58. Morgan HD, Santos F, Green K, Dean W, Reik W. Epigenetic reprogramming in mammals. Hum Mol Genet 2005; 14 Spec No 1:R47–58.

59. Dean W, Santos F, Stojkovic M, Zakhartchenko V, Walter J, Wolf E, et al. Conservation of methylation reprogramming in mammalian development: aberrant reprogramming in cloned embryos. Proc Natl Acad Sci U S A 2001; 98:13734–8.

60. Santos F, Hendrich B, Reik W, Dean W. Dynamic reprogramming of DNA methylation in the early mouse embryo. Dev Biol 2002; 241:172–82.

61. Barlow DP, Bartolomei MS. Genomic imprinting in mammals. Cold Spring Harb Perspect Biol 2014; 6.

62. Seki Y, Hayashi K, Itoh K, Mizugaki M, Saitou M, Matsui Y. Extensive and orderly reprogramming of genome-wide chromatin modifications associated with specification and early development of germ cells in mice. Dev Biol 2005; 278:440–58.

63. Sato S, Yoshimizu T, Sato E, Matsui Y. Erasure of methylation imprinting of Igf2r during mouse primordial germ-cell development. Mol Reprod Dev 2003; 65:41–50.

64. Swales AK, Spears N. Genomic imprinting and reproduction. Reproduction 2005; 130:389–99.

65. Ferguson-Smith AC. Genomic imprinting: the emergence of an epigenetic paradigm. Nat Rev Genet 2011; 12:565–75.

66. Bagislar S, Ustuner I, Cengiz B, Soylemez F, Akyerli CB, Ceylaner S, et al. Extremely skewed X-chromosome inactivation patterns in women with recurrent spontaneous abortion. Aust N Z J Obstet Gynaecol 2006; 46:384–7.

67. Gendrel AV, Heard E. Noncoding RNAs and epigenetic mechanisms during X-chromosome inactivation. Annu Rev Cell Dev Biol 2014; 30:561–80.

68. Fukuda A, Tomikawa J, Miura T, Hata K, Nakabayashi K, Eggan K, et al. The role of maternal-specific H3K9me3 modification in establishing imprinted X-chromosome inactivation and embryogenesis in mice. Nat Commun 2014; 5:5464.

69. Wang J, Zhang Y, Xu K, Mao X, Xue L, Liu X, et al. Genome-wide screen of DNA methylation changes induced by low dose X-ray radiation in mice. PloS One 2014; 9:e90804.

70. Feil R, Fraga MF. Epigenetics and the environment: emerging patterns and implications. Nat Rev Genet 2011; 13:97–109.

71. Blewitt ME, Vickaryous NK, Paldi A, Koseki H, Whitelaw E. Dynamic reprogramming of DNA methylation at an epigenetically sensitive allele in mice. PLoS Genet 2006; 2:e49.

72. Morgan HD, Sutherland HG, Martin DI, Whitelaw E. Epigenetic inheritance at the agouti locus in the mouse. Nat Genet 1999; 23:314–8.

73. Farthing CR, Ficz G, Ng RK, Chan CF, Andrews S, Dean W, et al. Global mapping of DNA methylation in mouse promoters reveals epigenetic reprogramming of pluripotency genes. PLoS Genet 2008; 4:e1000116.

74. Borgel J, Guibert S, Li Y, Chiba H, Schubeler D, Sasaki H, et al. Targets and dynamics of promoter DNA methylation during early mouse development. Nat Genet 2010; 42:1093–100.

75. Suter CM, Martin DI, Ward RL. Germline epimutation of MLH1 in individuals with multiple cancers. Nat Genet 2004; 36:497–501.

76. Goel A, Nguyen TP, Leung HC, Nagasaka T, Rhees J, Hotchkiss E, et al. De novo constitutional MLH1 epimutations confer early-onset colorectal cancer in two new sporadic Lynch syndrome cases, with derivation of the epimutation on the paternal allele in one. Int J Cancer 2011; 128:869–78.

77. Lister R, Pelizzola M, Dowen RH, Hawkins RD, Hon G, Tonti-Filippini J, et al. Human DNA methylomes at base resolution show widespread epigenomic differences. Nature 2009; 462:315–22.

78. Hammoud SS, Nix DA, Zhang H, Purwar J, Carrell DT, Cairns BR. Distinctive chromatin in human sperm packages genes for embryo development. Nature 2009; 460:473–8.

79. Hammoud SS, Low DH, Yi C, Carrell DT, Guccione E, Cairns BR. Chromatin and transcription transitions of mammalian adult germline stem cells and spermatogenesis. Cell Stem Cell 2014; 15:239–53.

80. Brykczynska U, Hisano M, Erkek S, Ramos L, Oakeley EJ, Roloff TC, et al. Repressive and active histone methylation mark distinct promoters in human and mouse spermatozoa. Nat Struct Mol Biol 2010; 17:679–87.

81. Heard E, Martienssen RA. Transgenerational epigenetic inheritance: myths and mechanisms. Cell 2014; 157:95–109.

82. Kovalchuk O, Baulch JE. Epigenetic changes and nontargeted radiation effects–is there a link? Environ Mol Mutagen 2008; 49:16–25.

83. Lima F, Ding D, Goetz W, Yang AJ, Baulch JE. High LET (56)Fe ion irradiation induces tissue-specific changes in DNA methylation in the mouse. Environ Mol Mutagen 2014; 55:266–77.

84. Chaudhry MA, Omaruddin RA. Differential DNA methylation alterations in radiation-sensitive and -resistant cells. DNA Cell Biol 2012; 31:908–16.

85. Luzhna L, Ilnytskyy Y, Kovalchuk O. Mobilization of LINE-1 in irradiated mammary gland tissue may potentially contribute to low dose radiation-induced genomic instability. Genes Cancer 2015; 6:71–81.

86. Lee Y, Kim YJ, Choi YJ, Lee JW, Lee S, Cho YH, et al. Radiation-induced changes in DNA methylation and their relationship to chromosome aberrations in nuclear power plant workers. Int J Radiat Biol 2015; 91:142–9.

87. Ye S, Yuan D, Xie Y, Pan Y, Shao C. Role of DNA methylation in long-term low-dose gamma-rays induced adaptive response in human B lymphoblast cells. Int J Radiat Biol 2013; 89:898–906.

88. Newman MR, Sykes PJ, Blyth BJ, Bezak E, Lawrence MD, Morel KL, et al. A single whole-body low dose X-irradiation does not affect L1, B1 and IAP repeat element DNA methylation longitudinally. PloS One 2014; 9:e93016.

89. Kovalchuk O, Burke P, Besplug J, Slovack M, Filkowski J, Pogribny I. Methylation changes in muscle and liver tissues of male and female mice exposed to acute and chronic low-dose X-ray-irradiation. Mutat Res 2004; 548:75–84.

90. Tryndyak VP, Kovalchuk O, Pogribny IP. Loss of DNA methylation and histone H4 lysine 20 trimethylation in human breast cancer cells is associated with aberrant expression of DNA methyltransferase 1, Suv4-20h2 histone methyltransferase and methyl-binding proteins. Cancer Biol Ther 2006; 5:65–70.

91. Pogribny I, Koturbash I, Tryndyak V, Hudson D, Stevenson SM, Sedelnikova O, et al. Fractionated low-dose radiation exposure leads to accumulation of DNA damage and profound alterations in DNA and histone methylation in the murine thymus. Mol Cancer Res 2005; 3:553–61.

92. Bae S, Kim K, Cha HJ, Choi Y, Shin SH, An IS, et al. Altered microRNA expression profiles are involved in resistance to low-dose ionizing radiation in the absence of BMI1 in human dermal fibroblasts. Int J Oncol 2014; 45:1618–28.

93. Tabe Y, Hatanaka Y, Nakashiro M, Sekihara K, Yamamoto S, Matsushita H, et al. Integrative genomic and proteomic analyses identifies glycerol-3-phosphate acyltransferase as a target of low-dose ionizing radiation in EBV infected-B cells. Int J Radiat Biol 2016; 92:24–34.

94. Stankevicins L, Almeida da Silva AP, Ventura Dos Passos F, Dos Santos Ferreira E, Menks Ribeiro MC, David MG, et al. MiR-34a is up-regulated in response to low dose, low energy X-ray induced DNA damage in breast cells. Radiat Oncol 2013; 8:231.

95. Wang B, Li D, Sidler C, Rodriguez-Juarez R, Singh N, Heyns M, et al. A suppressive role of ionizing radiation-responsive miR-29c in the development of liver carcinoma via targeting WIP1. Oncotarget 2015; 6:9937–50.

96. Johnstone SE, Baylin SB. Stress and the epigenetic landscape: a link to the pathobiology of human diseases? Nat Rev Genet 2010; 11:806–12.

97. Franco R, Schoneveld O, Georgakilas AG, Panayiotidis MI. Oxidative stress, DNA methylation and carcinogenesis. Cancer Lett 2008; 266:6–11.

98. Gu X, Sun J, Li S, Wu X, Li L. Oxidative stress induces DNA demethylation and histone acetylation in SH-SY5Y cells: potential epigenetic mechanisms in gene transcription in Abeta production. Neurobiol Aging 2013; 34:1069–79.

99. Feng B, Ruiz MA, Chakrabarti S. Oxidative-stress-induced epigenetic changes in chronic diabetic complications. Can J Physiol Pharmacol 2013; 91:213–20.

100. Sundar IK, Caito S, Yao H, Rahman I. Oxidative stress, thiol redox signaling methods in epigenetics. Methods Enzymol 2010; 474:213–44.

101. Galligan JJ, Rose KL, Beavers WN, Hill S, Tallman KA, Tansey WP, et al. Stable histone adduction by 4-oxo-2-nonenal: a potential link between oxidative stress and epigenetics. J Am Chem Soc 2014; 136:11864–6.

102. McCabe MT, Ott HM, Ganji G, Korenchuk S, Thompson C, Van Aller GS, et al. EZH2 inhibition as a therapeutic strategy for lymphoma with EZH2-activating mutations. Nature 2012; 492:108–12.

103. Roche J, Nasarre P, Gemmill R, Baldys A, Pontis J, Korch C, et al. Global decrease of histone H3K27 acetylation in ZEB1-induced epithelial to mesenchymal transition in lung cancer cells. Cancers 2013; 5:334–56.

104. Petruk S, Black KL, Kovermann SK, Brock HW, Mazo A. Stepwise histone modifications are mediated by multiple enzymes that rapidly associate with nascent DNA during replication. Nat Commun 2013; 4:2841.

105. Safi SZ, Qvist R, Yan GO, Ismail IS. Differential expression and role of hyperglycemia induced oxidative stress in epigenetic regulation of beta1, beta2 and beta3-adrenergic receptors in retinal endothelial cells. BMC Med Genomics 2014; 7:29.

106. Cuozzo C, Porcellini A, Angrisano T, Morano A, Lee B, Di Pardo A, et al. DNA damage, homology-directed repair, and DNA methylation. PLoS Genet 2007; 3:e110.

107. Meilinger D, Fellinger K, Bultmann S, Rothbauer U, Bonapace IM, Klinkert WE, et al. Np95 interacts with de novo DNA methyltransferases, Dnmt3a and Dnmt3b, and mediates epigenetic silencing of the viral CMV promoter in embryonic stem cells. EMBO Rep 2009; 10:1259–64.

108. Wei D, Loeken MR. Increased DNA methyltransferase 3b (Dnmt3b)-mediated CpG island methylation stimulated by oxidative stress inhibits expression of a gene required for neural tube and neural crest development in diabetic pregnancy. Diabetes 2014; 63:3512–22.

109. Thanan R, Techasen A, Hou B, Jamnongkan W, Armartmuntree N, Yongvanit P, et al. Development and characterization of a hydrogen peroxide-resistant cholangiocyte cell line: A novel model of oxidative stress-related cholangiocarcinoma genesis. Biochem Biophys Res Commun 2015; 464:182–8.

110. Szumiel I. Ionizing radiation-induced oxidative stress, epigenetic changes and genomic instability: the pivotal role of mitochondria. Int J Radiat Biol 2015; 91:1–12.

111. Avila JG, Echeverri I, de Plata CA, Castillo A. Impact of oxidative stress during pregnancy on fetal epigenetic patterns and early origin of vascular diseases. Nutr Rev 2015; 73:12–21.

112. Kloypan C, Srisa-Art M, Mutirangura A, Boonla C. LINE-1 hypomethylation induced by reactive oxygen species is mediated via depletion of S-adenosylmethionine. Cell Biochem Funct 2015; 33:375–85.

113. Goodarzi AA, Jeggo P, Lobrich M. The influence of heterochromatin on DNA double strand break repair: Getting the strong, silent type to relax. DNA Repair 2010; 9:1273–82.

114. Ahel D, Horejsi Z, Wiechens N, Polo SE, Garcia-Wilson E, Ahel I, et al. Poly(ADP-ribose)-dependent regulation of DNA repair by the chromatin remodeling enzyme ALC1. Science 2009; 325:1240–3.

115. Nishida N, Arizumi T, Takita M, Kitai S, Yada N, Hagiwara S, et al. Reactive oxygen species induce epigenetic instability through the formation of 8-hydroxydeoxyguanosine in human hepatocarcinogenesis. Dig Dis 2013; 31:459–66.

116. Ponnusamy L, Mahalingaiah PK, Singh KP. Chronic oxidative stress increases resistance to doxorubicin-induced cytotoxicity in renal carcinoma cells potentially through epigenetic mechanism. Mol Pharmacol 2016; 89:27–41.

117. Basso M, Ratan RR. Transglutaminase is a therapeutic target for oxidative stress, excitotoxicity and stroke: a new epigenetic kid on the CNS block. J Cereb Blood Flow Metab 2013; 33:809–18.

118. Rahman I. Oxidative stress, transcription factors and chromatin

remodelling in lung inflammation. Biochemi Pharmacol 2002; 64:935–42.

119. Mishra PK, Raghuram GV, Jain D, Jain SK, Khare NK, Pathak N. Mitochondrial oxidative stress-induced epigenetic modifications in pancreatic epithelial cells. Int J Toxicol 2014; 33:116–29.

120. Khanal T, Kim D, Johnson A, Choubey D, Kim K. Deregulation of NR2E3, an orphan nuclear receptor, by benzo(a)pyrene-induced oxidative stress is associated with histone modification status change of the estrogen receptor gene promoter. Toxicol Lett 2015; 237:228–36.

121. Vrtacnik P, Marc J, Ostanek B. Hypoxia mimetic deferoxamine influences the expression of histone acetylation- and DNA methylation-associated genes in osteoblasts. Connect Tissue Res 2015; 56:228–35.

122. Paredes-Gonzalez X, Fuentes F, Su ZY, Kong AN. Apigenin reactivates Nrf2 anti-oxidative stress signaling in mouse skin epidermal JB6 P + cells through epigenetics modifications. AAPS J 2014; 16:727–35.

123. Yang B, Wagner J, Damaschke N, Yao T, Wuerzberger-Davis SM, Lee MH, et al. A novel pathway links oxidative stress to loss of insulin growth factor-2 (IGF2) imprinting through NF-kappaB activation. PloS One 2014; 9:e88052.

124. Fernandez-Palomo C, Seymour C, Mothersill C. Inter-relationship between low-dose hyper-radiosensitivity and radiation-induced bystander effects in the human T98G glioma and the epithelial HaCaT cell line. Radiat Res 2016; 185:124–33.

125. Ishii K, Hosoi Y, Ono T, Sakamoto K. Enhanced proliferation and IL-1 production of mouse splenocytes by low-dose whole-body X-irradiation. Physiol Chem Phys Med NMR 1996; 28:7–14.

126. Glover D, Little JB, Lavin MF, Gueven N. Low dose ionizing radiation-induced activation of connexin 43 expression. Int J Radiat Biol 2003; 79:955–64.

127. Klokov D, Leskov K, Araki S, Zou Y, Goetz EM, Luo X, et al. Low dose IR-induced IGF-1-sCLU expression: a p53-repressed expression cascade that interferes with TGFbeta1 signaling to confer a pro-survival bystander effect. Oncogene 2013; 32:479–90.

128. Temme J, Bauer G. Low-dose gamma irradiation enhances superoxide anion production by nonirradiated cells through TGF-beta1-dependent bystander signaling. Radiat Res 2013; 179:422–32.

129. Pandey BN, Kumar A, Ali M, Mishra KP. Bystander effect of conditioned medium from low and high doses of gamma-irradiated human leukemic cells on normal lymphocytes and cancer cells. J Environ Pathol Toxicol Oncol 2011; 30:333–40.

130. Plata Mdel M, Williams L, Seki Y, Hartil K, Kaur H, Lin CL, et al. Critical periods of increased fetal vulnerability to a maternal high fat diet. Reprod Biol Endocrinol 2014; 12:80.

131. Valentin J. Avoidance of radiation injuries from medical interventional procedures. Ann ICRP 2000; 30:7–67.

132. Mulder EJ, Robles de Medina PG, Huizink AC, Van den Bergh BR, Buitelaar JK, Visser GH. Prenatal maternal stress: effects on pregnancy and the (unborn) child. Early Hum Dev 2002; 70:3–14.

133. Godfrey KM, Barker DJ. Fetal programming and adult health. Public Health Nutr 2001; 4:611–24.

134. Barker DJ. Fetal programming of coronary heart disease. Trends Endocrinol Metab 2002; 13:364–8.

135. Hall EJ, Giaccia AJ. Radiobiology for the radiobiologist. Philadelphia, PA: JB Lippencott Co. 1994.

136. Valentin J. Biological effects after prenatal irradiation (embryo and fetus): ICRP Publication 90 Approved by the Commission in October 2002. Ann ICRP 2003; 33:1–206.

137. Thompson LP, Al-Hasan Y. Impact of oxidative stress in fetal programming. J Pregnancy 2012; 2012:582748.

138. Stangenberg S, Nguyen LT, Chen H, Al-Odat I, Killingsworth MC, Gosnell ME, et al. Oxidative stress, mitochondrial perturbations and fetal programming of renal disease induced by maternal smoking. Int J Biochem Cell Biol 2015; 64:81–90.

139. Peuchant E, Brun JL, Rigalleau V, Dubourg L, Thomas MJ, Daniel JY, et al. Oxidative and antioxidative status in pregnant women with either gestational or type 1 diabetes. Clin Biochem 2004; 37:293–8.

140. Block G, Dietrich M, Norkus EP, Morrow JD, Hudes M, Caan B, et al. Factors associated with oxidative stress in human populations. Am J Epidemiol 2002; 156:274–85.

141. Franco MC, Kawamoto EM, Gorjao R, Rastelli VM, Curi R, Scavone C, et al. Biomarkers of oxidative stress and antioxidant status in children born small for gestational age: evidence of lipid peroxidation. Pediatr Res 2007; 62:204–8.

142. Bayhan G, Kocyigit Y, Atamer A, Atamer Y, Akkus Z. Potential atherogenic roles of lipids, lipoprotein(a) and lipid peroxidation in preeclampsia. Gynecol Endocrinol 2005; 21:1–6.

143. Atamer Y, Kocyigit Y, Yokus B, Atamer A, Erden AC. Lipid peroxidation, antioxidant defense, status of trace metals and leptin levels in preeclampsia. Eur J Obstet Gynecol Reprod Biol 2005; 119:60–6.

144. Roghair RD, Miller FJ Jr., Scholz TD, Lamb FS, Segar JL. Endothelial superoxide production is altered in sheep programmed by early gestation dexamethasone exposure. Neonatology 2008; 93:19–27.

145. Rosenfeld CS. Animal models to study environmental epigenetics. Biol Reprod 2010; 82:473–88.

146. Dolinoy DC. The agouti mouse model: an epigenetic biosensor for nutritional and environmental alterations on the fetal epigenome. Nutr Rev 2008; 66:S7–11.

147. Klebig ML, Wilkinson JE, Geisler JG, Woychik RP. Ectopic expression of the agouti gene in transgenic mice causes obesity, features of type II diabetes, and yellow fur. Proc Natl Acad Sci U S A 1995; 92:4728–32.

148. Bernal AJ, Dolinoy DC, Huang D, Skaar DA, Weinhouse C, Jirtle RL. Adaptive radiation-induced epigenetic alterations mitigated by antioxidants. FASEB J 2013; 27:665–71.

149. Kang KA, Zhang R, Kim GY, Bae SC, Hyun JW. Epigenetic changes induced by oxidative stress in colorectal cancer cells: methylation of tumor suppressor RUNX3. Tumour Biol 2012; 33:403–12.

150. Patterson AJ, Xiao D, Xiong F, Dixon B, Zhang L. Hypoxia-derived oxidative stress mediates epigenetic repression of PKCepsilon gene in foetal rat hearts. Cardiovasc Res 2012; 93:302–10.

151. Nadasi E, Clark JS, Szanyi I, Varjas T, Ember I, Baliga R, et al. Epigenetic modifiers exacerbate oxidative stress in renal proximal tubule cells. Anticancer Res 2009; 29:2295–9.

152. Rosenfeld CS, Sieli PT, Warzak DA, Ellersieck MR, Pennington KA, Roberts RM. Maternal exposure to bisphenol A and genistein has minimal effect on A(vy)/a offspring coat color but favors birth of agouti over nonagouti mice. Proc Natl Acad Sci U S A 2013; 110:537–42.

153. Dolinoy DC, Huang D, Jirtle RL. Maternal nutrient supplementation counteracts bisphenol A-induced DNA hypomethylation in early development. Proc Natl Acad Sci U S A 2007; 104:13056–61.

154. Redpath JL, Antoniono RJ. Induction of an adaptive response against spontaneous neoplastic transformation in vitro by low-dose gamma radiation. Radiat Res 1998; 149:517–20.

155. Shadley JD, Afzal V, Wolff S. Characterization of the adaptive response to ionizing radiation induced by low doses of X rays to human lymphocytes. Radiat Res 1987; 111:511–7.

156. Joiner MC, Lambin P, Malaise EP, Robson T, Arrand JE, Skov KA, et al. Hypersensitivity to very-low single radiation doses: its relationship to the adaptive response and induced radioresistance. Mutat Res 1996; 358:171–83.

157. Phan N, De Lisio M, Parise G, Boreham DR. Biological effects and adaptive response from single and repeated computed tomography scans in reticulocytes and bone marrow of C57BL/6 mice. Radiat Res 2012; 177:164–75.

RADIATION RESEARCH **188**, 539–546 (2017)
0033-7587/17 $15.00

DOI: 10.1667/RR14864.1

REVIEW

Impact of Ionizing Radiation on the Cardiovascular System: A Review

Stephanie Puukila,[a,1] Jennifer A. Lemon,[b] Simon J. Lees,[c] T. C. Tai,[d] Douglas R. Boreham[d,e] and Neelam Khaper[c,2]

[a] *Department of Biology, Lakehead University, Thunder Bay, ON, P7B 5E1, Canada;* [b] *Medical Physics and Applied Radiation Sciences, McMaster University, Hamilton ON, L8S 4L8, Canada;* [c] *Northern Ontario School of Medicine, Lakehead University, Thunder Bay, ON P7B 5E1, Canada;* [d] *Northern Ontario School of Medicine, Laurentian University, Sudbury, ON P3E 2C6, Canada; and Bruce Power, Tiverton, ON, N0G 2T0 Canada*

Puukila, S., Lemon, J. A., Lees, S. J., Tai, T. C., Boreham, D. R. and Khaper, N. Ionizing Radiation and the Heart: A Review. *Radiat. Res.* 188, 539–546 (2017).

Radiation therapy has become one of the main forms of treatment for various types of cancers. Cancer patients previously treated with high doses of radiation are at a greater risk to develop cardiovascular complications later in life. The heart can receive varying doses of radiation depending on the type of therapy and can even reach doses in the range of 17 Gy. Multiple studies have highlighted the role of oxidative stress and inflammation in radiation-induced cardiovascular damage. Doses of ionizing radiation below 200 mGy, however, have been shown to have beneficial effects in some experimental models of radiation-induced damage, but low-dose effects in the heart is still debated. Low-dose radiation may promote heart health and reduce damage from oxidative stress and inflammation, however there are few studies focusing on the impact of low-dose radiation on the heart. In this review, we summarize recent studies from animal models and human data focusing on the effects and mechanism(s) of action of radiation-induced damage to the heart, as well as the effects of high and low doses of radiation and dose rates.

INTRODUCTION

The use of ionizing radiation has become common practice in the treatment of cancer and medical diagnostics. It is estimated that more than 50% of patients with cancer are treated with radiotherapy (*1*). In Canada, medical diagnostic procedures account for roughly 40% of the average annual radiation dose in North America (*2*). Therefore, it is important to understand how cells and tissues respond to radiation. The absorption of radiation by living cells can directly disrupt atomic structures, producing chemical and biological changes. In the clinic, gamma and X rays, are the most commonly used types of ionizing radiation, exert about 70–80% of their effects indirectly through the generation of free radicals (*3–5*). Linear energy transfer (LET) influences the relative biological effectiveness of different radiation qualities, with high-LET radiation resulting in highly complex clusters of DNA damage, relative to simple evenly distributed patterns produced by low-LET radiation (*6–11*).

Previously, it was thought that early biochemical modifications that occur during or shortly after irradiation were due to the immediate effects produced by radiation exposure. However, cellular damage caused by oxidative changes may continue to arise for days and months after the initial exposure, likely due to continuous generation of reactive oxygen species (ROS) as a result of chain reactions typically propagated by lipid peroxidation (*6*, *12*, *13*). Radiation-induced oxidative stress has been shown to spread from irradiated cells to unirradiated neighboring (i.e., bystander) cells through gap junctions, membrane channels and paracrine mechanisms (*15–17*). Moreover, the bystander cells and their progeny exhibit neoplastic transformation as well as a wide range of oxidative damage, including elevated protein carbonyls, lipid peroxidation and genomic instability (*6*, *18*).

HIGH-DOSE RADIATION

The adverse cardiac effects of high-dose radiation in humans have been recognized where cases of heart disease were reported after radiotherapy. High doses of radiation used in cancer treatment have been shown to damage cardiac tissue, leading to cardiac dysfunction and cardiovascular disease (CVD). The dose of radiation the heart will receive depends on the type of radiation therapy. For example, when radiation is used for breast cancer therapy, doses to the heart can range from 3–17 Gy (*19*). A study conducted in 2,168 breast cancer patients reported that coronary events risk increased by

[1] Scholar-in-Training, Radiation Research Society.

[2] Address for correspondence: Medical Sciences Division, Northern Ontario School of Medicine, Lakehead University, 955 Oliver Road, Thunder Bay, ON P7B 5E1, Canada; e-mail: nkhaper@nosm.ca.

7.4% per Gy to the heart (*20*). Analyses on 8 randomized trials have found a 62% increase in cardiac deaths among breast cancer patients treated with radiation therapy (*21*, *22*).

Radiation-Induced Cardiovascular Complications

Oxidative stress and chronic inflammation have both been implicated in CVD. ROS has been shown to contribute to the development of cardiac remodeling processes including fibrosis, apoptosis and hypertrophy (*23*). Radiation exposure of tissue has been shown to increase cytokines, chemokines, growth factors, as well as ROS, thus perpetuating an inflammatory response over time (*24*). Also, studies on atomic bombs survivors have found elevated inflammatory markers and immune response modulation, which is discussed in more detail later in this review. Inflammation is also an integral component of the host response to tissue injury or host invasion and plays a particularly active role after myocardial infarction (MI). Stimulation of cytokines also contribute to molecular and phenotypic changes in cardiac myocytes including apoptosis, hypertrophy and contractile dysfunction (*23*). Radiation-induced CVD can include pericarditis, pericardial and myocardial fibrosis and coronary artery disease (CAD) (*25–27*). Acute effects are rare, but can occur during radiation treatment (*28*, *29*). Chronic pericarditis typically presents within 12 months of therapy, but may present months to years after completion of radiation treatment; with up to 20% of patients developing symptoms within 10 years of treatment (*27–29*). Radiation-induced myocardial fibrosis develops from the proliferation of collagen separating or replacing myocytes, leading to ischemia and in severe cases heart failure (*25*, *27*). Myocardial fibrosis typically develops at radiation doses above 30 Gy, is often asymptomatic and differs from other CVD because it can occur in the absence of an inflammatory response (*28*). Radiation damage has been reported to lead to reduced myocardial compliance through microvascular insufficiency and ischemia, which can result in interstitial fibrosis (*28*). Radiation-induced CAD resembles atherosclerotic CAD, however, exposure to radiation has been shown to lead to a fibrous plaque (*25*, *28*). There is increased proliferation of myofibroblasts and lipid containing macrophages that form plaques which can lead to ischemic heart disease and MI (*25*, *29*). Valvular lesions and calcification have also been described in irradiated patients (*25*, *30*) where coronary lesions caused by radiation therapy is the most significant cause of mortality from radiation-induced heart disease (*30*). Current literature suggests that there are three proposed mechanisms of radiation-induced CAD: ultrastructural damage to capillary networks which can ultimately lead to ischemia (*29*, *31*, *32*), structural damage to the epicardial arteries (*29*, *33*) and sustained inflammatory response attributed to NF-κB activation (*29*, *34*, *35*).

Atomic Bomb Survivors

Survivors of radiation exposure have been shown to develop cardiovascular disease years after exposure. Studies of survivors from the atomic bombs in Hiroshima and Nagasaki have shown there is a risk of developing cardiovascular disease (*36*, *37*). The radiation from the bombs was composed predominantly of γ rays and resulted in absorbed doses up to 4 Gy in survivors (*36*, *38*). Mortality from CVD was significantly increased >40 years after single whole body high-dose exposure (*36*, *37*). In fact, stroke and heart disease combined accounted for 1/3 of high-dose radiation associated deaths of atomic bomb survivors compared with cancer (*36*, *39*). For heart disease alone the estimated relative risk per Gy was 14% (*39*). Radiation-induced chronic low-grade inflammation has also been reported in this cohort. It was found that plasma levels of tumor necrosis factor (TNF)-α and interleukin (IL)-10 increased slightly in the high-dose group (over 1.5 Gy) while interferon (IFN)-γ, immunoglobulin (Ig)A, IgM and erythrocyte sedimentation rate increased with increased radiation dose (from 5 mGy to over 1.5 Gy) (*21*, *40*, *41*). There are several studies that investigated the long-term effects of the atomic bomb on the T-cell system. The level of CD4 T cells was significantly decreased with increased radiation dose in atomic bomb survivors. Also, the prevalence of MI was significantly higher in the survivors with a lower proportion of CD4 T cells (*42*). The response of T cells to mitogens, specifically the ability to produce IL-2, in atomic bomb survivors was also investigated. It was found that, of survivors examined, those exposed to higher doses (1.5 Gy) contained significantly fewer IL-2 producing CD4 T cells than those exposed to a lower dose (5 mGy) (*43*). Kusunoki *et al*. suggest the elevated levels of inflammatory markers found in survivors can be attributed, at least in part, to premature T-cell immunosenescence. This may also be involved in the development of aging-associated and inflammation related diseases observed in survivors (*44*).

Radiation therapy

Clinical investigations on how high-dose radiation affects the heart are difficult to conduct since cardiovascular events may occur years after completing radiotherapy (*35*). Most studies have examined physiological changes with limited information of the molecular mechanisms associated with cardiac response to radiation (summarized in Table 1). Irradiated arteries from patients undergoing a resection of a tumor in the head and neck region, or breast reconstruction after a mastectomy for breast cancer showed significant intimal thickening (*45*). Proteoglycan deposition and inflammatory cell infiltration were also increased in irradiated arteries (*45*). An increased risk of coronary heart disease after radiotherapy for peptic ulcer disease has been observed, where part of the heart received very high doses ranging from 7.6–18.4 Gy (*46*). Patients who receive

TABLE 1
Summary of Recent Studies on the Effect of Cell, Tissue or Whole-Body Ionizing Irradiation on the Cardiovascular System

Dose	Cell/tissue studies	Animal studies	Clinical studies
<200 mGy	NA	Decreased DNA damage (*84*) Reduced atherosclerosis lesions and serum cholesterol (*91*) Decreased oxidative stress, inflammation and fibrosis Increased capillary density (*95*) Changes in collagen IV (*97*) Enhancement of TNF-α and fibrinogen (*95*)	NA
200–900 mGy	N/A	Reduced atherosclerosis lesions and cholesterol (*91*) Increased capillary density (*95*) Changes in collagen IV (*95*) Enhancement of TNF-α and fibrinogen (*95*)	NA
1–4 Gy	Impaired cardiac myocyte calcium handling (*64*)	Increased inflammation (*66*) Increased ROS and mitochondrial dysfunction (*90*)	Increased development of cardiovascular disease (*35*) Increased inflammation (*3, 40*) Increased sedimentation rate (*40*) Increased plasma level of immunoglobulin (*40*) Decreased IL-2 producing CD4 T cells (*42*)
5–8 Gy	Increased ROS and mitochondrial dysfunction (*62*) Increased expression of oxidative stress, heat shock proteins and p53 target genes (*74*)	Increased myocardial fibrosis (*75*) Reduced left ventricular diameter (*75*) Elevated systemic inflammation (*75*)	Increased risk of coronary heart disease (*45*) Increased risk of MI, angina, pericarditis and valvular disease (*46*)
>8 Gy	Develop CAD after irradiation for Hodgkin's disease (*23*) Increased apoptosis (*63*) Mitochondrial dysfunction (*63*) Increased mitochondrial mass (*63*) Decreased succinate-driven state 2 respiration (*63*) Drop in aortic output (*64*)	Increased fibrosis and inflammation (*72*) Cellular peri-arterial fibrosis and irregular collagen deposition (*73*) Reduced global radial and circumferential strain (*73*) Increased myocardial fibrosis and systemic inflammation (*75*) Reduced left ventricular diameter (*75*)	Development of CAD after irradiation for Hodgkin's disease (*21*) Myocardial fibrosis (*27*) Intimal thickening (*44*) Proteoglycan deposition (*44*) Inflammatory cell infiltration (*44*)

radiation therapy for breast cancer treatment are particularly at risk of developing heart disease. One study investigated heart disease in women treated for breast cancer in Denmark and Sweden between 1976–2006 who received radiotherapy with mean doses of 6.3 and 2.7 Gy to the heart for left-sided and right-sided breast cancers, respectively. They reported significant increases in incidence for MI, angina, pericarditis and valvular disease (*47*). Early Breast Cancer Trialists' Collaborative Group data has shown that relative risk of cardiac death was related to the estimated mean cardiac dose, and that risk increased by 3% per Gy (*48*). Tjessem *et al*. investigated hypofractionated radiation therapy in breast cancer patients who received either 10 fractions of 4.3 Gy ×2/week (43 Gy total dose) or 20 fractions of 2.5 Gy ×5/week (50 Gy total dose). They found patients who received a lower total dose, but higher dose per fraction, had an increased risk of developing fatal ischemic heart disease compared to the group with lower dose fractions (*49*). This suggested that even if the total dose is lower, a higher dose per fraction was more harmful than a lower dose per fraction with a higher total dose. It appears that NF-κB activation may be involved in radiation induced cardiac damage. NF-κB was shown to be activated in arterial biopsies from human conduit arteries of patients who had previously received radiation therapy (*34*).

Radiation therapy patients treated as children and adolescents appear to be at the highest relative risk of a fatal cardiovascular complication when compared to age-matched untreated subjects (*50*, *51*). These patients have an increased risk for CAD, valvular heart disease, congestive heart failure and sudden death, with the risk being particularly high in patients treated before the age of 40

years (*21*, *52–55*). Due to the location and treatment regime for Hodgkin's disease, death due to cardiac disease is estimated to be responsible for about one quarter of the non-cancer mortality in these patients (*50*, *53*, *56–58*) The risk of cardiac-related deaths in survivors of Hodgkin's disease is estimated to be between 9.3 and 28 per 10,000 patients, with MI causing over two-thirds of the cardiac mortality observed in irradiated Hodgkin's disease patients (*50*, *53*, *58–60*). For example, a patient with Hodgkin's disease and who had completed radiation therapy to the mediastinum and neck (total of 40 Gy) was shown to have multiple cardiovascular complications leading to the development of CAD (*21*). In another study a 56-year-old woman who had previously been treated for Hodgkin's disease had signs of heart failure and myocardial fibrosis (*61*). It's been observed that increased death in Hodgkin's disease survivors took only a little over 10 years for the cumulative risk of fatality from ischemic heart disease to rapidly increase (*50*, *56*). These studies advocate for a reduction of dose levels in Hodgkin's disease treatment, but difficulties in implementing this strategy remain due to the patient-specific nature of treating Hodgkin's disease. Also, comparing patients that are unhealthy (cancer, immunocompromised, etc.) to healthy unirradiated individuals has several confounding factors that may bias the interpretation of the effects of radiation on the cardiovascular system.

Animal Studies

As clinical studies of the effects of radiation on the heart are limited, animal models aid to better understand the mechanism(s) of action of high doses of radiation similar to those used in cancer therapy. Oxidative stress appears to be associated with high-dose radiation-induced cardiac damage in animal models. Benderitter *et al*. exposed adult male rats to a single 20 Gy X-ray dose to the heart, which resulted in cardiac dysfunction at 1-month postirradiation accompanied by a decrease in cardiac vitamin E and an increase in Mn-superoxide dismutase and glutathione peroxidase levels at 4 months postirradiation. Based on these findings it was concluded that antioxidant defenses were activated relatively long after irradiation due to the sustained production of free radicals (*62*). Exposure of rat aorta smooth muscle cell line to 5 Gy γ radiation resulted in increased levels of ROS within minutes that disappeared within 30 min. Mitochondrial dysfunction was detected after 12 h and mitochondrial ROS and oxidation of mitochondrial DNA was observed 24 h postirradiation (*63*). Sridharan *et al*. investigated the effect of radiation on mitochondrial membrane of rat hearts where the rats received a single 21 Gy X-ray dose to the heart. They found there was an increase in apoptosis, reduction in mitochondrial membrane potential, increased calcium-induced mitochondrial permeability transition pore opening, increased mitochondrial mass and decreased succinate-driven state 2 respiration, suggesting that local heart irradiation caused mitochondrial dysfunction (*64*). Moreover, radiation induced oxidative stress impacts cardiac myocytes calcium handling. Isolated ventricular myocytes and the mediastinal area of anaesthetized mice were exposed to 4 and 20 Gy X-ray doses, respectively. Calcium transient amplitudes and sarcoplasmic reticulum calcium load decreased in a dose dependent manner. Exposure led to increased ROS levels, which activated Ca^{+}/calmodulin-dependent protein kinase II, leading to impaired Ca^{+} handling and ultimately cardiac dysfunction (*65*).

As radiation is known to cause damage to DNA the role of tumor suppressor protein p53 in radiation-induced myocardial injury has also been investigated. Mice with an endothelial cell-specific deletion of p53 underwent whole-heart X-ray irradiation. After a single12 Gy dose or 10 daily fractions of 3 Gy, the lifespan of p53 deficient mice was significantly decreased compared to wild-type irradiated controls. Histopathogy examination showed multifocal areas of degeneration and necrosis in the myocardium. Whole-heart 12 Gy irradiation led to impaired systolic function, cardiac hypertrophy, vascular remodeling, myocardial hypoxia, necrosis and ischemia. Mice lacking p21, a transcriptional target of p53, also developed myocardial degeneration, necrosis, systolic dysfunction and cardiac hypertrophy after whole-heart 12 Gy irradiation (*66*).

Inflammation and fibrosis, like oxidative stress are also implicated in several cardiac disease conditions. Radiation has been shown to induce inflammatory response. A study by Azimzadeh *et al*. found hearts from mice that received whole-body 3 Gy γ irradiation had altered expression of several inflammatory mediators and antioxidants compared to nonirradiated controls (*67*). Upregulation of cytokines, such as IL-6 and IL-8, have been observed after endothelial cell irradiation in a time and dose dependent manner (*26*, *68*). Elevated cytokines can promote interstitial fibrosis and collagen deposition. Increased TNF-α and TGF-β levels have been shown to correlate closely with the deposition of collagen (*23*, *69*). Radiation-induced fibrosis involves the interaction of several cytokines and growth factors, fibroblast proliferation and differentiation, as well as matrix remodeling (*70*, *71*). Premature differentiation of progenitor fibroblasts to fibrocytes can also be radiation induced, potentially leading to enhanced collagen synthesis (*72*). Hearts from rats that received 15 or 18 Gy chest γ irradiation revealed significant myocardial fibrosis and necrosis when compared to controls. Protein and gene expression of transcription factor peroxisome proliferator-activated receptors (PPAR), tissue inhibitor of metalloproteinase-1 (TIMP-1), and TGF-β were also significantly higher in the irradiated hearts (*73*). The impact of high-dose radiation on coronary microvasculature and ventricular function of rats exposed to 10 Gy whole-body X-ray radiation has also been examined. Radiation exposure resulted in cellular peri-arterial fibrosis and irregular collagen deposition thereby altering endothelial and cardiac function (*74*). A study using microarray analysis with rat fibroblasts and cardiac myocytes irradiated with 8 Gy

showed increased oxidative stress, heat-shock proteins and expression of p53 target genes. Moreover, extracellular matrix formation and lipid metabolism gene expression was increased in fibroblasts, while antioxidant and cytokine gene expression were increased in cardiac myocytes suggesting that gene expression response subsequent to radiation exposure is cell specific (*75*). Nonhuman primates have also been used to examine the late effects of whole-body γ irradiation on the heart. Male rhesus macaques received a single total-body dose of 6.5–8.4 Gy γ irradiation where it was demonstrated that radiation led to increased myocardial fibrosis, reduced left ventricular dimension and elevated systemic inflammation (*76*).

It is clear that cardiac damage due to high doses of radiation is a result of increased ROS and inflammation, which can in turn lead to increased fibrosis (summarized in Table 1). Further studies are required to fully understand the mechanism(s) of action and long-term effects so mitigation strategies can be developed to help protect patients from high-dose exposures.

LOW-DOSE RADIATION

While it is well known that high doses of radiation are harmful to long-term cardiac function, it appears that low doses of radiation may not be detrimental and, under certain circumstances, may induce mechanisms that could be beneficial. The definition of low-dose radiation (LDR) varies depending upon the endpoint but for cardiovascular effects it has been proposed to be doses below 200 mGy (*77*). The existence of beneficial responses indicates that the dose-response relationships for some biological effects is not linear and not proportional to dose (*78*). It is suggested that a sudden, yet nonlethal, rise of toxin concentration in a biological system will tend to elicit stress responses and stimulate adaptation, usually as protective mechanisms (*79–81*). This is likely due to involvement of an innate immune response and decreased inflammation. LDR has also been shown to reduce the development of tumor growth, suppress tumor metastases and autoimmune diseases (*82–84*). Taylor *et al*. investigated DNA damage induced by increasing levels of ^{18}F-FDG injection, commonly used for PET scans and demonstrated that at 72 h post-injection the highest injection activities used (14.80 MBq) did not lead to residual DNA damage in hematopoetic tissue, but instead decreased the level of damage below controls (*85*). However, the effect of ^{18}F-FDG injection on the heart has yet to be elucidated. The same group investigated cancer risk in cancer-prone *Trp53*$^{+/-}$ mice that received either 10 mGy γ rays or 10 mGy ^{18}F-FDG injection. Neither 10 mGy irradiation significantly modified the frequency or latency of tumourigenesis relative to unirradiated control mice. The 10 mGy γ rays and 10 mGy ^{18}F-FDG doses also did not alter the formation of tissue specific lesions on the hearts of these animals (*86*). Because the repair mechanisms induced by low-dose radiation is suggested to have an all-or-nothing response, it not only repairs the small amount of damage induced by radiation, but also repairs damage missed by the cell's normal housekeeping systems, which consequently has the capacity to further reduce the risk due to exposure to other toxins (*87*, *88*). Increasing evidence indicates that adaptive responses can occur after either a single acute low dose, as well as protracted low-dose-rate exposures to X ray or γ radiation (*79*, *89*, *90*).

Low-Dose Radiation and The Heart

The impact of radiation on mitochondrial function in mice hearts exposed to either a low dose (0.2 Gy) or a high dose (2 Gy) of radiation has been studied. The mitochondria exposed to high-dose radiation showed functional impairment reflected as partial deactivation of Complex I and Complex III, decreased succinate-driven respiratory capacity, increased levels of ROS and enhanced oxidation of mitochondrial proteins, whereas a low dose of radiation had no effect on mitochondrial function (*91*). Studies have demonstrated that low-dose radiation has beneficial effects against atherosclerotic progression in atherosclerosis prone *ApoE*$^{-/-}$ mice that were exposed to either 25, 50, 100 or 500 mGy at either low-dose rate (1.0 mGy/min) or high-dose rate (150 mGy/min). Low-dose-rate exposure at early stages reduced lesion frequency and size in early stages of atherosclerosis with no significant impact on total serum cholesterol. Low-dose exposure at late stages of disease reduced average lesion size and decreased total serum cholesterol. High-dose-rate exposure during early-stage disease produced both protective and detrimental effects suggesting that low-dose radiation, particularly low-dose-rate exposures, slow the progression of atherosclerotic disease regardless of disease stage at time of exposure (*92*). The same group also investigated the influence of low doses (25–500 mGy) on disease progression in *ApoE*$^{-/-}$ mice with reduced *p53* function (*Trp53*$^{+/-}$). When exposed to low doses in early stages of atherosclerosis, lesion growth and frequency were decreased accompanied by the progression of lesion severity in the aortic root in *Trp53*$^{+/-}$ mice. Exposure of *Trp53*$^{+/-}$ mice at later stages of disease did not demonstrate these beneficial effects. In fact, radiation exposure accelerated lesion growth and increased serum cholesterol levels indicating that reduced *p53* function does not influence the protective effects of low-dose exposure against early stage atherosclerosis, however exposed to the same doses at late stage disease reduced *p53* function produced detrimental effects (*93*).

Low-dose radiation has also been shown to impact type 1 diabetes in a mouse model that received a whole-body 25-mGy dose. It was demonstrated that LDR caused a significant decrease in oxidative damage and fibrosis and gene expression and protein levels of IL-18, TNF-α, plasminogen activator inhibitor (PAI)-1 and monocyte chemoattractant protein (MCP)-1 when compared to unirradiated diabetic mice, while intercellular adhesion

molecule-1 did not change. These results suggested that while LDR has an effect on the inflammatory response in cardiac pathogenesis caused by diabetes, each inflammatory mediator may have its own mechanism and pathway that may or may not be influenced by LDR (*94*).

A study in *ApoE*$^{-/-}$ mice, which received 0.2 and 2 Gy local irradiation to the heart, investigated inflammatory infiltration and fibrosis. The 0.2 Gy treatment induced premature death in the knockout mice compared to wild-type controls suggesting increased sensitivity of *ApoE*$^{-/-}$ mice to LDR. The lower dose also led to left ventricle dysfunction observed at 20-weeks postirradiation, while mild hypertrophy appeared at 40 weeks and was sustained at 60 weeks in the *ApoE*$^{-/-}$ mice. Both knockout and wild-type strains of mice exhibited contractile dysfunction with a mild, but significant, decrease in ejection and shortening fraction. Acute inflammatory infiltrate was observed in scarring areas with accumulation of M1-macrophages and secretion of IL-6 in *ApoE*$^{-/-}$ mice after 0.2 and 2 Gy. Moreover, both 0.2 and 2 Gy exposure in *ApoE*$^{-/-}$ mice resulted in increased fibrosis markers TGF-β1 and PAI-1 (*95*). Another study with hearts of *ApoE*$^{-/-}$ mice found that whole-body low-dose γ irradiations (25–500 mGy), induced increased capillary density, changes in collagen IV and enhancement of TNF-α and fibrinogen. The investigators conclude that these effects are likely reflecting compensatory regulations in the heart (*96*).

There is a paucity of information on how low-dose radiation affects the heart and therefore further research must be conducted to better understand the possible beneficial or detrimental effects of LDR on the heart. Future research on the effects of LDR on the heart should focus on the mechanism(s) of oxidative stress, inflammation and the immune response, as well as the short and long term effects on the heart from radiation used in diagnostic imaging.

CONCLUSIONS

As the use of ionizing radiation in medical procedures becomes common practice it is necessary to understand its long-term impact on patients. High doses of radiation used in cancer treatment have been shown to lead to cardiac dysfunction over time. The mechanisms of action predominantly involve increased oxidative stress as well as inflammation. While the effects of high dose radiation on the heart are better known, there is little knowledge on the effects of LDR. Some studies suggest that LDR may be beneficial and trigger protective cellular responses, while other studies show increased risk of cardiovascular disease. Future studies are required to advance the understanding of the mechanism(s) that regulate a response against oxidative stress induced cellular damage as it relates to cardiac function. Further understanding of the effects of low dose ionizing radiation could lead to advances in patient care and reduce the detrimental impact of radiation therapy on cardiac function.

ACKNOWLEDGMENTS

The authors would like to acknowledge H. Forsyth and A. Homagain for their aid in editing the manuscript. This work was supported by Bruce Power and Mitacs.

Received: June 16, 2017; accepted: August 15, 2017; published online: September 5, 2017

REFERENCES

1. Siegel R, DeSantis C, Virgo K, Stein K, Mariotto A, Smith T, et al. Cancer treatment and survivorship statistics. CA Cancer J Clin 2012; 62(4):220–41.
2. 2. Canadian Nuclear Safety Commission. Dose from artificial sources of radiation. (cited 2016 Apr 27) (http://nuclearsafety.gc.ca/)
3. Niemantsverdriet M, van Goethem M-J, Bron R, Hogewerf W, Brandenburg S, Langendijk JA, et al. High and low LET radiation differentially induce normal tissue damage signals. Int J Radiat Oncol Biol Phys 2012; 83(4):1291–7.
4. Jones B, Dale RG, Cárabe-Fernández A. Charged particle therapy for cancer: The inheritance of the Cavendish scientists? Appl Radiat Isot 2009; 67(3):371–7.
5. Schulz-Ertner D, Tsujii H. Particle radiation therapy using proton and heavier ion beams. J Clin Oncol 2007; 25(8):953–64.
6. Azzam EI, Jay-Gerin J-P, Pain D. Ionizing radiation-induced metabolic oxidative stress and prolonged cell injury. Cancer Lett 2012; 327(1–2):48–60.
7. Kryston TB, Georgiev AB, Pissis P. Role of oxidative stress and DNA damage in human carcinogenesis. Mutat Res Mol Mech Mutagen 2011; 711(1):193–201.
8. Ottolenghi A, Merzagora M, Paretzke HG. DNA complex lesions induced by protons and alpha-particles: track structure characteristics determining linear energy transfer and particle type dependence. Radiat Environ Biophys 1997; 36(2):97–103.
9. Goodhead DT. Energy deposition stochastics and track structure: what about the target? Radiat Prot Dosimetry 2006; 122(1–4): 3–15.
10. Ward JF. Biochemistry of DNA lesions. Radiat Res Suppl 1985; 8:S103–11.
11. Georgakilas AG. From chemistry of DNA damage to repair and biological significance. Comprehending the future. Mutat Res 2011; 711(1–2):1–2.
12. Petkau A. Role of superoxide dismutase in modification of radiation injury. Br J Cancer Suppl 1987; 8:87–95.
13. Riley PA. Free radicals in biology: oxidative stress and the effects of ionizing radiation. Int J Radiat Biol 1994; 65(1):27–33.
14. Giordano FJ. Oxygen, oxidative stress, hypoxia, and heart failure. J Clin Invest 2005; 115(3):500–8.
15. Azzam EI, de Toledo SM, Little JB. Oxidative metabolism, gap junctions and the ionizing radiation-induced bystander effect. Oncogene 2003; 22(45):7050–7.
16. Hei TK, Zhou H, Chai Y, Ponnaiya B, Ivanov VN. Radiation induced non-targeted response: mechanism and potential clinical implications. Curr Mol Pharmacol 2011; 4(2):96–105.
17. Mothersill C, Seymour CB. Radiation-induced bystander effects–implications for cancer. Nat Rev Cancer 2004; 4(2):158–64.
18. Buonanno M, de Toledo SM, Azzam EI. Increased frequency of spontaneous neoplastic transformation in progeny of bystander cells from cultures exposed to densely ionizing radiation. PLoS One 2011; 6(6):e21540.
19. Darby SC, Cutter DJ, Boerma M, Constine LS, Fajardo LF,

Kodama K, et al. Radiation-related heart disease: current knowledge and future prospects. Int J Radiat Oncol Biol Phys 2010; 76(3):656–65.

20. Darby SC, Ewertz M, McGale AM, Bennet U, Blom-Goldman D, Bronnum D, et al. Risk of ischemic heart disease in women after radiotherapy for breast cancer. N Engl J Med 2013; 368(11): 987–98.
21. Yusuf SW, Sami S, Daher IN. Radiation-induced heart disease: a clinical update. Cardiol Res Pract 2011; 2011:1–9.
22. Cuzick J, Stewart H, Rutqvist L, Houghton J, Edwards R, Redmond C, et al. Cause-specific mortality in long-term survivors of breast cancer who participated in trials of radiotherapy, J Clin Oncol 1994; 12(3):447–53.
23. Nian M, Lee P, Khaper N, Liu P. Inflammatory cytokines and postmyocardial infarction remodeling. Circ Res 2004; 94(12): 1543–53.
24. Schaue D, Micewicz ED, Ratikan JA, Xie MW, Cheng G, McBride WH. Radiation & inflammation, Semin Radiat Oncol 2015; 25(1):4–10.
25. Darby SC, Cutter DJ, Boerma M, Constine LS, Fajardo LF, Kodama K, et al. Radiation-related heart disease: current knowledge and future prospects. Int J Radiat Oncol Biol Phys 2010; 76(3):656–65.
26. Schultz-Hector S, Trott K-R. Radiation-induced cardiovascular diseases: is the epidemiologic evidence compatible with the radiobiologic data? Int J Radiat Oncol Biol Phys 2007; 67(1):10–8.
27. Gagliardi G, Constine LS, Moiseenko V, Correa C, Pierce LJ, Allen AM, et al. Radiation dose-volume effects in the heart. Int J Radiat Oncol Biol Phys 2010; 76(3):S77–85.
28. Heidenreich PA, Kapoor JR. Radiation induced heart disease: systemic disorders in heart disease. Heart 2009; 95(3):252–8.
29. Filopei J, Frishman W. Radiation-induced heart disease. Cardiol Rev 2012; 20(4):184–8.
30. Veinot JP, Edwards WD. Pathology of radiation-induced heart disease: A surgical and autopsy study of 27 cases. Hum Pathol 1996; 27(8):766–73.
31. Fajardo LF, Stewart JR. Pathogenesis of radiation-induced myocardial fibrosis. Lab Invest 1973; 29(2):244–57.
32. Greenwood RD, Rosenthal A, Cassady R, Jaffe N, Nadas AS. Constrictive pericarditis in childhood due to mediastinal irradiation. Circulation 1974; 50(5):1033–9.
33. Schultz-Hector S, Balz K. Radiation-induced loss of endothelial alkaline phosphatase activity and development of myocardial degeneration. An ultrastructural study. Lab Invest 1994; 71(2): 252–60.
34. Halle M, Gabrielsen A, Paulsson-Berne G, Gahm C, Agardh HE, Farnebo F, et al. Sustained inflammation due to nuclear factor-kappa B activation in irradiated human arteries. J Am Coll Cardiol 2010; 55(12):1227–36.
35. Weintraub NL, Jones WK, Manka D. Understanding radiation-induced vascular disease. J Am Coll Cardiol 2010; 55(12):1237–9.
36. Baker JE, Moulder JE, Hopewell JW. Radiation as a risk factor for cardiovascular disease. Antioxid Redox Signal 2011; 15(7): 1945–56.
37. Preston DL, Shimizu Y, Pierce DA, Suyama A, Mabuchi K. Studies of mortality of atomic bomb survivors. Report 13: Solid cancer and noncancer disease mortality: 1950–1997. Radiat Res 2003; 160(4):381–407.
38. Straume T, Rugel G, Marchetti AA, Rühm W, Korschinek G, McAninch JE, et al. Measuring fast neutrons in Hiroshima at distances relevant to atomic-bomb survivors. Nature 2003; 424(6948):539–42.
39. Shimizu Y, Kodama K, Nishi N, Kasagi F, Suyama A, Soda M, et al. Radiation exposure and circulatory disease risk: Hiroshima and Nagasaki atomic bomb survivor data, 1950-2003. BMJ 2010; 340.
40. Hayashi T, Kusunoki Y, Hakoda M, Morishita Y, Kubo Y, Maki M, et al. Radiation dose-dependent increases in inflammatory response markers in A-bomb survivors. Int J Radiat Biol 2003; 79(2):129–36.
41. Hayashi T, Morishita Y, Kubo Y, Kusunoki Y, Hayashi I, Kasagi F, et al. Long-term effects of radiation dose on inflammatory markers in atomic bomb survivors. Am J Med 2005; 118(1):83–6.
42. Kusunoki Y, Kyoizumi S, Yamaoka M, Kasagi F, Kodama K, Seyama T. Decreased proportion of CD4 T cells in the blood of atomic bomb survivors with myocardial infarction. Radiat Res 1999; 152(5):539.
43. Kusunoki Y, Hayashi T, Morishita Y, Yamaoka M, Maki M, Bean MA, et al. T-cell responses to mitogens in atomic bomb survivors: a decreased capacity to produce interleukin 2 characterizes the T cells of heavily irradiated individuals. Radiat Res 2001; 155(1): 81–8.
44. Kusunoki Y, Yamaoka M, Kubo Y, Hayashi T, Kasagi F, Douple EB, et al. T-cell immunosenescence and inflammatory response in atomic bomb survivors. Radiat Res 2010; 174(6):870–6.
45. Russell NS, Hoving S, Heeneman S, Hage JJ, Woerdeman LAE, de Bree R, et al. Novel insights into pathological changes in muscular arteries of radiotherapy patients. Radiother Oncol 2009; 92(3):477–83.
46. Carr ZA, Land CE, Kleinerman RA, Weinstock RW, Stovall M, Griem ML, et al. Coronary heart disease after radiotherapy for peptic ulcer disease. Int J Radiat Oncol Biol Phys 2005; 61(3): 842–50.
47. McGale P, Darby SC, Hall P, Adolfsson J, Bengtsson N-O, Bennet AM, et al. Incidence of heart disease in 35,000 women treated with radiotherapy for breast cancer in Denmark and Sweden. Radiother Oncol 2011; 100(2):167–75.
48. Early Breast Cancer Trialists' Collaborative Group. Long term toxicity of radiation therapy. In: Update of the Early Breast Cancer Trialists' Collaborative group overview of radiation therapy for early breast cancer. Chicago: American Society of Clinical Oncology Annual Meeting; 2007.
49. Tjessem KH, Johansen S, Malinen E, Reinertsen KV, Danielsen T, Fossa SD, Fossa A. Long-tern cardiac mortility after hypofractionated radiation therapy in breast cancer. Int J Radiat Oncol Biol Phys 2013; 87(2):337–43.
50. Adams MJ, Hardenbergh PH, Constine LS, Lipshultz SE. Radiation-associated cardiovascular disease. Crit Rev Oncol Hematol 2003; 45(1):55–75.
51. Hancock SL, Donaldson SS, Hoppe RT. Cardiac disease following treatment of Hodgkin's disease in children and adolescents. J Clin Oncol 1993; 11(7):1208–15.
52. Aleman BMP, van den Belt-Dusebout AW, Klokman WJ, Van't Veer MB, Bartelink H, van Leeuwen FE. Long-term cause-specific mortality of patients treated for Hodgkin's disease. J Clin Oncol 2003; 21(18):3431–9.
53. Hoppe RT. Hodgkin's disease: complications of therapy and excess mortality. Ann Oncol 1997; 8(1):115–8.
54. Ng AK, Bernardo MP, Weller E, Backstrand KH, Silver B, Marcus KC, et al. Long-term survival and competing causes of death in patients with early-stage Hodgkin's disease treated at age 50 or younger. J Clin Oncol 2002; 20(8):2101–8.
55. Swerdlow AJ, Higgins CD, Smith P, Cunningham D, Hancock BW, Horwich A, et al. Myocardial infarction mortality risk after treatment for Hodgkin disease: a collaborative British cohort study. J Natl Cancer Inst 2007; 99(3):206–14.
56. Reinders JG, Heijmen BJ, Olofsen-van Acht MJ, van Putten WL, Levendag PC. Ischemic heart disease after mantlefield irradiation for Hodgkin's disease in long-term follow-up. Radiother Oncol 1999; 51(1):35–42.
57. Creutzberg CL, Visser AG, De Porre PM, Meerwaldt JH, Althof VG, Levendag PC. Accuracy of patient positioning in mantle field irradiation. Radiother Oncol 1992; 23(4):257–64.
58. Mauch PM, Kalish LA, Marcus KC, Shulman LN, Krill E, Tarbell

NJ, et al. Long-term survival in Hodgkin's disease relative impact of mortality, second tumors, infection, and cardiovascular disease. Cancer J Sci Am 1995; 1(1):33–42.

59. Aisenberg AC. Problems in Hodgkin's disease management. Blood 1999; 93(3):761–79.

60. Hancock SL, Tucker MA, Hoppe RT. Factors affecting late mortality from heart disease after treatment of Hodgkin's disease. JAMA 1993; 270(16):1949–55.

61. *61*. O H-Icí D, Garot J. Radiation-induced heart disease. Circ Heart Fail 2011; 4(1):e1–2.

62. Benderitter M, Maingon P, Abadie C, Assem M, Maupoil V, Briot F, et al. Effect of in vivo heart irradiation on the development of antioxidant defenses and cardiac functions in the rat. Radiat Res 1995; 144(1):64.

63. Yoshida T, Goto S, Kawakatsu M, Urata Y, Li T-S. Mitochondrial dysfunction, a probable cause of persistent oxidative stress after exposure to ionizing radiation. Free Radic Res 2012; 46(2): 147–53.

64. Sridharan V, Aykin-Burns N, Tripathi P, Krager KJ, Sharma SK, Moros EG, et al. Radiation-induced alterations in mitochondria of the rat heart. Radiat Res 2014; 181(3):324–34.

65. Sag CM, Wolff HA, Neumann K, Opiela M-K, Zhang J, Steuer F, et al. Ionizing radiation regulates cardiac Ca handling via increased ROS and activated CaMKII. Basic Res Cardiol 2013; 108(6):385.

66. Lee C-L, Moding EJ, Cuneo KC, Li Y, Sullivan JM, Mao L, et al. p53 functions in endothelial cells to prevent radiation-induced myocardial injury in mice. Sci Signal 2012; 5(234):ra52.

67. Azimzadeh O, Scherthan H, Sarioglu H, Barjaktarovic Z, Conrad M, Vogt A, et al. Rapid proteomic remodeling of cardiac tissue caused by total body ionizing radiation. Proteomics 2011; 11(16): 3299–311.

68. Van Der Meeren A, Squiban C, Gourmelon P, Lafont H, Gaugler MH. Differential regulation by IL-4 and IL-10 of radiation-induced IL-6 and IL-8 production and ICAM-1 expression by human endothelial cells. Cytokine 1999; 11(11):831–8.

69. Deten A, Hölzl A, Leicht M, Barth W, Zimmer HG. Changes in extracellular matrix and in transforming growth factor beta isoforms after coronary artery ligation in rats. J Mol Cell Cardiol 2001; 33(6):1191–207.

70. Nguyen TD, Maquart F-X, Monboisse J-C. Ionizing radiations and collagen metabolism: from oxygen free radicals to radio-induced late fibrosis. Radiat Phys Chem 2005; 72(2):381–6.

71. Rødningen OK, Overgaard J, Alsner J, Hastie T, Børresen-Dale A-L. Microarray analysis of the transcriptional response to single or multiple doses of ionizing radiation in human subcutaneous fibroblasts. Radiother Oncol 2005; 77(3):231–40.

72. Herskind C, Rodemann HP. Spontaneous and radiation-induced differentiation of fibroblasts. Exp Gerontol 2000; 35(6–7):747–55.

73. Gao S, Wu R, Zeng Y. Up-regulation of peroxisome proliferator-activated receptor gamma in radiation-induced heart injury in rats. Radiat Environ Biophys 2012; 51(1):53–9.

74. Baker JE, Fish BL, Su J, Haworth ST, Strande JL, Komorowski RA, et al. 10 Gy total body irradiation increases risk of coronary sclerosis, degeneration of heart structure and function in a rat model. Int J Radiat Biol 2009; 85(12):1089–100.

75. Boerma M, van der Wees CGC, Vrieling H, Svensson JP, Wondergem J, van der Laarse A, et al. Microarray analysis of gene expression profiles of cardiac myocytes and fibroblasts after mechanical stress, ionising or ultraviolet radiation. BMC Genomics 2005; 6:6.

76. DeBo RJ, Lees CJ, Dugan GO, Caudell DL, Michalson KT, Hanbury DB, et al. Late effects of total-body gamma irradiation on cardiac structure and function in male rhesus macaques. Radiat Res 2016; 186(1):55–64.

77. National Council on Radiation Protection and Measurements. Exposure of the population in the United States and Canada from natural background radiation : recommendations of the National Council on Radiation Protection and Measurements. The Council; 1987. 209 p.

78. Zarate N, Wang XY, White EJ, Boreham D, Rangachari PK, Huizinga JD. Low doses of ionizing radiation can prevent radiation-induced colonic epithelial hyporesponsiveness to muscarinic agonists. Int J Radiat Biol 2006; 82(12):887–98.

79. Feinendegen LE. Evidence for beneficial low level radiation effects and radiation hormesis. Br J Radiol 2005; 78(925):3–7.

80. Calabrese EJ, Baldwin LA. Toxicology rethinks its central belief. Nature 2003; 421(6924):691–2.

81. Khaper N, Bryan S, Dhingra S, Singal R, Bajaj A, Pathak CM, et al. Targeting the vicious inflammation-oxidative stress cycle for the management of heart failure. Antioxid Redox Signal 2010; 13(7):1033–49.

82. Kojima S, Nakayama K, Ishida H. Low dose gamma-rays activate immune functions via induction of glutathione and delay tumor growth. J Radiat Res 2004; 45(1):33–9.

83. Nowosielska EM, Wrembel-Wargocka J, Cheda A, Lisiak E, Janiak MK. Enhanced cytotoxic activity of macrophages and suppressed tumor metastases in mice irradiated with low doses of X- rays. J Radiat Res 2006; 47(3–4):229–36.

84. Tanaka T, Tago F, Fang S-P, Shimura N, Kojima S. Repeated 0.5-Gy gamma-ray irradiation attenuates autoimmune manifestations in MRL-lpr/lpr mice. Int J Radiat Biol 2005; 81(10):731–40.

85. Taylor K, Lemon JA, Boreham DR. Radiation-induced DNA damage and the relative biological effectiveness of 18F-FDG in wild-type mice. Mutagenesis 2014; 29(4):279–87.

86. Taylor K, Lemon JA, Phan N, Boreham DR. Low-dose radiation from 18F-FDG PET does not increase cancer frequency or shorten latency but reduces kidney disease in cancer-prone Trp53+/- mice. Mutagenesis 2014; 29(4):289–94.

87. Gori T, Münzel T. Biological effects of low-dose radiation: of harm and hormesis. Eur Heart J 2011; 33:292–5.

88. Kaiser J. Hormesis. Sipping from a poisoned chalice. Science 2003; 302(5644):376–9.

89. Pollycove M, Feinendegen LE. Radiation-induced versus endogenous DNA damage: possible effect of inducible protective responses in mitigating endogenous damage. Hum Exp Toxicol 2003; 22(6):290–306.

90. Feinendegen LE. Relative implications of protective responses versus damage induction at low dose and low-dose-rate exposures, using the microdose approach. Radiat Prot Dosimetry 2003; 104(4):337–46.

91. Barjaktarovic Z, Schmaltz D, Shyla A, Azimzadeh O, Schulz S, Haagen J, et al. Radiation-induced signaling results in mitochondrial impairment in mouse heart at 4 weeks after exposure to X-rays. PLoS One 2011; 6(12):e27811.

92. Mitchel REJ, Hasu M, Bugden M, Wyatt H, Little MP, Gola A, et al. Low-dose radiation exposure and atherosclerosis in ApoE$^{-/-}$ mice. Radiat Res 2011; 175(5):665–76.

93. Mitchel REJ, Hasu M, Bugden M, Wyatt H, Hildebrandt G, Chen Y-X, et al. Low-dose radiation exposure and protection against atherosclerosis in ApoE(-/-) mice: the influence of P53 heterozygosity. Radiat Res 2013; 179(2):190–9.

94. Zhang C, Jin S, Guo W, Li C, Li X, Rane MJ, et al. Attenuation of diabetes-induced cardiac inflammation and pathological remodeling by low-dose radiation. Radiat Res 2011; 175(3):307–21.

95. Monceau V, Meziani L, Strup-Perrot C, Morel E, Schmidt M, Haagen J, et al. Enhanced sensitivity to low dose irradiation of ApoE-/- mice mediated by early pro-inflammatory profile and delayed activation of the TGFβ1 cascade involved in fibrogenesis. PLoS One 2013; 8(2):e57052.

96. Mathias D, Mitchel REJ, Barclay M, Wyatt H, Bugden M, Priest ND, et al. Low-dose irradiation affects expression of inflammatory markers in the heart of ApoE-/- mice. PLoS One 2015; 10(3): e011966.